LIST OF ABBREVIATIONS

a.a.	amino acid
AIF	apoptosis-inducing factor
AM	acetoxymethyl ester
AMP	adenosine monophosphate
APAF-1	apoptotic protease-activating factor-1
ASK1	apoptotic signaling kinase 1
ATG5	autophagy protein 5
ATP	adenosine-5'-triphosphate
Bad	Bcl-2-associated agonist of cell death
BAPTA	1,2-bis(o-aminophenoxy)ethane-N,N,N',N'-tetraacetic acid
Bak	Bcl-2 antagonist/killer
Bax	Bcl-2-associated X protein
Bcl	B-cell lymphoma
BH	Bcl-2 homology
Bid	BH3-interacting domain death agonist
Bik	Bcl-2-interacting killer
Bim	Bcl-2-interacting mediator of cell death
BMF	Bcl-2-modifying factor
Bok	Bcl-2-related ovarian killer
$[Ca^{2+}]_{cyt}$	free cytosolic Ca^{2+} concentration
$[Ca^{2+}]_{ER}$	ER Ca^{2+} concentration
$[Ca^{2+}]_{m}$	mitochondrial Ca^{2+} concentration
CaBP	Ca^{2+}-binding protein
CaM	calmodulin
CaMK	Ca^{2+}/calmodulin-dependent protein kinase
cAMP	cyclic AMP
caspase	cystein-aspartic protease
CICR	Ca^{2+}-induced Ca^{2+} release
CLL	Chronic lymphocytic leukemia
CRAC	Ca^{2+} release -activated channel
CRT	calreticulin
Cyt c	cytochrome c
DAG	diacylglycerol
DD	death domain
DISC	death-induced signaling complex
DLBCL	diffuse large B-cell lymphoma
DTT	dithiothreitol
dYT	double yeast, tryptophan
ECL	enhanced chemiluminescence
EDTA	ethylenediaminetetraacetic acid
EGTA	ethylene glycol tetraacetic acid
ER	endoplasmic reticulum
FADD	Fas-associated death DD protein
FAS	apoptosis-stimulating fragment
FLIP	FLICE-inhibitory protein
GAPDH	glyceraldehyde 3-phosphate dehydrogenase
GPCR	G protein-coupled receptor
Grp75	glucose-regulated protein 75
GST	glutathione S-transferase
h	hour(s)
HBSS	Hank's balanced salt solution
HEPES	(4-(2-hydroxyethyl)-1-piperazineethanesulfonic acid
IAP	inhibitor of apoptosis
IDP	IP_3R-derived peptide
IgM	immunoglobulin M
IICR	IP_3-induced Ca^{2+} release
IMM	inner mitochondrial membrane
IMS	inner mitochondrial space

IP_3	inositol 1,4,5-trisphosphate
IP_3R	IP_3 receptor
IPTG	isopropyl-β-D-thiogalactoside
JNK	c-Jun N-terminal Kinase
kDa	kilodalton
LBD	ligand-binding domain
MAMs	mitochondrial-associated membranes
Mcl-1	myeloid cell leukemia sequence 1
MCU	mitochondrial Ca^{2+} uniporter
MEF	mouse embryonic fibroblast
MFN	mitofusin
min	minute(s)
MOMP	mitochondrial outer-membrane permeabilization
NCX	Na^{+}/Ca^{2+}-calcium exchanger
NFAT	Nuclear factor of activated T cells
OMM	outer mitochondrial membrane
PAGE	polyacrylamide gel electrophoresis
PARP	poly-ADP-ribose polymerase
PBS	phosphate-buffered saline
PE	phosphatidylethanolamine
PI3K	phosphatidylinositol 3-kinase
PIP_2	phosphatidylinositol 4,5-bis-phosphate
PKB	protein kinase B/AKT
PKC	protein kinase C
PLC	phospholipase C
PMCA	plasma-membrane Ca^{2+} ATPase
PML	promyelocytic leukemia protein
PP2B	protein phosphatase 2B/calcineurin
PTP	permeability transition pore
PUMA	p53-upregulated modulator of apoptosis
PVDF	polyvinylidene fluoride
RIPA	radioimmunoprecipitation assay
ROC	receptor operated channel
RyR	ryanodine receptor
SDS	sodium dodecyl sulfate
SEM	standard error of the mean
SERCA	sarco-endoplasmic reticulum Ca^{2+} ATPase
Smac/DIABLO	small mitochondria-derived activator of caspase/direct inhibitor of apoptosis-binding protein with low pI
SOC	store-operated channel
SPCA	secretory pathway Ca^{2+} ATPase
SR	sarcoplasmic reticulum
STIM	Stromal interaction molecule
STS	staurosporine
TCR	T cell receptor
TG	thapsigargin
TM	transmembrane
TMD	transmembrane domain
TNF	tumor necrosis factor
TRAIL	TNF-alpha-related apoptosis-inducing ligand
VDAC	voltage-dependent anion channel
VOC	voltage-operated channel

GENERAL INTRODUCTION

GENERAL INTRODUCTION

The introductory material presented in this section is partly based on the following reviews:

- **Giovanni Monaco**, Tim Vervliet, Haidar Akl, Geert Bultynck (2013). The selective BH4-domain biology of Bcl-2-family members: IP_3Rs and beyond. *Cellular and Molecular Life Sciences, 2013 Apr; 70(7):1171-83*.

- Jean-Paul Decuypere, **Giovanni Monaco**, Geert Bultynck, Ludwig Missiaen, Humbert De Smedt, Jan B. Parys (2011). The IP_3 receptor-mitochondria connection in apoptosis and autophagy. *Biochimica et Biophysica Acta (BBA)-Molecular Cell Research*, 2011 May; 1813(5):1003-13.

GENERAL INTRODUCTION

1 Cell death: suicidal, criminal or both?

A single cell of a multicellular organism is an active participant of its milieu, constantly adapting to the changing physiological demands and to contingent extracellular stressors. It strives against many different types of stress like nutrients deprivation, chemical stress, oxidative stress, irradiation, pathogens, *etc.* In response to these stressful circumstances, cells face an almost Shakespearean dilemma: to die or not to die? Under low-stress conditions, they may attempt to cope with the injury by taking pro-survival measures and meanwhile repair the damages. The best example of such a lifespan-extending strategy is autophagy [from the Greek "to eat" ("phagy") oneself ("auto")] [1]. Stressed cells that underwent autophagy generate energy and metabolites by digesting their own organelles and macromolecules in a sort of cell self-cannibalism. However, if the aforementioned stress conditions are too severe or prolonged over time then the cell is on a one-way trip to death. The sentence of cell death may just follow the failure in the autophagic-adaptive response [2] or occur *via* two different processes known as necrosis (from the Greek "nekros," for corpse) and apoptosis (from a Greek compound word that suggests "the falling off of leaves") [3, 4] (Fig.1, next page). Necrosis is generally considered a pathological and often "accidental" form of cell death in response to extremely harsh physicochemical insults. Apoptotic cell death is instead a tightly controlled cell suicide program not necessarily detrimental for the whole organism. The two forms of cell demise overlap to some extent and apoptosis may in some cases progress to necrosis. Moreover, it became clear that an intermediate situation between the two exists (called necroptosis) which is phenotypically similar to necrosis but relies on a genetic program [5-7]. Even more complicated, cell death might also proceed by following additional routes which have been recently identified but are not yet well characterized (such as anoikis, entosis, parthanatos, *etc*., see [7]).

As for the necrotic cells, they are morphologically characterized by a general cell swelling which leads to membrane permeabilization and cell lysis. The intracellular material is thereby released in the extracellular environment and causes a sustained inflammatory response. Contrarily, apoptosis is an “implosive”-death mode because it doesn’t compromise cell integrity. Apoptotic cells drastically shrink, lose contacts with their neighbors, their DNA becomes fragmented and their cell membrane protrudes forming blebs. As a result, small vesicles incorporating various cell fragments shed from the cellular surface. These so-called apoptotic bodies present a distinctive plasma-membrane reorganization [8, 9] that guarantees their prompt recognition and phagocytic removal by macrophages and neighboring cells. Since no inflammation follows, apoptosis can be seen as a “stealth” way to remove superfluous or damaged cells without causing harm to the healthy cells. If the removal of apoptotic bodies is delayed or nonexistent, as in cell-culture conditions, secondary necrosis follows apoptosis [10, 11].

The next subsections will provide an overview of apoptosis with a definition of the main intracellular events, which take place upstream to the morphological rearrangements just mentioned.

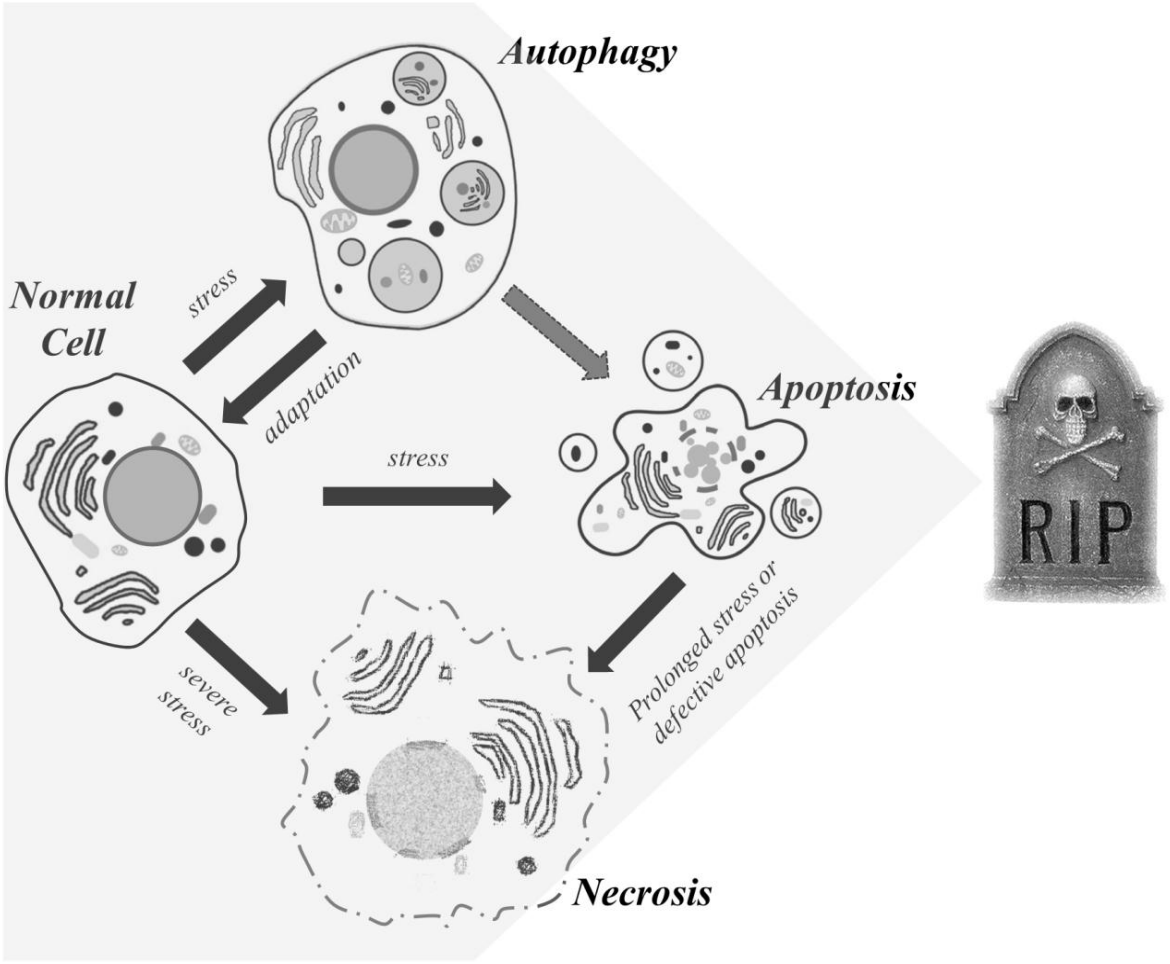

Fig. 1: The basic ways by which cells deal with stress. Under stress conditions, cellular adaptation may result *via* a hand-to-mouth strategy (autophagy). Alternatively, intracellular component are "packaged" towards cell suicide (apoptosis). However, if the injury is too severe or prolonged over time, the only way to go is a crude cell explosion (necrosis/necroptosis). In some cases a particular cell response can progress to the other. Adapted from [12].

1.1 Molecular components of apoptosis signaling

Apoptotic cell death is an evolutionary conserved form of programmed cell death. This process is crucial for both embryonic development and adult-tissue homeostasis by ensuring the physiological removal of redundant, infected, damaged or transformed cells. Every day, in an impulse of unconscious altruism, almost 70 billion of our cells decide to sacrifice themselves for the sake of the whole organism [13, 14]. In contrast, a defective "cell suicide" can lead to pathophysiological conditions such as cancer or neurodegenerative and autoimmune diseases due, respectively, to excessive cell proliferation or uncontrolled cell death [15, 16].

Once the apoptotic response is triggered, the death sentence may be pronounced at the cell surface or directly involve the cell inner space. In vertebrates, this *a priori* distinction justifies the definition of two different but often interconnected apoptotic routes, the extrinsic and the intrinsic pathway [17] (see Fig. 2). The former is particularly important for the immune response and tolerance, the latter has more relevance in tissue homeostasis and stress responses [10, 18]. Both pathways may occur concomitantly and are eventually associated with the downstream release of apoptotic mediators from intracellular organelles and activation of enzymes responsible for the ordered breakdown of the cell [19]. Among these enzymes, the most relevant to the apoptotic cell dismantling are certainly the "cysteine aspartate" proteases (caspases). As suggested by the name, these proteases exploit their catalytic site, containing a highly conserved cysteine residue, to specifically cleave their substrates at the level of internal aspartic-acid residues. Two different classes of caspases are instrumental in apoptosis: the initiator caspases (caspase-2, -8, -9, -10 and -12) and the effector caspases (caspase-3, -6 and -7) [20]. Both classes are initially dormant in the cell as inactive precursors (procaspases) that need to be further processed. Upon apoptosis induction, the initiator caspases are activated as a consequence of a clustering process. Successively,

these fully active proteases activate, *via* a hierarchical proteolytic cascade, the effector caspases. The latter are the ones in charge of executing the cell-death process by cleaving several substrates including cytoskeletal proteins, transcription factors or DNA-repair enzymes such as PARP (poly-ADP-ribose polymerases) [21]. What follows is the series of cell morphological changes already described as apoptosis trademarks. The only exceptions to this general cascade model are represented by the endoplasmic reticulum (ER)-stress- and the perforin/granzyme B-induced apoptosis [10, 22]. In both cases the initiator-caspases step may be bypassed in favor of a direct activation of the effector caspases, however the detailed description of these pathways goes beyond the scope of this introduction.

1.1.1 The extrinsic pathway

The extrinsic pathway, also known as "death-receptor pathway", is triggered outside the cell through the activation of pro-apoptotic receptors (Fig. 2, right). Hence, extracellular death ligands, like the tumor necrosis factor (TNF), the TNF-related apoptosis-inducing ligand (TRAIL) or the apoptosis-stimulating fragment (FAS), interact with their corresponding death receptors on the cell surface. Upon ligation, receptors aggregate in the cell membrane by means of their characteristic death domains (DD) and become activated [23]. Next, the apoptotic signal propagates to the cell-inner space *via* the association of other DD-containing proteins with the cytoplasmic domains of the receptors. Such adaptor proteins are defined as Fas-associated death domain (FADD) and in turn recruit the initiator procaspases-8 and -10 to form a macromolecular complex, called death-induced signaling complex (DISC). The DISC assembly leads to the full activation of the mentioned initiator caspases that are now able to cleave and activate the effector caspases-3, -6 and -7.

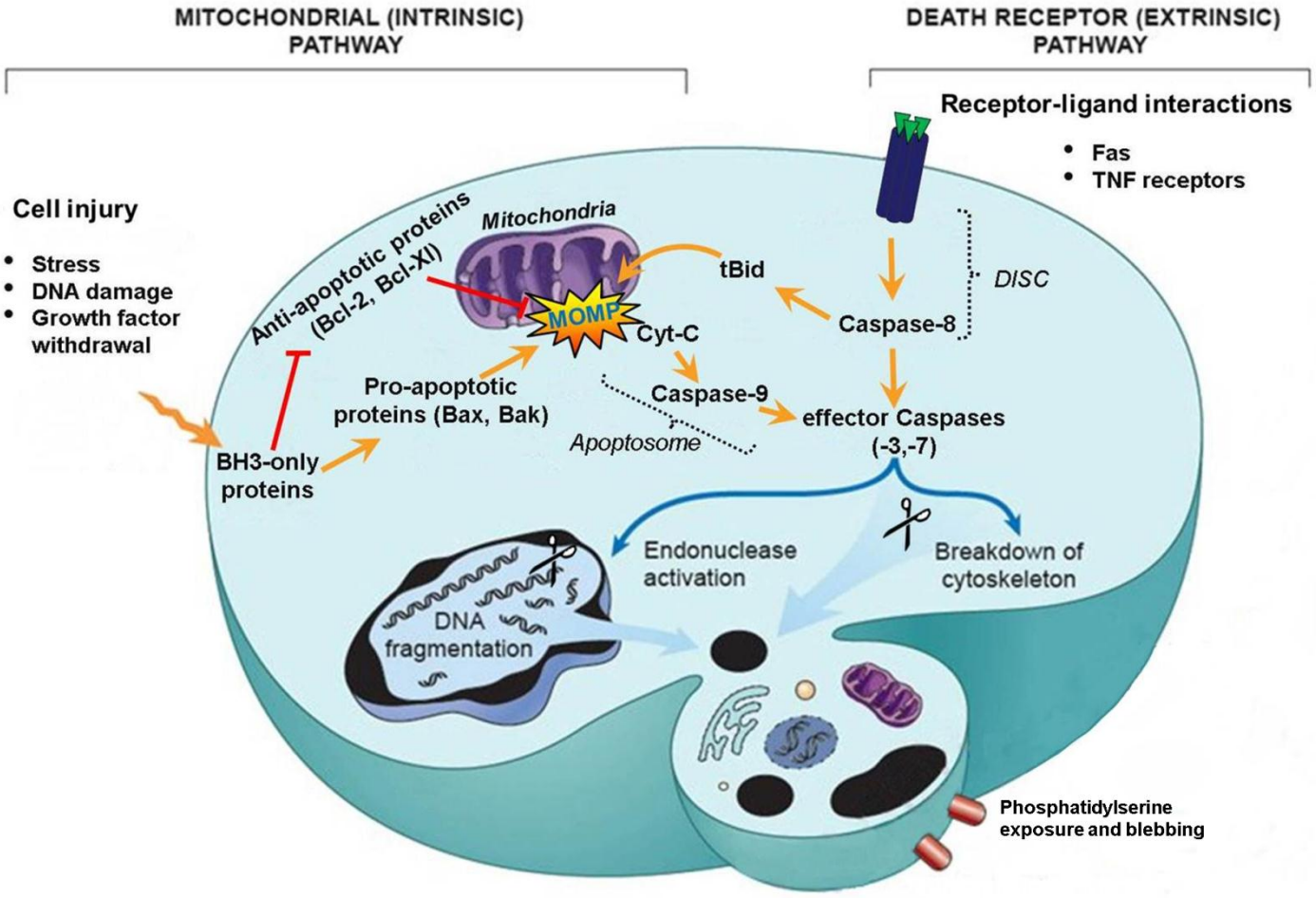

Fig. 2: The intrinsic and extrinsic apoptotic pathway. In the intrinsic or mitochondrial pathway (left), apoptotic sensors and effectors (BH3-only proteins, Bax, Bak) interplay towards MOMP induction and release of Cytochrome c. Cytochrome c promotes the formation of the apoptosome, where caspase-9 is activated and cleaves effector caspases. In the extrinsic pathway (right), a death ligand such as TNF, TRAIL or Fas Ligand transmits the apoptotic signal to the initiator caspase-8 which directly cleaves and activates the effector caspases or additionally the pro-apoptotic protein Bid to induce MOMP. In both cases, the brakes to MOMP are provided by the anti-apoptotic proteins (Bcl-2, Bcl-Xl *etc.*). Adapted from [24].

In cells with a poorly formed DISC, the apoptotic signaling is strengthened through the simultaneous caspase-8 stimulation of the intrinsic pathway [25], as will be described in section 1.2.2. Conversely, the recruitment to the DISC of a class of competitive inhibitors, known as FLICE-inhibitory proteins (FLIPs), contravenes the seminal activation of the initiator caspase-8 and therefore the downstream proteolytic cascade [26].

1.1.2 The intrinsic pathway and the mitochondrial outer membrane permeabilization (MOMP)

The intrinsic pathway is initiated in response to various types of non-receptor-mediated stressors ranging from DNA damage to drug cytotoxicity. This apoptotic route is often addressed as the mitochondrial pathway given that mitochondria are here the key players [27] (Fig. 2, left). Mitochondria are double-membrane intracellular organelles typically responsible for the cell's energy supply. They act as the "power plants" of the cell by converting the electrochemical gradient established across their inner membrane into adenosine-5'-triphosphate (ATP), the main energy source of cells [28]. Beyond the basal metabolism, the mitochondrial production of ATP also drives many apoptotic events of both the extrinsic and the intrinsic pathway [29]. Ironically, the crucial event in the intrinsic pathway is the partial loss of mitochondrial integrity and consequently of mitochondrial membrane potential. This is due to the MOMP event which represents, in most cases, the one-way ticket towards apoptosis initiation and propagation [30]. Permeabilized mitochondria release several pro-death factors from the inner mitochondrial space (IMS) into the cytosol *e.g.* Cytochrome C (Cyt c), second mitochondria-derived activator of caspase (Smac/DIABLO), apoptosis inducing factor (AIF), OMI/htra2 and endonuclease G [31]. All these molecules are successively, directly or indirectly, facilitating the activation of the caspases. In more detail, Cyt c is in its normal function involved in mitochondrial respiration, but upon release in the

cytosol it binds to a specific adaptor protein named apoptotic protease-activating factor-1 (APAF-1). In turn, APAF-1 acts, similarly to the FADD proteins in the extrinsic pathway, by oligomerizing and mediating the recruitment of the initiator caspase-9. Therefore, a caspase-activation platform similar to the DISC, here termed "apoptosome", is assembled and ready to "turn on" the proteolytic activity of the executioner caspase-3. As listed previously, the promoting role of Cyt c in the described cascade of events is assisted by the role of the other proteins released from the IMS. Smac/Diablo and OMI/htra2 antagonize the inhibitor of apoptosis (IAPs) proteins, members of a protein family with the ability to directly inhibit caspases. On the other hand, endonuclease G and AIF are mitochondrial nucleases which play a role in chromatin condensation and DNA fragmentation once freed in the cytosol [32]. Numerous models have been proposed for explaining MOMP execution, including the formation of a putative megapore, better known as permeability transition pore (PTP) [33, 34]. The latter is a multi-protein complex spanning the inner and outer membranes of the mitochondria that would provoke mitochondrial swelling and rupture of the outer membrane. However, the currently most accepted model suggests a less harsh scenario wherein a set of proteins of the Bcl-2 family (see section 1.2.2.) induces the formation of multimeric channel complexes to guide the release of the aforementioned apoptogens. In detail, mitochondrial permeabilization seems mainly due to a couple of Bcl-2 "effectors" proteins termed Bax and Bak which oligomerize in the outer mitochondrial membrane (OMM) [35]. Unlike Bak, Bax is primarily a cytosolic protein and undergoes conformational rearrangements for being able to accumulate on the OMM [36]. The other Bcl-2-family relatives are engaged in a complex set of interactions aimed at the regulation of Bax/Bak-mediated MOMP [37].

The next paragraphs discuss in detail the Bcl-2-family dynamics towards a pro- or anti-MOMP outcome.

1.2 Pro- and anti-apoptotic Bcl-2-family members

The pioneering observations concerning the Bcl-2-protein family were made in the context of hematological systems or cancers originating from these cells. This protein family derives indeed its name from the discovery, more than 2 decades ago, of B-cell lymphoma 2 (*BCL2*), the firstly revealed anti-death gene. Excessive expression of the *BCL2* gene was thereby proven to be associated with the survival advantage observed for hematological cancer cells [38, 39]. Thereafter, a new research field was set in motion and led to the progressive discovery and characterization of many other Bcl-2 family members. Currently, more than 20 members [40, 41] are known and are classified as pro-apoptotic or anti-apoptotic according to their ability to, respectively, promote or prevent MOMP.

1.2.1 Structure-function relationship for Bcl-2 proteins

A further subdivision of the two opposing classes is based on the presence of one or more of the four structurally conserved alpha-helical regions defined Bcl-2-homology domains (BH domains) [42]. The resulting three sub-families are defined as: 1) the pro-apoptotic-"BH3-only" proteins (*e.g.* Bid, Bim, Bad, PUMA, Noxa); 2) the pore-promoting- or "effector"-multidomain proteins (*e.g.* Bax and Bak, already mentioned above) and 3) the anti-apoptotic-Bcl-2-like proteins (*e.g.* Bcl-2, Bcl-Xl, Mcl-1, Bcl-w, A1) (see Fig. 3). The last two sub-families share all four homologous regions even though the presence of the BH4 domain in the multi- domain pro-apoptotic proteins is still under debate [42, 43]. Moreover, they have a similar structural organization with a central hydrophobic helix surrounded by at least five amphipathic helices. The last helical portion, including one or more of the most C-terminal

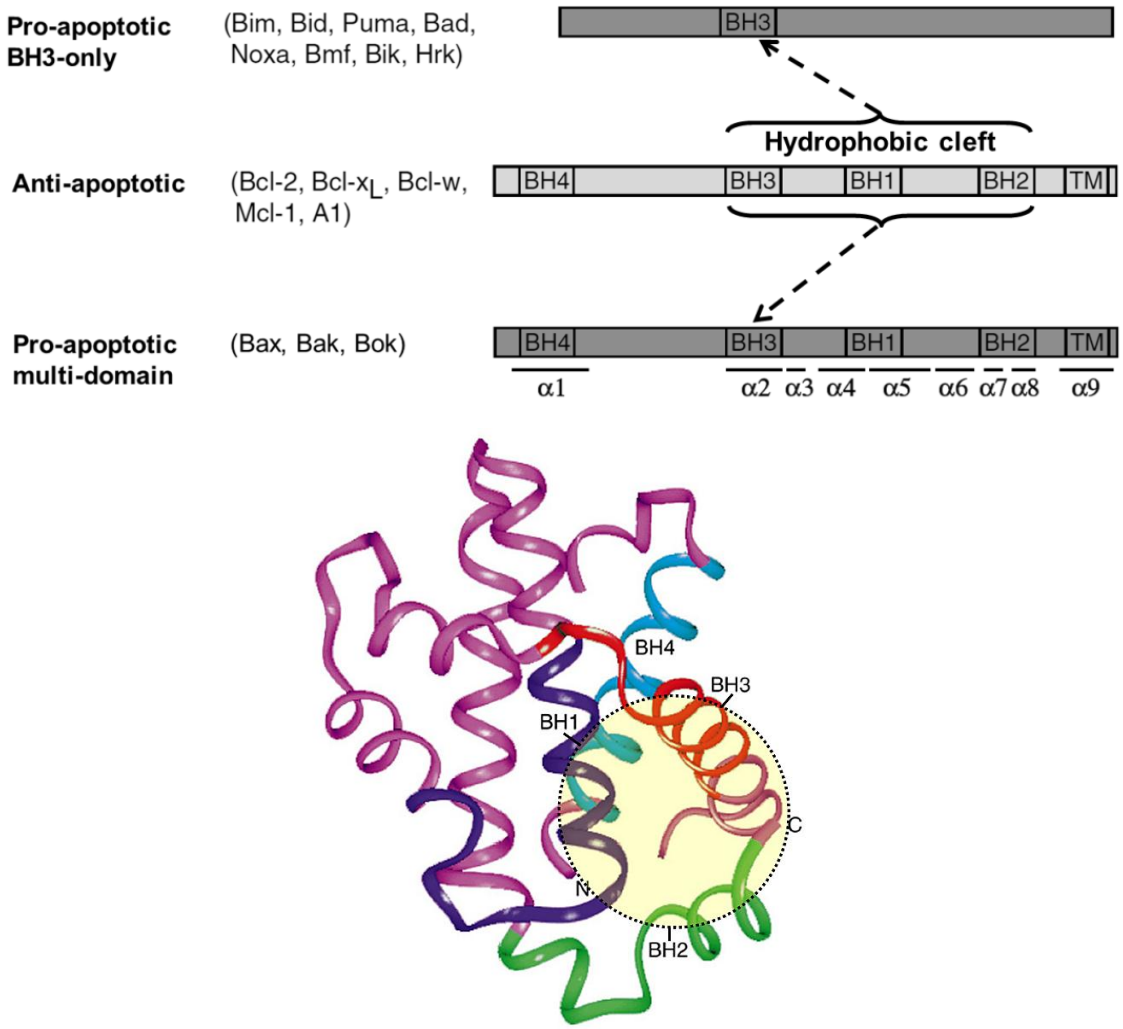

Fig. 3: Classification of the Bcl-2-family members according to their structure and function. (Upper scheme) Bcl-2-family proteins can either have one (BH3-only), three/four (pro-apoptotic multidomain) or four (anti-apoptotic multidomain) BH domains. The hydrophobic cleft formed by BH3, 1 and 2 domains of the anti-apoptotic proteins (highlighted at the bottom Bcl-Xl structure with a yellow circle) is in charge of binding and inhibiting the pro-apoptotic members (multidomain or BH3-only) at the level of their BH3 domain. The molecular and functional role of BH4 domain (light blue) is under debate. Not shown in the bottom figure is a large, unstructured loop between residues 26–76 in the protein. Adapted from [35, 44].

helices, is considered as their transmembrane domain (TMD) which allows the permanent or temporary insertion into cellular membranes [45-49]. On the contrary, the BH3-only proteins, apart from containing a single BH motif, as their name indicates, are very heterogeneous and unstructured proteins often deprived of a TMD. According to the mainframe model, a network of reciprocal interactions is built up by the triad of these Bcl-2 sub-families in order to modulate MOMP occurrence [30]. Generally, Bcl-2-proteins interactivity relies on a key three-dimensional protein structure termed “hydrophobic cleft”, shaped on the surface of the anti-apoptotic proteins by the helices of their BH1, BH2 and BH3 domains. The hydrophobic cleft serves as a selective binding pocket for the BH3 domain of the other Bcl-2 sub-families belonging to the pro-apoptotic group (see Fig. 3). Besides the BH1, BH2 and BH3 domain, the anti-apoptotic Bcl-2-family members, like Bcl-2 and Bcl-Xl, require also the N-terminal BH4 domain for retaining their anti-apoptotic activity [50-52]. However, the role of the BH4 domain in Bcl-2's pro-survival activity is not as well understood as that of the other three BH domains and often controversial [53-55].

1.2.2 Interplay of Bcl-2 proteins at the mitochondria

In unstressed conditions, the pro-MOMP activity of the pro-apoptotic Bcl-2 group (multidomain and BH3-only proteins) is neutralized by the interaction with their anti-apoptotic Bcl-2 relatives on the OMM or in the cytosol. In response to an intrinsic apoptotic stimulus, the BH3-only proteins act as sensors and get activated by transcriptional induction (PUMA and Noxa), post-translational modification (Bad) or both [30, 56]. An important exception concerns the BH3-only protein Bid which is cleaved to form its active truncated counterpart (tBid) by caspase-8 and makes, as already anticipated in 1.2.1, a strong link between extrinsic and intrinsic apoptotic pathways [25]. Once active, the BH3-only proteins translocate to the OMM and either stimulate Bax and Bak pore-forming activity or alleviate

the function of the anti-apoptotic Bcl-2 proteins, thereby favoring MOMP and its already described effects [40, 41, 57] (see Fig. 4). Some of the BH3-only proteins (*e.g.* Bid and Bim) are able to interact with both the anti-apoptotic repertoire as well as the MOMP-"effectors", Bax and Bak. They are addressed as ''activators" since they are directly responsible of unleashing Bax and Bak pro-MOMP activity. Other BH3-only proteins are solely able to bind the anti-apoptotic repertoire and are referred to as ''sensitizers'' (*e.g.* Bad, Noxa, Bmf) (see Fig. 4, upper frame). Their role is to lower the threshold for apoptosis by simultaneously occupying anti-apoptotic members and releasing activators in favor of Bax and Bak oligomerization. Importantly, the interaction between anti-apoptotic proteins and the sensitizer BH3-only proteins displays a high degree of selectivity [58-61]. For instance, while the BH3 domain of Bad mainly targets Bcl-2, Bcl-Xl, Bcl-W, the BH3 domain of Noxa mostly targets Mcl-1 and not the other sensitizers. Such selectivity has been exploited in oncology research to develop BH3-domain mimetics which can disturb a specific subset of interactions between the anti-apoptotic and the BH3-only proteins. In this way it is possible to target only the anti-apoptotic proteins to which the particular cancer type is addicted for survival. A good example comes from the new generation of BH3-mimetic compounds like ABT-737 and ABT-199, derived from the BH3 domain of Bad and developed against hematological malignancies [63-66]. They selectively target the hydrophobic cleft of Bcl-2 and Bcl-Xl (ABT-737) or only Bcl-2 (ABT-199), and thereby displace the BH3-only proteins, therefore deputizing the sensitizers activity.

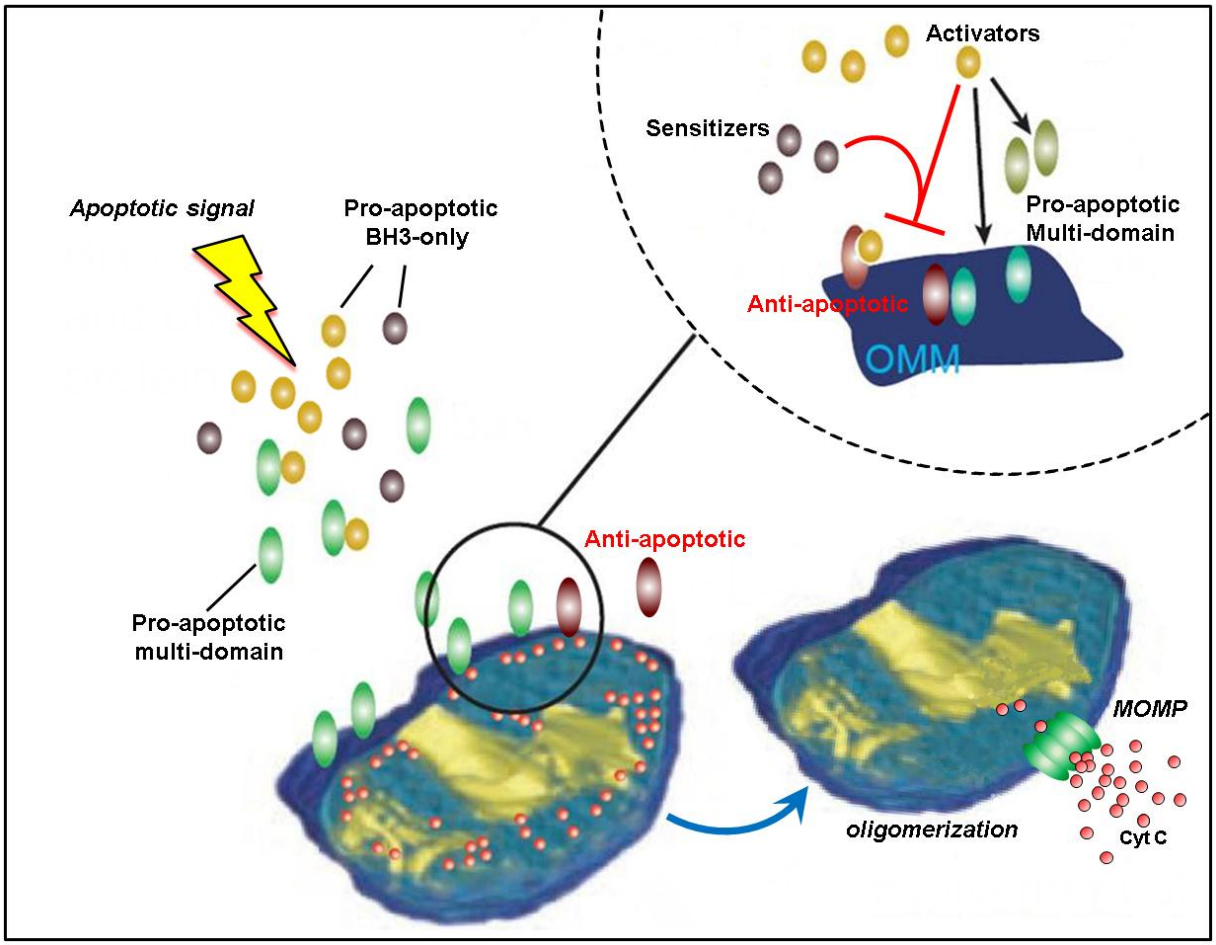

Fig. 4: Overview of the Bcl-2 proteins in action for regulating MOMP. Apoptotic stimuli engage the activity of a subgroup of the pro-apoptotic Bcl-2 proteins, the BH3-only members, which in turn stimulate pro-MOMP Bax and Bak oligomerization or alleviate the function of the anti-apoptotic members. Upper frame: some BH3-only proteins can perform both roles (activators) and others only the latter (sensitizers). Adapted from [62].

Hitherto the function of Bcl-2 proteins in apoptosis has been described with respect to their OMM interplay but a considerable portion of the Bcl-2 family resides elsewhere in the cell [67-69]. The other important site where Bcl-2 proteins act to decide cell fate is the ER. This multifunctional organelle is at some positions in close proximity to the mitochondria and, in tandem with them, plays a major role in regulating intracellular Ca^{2+} signaling, as discussed in detail in section 2.

2 Intracellular Ca^{2+} homeostasis and cell death

Apart from its well-known role as primary mineral component of the skeletal system, Ca^{2+} is an essential messenger molecule at the cellular level. Ca^{2+} signals set up and/or regulate a plethora of processes within (intracellular) and between (extracellular/intercellular) cells, such as DNA transcription, cell cycle regulation, differentiation, cell motility/migration, muscle contraction/relaxation, neurotransmission and also cell fate [70]. Interestingly, it is believed that intracellular Ca^{2+} signaling evolved from the initial tendency of primitive unicellular eukaryotes to exclude Ca^{2+} from their inner space. This behavior emerged as a way to avoid intrinsic cytotoxicity of Ca^{2+} in the cytosol [71]. However, further in evolution, intracellular Ca^{2+} homeostasis was exploited by the cell to assemble a versatile signaling network with very different spatial and temporal dynamics. The formation of the correct spatio-temporal Ca^{2+} signals is guaranteed by an extensive cellular machinery named the Ca^{2+} toolkit [72, 73]. It comprises various Ca^{2+}-binding (buffers, effectors) and Ca^{2+}-transporting (channels, pumps, exchangers) proteins, present mainly in the cytosol, plasma membrane, ER and mitochondria. Although this Ca^{2+}-homeostatic machinery should provide a normal cell function, yet the very same system can also provoke robust, prolonged and potentially deadly increases of the free cytosolic Ca^{2+} concentration ($[Ca^{2+}]_{cyt}$) in response to cell stress or injury. These toxic Ca^{2+} signals are due to excessive Ca^{2+} entry from the extracellular space, defective Ca^{2+} extrusion

from the cell, increased release from intracellular Ca^{2+} stores or combinations of the above [74]. In line with this, many apoptotic inducers are reported to exploit Ca^{2+}-dependent pathways to carry out their apoptotic action. These inducers encompass physiological as well as pharmacological factors and include hormones as corticosteroids, angiotensin II and testosterone, factors such as tumor necrosis factor, arachidonic acid, ceramide, NO and H_2O_2, and pharmacological agents such as staurosporine, thapsigargin and cisplatin [75, 76].

The work presented in this thesis concerns the role of the intracellular Ca^{2+} stores in apoptotic cell death, therefore after a better description of the Ca^{2+} toolkit we will mainly focus on the function of the ER as the principal intracellular Ca^{2+} store.

2.1 Intracellular Ca^{2+} signaling: the Ca^{2+} toolkit

In resting cells, the Ca^{2+} toolkit ensures that $[Ca^{2+}]_{cyt}$ is always maintained around 10.000-fold lower (with an approximate value of 100 nM) than the extracellular matrix, by extruding Ca^{2+}, chelating Ca^{2+} in the cytosol or sequestering Ca^{2+} in cellular stores [70]. The major components of this Ca^{2+} "OFF" mode are summarized below. First of all, the plasma-membrane Ca^{2+} ATPase (PMCA) actively pumps Ca^{2+} out of the cell [77]. On the same location, the Na^+/Ca^{2+} exchanger (NCX) plays a role in removing intracellular Ca^{2+} in exchange for Na^+, thereby driven by the Na^+ gradient over the plasma membrane. Intracellularly, the ER, or its counterpart in muscle cells, the sarcoplasmic reticulum (SR), is the organelle in charge of sequestering Ca^{2+} from the cytosolic space. Here, the Ca^{2+} pump sarco-endoplasmic reticulum Ca^{2+} ATPase (SERCA) guarantees, in concert with a set of Ca^{2+}-buffering proteins (calreticulin, calnexin, *etc.*), a net ER/SR luminal Ca^{2+} concentration ($[Ca^{2+}]_{ER}$) in the range of ~1 mM [70, 78]. Additionally, SERCAs and other pumps known as secretory-pathway Ca^{2+} ATPases (SPCA) are also involved in the Ca^{2+} loading of membrane-bound compartments like the Golgi complex and the secretory vesicles. $[Ca^{2+}]_{cyt}$ in the cytosol

is buffered by another set of Ca^{2+}-buffering proteins comprising calbindins, parvalbumins and calretinin, and it can be "sensed" by Ca^{2+}-sensor proteins such as calmodulin [79].

Upon cell activation, in response to membrane depolarization, stretch, noxious stimuli, extracellular agonists or depletion of intracellular Ca^{2+} stores, the $[Ca^{2+}]_{cyt}$ can rise transiently up to 1-10 μM. This "ON" mode is elicited through i) the Ca^{2+} influx in the cytoplasm from the virtually unlimited extracellular sources and ii) the Ca^{2+} release from the intracellular stores, mainly the ER and, to a lesser extent, the Golgi apparatus. On the plasma membrane, a large family of Ca^{2+}-entry channels mediates the Ca^{2+} influx. They are classified, by their activation mechanism, as voltage-operated channels (VOCs), store-operated channels (SOCs) or receptor-operated channels (ROCs). VOCs are activated by membrane depolarization, SOCs sense the emptying of the ER Ca^{2+} store in order to induce the store-operated Ca^{2+} entry (SOCE) while ROCs respond to binding of external stimuli *e.g.* ATP, glutamate or other transmitters [80, 81]. Notably, the prototypical SOC channel is represented by the Ca^{2+} release-activated channels (CRACs). The ER-Ca^{2+} depletion is sensed by the stromal interaction molecules (STIM) 1 and 2, which bind and activate the pore-forming subunit of the CRAC channel, better known as ORAI, leading to the slow replenishment of the ER with Ca^{2+} [82].

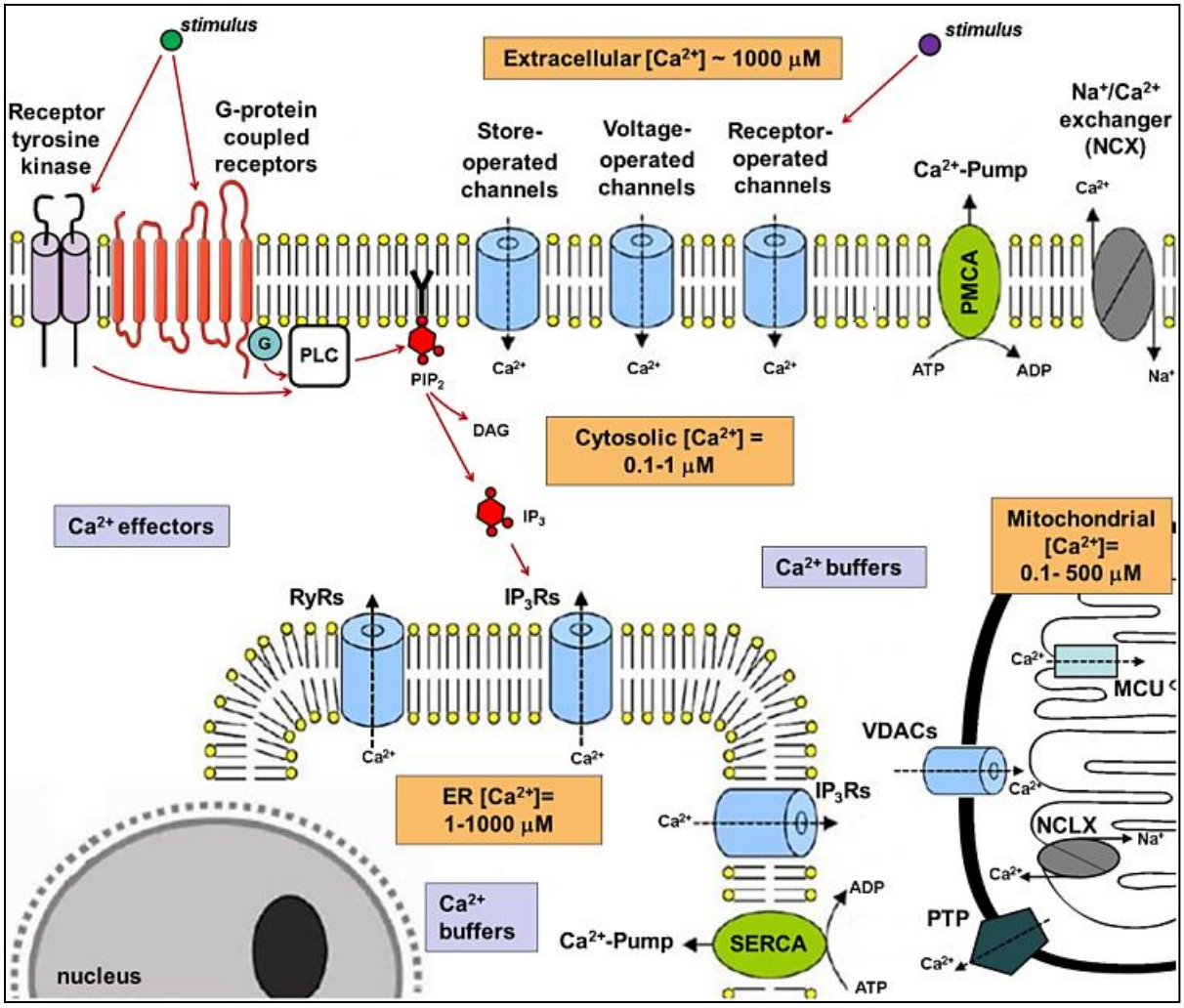

Fig. 5: Major components of the Ca^{2+}-signaling toolkit. In the "ON" mode, Ca^{2+} channels (depicted in blue) increase $[Ca^{2+}]_{cyt}$ by two mechanisms: 1) entry of external Ca^{2+} *via* plasma-membrane channels; 2) release of Ca^{2+} from internal stores *via* Ca^{2+} release channels, such as IP_3Rs. The IP_3R activation proceeds *via* a signaling cascade involving G-coupled or tyrosine-kinase receptors, phospholipase C (PLC) and IP_3 diffusion. Return to resting conditions, "OFF mode", is ensured by pumps (depicted in green) and the Na^+/Ca^{2+}exchanger. Ca^{2+} is taken up by internal stores or extruded out of the cell. Mitochondria play a special role in the ER-mitochondria Ca^{2+} cross-talk (see text). Adapted from [83].

On the other hand, the release of Ca^{2+} from intracellular stores is mediated by a group of Ca^{2+} channels primarily located on ER membranes. The opening of these channels is driven by diffusible messengers, among which inositol 1,4,5-trisphosphate (IP_3) and Ca^{2+} itself are the most relevant (as will be discussed in more detail in the next section). Successively, the induced Ca^{2+} transients are decoded by Ca^{2+}-binding proteins, which act as cytosolic Ca^{2+} sensors (*e.g.* calmodulin) [78]. The latter activate downstream effectors towards the execution of a specific Ca^{2+}-dependent process or alternatively can function themselves as Ca^{2+} effectors. Once the downstream targets have been activated, cytosolic Ca^{2+} signaling goes "OFF" again by means of the Ca^{2+}-pump mechanisms defined above, in order to rapidly restore the resting conditions. A special role is played, in both ON and OFF mechanisms, by mitochondria due to their close proximity to the ER [84]. They preferentially take up Ca^{2+} released from the ER through the concerted action of the voltage-dependent anion channels (VDACs), mainly the VDAC-1 isoform [85], and the recently identified mitochondrial Ca^{2+} uniporter (MCU) [86]. Once the $[Ca^{2+}]_{cyt}$ has returned to resting levels, the mitochondrial Na^+/Ca^{2+} exchanger (NCLX) and the permeability-transition-pore (PTP) [87] complex take care of slowly releasing the Ca^{2+} back to the cytosol and further to the ER store.

2.2 *Ca^{2+} release from ER*

The ER is known as the protein-processing factory of the cell, whereby all the different polypeptides are assisted for proper folding in order to exert their cellular function. On the other hand, the ER is also involved in other essential cellular activities such as the synthesis of lipids or, as highlighted above, the regulation of Ca^{2+} signaling [88]. While SERCAs ensures the filling state, the release of Ca^{2+} from the ER and SR membranes is commonly mediated by intracellular Ca^{2+}-release channels such as the inositol IP_3 receptors (IP_3Rs) and their close relatives, the ryanodine receptors (RyRs). IP_3Rs are channels ubiquitously expressed in most

cell types whereas RyRs are mainly present in excitable cell types, like muscle cells or neurons, and in a limited set of non-excitable cells. Both classes of channels share significant structural and functional similarities [89, 90]. However, only IP_3R-channel opening is triggered by the second messenger IP_3 with a consequent increase in $[Ca^{2+}]_{cyt}$. The main route towards IP_3 production initiates at the cellular surface whereon several agonists (*e.g.* hormones, growth factors *etc.*) bind and activate G protein-coupled receptors or tyrosine kinase-coupled receptors (see Fig. 5). In turn, these receptors can stimulate different isoforms of phospholipase C (PLC), accountable for the enzymatic hydrolysis of the membrane phospholipid phosphatidylinositol bis-phosphate (PIP_2) in IP_3 and diacylglycerol (DAG). The lipophilic DAG remains associated to the membrane environment while IP_3, being a water-soluble molecule, diffuses away from its production site and eventually interacts with its receptor, the IP_3R, on the ER surface. Additionally, the channel opening of both IP_3Rs and RyRs is under control of the local $[Ca^{2+}]_{cyt}$. Ca^{2+} modulation is biphasic with high $[Ca^{2+}]$ resulting in channel closure and a low $[Ca^{2+}]$ in channel opening. The latter mechanism, known as Ca^{2+}-induced Ca^{2+} release (CICR) [73], allows the cellular propagation of an initially localized Ca^{2+} signal by activating neighboring Ca^{2+}-channels. Thus, CICR chiefly contributes to the high degree of spatial and temporal diversity of the Ca^{2+} signals, besides the role of the other Ca^{2+}-toolkit players. In this scenario, the firing of different Ca^{2+} channels will vary in space and time depending on the sensitivity to the Ca^{2+}-mobilizing agents, on accessory modulatory mechanisms (*e.g.* phosphorylation) and, consequently to CICR, on the level of channel clustering. In response to weak stimuli, a small amount of IP_3 is produced and triggers individual channels to open and release Ca^{2+} "blips" or "quarks" [91, 92]. Stronger stimuli, in contrast, are able to activate a series of channels within a cluster and produce Ca^{2+} "puffs". More global Ca^{2+} signals are generated when neighboring clusters, along the ER membrane, are excited by a CICR "wave". The neighboring mitochondria can

sustain the ER Ca^{2+} release by buffering the $[Ca^{2+}]_c$ at the mouth of the channels and therefore reducing the negative feedback by local Ca^{2+} [84]. Finally, the emptying of the ER-Ca^{2+} store and lowering of the luminal Ca^{2+} concentration, negatively regulates IP_3Rs and RyRs, thus closing them and preventing the accumulation of cytotoxic $[Ca^{2+}]_{cyt}$ [93].

2.3 ER Ca^{2+} release and cell fate: the implications of the ER-mitochondria cross-talk

Ca^{2+} discharged from the ER is implicated in a multitude of events that participate in cell-death progression or prevention. Cytosolic Ca^{2+} transients activate multiple enzymes (NO synthases, calcineurin, transglutaminase, calpain, kinases, phospholipases or endonucleases) involved in controlling the breakdown of various cellular constituents [94] or in tuning the activity of the apoptotic machinery (see Fig. 6). For instance, calpain's proteolytic activity can: 1) unleash the pro-apoptotic potential of AIF, Bid, Bax and caspase-12; 2) abolish the pro-survival effect of XIAP (X-linked inhibitor of apoptosis protein) on caspases [94-96] or 3) contribute to apoptosis induction by inhibiting autophagy *via* the cleavage of the autophagy protein 5 (ATG5), which is required for the autophagosome formation [97]. Interestingly, a slight increase of $[Ca^{2+}]_{cyt}$ could also activate the Ca^{2+}/calmodulin-dependent protein kinases (CaMKs) whose signaling converges into the regulation of some other kinases controlling cell fate. More precisely, there is clear evidence that CaMKII can phosphorylate the apoptotic signaling kinase 1 (ASK1), which finally leads to the activation of the multifunctional c-Jun N-terminal Kinase (JNK) [98]. The sustained activation of JNK is associated with apoptosis, whereas the acute and transient activation of JNK is involved in cell proliferative or survival pathways [99]. Simultaneously, downstream of the same CaMK-signaling cascade, the Ca^{2+}/calmodulin-dependent protein kinase kinase (CaMKK) can induce the protein kinase B (PKB/Akt), which in turn promotes the phosphorylation of Bad and its pro-survival sequestration by the 14–3–3 adaptor protein [100]. In the latter scenario, the Ca^{2+}-dependent

phosphatase known as calcineurin can play the opposite role by dephosphorylating Bad and guiding its pro-MOMP translocation into the mitochondria. Remarkably, the same phosphatase is able to dephosphorylate the Ca^{2+}-sensitive transcription factor NFATc (nuclear factor of activated T cells) and favor its pro-survival activity at the nucleus [101].

The ambivalence of Ca^{2+} signaling in cell-fate decisions assumes an even greater significance in relation to the ER-mitochondria close proximity. This local coupling was originally described in the functional context of lipid biosynthesis and lipid/protein trafficking [102, 103]. Later it became clear that the close connection of mitochondria to the ER, the largest intracellular Ca^{2+} store, was also ideally suited for mediating the cross-talk of Ca^{2+} among these two organelles [104]. As mentioned in section 2.1, mitochondria express different Ca^{2+}-transport systems, which implies the crossing of two membranes, namely first the OMM and subsequently the inner mitochondrial membrane (IMM). In contrast with other organelles, mitochondrial Ca^{2+} uptake is not driven by pumps but by the large electrochemical gradient ($\Delta\Psi m = -180$ mV) between the inside and outside of energized mitochondria [84]. Since such Ca^{2+}-uptake system showed low-affinity properties, the shuttling of Ca^{2+} between the ER and the mitochondria was partially overlooked and initially considered as a mere buffering event to control the amount of available Ca^{2+}. However, Ca^{2+} released from the ER creates local microdomains at the ER-mitochondria interface with relatively high concentrations of the ion. Comparative experiments indeed estimated that the Ca^{2+} concentration reaches at least 16 μM [105] in these inter-organellar "hotspots". Besides, IP_3Rs and VDAC-1, by facing each other at the ER-mitochondria interface [85], build up a fast-track pathway for the efficient transfer of Ca^{2+}. Consistently, the vast set of other proteins which crowd the ER-mitochondria interface (*e.g.* promyelocytic leukemia (PML) protein, the chaperone glucose-regulated protein 75 (Grp75), mitofusins (MFNs), the PKB/Akt, sigma-1 receptor, Bcl-2-family members *etc.*) may speed up or slow down the preferential Ca^{2+} trafficking [106, 107]. Such

inter-organellar Ca^{2+} shuttling is directly or indirectly determining cell fate by affecting the mitochondrial pro-death or pro-survival mechanisms. A very important factor hereby is the magnitude of the Ca^{2+} signal received by the mitochondria. Both the steady-state Ca^{2+}-filling level of the ER [34] as well as the IP_3R activity [108] govern the amount of transferred Ca^{2+}. On the pro-survival side, it was shown that the constitutive or agonist-triggered transfer of low amount of Ca^{2+} from the ER to the mitochondria is essential for the production of ATP through oxidative phosphorylation [109]. ATP production is here required to sustain the proper energy supply of the cell, and also to specifically regulate the activity of ATP-sensitive proteins located nearby (*e.g.* the ATPase SERCA and the IP_3Rs) as a feedback control system on cytosolic Ca^{2+} signaling. Additionally, other mitochondrial processes as fatty-acid oxidation, amino-acid catabolism and the regulation of some mitochondrial proteins (enzymes or carriers) are also dependent on the mitochondrial Ca^{2+} concentration ($[Ca^{2+}]_m$) [110-112]. If this basal Ca^{2+} transfer is too low, the increase in catabolic AMP over ATP will activate autophagy as an adaptive pro-survival mechanism [113]. On the pro-death side, either too low or too high Ca^{2+} cross-talk is implicated in the initiation and propagation of cellular processes such as autophagic, apoptotic and necrotic cell death. Possibly, the choice among these three mechanisms depends on the intensity of injury and on the status of the cell - *e.g.* the resting concentration of ATP and the mitochondrial status very much influence the mode of cellular death [74]. For instance, during small insults, autophagy may lose its pro-survival role when mitochondria that are still intact but latently dysfunctional or deprived of Ca^{2+} [114, 115], consume the barely sufficient cytosolic ATP to sustain their membrane potential. The ensuing bioenergetic crisis causes cell death referable to as autophagic cell death because it occurs together with the accumulation of the typical double-membrane autophagic vacuoles [7].

On the other hand, mitochondrial Ca^{2+} overloading has been proven to compromise the integrity of mitochondria, inducing MOMP and eventually apoptotic or necrotic cell death.

The road to apoptosis requires a residual ATP production but if the insult towards the mitochondria is too severe and the Ca^{2+}-dependent energy production too strongly impeded, cell death by necrosis will ensue instead [74, 106, 116].

As discussed above, the ER protagonists in the preferential Ca^{2+} communication between the ER and the mitochondria are the IP_3Rs. Therefore, in the following section, a proper presentation of this Ca^{2+}-channel family is provided.

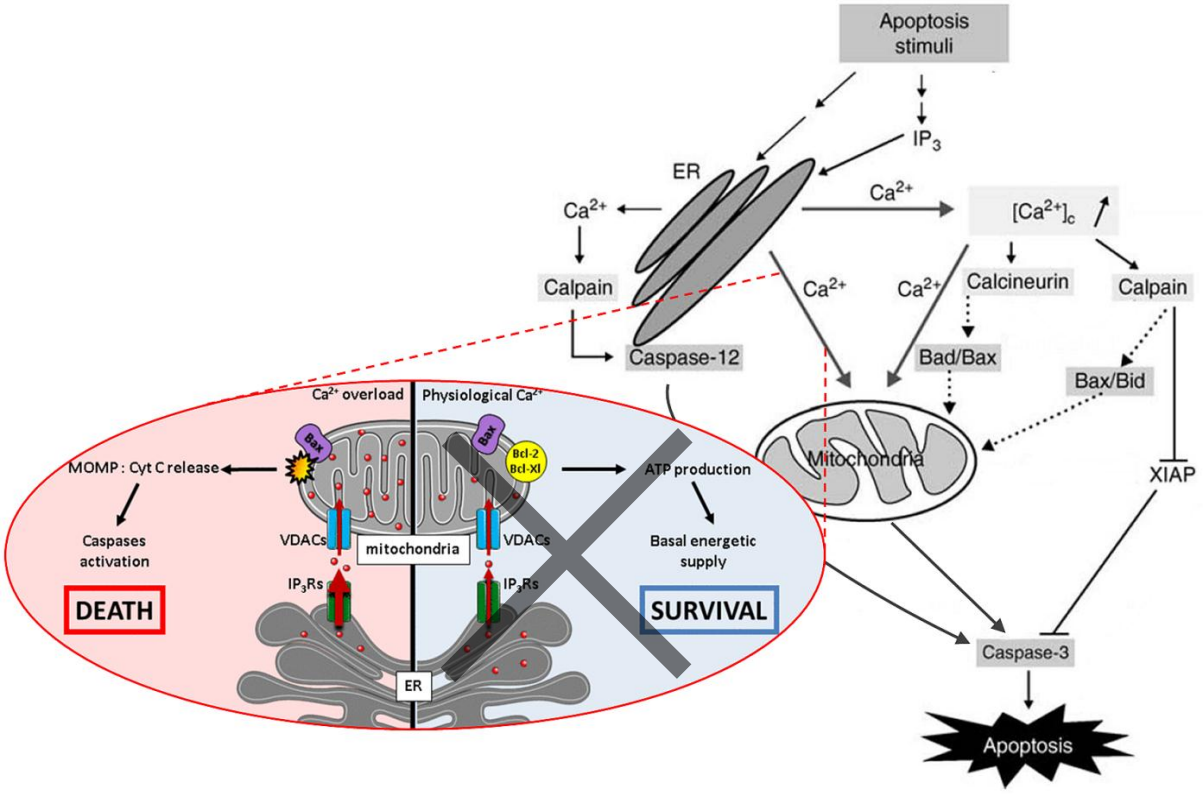

Fig. 6: Possible mechanisms of Ca^{2+} signaling in apoptosis with a focus on the ER-mitochondria cross-talk. In response to apoptotic stimuli, the excessive Ca^{2+} released from ER can bind to Ca^{2+}-dependent enzymes, such as calpain and calcineurin, and activate their downstream targets including some Bcl-2-family proteins. Alternatively, the released Ca^{2+} may be directly taken up by the closely juxtaposed mitochondria (see frame for ER-mitochondria Ca^{2+} cross-talk) and instead of favoring bioenergetics (crossed side) would lead to MOMP and cell death. Adapted from [95].

2.4 IP_3R structure and regulation

The IP_3R forms a multimeric structure consisting of 4 subunits of about 310 kDa (approximately 2700 a.a.) [117]. Each IP_3R subunit comprises an N-terminal ligand-binding domain (LBD) exposing the IP_3-binding site, a central regulatory/coupling domain, the Ca^{2+}-channel region, with 6 TMDs, and a short cytoplasmic C-terminal tail or gating domain (Fig. 7). In *Mammalia*, three genes encode for IP_3Rs (IP_3R1, IP_3R2 and IP_3R3) and the diversity is further increased by splicing events together with the possibility of homo- and heteromeric channels. IP_3 is the physiological activator of all IP_3R isoforms, though the rank order of the affinity for IP_3 is $IP_3R2 > IP_3R1 > IP_3R3$ [108]. IP_3R1 shares around 60% of identity with the other 2 isoforms [118, 119] and shows the highest expression levels and tissue distribution. However, most cell types express a combination of these three IP_3R isoforms with very distinct subcellular localizations and expression patterns [90]. This allows them to set up specific intracellular Ca^{2+} signals in response to many specific cellular requirements. As mentioned in the previous section, IP_3 teams up with Ca^{2+} as a co-agonist to regulate the IP_3R. IP_3-induced Ca^{2+} release (IICR) is indeed stimulated or inhibited by, respectively, low (< 300 nM) or high concentrations of Ca^{2+} near the pore [120-122]. The way in which Ca^{2+} biphasically regulates the IP_3Rs is still not clarified, but it has been proposed to involve at least an inhibitory and a stimulatory Ca^{2+}-binding site located in the LBD. In the resting state, the N-terminal portion of the LBD (a.a. 1-225 in IP_3R1) functions as a "suppressor domain", preventing the binding of IP_3 to its binding core located more distally in the LBD (a.a. 226-576 in IP_3R1). Under these conditions, the pore region may become sealed by the reciprocal interaction between the N- and C-terminal regions of the receptor. Upon IP_3 binding to the IP_3-binding core, a conformational change is induced in order to sensitize a Ca^{2+}-binding site. The subsequent binding of Ca^{2+} leads to a further conformational change that removes the N-terminal/C-terminal interaction and opens the gate [90, 123].

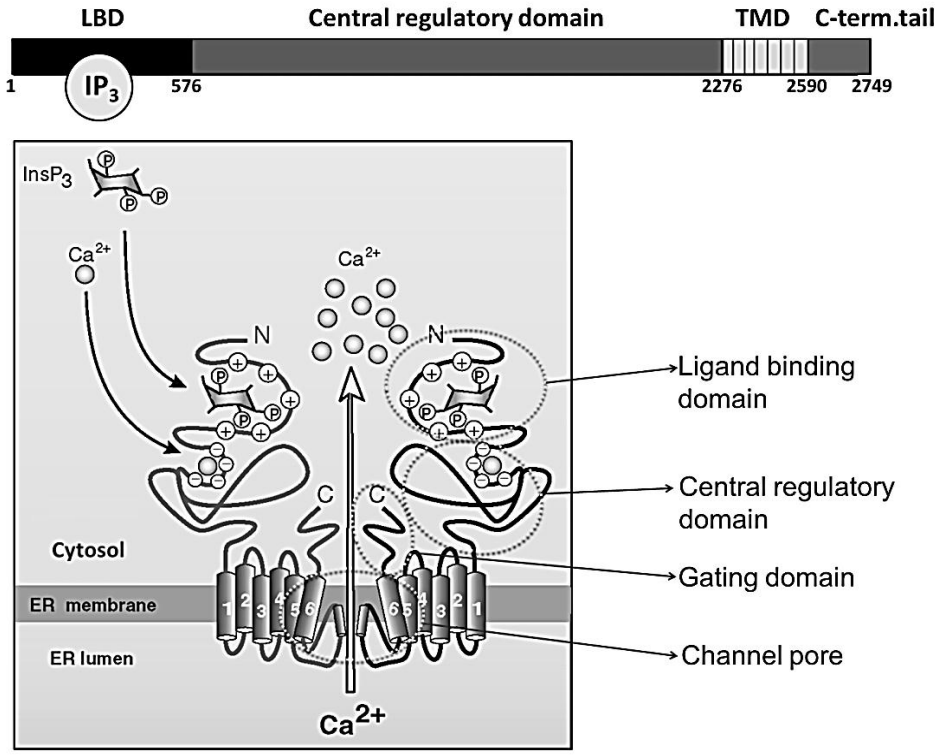

Fig. 7: Schematic representation of the IP_3R structure. The upper part of the figure depicts the primary sequence of IP_3R1 with the different functional domains (ligand-binding domain [LBD] with IP_3 bound to it, central regulatory domain, transmembrane domain [TMD] and C-terminal tail [gating domain]). In the lower part, two of the channel subunits that make up the tetramer are shown and each functional domain is highlighted with a dotted circle. The channel is shown with the gate region opened in response to IP_3 and Ca^{2+} binding. Adapted from [123].

Recent data indicate that the central regulatory domain together with the "suppressor domain" are, during the activated state, in charge of relaying the IP_3- and Ca^{2+}-stimulatory signals down to the transmembrane region of the channel [90, 124]. Further modulation is performed by ATP, which modifies the sensitivity of the channel to Ca^{2+}, and by a list of more than 50 different regulatory proteins or compounds with either stimulatory or inhibitory effects (see reviews [125-127]). Such a list notably includes protein kinases and phosphatases, responsible for the IP_3R-phosphorylation status [128], as well as proteins involved in apoptosis. Hereinafter the regulation of ER Ca^{2+} fluxes by pro- and anti-apoptotic proteins will be discussed with a special attention to IP_3Rs.

3 Apoptosis-regulatory proteins control ER-mitochondria Ca^{2+} cross-talk

Not as widely recognized, but also of considerable importance, is the cell-fate determining role of the apoptosis-regulatory proteins in the ER-mitochondria Ca^{2+} axis described above. In this paradigm, proteins such as the Bcl-2-family members act at the ER-mitochondria interface, to prevent or promote apoptosis well upstream of the MOMP step. At the ER surface, effects were described on the SERCA pumps, responsible for loading the ER Ca^{2+} stores, on ER Ca^{2+} buffers such as calreticulin, on the Ca^{2+} content of the ER, and on the main Ca^{2+}-release channels, the IP_3Rs [129-132]. At the mitochondria, anti-apoptotic Bcl-2 proteins showed the ability to regulate VDAC-1-channel activity or oligomerization state [133, 134]. Complementarily, post-MOMP proteins have also been reported to act at the ER-mitochondria Ca^{2+} loop (see section 3.2 for details).

3.1 Regulation upstream of MOMP

3.1.1 Pro- and anti-apoptotic Bcl-2 proteins exert opposing effects on ER-Ca^{2+} handling

Bcl-2, the anti-apoptotic progenitor of the Bcl-2 family, was firstly reported to affect ER Ca^{2+} fluxes back at the beginning of the 90s [135, 136]. Since then, it has become increasingly clear that the ER, the main intracellular Ca^{2+} store, is tightly controlled by Bcl-2-family members. Shortly after, a groundbreaking study [137, 138] succeeded in partly elucidating the mechanism of action of the anti-apoptotic Bcl-2 proteins at the ER. It was indeed found that Bcl-2 overexpression at the ER enhanced the ER Ca^{2+}-leak rate and thus reduced the basal $[Ca^{2+}]_{ER}$. As a result, the IP_3R-mediated Ca^{2+} signals originating from the ER were dampened in concert with the Ca^{2+} signaling to the mitochondria. In line with these observations, Palmer and colleagues, by using an improved genetically-encoded Ca^{2+} sensor, showed Bcl-2's ability to decrease the $[Ca^{2+}]_{ER}$ as well as to alter the IICR [139]. It was originally

hypothesized that this ER-empting effect of Bcl-2 was due to its potential pore-forming ability in the ER membrane (similarly to Bax on OMM) [140, 141] in view of the resemblance of Bcl-2 and Bcl-Xl structures to bacterial toxins. However, a subsequent study would exclude this possibility [142] and suggested instead a modulation of the ER Ca^{2+}-loading/release machinery. The anti-apoptotic Bcl-2-family members were proposed to molecularly interact with SERCAs [143-145]. Hence, Bcl-2 was found to inactivate SERCA2b and SERCA1, respectively the house-keeping and the skeletal muscle type Ca^{2+}-pump isoforms, thereby lowering the content of SR/ER Ca^{2+} stores [146, 147]. Additionally, another study showed a decline in SERCA2b- and calreticulin-protein levels following Bcl-2 overexpression [129]. However, Bcl-2 did not show a consistent reduction of SERCA-protein levels or activity in other experimental circumstances [136, 143, 148-150]. Another possible explanation for the decrease in ER-Ca^{2+} content could then be a regulation of IP_3Rs by Bcl-2-family members. Several groups have addressed this possibility and reported an indirect or direct effect of Bcl-2 on IP_3Rs. In the former case, the first strong evidences supported the argument that, in the absence of Bax and Bak, unopposed Bcl-2 leads to IP_3R1 hyperphosphorylation, which in turn increases the firing of IP_3R1 and the slow ER Ca^{2+} discharge [151, 152]. Nonetheless, further studies have challenged this general claim. Apparently, in different cell types or experimental conditions, the ER Ca^{2+} content was not affected by the presence of Bcl-2 [153], suggesting that this effect may strictly depend on the activity of a specific IP_3R isoform or on post-translational modifications of both IP_3Rs and Bcl-2 itself. A proof of concept comes from the phosphorylation of Bcl-2 by JNK which impacts on its effects on both, ER Ca^{2+} homeostasis and anti-apoptotic function [149]. Whether Bcl-2 phosphorylation modulates its binding to the IP_3R and/or regulates IICR is however presently not known. In line with the clues just mentioned, Bcl-2 was also reported to suppress IP_3R activity by recruiting calcineurin/protein phosphatase 2b (PP2B) [154, 155] or the protein phosphatase (PP1) [156] on IP_3Rs. An

additional indirect effect of the Bcl-2-family members on IP_3Rs implicates the control of the protein-expression levels. For instance, Bcl-Xl overexpression has been shown to reduce the level of IP_3Rs in cells *via* a decreased binding of the transcription factor nuclear factor of activated T cells, cytoplasmic 2 (NFATc2) to the IP_3R promoter [150]. Finally, most of the claims regarding the effects of pro-apoptotic Bcl-2 proteins were extrapolated from the findings concerning the role of the ER-store loading [151, 152]. Thereby, it has been proposed that in contrast to anti-apoptotic Bcl-2 proteins, Bax and Bak elevate $[Ca^{2+}]_{ER}$, trigger ER Ca^{2+} release and mitochondrial uptake. This hypothesis was partially supported by the demonstrated ability of Bax and Bak to localize and oligomerize at ER membranes [157, 158]. A role in the mechanism of Bax/Bak-dependent ER Ca^{2+} release has also been reported for several BH3-only proteins, including Bik and PUMA [159-161].

More recent work indicated that anti-apoptotic Bcl-2 proteins do not primarily act by altering the ER Ca^{2+}-store content. Instead, they directly target IP_3Rs and may function as endogenous regulators of IP_3Rs [148, 162, 163], but the precise mechanisms involved are still debated.

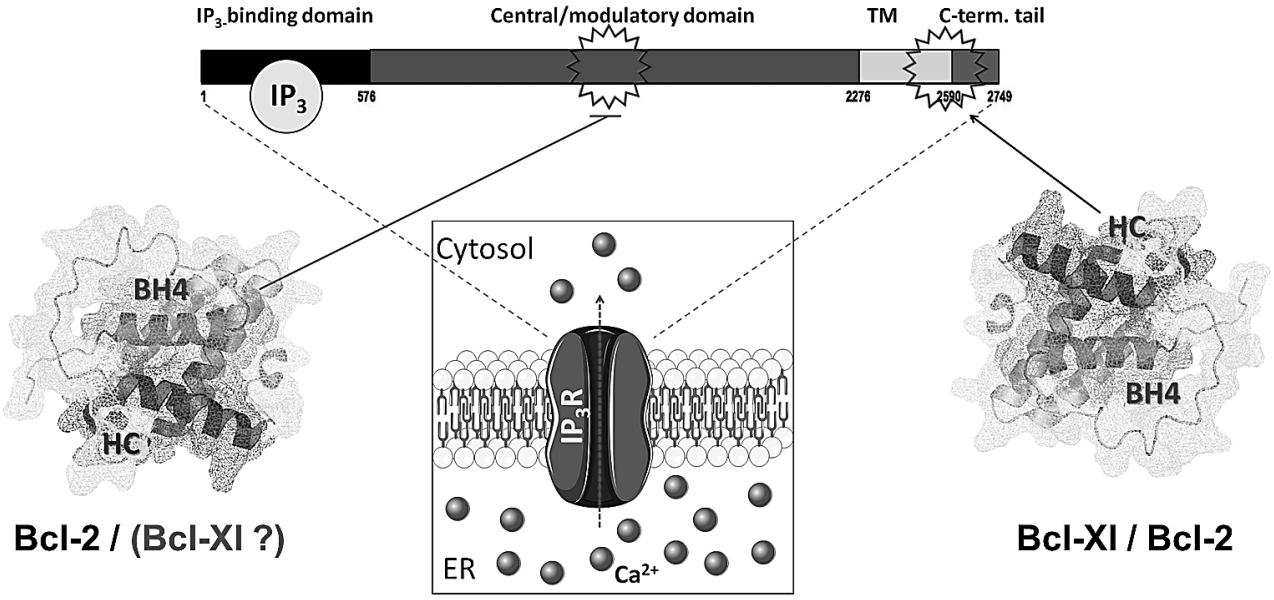

Fig. 8: Main interactions reported for Bcl-2 and Bcl-Xl with the IP_3Rs channels. First Bcl-Xl and then Bcl-2 have been proven to interact with the C-terminal domain of the IP_3Rs (close to the channel pore) possibly through their hydrophobic clefts (HC) or another domain than the BH4 domain. In this paradigm, both proteins increase the IP_3R's sensitivity to basal IP_3 levels and promote pro-survival Ca^{2+} oscillations (left). Perhaps most importantly, Bcl-2 through its BH4 domain has been shown to target the central, modulatory domain of the IP_3R, thereby reducing large global pro-apoptotic Ca^{2+} transients (left). The role of Bcl-Xl-BH4 domain on the IP_3Rs is unknown. Taken from [164].

3.1.2 Anti-apoptotic Bcl-2 proteins directly target IP_3Rs: Bcl-2 versus Bcl-Xl

The direct interaction of anti-apoptotic Bcl-2 proteins, like Bcl-2 and Bcl-Xl, with the IP_3Rs (see Fig. 8) regulates the channel properties in two convergent pro-survival ways: a) by reducing the sustained IP_3R-mediated Ca^{2+} release and thereby preventing mitochondrial Ca^{2+} overload, or b) by stimulating basal IP_3R-mediated Ca^{2+} oscillations in favor of a proper mitochondrial respiration (see also Fig. 9). This paradigm is nicely exemplified by the dual effect of Bcl-2 in mouse thymocytes, an immature T-cell model. On the one hand, Bcl-2 suppresses pro-apoptotic IP_3R-mediated Ca^{2+} transients (provoked by strong T cell-receptor stimulation) but on the other hand it has a role in maintaining pro-survival Ca^{2+} oscillations (provoked by weak T cell-receptor stimulation) [76, 165]. In line with the latter activity, Bcl-Xl interacting with the IP_3Rs promoted the sensitization of the IP_3R channel to low levels of

agonist stimulation [163, 166]. IP_3R/Bcl-Xl-complex formation in these conditions increased the frequency of Ca^{2+} oscillations, mitochondrial bioenergetics, and NFAT-mediated signaling in Bcl-Xl-overexpressing chicken B lymphocytes, while not affecting global agonist-induced Ca^{2+} transients. It was thereby very elegantly shown that Bcl-Xl protection against high [anti-IgM]-induced apoptosis was reduced in the absence of IP_3Rs [166]. The same study also suggested that the effect of Bcl-Xl on Ca^{2+} signaling depended on the type of IP_3R isoform. Bcl-Xl stimulated IP_3R-mediated Ca^{2+} oscillations for all three isoforms while it lowered $[Ca^{2+}]_{ER}$ in IP_3R3-, but not in IP_3R1- or IP_3R2-expressing cells. The effects of Bcl-Xl seemed to rely on its binding to the C-terminal region of the IP_3R, close to the Ca^{2+} channel pore (Fig. 8). As mentioned in 2.4, this C-terminal tail is also involved in the control of IP_3R-channel gating through interaction with other regulatory domains of the protein [167]. Thus, Bcl-Xl may thereby enhance the coupling between the N-terminal IP_3-binding domain and the C-terminal channel-pore opening, underlying the observed IP_3R sensitization. The C-terminal part of the IP_3R has been proposed to display structural features that mimic the BH3 domain of BH3-only proteins [168]. In this respect, one assumes that the hydrophobic cleft formed by BH3, BH1, and BH2 of all anti-apoptotic Bcl-2-family members may participate in the binding to the IP_3R. Finally, it has been recently described that not only Bcl-Xl but also Bcl-2 and Mcl-1 target this C-terminal site on IP_3Rs and cause IP_3R sensitization [169] perhaps favoring in this way mitochondrial metabolism and therefore survival (see also section 2.3). In contrast, Distelhorst and coworkers proposed that Bcl-2 reduces the excessive IP_3R-mediated Ca^{2+} release by binding to another site of the protein [162, 170]. This additional Bcl-2-binding site resides between amino acids 1389–1408 of IP_3R1. Bcl-2 binding to this region in the central, modulatory domain of the IP_3R caused an inhibition of the Ca^{2+}-flux properties of IP_3R in response to agonist stimulation (Fig. 8). Furthermore, a peptide corresponding to the Bcl-2-binding site on IP_3Rs (a.a. 1389–1408 of the mouse IP_3R1), called

IP_3R-derived peptide (IDP), completely abolished the binding of Bcl-2 to the IP_3Rs [130]. A cell-permeable version of IDP enhanced IP_3R-mediated Ca^{2+} signaling, thereby potentiating apoptotic signals, similarly to strong TCR stimulation. In this respect, IDP derepresses Bcl-2's inhibitory function on IP_3R1 by specifically targeting the BH4 domain of Bcl-2 and not its BH3 binding hydrophobic cleft. The BH4 domain of Bcl-2 is thus sufficient for binding and inhibiting the IP_3R, and for protecting against IP_3R1-mediated apoptosis [170]. Besides, the isolated Bcl-2-BH4 domain had already been previously proven to protect against apoptosis in many other experimental conditions [133, 171-173]. This indicates that the BH4 domain possesses an anti-apoptotic activity separated from or additive to the one mediated by the hydrophobic cleft of the anti-apoptotic-Bcl-2 proteins. In compliance, IDP targets Bcl-2 independently of the compounds that target the hydrophobic cleft, like the BH3-mimetic tools (*e.g.* ABT-737). Combining IDP with ABT-737 enhanced the potency of ABT-737 to induce cell death in lymphocytes obtained from chronic lymphocytic leukemia (CLL) patients [174]. Furthermore, applying a stabilized cell-permeable form of IDP (TAT-IDP^s) potently induced cell death through excessive IP_3R-mediated Ca^{2+}-release events in CLL cells, while TAT-IDP^s did not significantly reduce the survival of normal lymphocytes [175].

Collectively, these literature data suggests that Bcl-2 and Bcl-Xl may have separate and/or complementary pro-survival properties at the level of the IP_3R by targeting one or more of the protein regions with their hydrophobic cleft, their BH4 domain or the coordinate activity of the two.

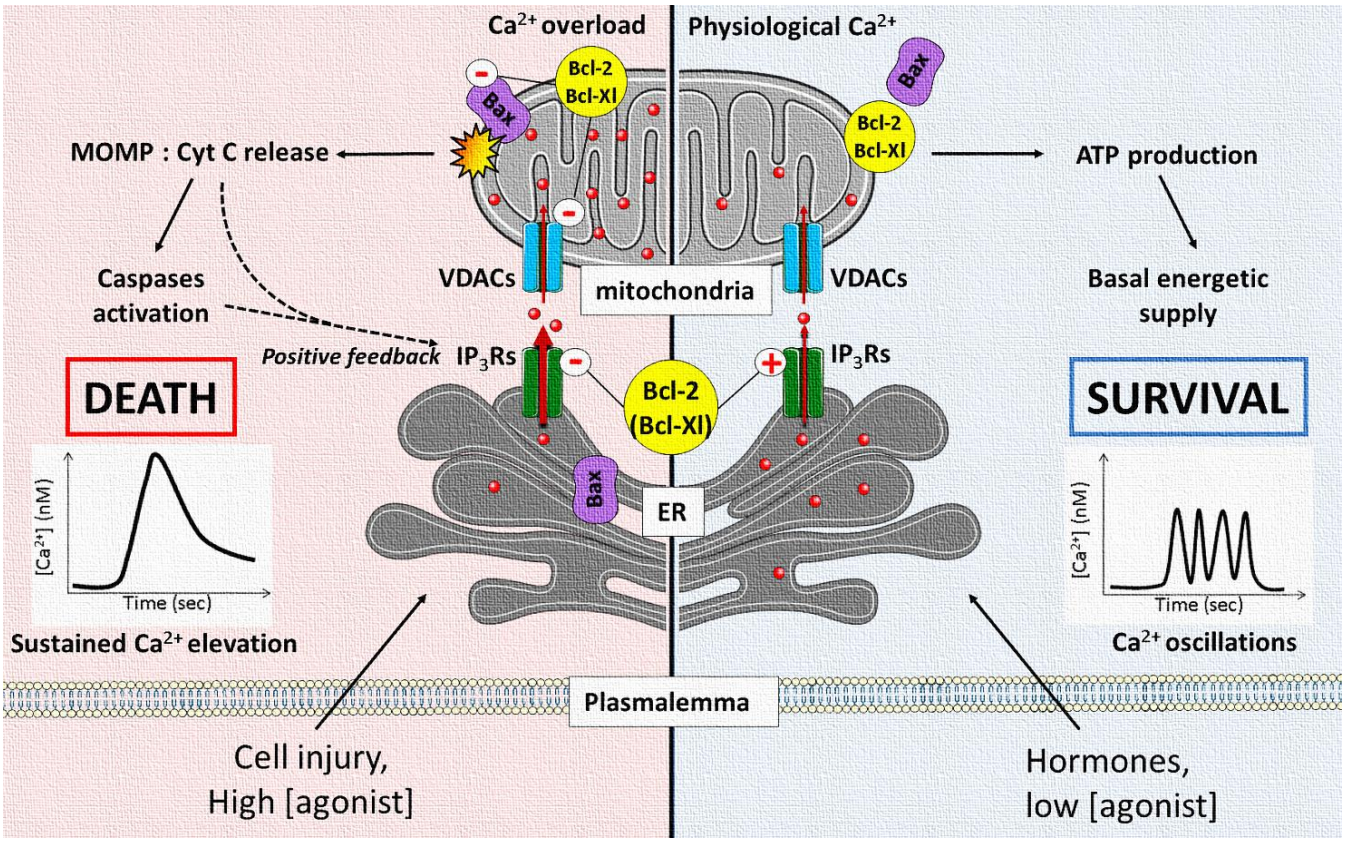

Fig. 9: Summary diagram representing the main roles of Bcl-2 and Bcl-Xl proteins in IP_3R-mediated apoptosis and survival. In healthy cells (right), a constitutive and oscillatory Ca^{2+} transfer from the ER to the mitochondria through channels like IP_3Rs and VDACs is necessary to meet the cellular energy requirements. In this scenario, the binding of Bcl-Xl/Bcl-2 to the IP_3Rs boosts the fueling of IP_3Rs into mitochondria and in turn favors ATP production *via* the IP_3R-dependent activity of the Krebs-cycle's enzymes. When a cell injury triggers an excessive IP_3Rs-transfer between the two organelles (left), mitochondria head to a lethal Ca^{2+}-overloading process which leads to Bax-promoted MOMP, release of the apoptogenic factors and caspases activation. Cyt c and caspase-3 act in a positive feedback loop to maintain ER Ca^{2+} release through the IP_3Rs. Here, Bcl-Xl and/or Bcl-2 may exert their protective role by: 1) heteromerizing with Bax and inhibit its pore forming activity, 2) acting on VDACs to decrease mitochondrial Ca^{2+}-uptake, 3) binding to the IP_3Rs and blocking the sustained IP_3R-cross-talk between ER and mitochondria. In the latter case, only the inhibitory binding of IP_3Rs by Bcl-2 has been reported. Inspired by [76].

3.2 Regulation downstream of MOMP

During the execution phase of apoptosis, IP_3Rs are transferring Ca^{2+} to mitochondria, and this transfer is affected by means of two regulatory systems involving downstream components of the apoptotic cascade: the mitochondrially released factor Cyt c and the executioner protease caspase-3 (see section 1.2). At the ER, Cyt c has been shown to interact with IP_3R1 at its C-terminus (a.a. 2621-2636) and thereby reduce the Ca^{2+}-dependent inhibition of channel opening [176]. This is supposed to lead to an uninhibited increase in ER Ca^{2+} release and would further amplify the apoptotic Ca^{2+} transfer to the mitochondria. Importantly, a peptide encompassing this C-terminal portion of the IP_3R can displace the interaction and prevent the Cyt c-dependent hyperactivation of the IP_3R channel [177]. Concerning the second mechanism, IP_3Rs are potential targets of the activated caspase-3, an even more downstream apoptotic player [178, 179]. The proteolytic activity of caspase-3 acts on a single highly conserved and caspase-specific DEVD (Asp-Glu-Val-Asp) cleavage site located on the IP_3R1 isoform. The channel cleaved at a.a. 1892 results in a constitutively open C-terminal channel domain, which maintains intact in the ER membrane [180]. This channel-only domain still contains the C-terminal TDMs and gating domain but lacks the N-terminus and the regulatory domains needed to keep the channel closed in the absence of IP_3. The ectopic expression of this C-terminal part of IP_3R1 was sufficient to induce a persistent, IP_3–independent, ER Ca^{2+} leak and thereby promote apoptosis. Both schemes involving caspase-3 cleavage and Cyt c binding generate a lethal mechanism on the IP_3Rs (see Fig. 9). Ca^{2+} released by IP_3Rs is transferred to the mitochondria, which in turn leads to Cyt c release and subsequent caspase-3 activation, both of which will feed forward to IP_3Rs and lead to more and persistent Ca^{2+} release (see also [181]). Very recently, also calpains have been caught in the act of cleaving the IP_3R during cell death perhaps by being involved in the same feedback mechanism [182].

AIMS AND OBJECTIVES

AIMS AND OBJECTIVES

As was explained in the "General Introduction", one aspect of the role of Bcl-2 and Bcl-Xl as cell-death antagonists consists in regulating the intracellular Ca^{2+} dynamics *via* their action on the ER-resident IP_3Rs. However, until now, there is no consensus on how these anti-apoptotic Bcl-2-family members regulate IP_3Rs and intracellular Ca^{2+} homeostasis, thereby controlling cell fate. Moreover, the molecular determinants underlying this role have not yet been fully characterized. The recent prospect of multiple interaction sites on IP_3Rs (central modulatory domain and C-terminal domain) and the involvement of different domains on Bcl-2/Bcl-Xl (BH4 domain and possibly hydrophobic cleft), were a challenge for addressing this issue. Importantly, although Bcl-2 and Bcl-Xl share high structural and biochemical similarities, particularly with respect to their BH4 domains, there are many indications that these proteins may have differential functions and it is not clear whether they affect IP_3Rs in the same way. Finally, the structural and molecular requirements of the BH4 domain necessary for interacting with IP_3Rs and for regulating Ca^{2+} release, have not yet been identified.

Hence, in this study we applied a multifaceted approach to compare side-by-side the molecular and functional regulation of IP_3Rs by Bcl-2 versus Bcl-Xl, with the main focus on the role of the BH4 domains derived from these proteins.

This general aim can be subdivided in 4 objectives:

I. *Investigate the regulation of IP_3R-mediated Ca^{2+} release by the BH4 domains of Bcl-2 versus Bcl-Xl*

II. *Evaluate the protective role of BH4-Bcl-2/BH4-Bcl-Xl against Ca^{2+}-dependent apoptosis*

III. *Identify the structural determinants of the isolated BH4 domain required for binding and modulating the IP_3Rs*

IV. *Characterize the interactions of Bcl-2 and Bcl-Xl with their proposed IP_3R1-binding sites*

The results of this study will lead to a better understanding of the molecular conversation between the IP_3R and Bcl-2/Bcl-Xl potentially exploitable to treat diseases characterized by excessive Ca^{2+}-mediated cell death or proliferation.

The research papers describing the results associated with one or more of the objectives are presented in the following sections.

RESULTS

PART I

Addressing objectives I, II, and III

Selective regulation of IP_3-receptor-mediated Ca^{2+} signaling and apoptosis by the BH4 domain of Bcl-2 versus Bcl-Xl

Giovanni Monaco[1#], Elke Decrock[2#], Haidar Akl[1], Raf Ponsaerts[1], Tim Vervliet[1], Tomas Luyten[1], Marc De Maeyer[3], Ludwig Missiaen[1], Clark W. Distelhorst[4], Humbert De Smedt[1], Jan B. Parys[1], Luc Leybaert[2], Geert Bultynck[1]

[1] Laboratory of Molecular and Cellular Signaling, Department of Molecular Cell Biology, Campus Gasthuisberg O/N-1 bus 802, Herestraat 49, BE-3000 Leuven, Belgium

[2] Department of Basic Medical Sciences, Physiology Group, Faculty of Medicine and Health Sciences, Ghent University, BE-9000 Gent, Belgium

[3] Biomolecular Modelling, Biochemistry, Molecular and Structural Biology Section, Department of Chemistry, Celestijnenlaan 200G bus 2403, BE-3001 Heverlee, Belgium

[4] Departments of Medicine and Pharmacology, Comprehensive Cancer Center, Case Western Reserve University, Cleveland, OH 44106, USA

# These authors equally contributed to the work.

Cell Death Differ. 2012,19:295-309.

Open

Cell Death and Differentiation (2012) 19, 295–309

www.nature.com/cdd

Selective regulation of IP_3-receptor-mediated Ca^{2+} signaling and apoptosis by the BH4 domain of Bcl-2 *versus* Bcl-Xl

G Monaco[1,5], E Decrock[2,5], H Akl[1], R Ponsaerts[1], T Vervliet[1], T Luyten[1], M De Maeyer[3], L Missiaen[1], CW Distelhorst[4], H De Smedt[1], JB Parys[1], L Leybaert[2] and G Bultynck*[,1]

Antiapoptotic B-cell lymphoma 2 (Bcl-2) targets the inositol 1,4,5-trisphosphate receptor (IP_3R) via its BH4 domain, thereby suppressing IP_3R Ca^{2+}-flux properties and protecting against Ca^{2+}-dependent apoptosis. Here, we directly compared IP_3R inhibition by BH4-Bcl-2 and BH4-Bcl-Xl. In contrast to BH4-Bcl-2, BH4-Bcl-Xl neither bound the modulatory domain of IP_3R nor inhibited IP_3-induced Ca^{2+} release (IICR) in permeabilized and intact cells. We identified a critical residue in BH4-Bcl-2 (Lys17) not conserved in BH4-Bcl-Xl (Asp11). Changing Lys17 into Asp in BH4-Bcl-2 completely abolished its IP_3R-binding and -inhibitory properties, whereas changing Asp11 into Lys in BH4-Bcl-Xl induced IP_3R binding and inhibition. This difference in IP_3R regulation between BH4-Bcl-2 and BH4-Bcl-Xl controls their antiapoptotic action. Although both BH4-Bcl-2 and BH4-Bcl-Xl had antiapoptotic activity, BH4-Bcl-2 was more potent than BH4-Bcl-Xl. The effect of BH4-Bcl-2, but not of BH4-Bcl-Xl, depended on its binding to IP_3Rs. In agreement with the IP_3R-binding properties, the antiapoptotic activity of BH4-Bcl-2 and BH4-Bcl-Xl was modulated by the Lys/Asp substitutions. Changing Lys17 into Asp in full-length Bcl-2 significantly decreased its binding to the IP_3R, its ability to inhibit IICR and its protection against apoptotic stimuli. A single amino-acid difference between BH4-Bcl-2 and BH4-Bcl-Xl therefore underlies differential regulation of IP_3Rs and Ca^{2+}-driven apoptosis by these functional domains. Mutating this residue affects the function of Bcl-2 in Ca^{2+} signaling and apoptosis.
Cell Death and Differentiation (2012) **19,** 295–309; doi:10.1038/cdd.2011.97; published online 5 August 2011

Pro- and anti-apoptotic B-cell lymphoma 2 (Bcl-2) family members control cell survival by regulating programmed cell death and autophagy.[1] The founding member is Bcl-2, a 26-kDa protein localized in the mitochondrial and endoplasmic-reticulum (ER) membranes. Members of this protein family are characterized by the presence of Bcl-2 homology domains (BH domains).[2,3] Although multidomain proapoptotic proteins contain three BH domains (BH1, BH2 and BH3), the antiapoptotic proteins, like Bcl-2 and Bcl-Xl, are characterized by an additional BH domain (BH4).[1] The BH1, BH3 and BH2 domains of the antiapoptotic Bcl-2 family proteins form a hydrophobic pocket that binds the BH3 domain of proapoptotic proteins, thereby counteracting their proapoptotic activity.[4] Besides this hydrophobic cleft, the BH4 domain is also essential for the antiapoptotic activity of Bcl-2.[5,6]

Moreover, Ca^{2+} signaling from the ER to the mitochondria plays an important role in apoptosis initiation.[7] Several pro- and anti-apoptotic Bcl-2 proteins localize at the ER membrane, where they modulate Ca^{2+}-release events[8,9] (recently reviewed in Rong *et al.*[10] and Rizzuto *et al.*[11]). Bcl-2 proteins thereby influence mitochondrial function because of the close proximity of ER and mitochondrial membranes.[12–14] Ca^{2+} transfer via the ER–mitochondria connection plays a bimodal role in cell survival.[15,16] Small oscillatory Ca^{2+} signals promote survival by stimulating mitochondrial function and bioenergetics, whereas larger mitochondrial [Ca^{2+}] rises promote cell death by provoking mitochondrial outer

[1]Laboratory of Molecular and Cellular Signaling, Department of Molecular Cell Biology, Campus Gasthuisberg O/N-1 bus 802, Herestraat 49, BE-3000 Leuven, Belgium; [2]Department of Basic Medical Sciences, Physiology Group, Faculty of Medicine and Health Sciences, Ghent University, BE-9000 Gent, Belgium; [3]Biomolecular Modelling, Biochemistry, Molecular and Structural Biology Section, Department of Chemistry, Celestijnenlaan 200G bus 2403, BE-3001 Heverlee, Belgium and [4]Departments of Medicine and Pharmacology, Comprehensive Cancer Center, Case Western Reserve University, Cleveland, OH 44106, USA

*Corresponding author: G Bultynck, Laboratory of Molecular and Cellular Signaling, Department Molecular Cell Biology, Campus Gasthuisberg O/N-1 bus 802, Herestraat 49, BE-3000 Leuven, Belgium. Tel: +32 16 330215; Fax: +32 16 345991; E-mail: geert.bultynck@med.kuleuven.be

[5]These authors contributed equally to this work.

Keywords: apoptosis; antiapoptotic Bcl-2-family members; calcium signaling; endoplasmic reticulum; intracellular Ca^{2+}-release channels

Abbreviations: AI, apoptotic index; ATP, adenosine 5′-triphosphate; AUC, area under the curve; Bcl, B-cell lymphoma; BH domain, Bcl-2 homology domain; BSA, bovine serum albumin; Caspase, cysteine-dependent aspartate-specific protease; CED, cell death abnormal; c.p.m., counts per min; CytC, cytochrome *c*; DTR, Dextran Texas Red; EGTA, ethylene glycol tetraacetic acid; ER, endoplasmic reticulum; FACS, fluorescence-activated cell sorting; FITC, fluorescein isothiocyanate; GST, glutathione-*S*-transferase; HBSS, Hanks' balanced salt solution; HRP, horseradish peroxidase; IC, inhibitory concentration; IDP, IP_3R-derived peptide; IICR, IP_3-induced Ca^{2+} release; IP_3, inositol 1,4,5-trisphosphate; IP_3R, inositol 1,4,5-trisphosphate receptor; K_d, dissociation constant; MEF, mouse embryonic fibroblast; MOMP, mitochondrial outer membrane permeabilization; NFAT, nuclear factor of activated T cells; NF-κB, nuclear factor kappa-light-chain enhancer of activated B cells; PAC-1, first procaspase activating compound; PAGE, polyacrylamide gel electrophoresis; PARP, poly-(ADP-ribose)-polymerase; PBS, phosphate-buffered saline; PFA, paraformaldehyde; PI, propidium iodide; PVDF, polyvinylidene fluoride; RAF-1, v-raf-1 murine leukemia viral oncogene homolog 1; RAS, RAt Sarcoma; RU, resonance/response unit; SDS, sodium dodecyl sulfate; SPR, surface plasmon resonance; SERCA, sarcoplasmic-endoplasmic-reticulum Ca^{2+} adenosine triphosphatase; STS, staurosporine; TG, thapsigargin; VDAC, voltage-dependent anion channel

Received 02.12.10; revised 02.5.11; accepted 13.6.11; Edited by L Scorrano; published online 05.8.11

membrane permeabilization (MOMP).[11,13,14,17,18] Thus, both promoting cytosolic Ca^{2+} oscillations and blunting cytosolic Ca^{2+} transients underpin the antiapoptotic action of Bcl-2 family members.[19]

Different studies demonstrated that inositol 1,4,5-trisphosphate receptors (IP_3Rs) play a central role in this paradigm as targets of Bcl-2, Bcl-Xl and Mcl-1.[20–25] However, the localization of their interaction sites on the IP_3R as well as the physiological roles of these interactions remain unsolved. Different, not mutually exclusive, mechanisms have been proposed. (1) Increasing the ratio of anti- over pro-apoptotic Bcl-2 proteins caused IP_3R sensitization, enhancing basal IP_3R-mediated Ca^{2+} leak and reducing steady-state [Ca^{2+}] in the ER.[20] (2) Bcl-Xl interacted with the C-terminus of IP_3Rs, promoting spontaneous Ca^{2+} oscillations and enhancing mitochondrial bioenergetics.[23,26] (3) Bcl-2 directly inhibited IP_3Rs without altering steady-state ER Ca^{2+} levels.[21,22,27] Recently, the Bcl-2 interaction domain was identified in the central, modulatory region of the IP_3R (amino acids (a.a.) 1389–1408).[28] Disturbing endogenous IP_3R/Bcl-2 complexes potentiated IP_3-induced Ca^{2+} release (IICR) and sensitized cells toward proapoptotic Ca^{2+} signaling.[28] The BH4 domain of Bcl-2 was necessary and sufficient for interaction with the IP_3R.[29,30] (4) Bcl-Xl reduced the expression levels of IP_3Rs via a decreased binding of NFATc2 (nuclear factor of activated T cells, cytoplasmic, calcineurin-dependent 2) to the IP_3R promoter,[31] thereby reducing IICR.

Here, we directly compared the regulation of IP_3Rs by the BH4 domains of Bcl-2 and Bcl-Xl. Our results indicate that although the BH4 domain of Bcl-2 and Bcl-Xl are very similar in sequence and structure, a difference in one single residue between BH4-Bcl-2 and BH4-Bcl-Xl critically determined its IP_3R binding, suppression of IP_3R activity and protection against IP_3R-driven apoptosis.

Results

BH4-Bcl-2 and BH4-Bcl-Xl differentially regulate IICR. The structure of antiapoptotic Bcl-2 and of a monomeric subunit of the IP_3R1 is depicted in Figure 1a, including the interaction of Bcl-2 via its BH4 domain with the IP_3R1. The IP_3R-derived peptide (IDP; a.a. 1389–1408) corresponds to the Bcl-2-binding site on IP_3R1 and is therefore able to disrupt Bcl-2/IP_3R interaction in a competitive way. IDP completely alleviates the inhibitory action of the BH4 domain of Bcl-2 on IP_3Rs without affecting other BH4-domain targets, like voltage-dependent anion channel (VDAC) and calcineurin.[29] Thus, IDP is an excellent tool to decipher the role of IP_3R in the observed actions of BH4-Bcl-2 on intracellular Ca^{2+} signaling and cell death. Here, we directly compared the effect of BH4-Bcl-2 and BH4-Bcl-Xl on IICR using a unidirectional $^{45}Ca^{2+}$-flux assay in saponin-permeabilized mouse embryonic fibroblasts (MEF cells) in which the non-mitochondrial Ca^{2+} stores were loaded to steady state with $^{45}Ca^{2+}$. After adding 4 μM thapsigargin (TG), the efflux of $^{45}Ca^{2+}$ was followed in the presence of 1 mM ethylene glycol tetraacetic acid (EGTA). This assay allows the quantitative assessment of Ca^{2+}-efflux properties under unidirectional conditions in the absence of ER and mitochondrial Ca^{2+}-uptake activity. Ca^{2+} content (Figure 1b) and fractional loss (Figure 1c) were plotted as a function of time. Figure 1b shows that because of an inherent Ca^{2+} leak, the Ca^{2+} content of the stores slowly decreased over time, whereas adding IP_3 (3 μM) accelerated the decrease in Ca^{2+} content due to IICR, observed as a steep increase in the fractional loss (Figure 1c). The BH4 domains of Bcl-2 (BH4-Bcl-2; a.a. 6–30) and Bcl-Xl (BH4-Bcl-Xl; a.a. 1–24) were produced as synthetic peptides. A scrambled version of the BH4 domain of Bcl-2 (BH4-Bcl-2SCR) and a 'binding-deficient' version of BH4-Bcl-2, in which the surface-accessible residues were altered (BH4-Bcl-2BIND),[30] were used as negative controls. The $^{45}Ca^{2+}$-flux assays showed that BH4-Bcl-2 caused a potent concentration-dependent inhibition of IICR (Figures 1b and c). Importantly, BH4-Bcl-2 did not alter the Ca^{2+}-leak rate from the ER in the absence of IP_3. In contrast to BH4-Bcl-2, BH4-Bcl-2BIND and BH4-Bcl-2SCR did not inhibit IICR (Figure 1d and Supplementary Figures 1A and B). BH4-Bcl-2 inhibited IICR with a half-maximal inhibitory concentration (IC_{50}) of $\sim$30 μM and an IC_{100} of $\sim$100 μM (Figure 1d). Strikingly, BH4-Bcl-Xl did not inhibit IICR (estimated IC_{50} $>$500 μM)

Figure 1 Although the BH4 domains of Bcl-2 and Bcl-Xl are similar in sequence and structure, they differentially regulate IP_3R-mediated Ca^{2+} flux in permeabilized and intact cells. (**a**) Schematic presentation of the antiapoptotic Bcl-2-family members and the IP_3R. The N-terminal BH4 domain is unique for antiapoptotic members. The secondary structure and primary sequence of BH4-Bcl-2 and BH4-Bcl-Xl are very similar. The cylindrical tube represents the predicted α-helical structure (PSIPREDv2.7). The central modulatory domain of the IP_3R1, containing the Bcl-2-binding site (a.a. 1389–1408), is depicted (Dom3 = a.a. 923–1581). A peptide corresponding to a.a. 1389–1408 (IDP) could prevent binding of Bcl-2 to IP_3Rs. (**b**) Unidirectional $^{45}Ca^{2+}$ fluxes in permeabilized MEF cells plotted as $^{45}Ca^{2+}$ content (counts per min (c.p.m.)) as a function of time (min). Ca^{2+} release was activated by 3 μM IP_3 (gray bar) in the absence or presence of the different BH4-domain peptides (black bar). A typical experiment is shown. (**c**) Same experiment as in (**b**), but results are plotted as fractional loss (%/2 min) as a function of time. (**d**) IICR was quantified as the fractional loss after 2 min of IP_3 incubation minus the fractional loss before the IP_3 addition. IICR in the presence of vehicle was set as 100% and other values were normalized to this value. A dose-response curve is shown for BH4-Bcl-2, a non-binding mutant of BH4-Bcl-2 (BH4-Bcl-2BIND), BH4-Bcl-2 SCR and BH4-Bcl-Xl, obtained from three to four independent experiments. Data points represent mean ± S.E.M. (**e**) Intracellular Ca^{2+} signals in intact C6 glioma cells were monitored using Fluo-3. Cells were loaded with caged IP_3 (50 μM) and electroporated with different BH4-domain peptides (20 μM) and/or IDP. IP_3 was released by a UV flash and a rapid increase in cytosolic [Ca^{2+}] was observed. (**f**) Quantitative analysis of the area under the curve in (**e**) was obtained from at least six independent experiments and data are plotted as mean ± S.E.M. These data indicate that BH4-Bcl-2 significantly inhibited IICR, whereas the other BH4-domain peptides did not. IDP (20 μM) prevented the inhibition of IICR by BH4-Bcl-2. (**g**) A typical experiment in Fluo-3-loaded C6 glioma cells loaded with 20 μM of different BH4-domain peptides or IDP depicting Ca^{2+} signals in response to ATP (1 μM). For clarity reasons, Ca^{2+} responses in cells loaded with vehicle, BH4-Bcl-2, BH4-Bcl-2 + IDP or BH4-Bcl-Xl are shown. (**h**) Quantitative analysis of the area under the curve of the ATP-induced Ca^{2+} signals in intact Fluo-3-loaded C6 glioma cells loaded with the different BH4-domain peptides (20 μM) in response to 1 μM ATP (5-9 independent experiments). (**i**) Similar experiment as (**g**) except that cells were pretreated with EGTA (1 mM) 1 min before exposure to thapsigargin (TG; 2.5 μM). (**j**) Quantitative analysis of the area under the curve of the TG-induced Ca^{2+} responses (five independent experiments)

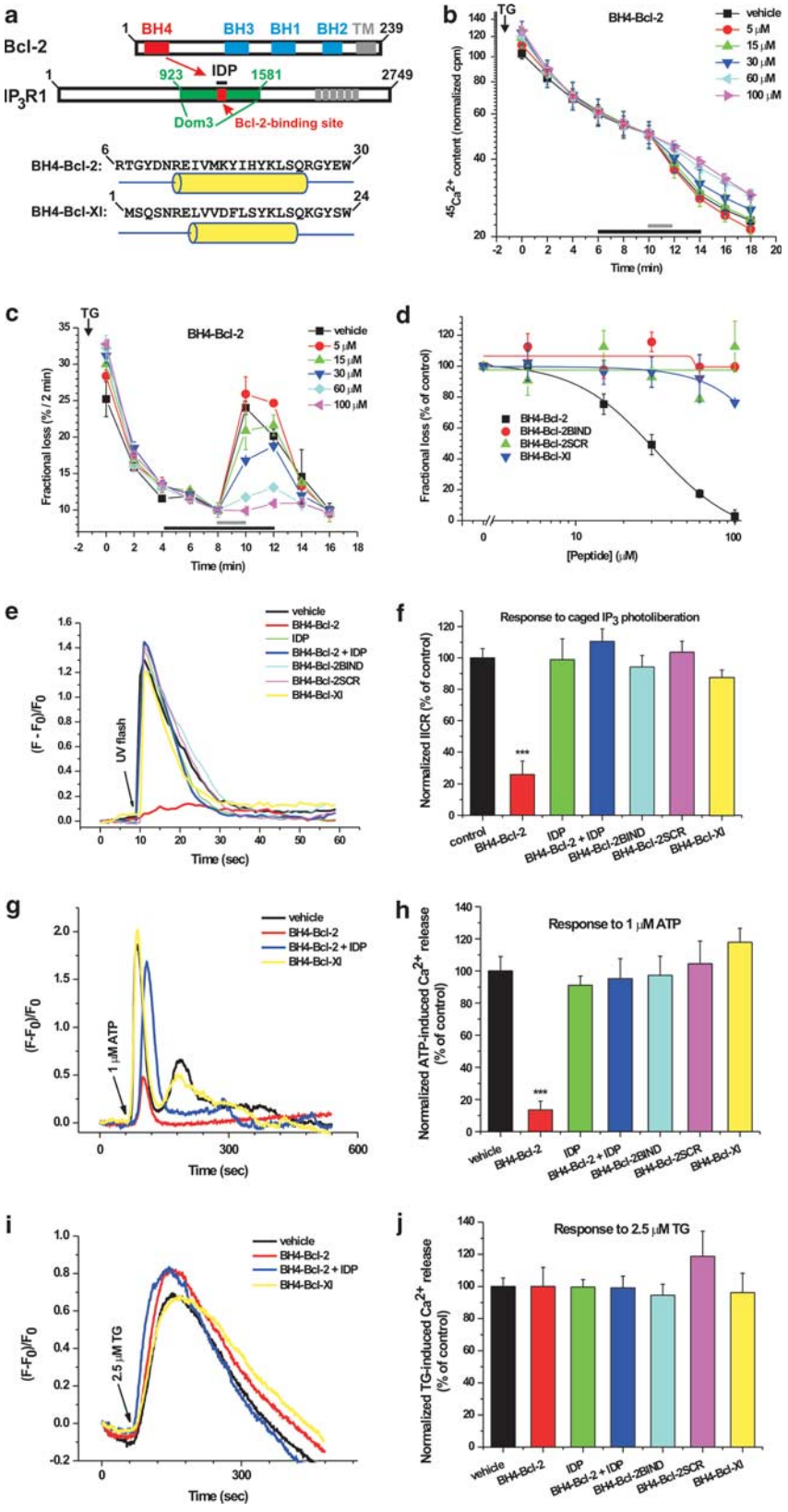
a
Bcl-2
BH4
BH3
BH1
BH2
TM
IDP
IP3R1
Dom3
Bcl-2-binding site
BH4-Bcl-2: RTGYDNREIVMKYIHYKLSQRGYEW
BH4-Bcl-Xl: MSQSNRELVVDFLSYKLSQKGYSW
b
BH4-Bcl-2
TG
vehicle
5 μM
15 μM
30 μM
60 μM
100 μM
45Ca2+ content (normalized cpm)
Time (min)
c
BH4-Bcl-2
Fractional loss (% / 2 min)
Time (min)
d
BH4-Bcl-2
BH4-Bcl-2BIND
BH4-Bcl-2SCR
BH4-Bcl-Xl
Fractional loss (% of control)
[Peptide] (μM)
e
vehicle
BH4-Bcl-2
IDP
BH4-Bcl-2 + IDP
BH4-Bcl-2BIND
BH4-Bcl-2SCR
BH4-Bcl-Xl
UV flash
(F - F0)/F0
Time (sec)
f
Response to caged IP3 photoliberation
Normalized IICR (% of control)
control
BH4-Bcl-2
IDP
BH4-Bcl-2 + IDP
BH4-Bcl-2BIND
BH4-Bcl-2SCR
BH4-Bcl-Xl
g
vehicle
BH4-Bcl-2
BH4-Bcl-2 + IDP
BH4-Bcl-Xl
1 μM ATP
(F-F0)/F0
Time (sec)
h
Response to 1 μM ATP
Normalized ATP-induced Ca2+ release (% of control)
i
vehicle
BH4-Bcl-2
BH4-Bcl-2 + IDP
BH4-Bcl-Xl
2.5 μM TG
(F-F0)/F0
Time (sec)
j
Response to 2.5 μM TG
Normalized TG-induced Ca2+ release (% of control)

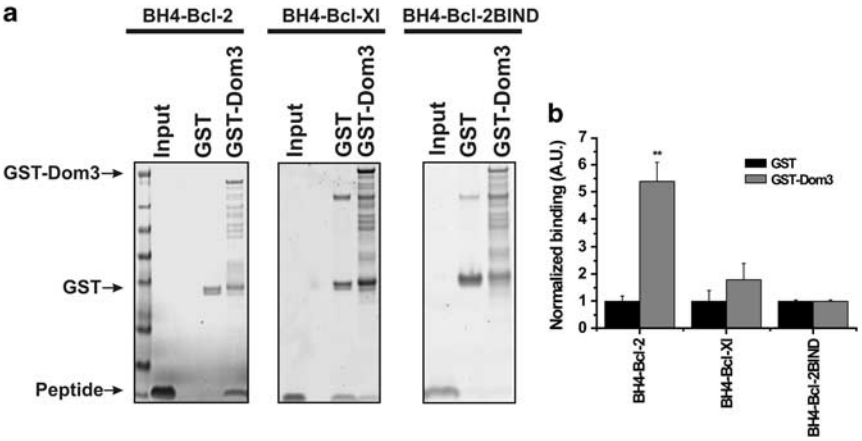

Figure 2 A GST-fusion protein corresponding to the central, modulatory domain of IP_3R1 binds BH4-Bcl-2, but not BH4-Bcl-Xl or BH4-Bcl-2BIND. (**a**) GST pull-down assays were used for assessing the binding of BH4-Bcl-2, BH4-Bcl-Xl or BH4-Bcl-2 BIND to either GST or GST-Dom3. Samples were analyzed via SDS-PAGE and total protein was stained. Bands corresponding to the BH4-domain peptides were quantified using ImageQuant. (**b**) The results of 3–7 independent experiments are plotted as mean ± S.E.M. **Significantly different from GST control ($P<0.01$)

(Figure 1d and Supplementary Figure 1C). We repeated the experiments using more physiological conditions, like 300 nM free Ca^{2+} (Supplementary Figure 2B), 1 μM free Ca^{2+} (Supplementary Figure 2C) and 1 mM Mg-ATP (Supplementary Figure 2D), and found that 40 μM BH4-Bcl-2 equally inhibited IICR.

Next, we examined the differential regulation of IP_3Rs by BH4-Bcl-2 and BH4-Bcl-Xl in C6 glioma cells, a cellular model optimized for *in situ* electroporation of membrane-impermeable molecules.[32,33] We loaded BH4-Bcl-2 or BH4-Bcl-Xl (both 20 μM) by electroporation and found that BH4-Bcl-2 inhibited IICR triggered by IP_3 photoliberation from its caged precursor in intact C6 cells (50 μM; Figures 1e and f), whereas BH4-Bcl-Xl did not. BH4-Bcl-2SCR and BH4-Bcl-2BIND control peptides did not reduce IICR. The inhibition by BH4-Bcl-2 was completely prevented by loading the cells with IDP (20 μM), indicating a competitive binding of BH4-Bcl-2 to IP_3Rs. Similar results were obtained using adenosine 5′-triphosphate (ATP; 1 μM), a physiological agonist provoking IP_3R-mediated Ca^{2+} release in these cells (Figures 1g and h). Finally, we assessed the TG (2.5 μM)-releasable Ca^{2+} in these cells 1 min after exposing the cells to EGTA (1 mM) and found no differences among the different conditions (Figures 1i and j). Hence, the decreased ATP-induced Ca^{2+} release in the presence of BH4-Bcl-2 was not because of decreased ER Ca^{2+}-store content.

These results indicate that BH4-Bcl-2 and BH4-Bcl-Xl differentially regulate IP_3R function independently of the ER Ca^{2+}-store content.

BH4-Bcl-2 and BH4-Bcl-Xl differentially bind to the central domain of the IP_3R. Next, we compared the binding of BH4-Bcl-2 and BH4-Bcl-Xl with glutathione-*S*-transferase (GST)-Dom3 (i.e. a.a. 923–1581 of IP_3R1; Figures 2a and b). Using GST pull-down assays, we found that BH4-Bcl-2, but not BH4-Bcl-Xl, strongly and specifically interacted with GST-Dom3. However, we consistently noticed a higher nonspecific binding of BH4-Bcl-Xl to GST than for BH4-Bcl-2. The reason for this is unclear. BH4-Bcl-2BIND was not pulled down by GST-Dom3 (Figures 2a and b), indicating that surface-accessible residues are important for interaction with IP_3Rs.

We also assessed the binding of GST-Dom3 to BH4-Bcl-2 and BH4-Bcl-Xl in a more quantitative manner using surface plasmon resonance (SPR). We monitored the binding of GST-Dom3 (Figures 3a–c) and GST (Supplementary Figures 3A–C and Figure 3e) to the streptavidin-coated sensor chip containing immobilized biotinylated peptides. Background signals obtained from the reference flow cell containing the scrambled peptides were subtracted to generate response curves. In each sensorgram, the association phase is plotted. GST (up to 40 μM) bound to neither biotin-BH4-Bcl-2 nor biotin-BH4-Bcl-Xl (Supplementary Figures 3A–C). GST-Dom3 displayed a concentration-dependent increase in resonance units, in the biotin-BH4-Bcl-2-containing flow cell (Figure 3a). This indicates a specific binding toward biotin-BH4-Bcl-2 with estimated dissociation constant (K_d) of $\sim$1 μM (Figure 3c). In the biotin-BH4-Bcl-Xl-containing flow cell (Figure 3b), GST-Dom3 resulted in significantly less increase in resonance units (Figure 3c).

We also monitored the binding of GST-Dom3 to biotin-BH4-Bcl-2BIND corrected for the response to the scrambled counterpart (Figure 3d). Clearly, GST-Dom3 did not specifically bind to biotin-BH4-Bcl-2BIND. The negative values in the sensorgrams indicate a slightly higher binding of GST-Dom3 to the scrambled version.

As the Bcl-2-binding site[28] is largely conserved among the different IP_3R isoforms, we compared the BH4-Bcl-2-binding properties of the GST-Dom3 (3.3 μM) derived from IP_3R1, IP_3R2 and IP_3R3 (Figures 3e and f). GST-Dom3 from all three IP_3R isoforms bound to biotin-BH4-Bcl-2 with roughly similar potencies (Figures 3e and f). The quality of the purified GST-fusion proteins was controlled using sodium dodecyl sulfate-polyacrylamide gel electrophoresis (SDS-PAGE; Figure 3g).

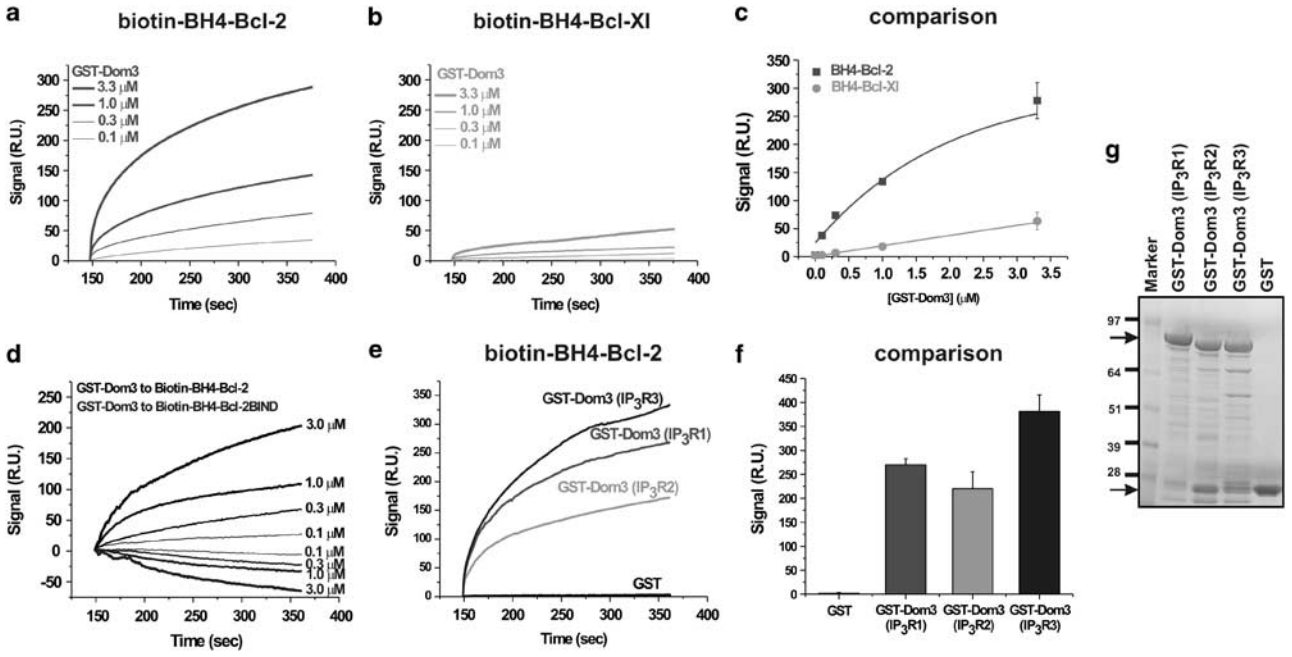

Figure 3 The central, modulatory domain of IP_3R1 binds to immobilized biotin-BH4-Bcl-2, but not to biotin-BH4-Bcl-Xl, in SPR experiments. (**a–c**) Sensorgrams are obtained after background correction for binding to the respective scrambled versions of the biotinylated BH4-domain peptides. The association phase is shown upon addition of different concentrations of purified GST-Dom3 to biotin-BH4-Bcl-2 (**a**) or biotin-BH4-Bcl-Xl (**b**). A typical experiment is shown. (**c**) The quantitative analysis of the binding properties of GST-Dom3 to either biotin-BH4-Bcl-2 or biotin-BH4-Bcl-Xl is shown. Values were obtained from three independent experiments and are plotted as mean ± S.E.M. (**d**) Sensorgrams representing the association phase of different concentrations of GST-Dom3 for the binding to either biotin-BH4-Bcl-2 or biotin-BH4-Bcl-2BIND. All curves are background corrected for binding to the respective scrambled peptides. (**e**) Sensorgrams representing the binding of purified GST-Dom3 (3.3 μM) obtained from IP_3R1, IP_3R2 and IP_3R3 to biotin-BH4-Bcl-2. GST (3.3 μM) was included as a control. (**f**) Quantitative analysis of the binding of purified GST and GST-Dom3 obtained from IP_3R1, IP_3R2 and IP_3R3 (all at 3.3 μM) to biotin-BH4-Bcl-2. Values were obtained from three independent experiments and are plotted as mean ± S.E.M. (**g**) A representative GelCode Blue-stained 4–12% Bis-Tris NUPAGE gel run in MOPS-SDS buffer showing the quality of the purified GST and GST-Dom3 derived from IP_3R1, IP_3R2 and IP_3R3 used in these SPR experiments. The upper arrow indicates the full-length GST-IP_3R-fusion proteins, whereas the lower arrow indicates parental GST

Identification of residues in BH4-Bcl-2 responsible for inhibiting IP_3Rs. Next, we investigated which residues in BH4-Bcl-2 are responsible for interaction with IP_3Rs. Based on a bioinformatics approach,[30] we successively changed the various predicted surface-accessible residues into alanines (Figure 4a) and investigated their properties toward inhibiting IICR as described in Figure 1. We applied 60 μM of the different BH4-Bcl-2 mutant peptides. This concentration, when used for wild-type BH4-Bcl-2, reduced the IICR to ~20% of its control value (Figure 4b). This analysis revealed that BH4-Bcl-2 acts as a discontinuous binding domain, in which every surface-accessible residue (Asp10, Arg12, Lys17, His20, Tyr21, Gln25, Arg26, Tyr28) contributed to the inhibition of IICR. In particular, Lys17, His20, Tyr21 or Arg26 seemed critical for the inhibitory properties of BH4-Bcl-2. Moreover, changing these residues into an Ala may indirectly affect the binding of BH4-Bcl-2 to IP_3Rs by altering its α-helical properties. It has to be noted that although minor changes in the secondary structure can occur, all Ala mutants displayed similar predicted α-helical properties as the wild-type BH4-Bcl-2 using PSIPRED vs3.0 (Supplementary Figure 4, http://bioinf.cs.ucl.ac.uk/psipred/).

Sequence alignment identifies a difference of one critical residue essential for differential IP_3R-inhibitory properties of BH4-Bcl-2 and BH4-Bcl-Xl. Sequence alignment shows that Lys17 (K17) in BH4-Bcl-2 corresponds to Asp11 (D11) in BH4-Bcl-Xl (Figure 5a), thereby introducing a charge change in the middle of the α-helical structure.[29,34,35] Hence, we made a mutant BH4-Bcl-2 peptide in which we replaced Lys17 by an aspartate (BH4-Bcl-2 K/D) and a mutant BH4-Bcl-Xl peptide in which we replaced Asp11 by a lysine (BH4-Bcl-Xl D/K). Strikingly, we found that BH4-Bcl-2 K/D failed to inhibit IICR, whereas BH4-Bcl-Xl D/K strongly reduced IICR (Figures 5b and c). Dose-response curves (Figure 5d) indicated that BH4-Bcl-2 and BH4-Bcl-Xl D/K inhibited IICR with an IC_{50} of 30 and 60 μM, respectively. In contrast, BH4-Bcl-Xl and BH4-Bcl-2 K/D were largely ineffective. The effects of the BH4-domain mutants on IICR were also observed in intact C6 glioma cells using caged IP_3 (Figures 5e and f). In contrast to BH4-Bcl-2, BH4-Bcl-2 K/D did not inhibit IICR in intact cells, whereas in contrast to BH4-Bcl-Xl, BH4-Bcl-Xl D/K was able to significantly reduce IICR. Similar results were obtained using the physiological agonist ATP (1 μM; Figure 5g), whereas none of the BH4-domain peptides did alter the amount of TG (2.5 μM)-releasable Ca^{2+} from the ER (Figure 5h).

The importance of this critical residue was underpinned by SPR experiments using immobilized biotin-BH4-Bcl-2 K/D and biotin-BH4-Bcl-Xl D/K. Consistent with the functional data, BH4-Bcl-2 K/D largely lost its ability to interact with

GST-Dom3 (Figure 5i), whereas BH4-Bcl-Xl D/K was able to bind GST-Dom3 (Figure 5j).

Taken together, these data indicate that one single residue difference between BH4-Bcl-2 and BH4-Bcl-Xl can explain their differential action on IP_3Rs.

BH4-Bcl-2 and BH4-Bcl-Xl differentially affect apoptosis. Next, we assessed whether BH4-Bcl-2 and BH4-Bcl-Xl displayed a difference in protection against apoptotic cell death in C6 glioma cells triggered by loading the cells with cytochrome *c* (CytC; 10 μM, 25 min) or by incubation with staurosporine (STS; 2 μM, 6 h). The apoptotic index (AI) was determined and expressed relative to the condition in which apoptosis was triggered in the absence of BH4 peptides (vehicle), which was set to 100%.

We first examined whether CytC interaction with the IP_3R contributed to CytC-induced apoptosis in the C6 cell model. The CytC–IP_3R interaction is part of a positive feedback loop that enhances cell death by promoting ER Ca^{2+} release through IP_3R channels.[36,37] We examined CytC-induced cell death in the absence and presence of a peptide matching the CytC-binding site on IP_3Rs (IP3RCYT; 50 μM). Cells loaded with IP3RCYT displayed a decrease of $\sim$50–60% in CytC-induced cell death (Figure 6a). These results indicate that part of the CytC-induced cell death was because of CytC binding to the IP_3Rs. We tested the different BH4-domain peptides (20 μM) in this cell system and found that both BH4-Bcl-2 and BH4-Bcl-Xl protected against CytC-induced cell death. However, BH4-Bcl-2 was significantly more potent in protecting than BH4-Bcl-Xl (Figure 6b). The BH4-Bcl-2SCR control did not protect at all. Importantly, changing Lys17 into Asp in BH4-Bcl-2 (BH4-Bcl-2 K/D) reduced the level of protection, thereby resembling BH4-Bcl-Xl. In contrast, changing Asp11 into Lys in BH4-Bcl-Xl (BH4-Bcl-Xl D/K) increased cell survival, thereby resembling BH4-Bcl-2.

To assess whether the difference in potency between BH4-Bcl-2 and BH4-Bcl-Xl is because of their differential action on the IP_3R, the BH4-domain peptides were loaded together with IDP competing with the IP_3R for binding of Bcl-2. IDP completely abolished the protective action of BH4-Bcl-2, but not that of BH4-Bcl-Xl (Figure 6c).

We also used STS, which acts upstream of the mitochondria and CytC release and initiates apoptosis via ER Ca^{2+}-release-dependent mechanisms.[38,39] STS induced apoptosis with a minor fraction of these cells displaying secondary necrosis (Figure 6d). Primary necrosis was not observed, as all propidium iodide (PI)-positive cells were also characterized by activated caspases (cysteine-dependent

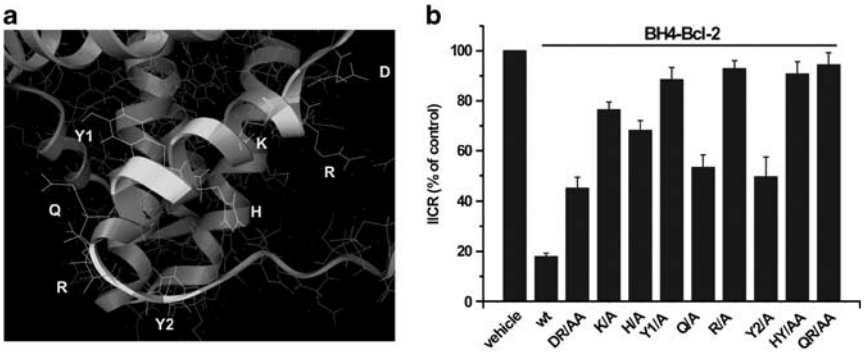

Figure 4 Determination of the residues in BH4-Bcl-2 critical for inhibiting IICR. (**a**) Zoomed picture of the BH4 domain of Bcl-2 showing its surface-accessible residues is depicted. (**b**) The inhibitory properties of different BH4-Bcl-2 mutant versions (60 μM), in which the surface-accessible residues were altered into alanines, were monitored in unidirectional $^{45}Ca^{2+}$-flux assays in permeabilized MEF cells. Four of the six single alanine mutations (K17A, H20A, Y21A and R26A) had the largest effect on the inhibitory action of the wild-type (wt) BH4-Bcl-2 domain

Figure 5 BH4-Bcl-2 and BH4-Bcl-Xl differ in one critical amino acid, which determines their effect on the IP_3R. (**a**) Aligned sequence of the BH4 domain of Bcl-2 and Bcl-Xl with indication of the surface-accessible residues (in color) is shown. The critical residue Lys17 in BH4-Bcl-2 is not conserved in BH4-Bcl-Xl (depicted in blue). The sequences of these BH4-domain peptides are indicated. (**b**) A typical experiment of a unidirectional $^{45}Ca^{2+}$-flux assay in permeabilized MEF cells, comparing the effect of BH4-Bcl-2, BH4-Bcl-Xl, BH4-Bcl-2 K/D and BH4-Bcl-Xl D/K (80 μM of peptides). (**c**) The quantification of the effects of the different BH4-domain peptides (80 μM) on IICR was obtained from three to four independent experiments. Data points represent mean ± S.E.M. *BH4-Bcl-2 and BH4-Bcl-Xl D/K are statistically different from control. $ BH4-Bcl-2 K/D is statistically different from BH4-Bcl-2. # BH4-Bcl-Xl D/K is statistically different from BH4-Bcl-Xl. (**d**) A dose-response curve for the different BH4-domain peptides was obtained from three independent experiments. Values are plotted as mean ± S.E.M. (**e**) Representative IP_3R-mediated Ca^{2+} traces in intact C6 glioma cells using caged IP_3 and UV photoliberation. (**f**) Quantitative analysis of the area under the curve, of the traces in (**e**), was obtained from at least six independent experiments and data are plotted as mean ± S.E.M. BH4-Bcl-2 and BH4-Bcl-Xl D/K significantly inhibited IICR, in contrast to BH4-Bcl-2 K/D and BH4-Bcl-Xl. *BH4-Bcl-2 and BH4-Bcl-Xl D/K are statistically different from control. $ BH4-Bcl-2 K/D is statistically different from BH4-Bcl-2. # BH4-Bcl-Xl D/K is statistically different from BH4-Bcl-Xl. (**g**) Similar experiment as in (**e** and **f**), except that Ca^{2+} signals were elicited by ATP (1 μM). Area under the curve of different control cells was determined and set at 100%. (**h**) Similar experiment as in (**e** and **f**), except that cells were pretreated for 1 min with EGTA (1 mM) and exposed to thapsigargin (TG, 2.5 μM). Area under the curve for control was determined and set at 100%. Statistically significant differences were considered at $P<0.05$ (single symbols), $P<0.01$ (double symbols) and $P<0.001$ (triple symbols). (**i**) Quantitative analysis of data obtained from three independent SPR experiments, in which the binding of different concentrations of GST-Dom3 to immobilized biotin-BH4-Bcl-2 was compared with its binding to immobilized biotin-BH4-Bcl-2 K/D. The maximal signal (resonance units) during the association phase was used in this analysis. (**j**) Quantitative analysis of data obtained from SPR experiments, in which the binding of GST-Dom3 to biotin-BH4-Bcl-Xl was compared with its binding to biotin-BH4-Bcl-Xl D/K. The maximal signal (resonance units) during the association phase was used in this analysis

aspartate-specific proteases). Results with STS were similar to those obtained with CytC loading (Figure 6e). Both BH4-Bcl-2 and BH4-Bcl-Xl, but not BH4-Bcl-2SCR, protected against STS-induced cell death. However, BH4-Bcl-2 was significantly more potent than BH4-Bcl-Xl. BH4-Bcl-2-mediated protection against STS was completely suppressed by IDP, whereas the effect of BH4-Bcl-Xl was independent of IDP.

As an additional control, we used first procaspase activating compound (PAC-1; 150 μM, 6 h), a direct procaspase-3 activating compound downstream of CytC.[40] These conditions caused apoptosis in $\sim$15% of the cell population. We found that BH4-Bcl-2 and BH4-Bcl-Xl did not protect against PAC-1-induced cell death, confirming that the target of these peptides is indeed upstream of caspase-3 (Figure 6f).

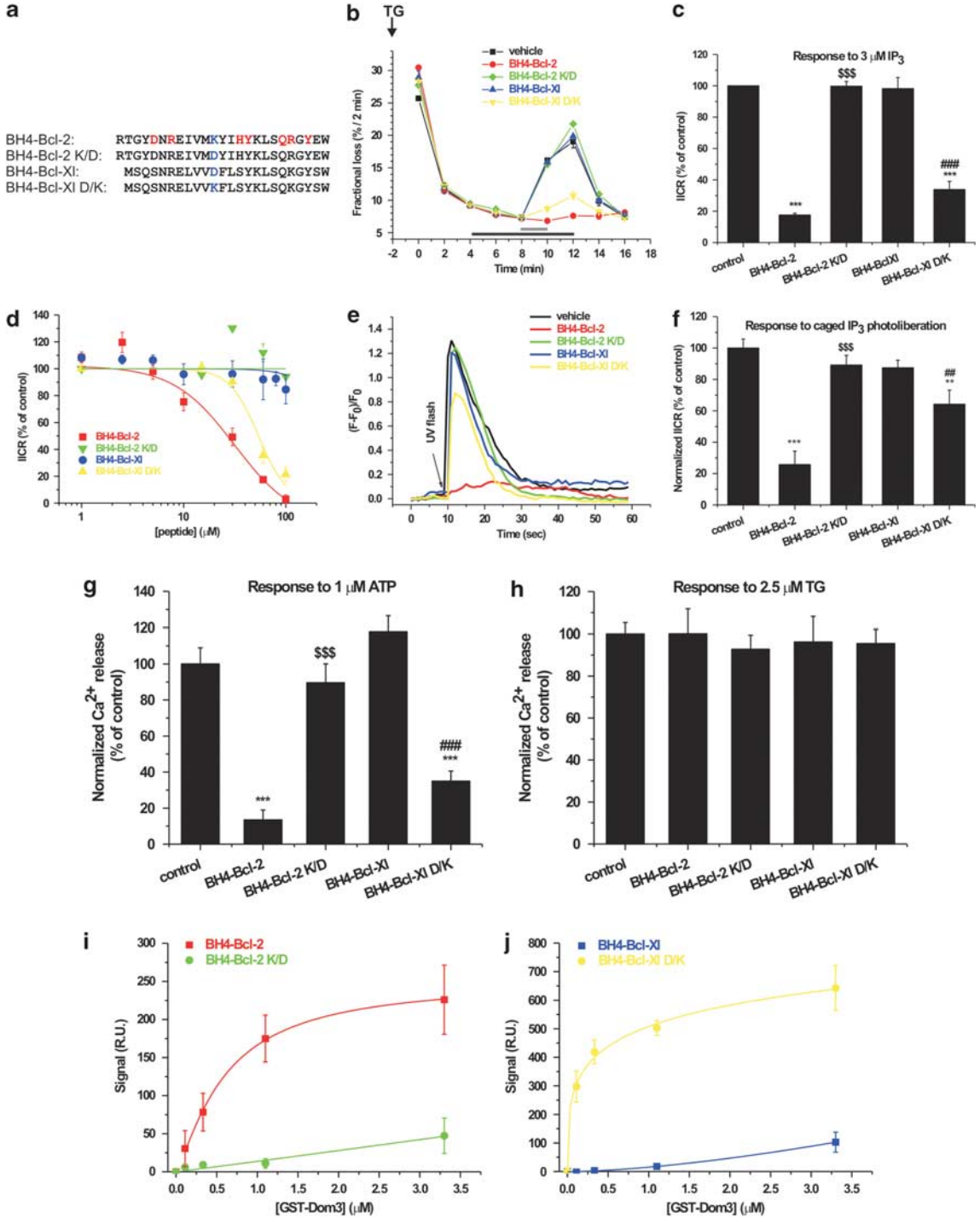

Co-loading of BH4-Bcl-2 with BH4-Bcl-Xl in C6 glioma cells did not display an additive effect toward their protection against CytC- and STS-induced cell death (Figure 6g and Supplementary Figure 5). The protective effects of both BH4-Bcl-2 and BH4-Bcl-Xl against CytC-induced apoptosis were ablated when the positive feedback loop of CytC on the IP_3R was prevented by co-loading IP3RCYT peptide (Figure 6h).

Collectively, these data indicate that the BH4 domains of Bcl-2 and Bcl-Xl both protect against apoptosis by acting on different targets upstream of caspase activation. Although the protective effect of BH4-Bcl-2 was stronger and largely dependent on its interaction with a specific binding site on the IP_3R, the protective effect of BH4-Bcl-Xl is independent of binding to the IP_3R. Nevertheless, in these paradigms

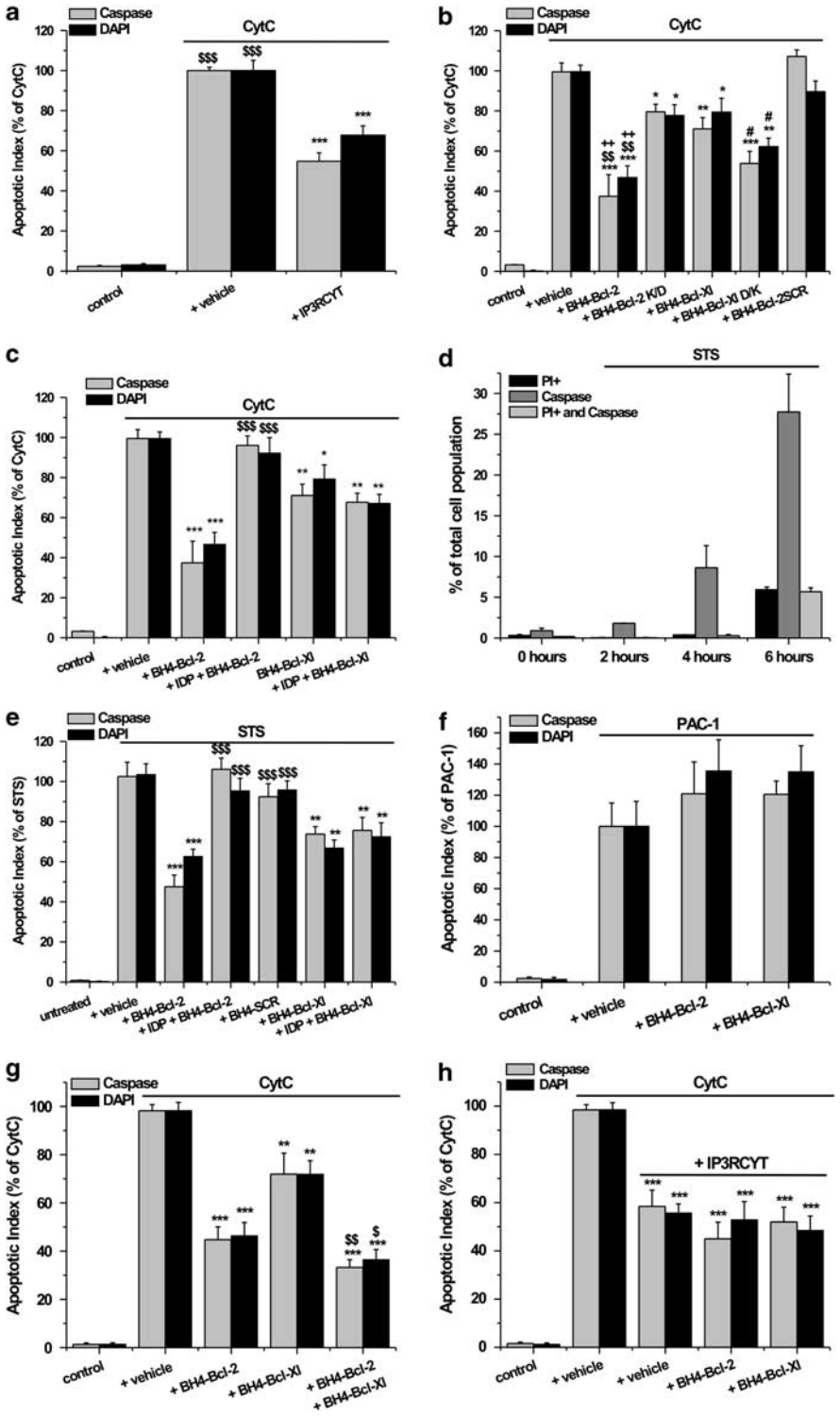

BH4-Bcl-Xl likely acts on a target that functions downstream of the IP_3R-signaling cascade.

Full-length Bcl-2 K/D is less efficient in binding IP_3Rs, inhibiting IP_3R activity and protecting against Ca^{2+}-dependent apoptosis. Finally, we tested whether the critical Lys17 identified in BH4-Bcl-2 plays a crucial role in the IP_3R-inhibitory action of full-length Bcl-2. Therefore, we mutated Lys17 into Asp in full-length 3xFLAG-Bcl-2, creating 3xFLAG-Bcl-2 K/D.

First, we compared the GST-Dom3-binding properties of 3xFLAG-Bcl-2 and 3xFLAG-Bcl-2 K/D by expressing these proteins in COS-1 cells and using GST pull-down assays (Figure 7a). We found that the binding of 3xFLAG-Bcl-2 K/D to GST-Dom3 was severely compromised compared with wild-type 3xFLAG-Bcl-2 (Figure 7b).

Next, we examined the effect of 3xFLAG-Bcl-2 and 3xFLAG-Bcl-2 K/D overexpression in COS-1 cells on ATP-induced Ca^{2+} release. We applied 1 μM ATP, a submaximal concentration for triggering Ca^{2+} signals, in Fura-2-loaded COS-1 cells. We monitored the Ca^{2+} signals in mCherry-transfected cells (Supplementary Figure 6). In each experiment, 10 cells were selected and calibrated Ca^{2+} signals were obtained. Typical Ca^{2+} responses in empty vector-, 3xFLAG-Bcl-2- and 3xFLAG-Bcl-2 K/D-transfected cells are shown in Figures 7c–e, respectively. Cells expressing 3xFLAG-Bcl-2 displayed blunted ATP-triggered Ca^{2+} signals in comparison with empty vector- or 3xFLAG-Bcl-2 K/D-transfected cells (Figure 7f). 3xFLAG-Bcl-2 was much more potent in inhibiting IP_3R-mediated Ca^{2+} signals than 3xFLAG-Bcl-2 K/D (Figure 7f). In addition, there was no difference for TG-induced Ca^{2+} signals (Figure 7g). Finally, we examined the effect of 3xFLAG-Bcl-2 and 3xFLAG-Bcl-2 K/D overexpression on the protection against STS-induced apoptosis. We used the cleavage of poly-(ADP-ribose)-polymerase (PARP), a downstream target of activated caspase-3, to monitor STS-induced apoptosis in transfected COS-1 cells (Figure 7h). Compared with control cells, 3xFLAG-Bcl-2 significantly reduced PARP cleavage upon STS treatment. 3xFLAG-Bcl-2 K/D was much less potent than 3xFLAG-Bcl-2 in preventing STS-induced PARP cleavage (Figure 7i).

We confirmed these findings in WEHI7.2 cells, which contain very low Bcl-2 levels. We created stable WEHI7.2 cell lines expressing either Bcl-2 or Bcl-2 K/D. First, western blotting analysis revealed that both stable cell lines displayed similar levels of Bcl-2 and Bcl-2 K/D (Figure 8a). Next, we monitored apoptosis by western blotting analysis with PARP antibodies (Figure 8b), annexin V-fluorescein isothiocyanate (FITC)/PI fluorescence-activated cell sorting (FACS) analysis (Figures 8c and d) and caspase-3-activity assay (Figure 8e). In all assays, Bcl-2 overexpression protected WEHI7.2 cells against STS-induced apoptosis, whereas Bcl-2 K/D was less effective than wild-type Bcl-2. These data correlate well with the IP_3R-binding and Ca^{2+}-signaling results obtained in COS-1 cells. Hence, Lys17 seems an important residue in the BH4 domain of full-length Bcl-2 for mediating Bcl-2-dependent inhibition of IP_3R-mediated Ca^{2+} signals and protection against STS-induced cell death.

Discussion

The major findings of this study are that (1) BH4-Bcl-2 and BH4-Bcl-Xl, although very similar in primary sequence and secondary structure,[29,34,35] act differentially on IP_3Rs, IICR and Ca^{2+}-dependent apoptosis; (2) one critical residue that has an opposite charge in BH4-Bcl-2 *versus* BH4-Bcl-Xl is responsible for their distinct biological properties; and (3) mutating this residue in the BH4 domain of full-length Bcl-2 decreases its ability to bind and inhibit IP_3Rs and to protect against apoptotic stimuli. We pinpointed one residue critical for inhibiting IP_3Rs in the sequence of BH4-Bcl-2 (Lys17) that was not conserved in BH4-Bcl-Xl (Asp11). This residue is of key importance for the specific action of BH4-Bcl-2 on the IP_3R. Changing Asp11 in BH4-Bcl-Xl into a Lys induced IP_3R binding and inhibition, leading to a BH4-Bcl-2-like function.

Bcl-2 and Bcl-Xl both act at the mitochondrial and the ER membranes, where they regulate ER Ca^{2+} dynamics via interaction with the IP_3R.[20–23,26] Several reports suggested that Bcl-2 predominantly inhibits proapoptotic Ca^{2+} transients, whereas Bcl-Xl predominantly stimulates

Figure 6 BH4-Bcl-2, but not BH4-Bcl-Xl, protects against CytC- and STS-induced apoptosis via its interaction with the IP_3R. (**a–c**) Loading of CytC (10 μM) in C6 glioma cells provoked a dramatic increase in the number of caspase-positive cells and cells with a fragmented nucleus (both quantified 25 min later) compared with cells loaded with buffer only ($ in (**a**) indicates that CytC significantly increases the apoptotic index compared with the control loading condition lacking CytC; the significance indication for CytC *versus* control was omitted from the other panels for clarity reasons). All results were obtained from four to eight independent experiments and are plotted as mean ± S.E.M. Statistically significant differences are indicated as in Figure 5. (**a**) Co-loading of the IP_3R peptide corresponding to the CytC-binding site (IP3RCYT 50 μM) together with CytC significantly (*) reduced the apoptotic index, indicating that CytC-induced apoptosis was amplified by its action on the IP_3R. (**b**) BH4-Bcl-2, BH4-Bcl-2 K/D, BH4-Bcl-Xl and BH4-Bcl-Xl D/K (20 μM) significantly (*) protected against CytC-induced apoptosis in both assays, but not BH4-Bcl-2SCR. However, BH4-Bcl-2 was significantly ($) more potent than BH4-Bcl-Xl. Furthermore, Bcl-2 is significantly more potent than Bcl-2 K/D (+), whereas Bcl-Xl D/K is significantly more potent than BH4-Bcl-Xl (#). (**c**) BH4-Bcl-2-mediated protection against CytC-induced apoptosis was alleviated by co-loading with 20 μM IDP, whereas the antiapoptotic activity of BH4-Bcl-Xl was not affected by IDP. Thus, BH4-Bcl-2, BH4-Bcl-Xl and BH4-Bcl-Xl + IDP significantly (*) reduced CytC-induced apoptosis, but not BH4-Bcl-2 + IDP. Furthermore, BH4-Bcl-2 + IDP is significantly ($) different from BH4-Bcl-2. (**d**) Characterization of the STS (2 μM)-induced cell death profile by analyzing the percentage of cells staining positive for propidium iodide (PI +), caspase activation (Caspase) and both PI and caspase activation (PI + and Caspase) as a function of time. (**e**) Similar approach as in (**c**) but with STS as an apoptotic trigger (applied in the medium for 6 h at 2 μM). (**f**) Similar approach as in (**a–c**), but with PAC-1, a small molecular activator of caspase-3, as an apoptotic trigger (applied in the medium for 6 h at 150 μM). (**g**) Effect of combining BH4-Bcl-2 and BH4-Bcl-Xl (both 20 μM) on CytC-induced apoptosis. *All conditions significantly reduced CytC-induced apoptosis. $^{\$}$The combination of BH4-Bcl-2 and BH4-Bcl-Xl is significantly different from BH4-Bcl-Xl, but not from BH4-Bcl-2. These results indicate no additive effect by combining BH4-Bcl-2 with BH4-Bcl-Xl. (**h**) Effect of BH4-Bcl-2 and BH4-Bcl-Xl on CytC-induced apoptosis in the presence of IP3RCYT peptide. *All conditions significantly reduced CytC-induced apoptosis. However, the protective effects of both BH4-Bcl-2 and BH4-Bcl-Xl were ablated in the presence of IP3RCYT peptide (50 μM) and thus did not significantly differ from the vehicle-treated condition

IP_3R-mediated prosurvival Ca^{2+} oscillations.[21–23,26,28] Nevertheless, other reports showed that Bcl-2 too may enhance IP_3R activity[20,25] and/or stimulate Ca^{2+} oscillations.[21,41] Hence, until now, it was not clear whether Bcl-2 and Bcl-Xl displayed distinct functional properties toward regulating IP_3Rs and thus Ca^{2+}-regulated apoptosis or whether they were similar in their action. As we recently showed that BH4-Bcl-2 was sufficient to protect against IP_3R-mediated apoptosis, we now made a direct comparison of the BH4-domain properties of Bcl-2 and Bcl-Xl by using synthetic peptides. Our study reveals a specific cellular function for the BH4 domain of Bcl-2 as a potent inhibitor of IICR and Ca^{2+}-dependent apoptosis, which is not shared by the BH4 domain of Bcl-Xl, although both motifs are very similar in sequence and structure. Our data indicate that this is because of a critical charge difference in one of the surface-accessible amino-acid residues. As a result, BH4-Bcl-Xl did not inhibit Ca^{2+} flux through the IP_3R. Nevertheless, BH4-Bcl-Xl protected against cell death.

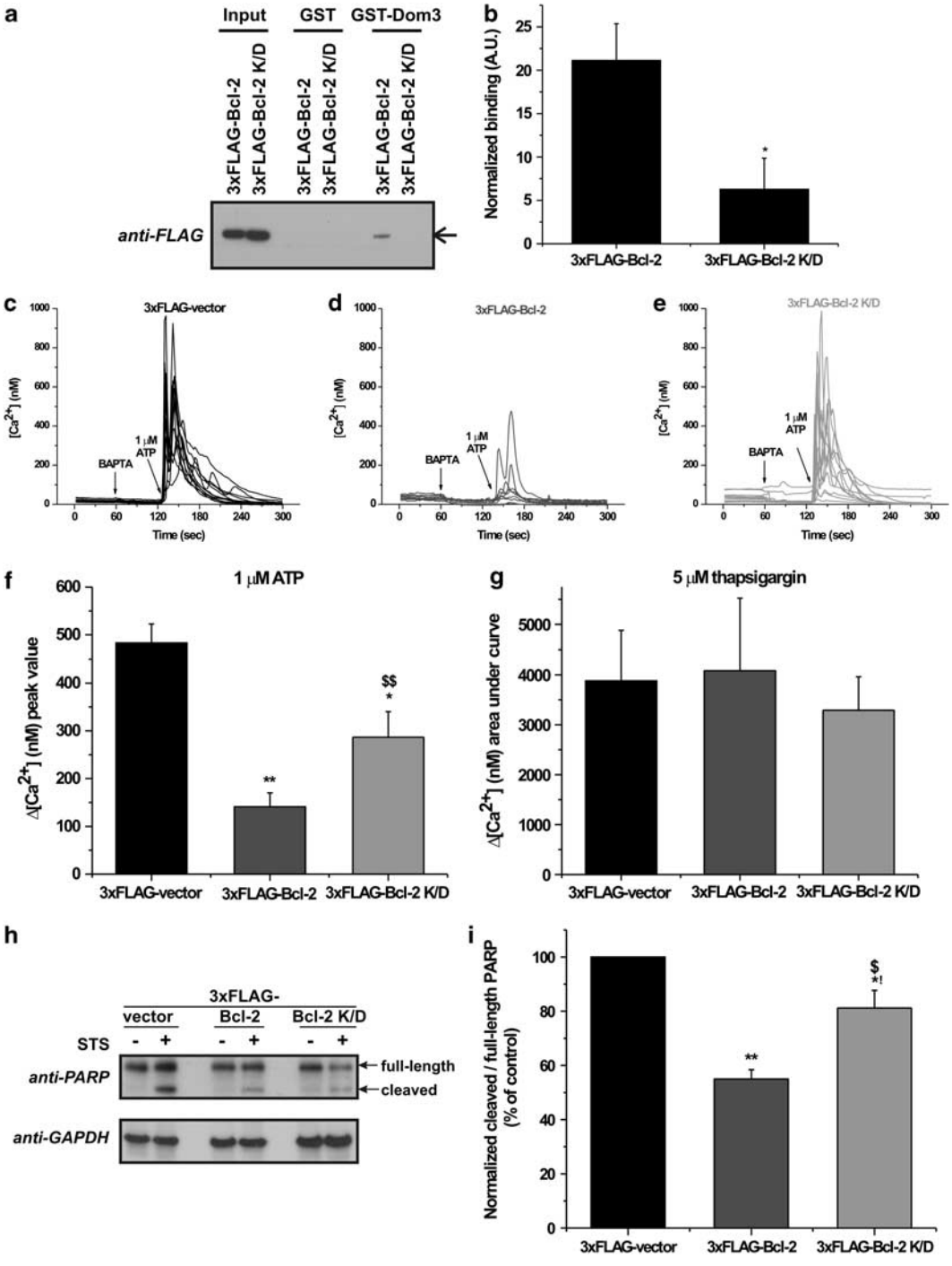

However, this effect was significantly smaller than for BH4-Bcl-2 and was not due to inhibition of IICR. This was concluded from the observation that IDP counteracting the effect of BH4-Bcl-2 did not interfere with the protective function of BH4-Bcl-Xl. Finally, using exogenous expression in COS-1 and WEHI7.2 cells, we demonstrated that the role of Lys17 is important for the action of full-length Bcl-2 on the IP_3R, as full-length Bcl-2 K/D was much less efficient in binding and inhibiting IP_3Rs as well as in protecting against apoptotic stimuli. We observed a weak binding of full-length Bcl-2 K/D (i.e. $\sim$20% of the binding of wild-type Bcl-2) to the IP_3R fragment, which indicates that residues other than Lys17 may contribute to the binding of full-length Bcl-2 to the IP_3R. This remaining binding of Bcl-2 K/D to IP_3R may be responsible for the weak inhibitory property of this protein on IP_3R-mediated Ca^{2+} signaling and its protective effects against STS-induced apoptosis. However, the latter may also be related to the antiapoptotic actions of Bcl-2 K/D through its hydrophobic cleft and may therefore suggest that its ability to scaffold proapoptotic BH3-domain proteins is unaffected by this mutation in the BH4 domain.

Clearly, whereas Bcl-2 exclusively interacts with the central domain of the IP_3R,[28] Bcl-Xl seems to interact with the C-terminal tail of the IP_3R.[23] The latter domain has been proposed to contain two putative BH3-like domains and may therefore interact with the hydrophobic cleft of Bcl-Xl.[24]

Besides the differential interaction with the IP_3R, Bcl-2 and Bcl-Xl could also differ with respect to other previously identified targets of the BH4 domain of Bcl-2-family members, as calcineurin, VDAC, RAF-1 (v-raf-1 murine leukemia viral oncogene homolog 1), RAS (RAt Sarcoma), CED (cell death abnormal)-4, paxillin and NF-κB (nuclear factor kappa-light-chain enhancer of activated B cells), all of which may play a role in apoptosis.[30] A side-by-side comparison between Bcl-2 and Bcl-Xl will be required to examine whether there is a distinct or preferential action of either domain on these targets and whether the critical sequence difference between BH4-Bcl-2 and BH4-Bcl-Xl revealed in this study affects their activity or selectivity. Furthermore, considering the preferential targeting of Bcl-Xl to the mitochondrial outer membrane,[42] we speculate that the protective action of BH4-Bcl-Xl may be mediated by modulating mitochondrial targets.[43] Although BH4-Bcl-2 and BH4-Bcl-Xl appear to have distinct targets, these targets likely do not function in completely independent pathways. Indeed, a combination of BH4-Bcl-2 and BH-Bcl-Xl did not provoke an additive protective effect and IP3RCYT abolished the protective effect of both BH4-Bcl-2 and BH4-Bcl-Xl against CytC-induced apoptosis. Thus, Bcl-Xl may act through its BH4 domain on a target downstream of the IP_3R, whereas other targets independently of the IP_3R/Ca^{2+}-signaling cascade cannot be excluded.

Our study may have important therapeutic consequences for cancers dependent on high levels of Bcl-2, like chronic lymphocytic leukemia.[44,45] It may be possible to target the BH4 domain of Bcl-2 in these malignancies, while preserving essential biological functions of Bcl-Xl in other cells.

To conclude, our study is the first to reveal a difference in the cellular activity of the BH4 domain of Bcl-2 and Bcl-Xl toward IP_3R regulation because of a single residue difference between both domains.

Materials and Methods

Peptides. All synthetic peptides were obtained from Thermo Electron (Osterode, Germany). Biotinylated peptides were obtained from Lifetein (South Pleinfield, NJ, USA). Table 1 provides an overview of the different peptides used in this study and their primary sequence.

Plasmid vector constructs. The pGEX-6p2 construct (Amersham Biosciences, GE Healthcare, Diegem, Belgium) encoding a.a. 923–1581 of mouse IP_3R1 Domain 3 was obtained as previously described.[28] pcDNA3.1 (-) mouse IP_3R2 and rat IP_3R3 were used as templates for the construction of pGEX-6p2 vectors encoding the corresponding regions of IP_3R2 (a.a. 913–1562) and IP_3R3 (a.a. 910–1427). Their respective coding regions were amplified by PCR using the following primers: IP_3R2 forward (5′-GCGGCGGGATCCAATGTCAT GAGGACCATCCACGG-3′); IP_3R2 reverse (5′-GCGGCGGAATTCCTAGAGCGTGT TGACCTGGCTG-3′); IP_3R3 forward (5′-GCGGCGGGATCCAACGTGCGGAGGTC CATCCAGGG-3′); IP_3R3 reverse (5′-GCGGCGGAATTCTCACAGAGCGCTCATGTGG GCATC-3′). PCR products were purified, digested with *Bam*HI and *Eco*RI (restrictions sites are underlined above) and ligated into *Bam*HI–*Eco*RI-treated pGEX-6p2 vector.

3xFLAG-Bcl-2 and -Bcl-Xl were generated by subcloning their respective full-length cDNAs into p3xFLAG-myc-CMV-24 vector (Sigma-Aldrich, Munich, Germany) at *Hind*III/*Bgl*II sites. The 3xFLAG-Bcl-2 K/D mutant was generated by PCR site-directed mutagenesis introducing GAT (D) to replace AAG (K) in wild-type Bcl-2-donor DNA. The following primers were used: 3F-Bcl-2 K/D forward (5′-GATAACCGGGAGATAGT GATGGATTACATCCATTATAAGCTGTCG-3′); 3F-Bcl-2 K/D reverse (5′-CGACAGCT TATAATGGATGTAATCCATCACTATCTCCCGGTTATC-3′).

The pSFFV-Neo and pSFFV-Neo-Bcl-2 vectors were kindly provided by Professor Clark W Distelhorst. The pSFFV-Neo-Bcl-2 K/D vector was also obtained by PCR site-directed mutagenesis. To introduce the desired point mutations, we designed and used the following primers: Neo-Bcl-2 K/D forward (5′-GACAAC CGGGAGATAGTGATGGACTACATCCATTATAAGCTGTCG-3′); Neo-Bcl-2 K/D reverse (5′-CGACAGCTTATAATGGATGTAGTCCATCACTATCTCCCGGTTGTC-3′). All constructs were verified by sequencing (Agowa AG, Berlin, Germany).

Figure 7 Mutating Lys17 into Asp in full-length Bcl-2 largely prevents the ability of Bcl-2 to bind to the IP_3R, inhibit IP_3R-mediated Ca^{2+} release and protect against STS-induced apoptosis in COS-1 cells. (**a**) Lysates from 3xFLAG-Bcl-2- and 3xFLAG-Bcl-2 K/D-overexpressing COS-1 cells were used in GST pull-down assays using purified GST-Dom3. A representative western blot using anti-FLAG antibodies is shown. (**b**) Immunoreactive bands of at least five independent experiments were quantified using ImageJ software. Values represent normalized values relative to their binding to GST. (**c–e**) COS-1 cells were co-transfected with mCherry plasmids and threefold excess of either empty vector (**c**), 3xFLAG-Bcl-2 plasmid (**d**) or 3xFLAG-Bcl-2 K/D plasmid (**e**). Only cells expressing the mCherry plasmid were monitored as F340/F380. Fura-2 signals were calibrated to obtain [Ca^{2+}] (nM). Representative Ca^{2+} traces obtained from 10 Fura-2-loaded COS-1 cells in response to ATP (1 μM) are shown. (**f**) Quantitative analysis of the amplitude of the ATP-induced Ca^{2+} signals in mCherry-expressing COS-1 cells transfected with either empty vector, 3xFLAG-Bcl-2 plasmid or 3xFLAG-Bcl-2 K/D plasmid obtained from six independent experiments (mean ± S.E.M.). *Both 3xFLAG-Bcl-2 and 3xFLAG-Bcl-2 K/D significantly reduce the peak [Ca^{2+}] in response to ATP. $^{\$}$3xFLAG-Bcl-2 K/D is significantly different from 3xFLAG-Bcl-2. (**g**) Quantitative analysis of the area under the curve of the TG-induced Ca^{2+} signal in these cells. (**h**) Western-blot analysis using anti-PARP antibodies for monitoring PARP cleavage upon STS treatment (1 μM for 6 h) in 3xFLAG-vector, 3xFLAG-Bcl-2 and 3xFLAG-Bcl-2 K/D-expressing COS-1 cells. GAPDH was used as a loading control. (**i**) Quantification of the immunoreactive bands of the ratio of the cleaved over the full-length PARP in the different transfected COS-1 cell populations from three independent experiments. The ratio of cleaved over full-length PARP obtained for control cells were set at 100% and the other ratios were normalized to this value. Both 3xFLAG-Bcl-2 and 3xFLAG-Bcl-2 K/D significantly (*) prevent STS-induced apoptosis compared with the empty-vector control, but 3xFLAG-Bcl-2 K/D is significantly ($) less potent than 3xFLAG-Bcl-2. Statistically significant differences are indicated as in Figure 5. We wish to remark that the results obtained with 3xFLAG-Bcl-2 K/D were borderline significantly (*!) different from the empty-vector control ($P = 0.051$)

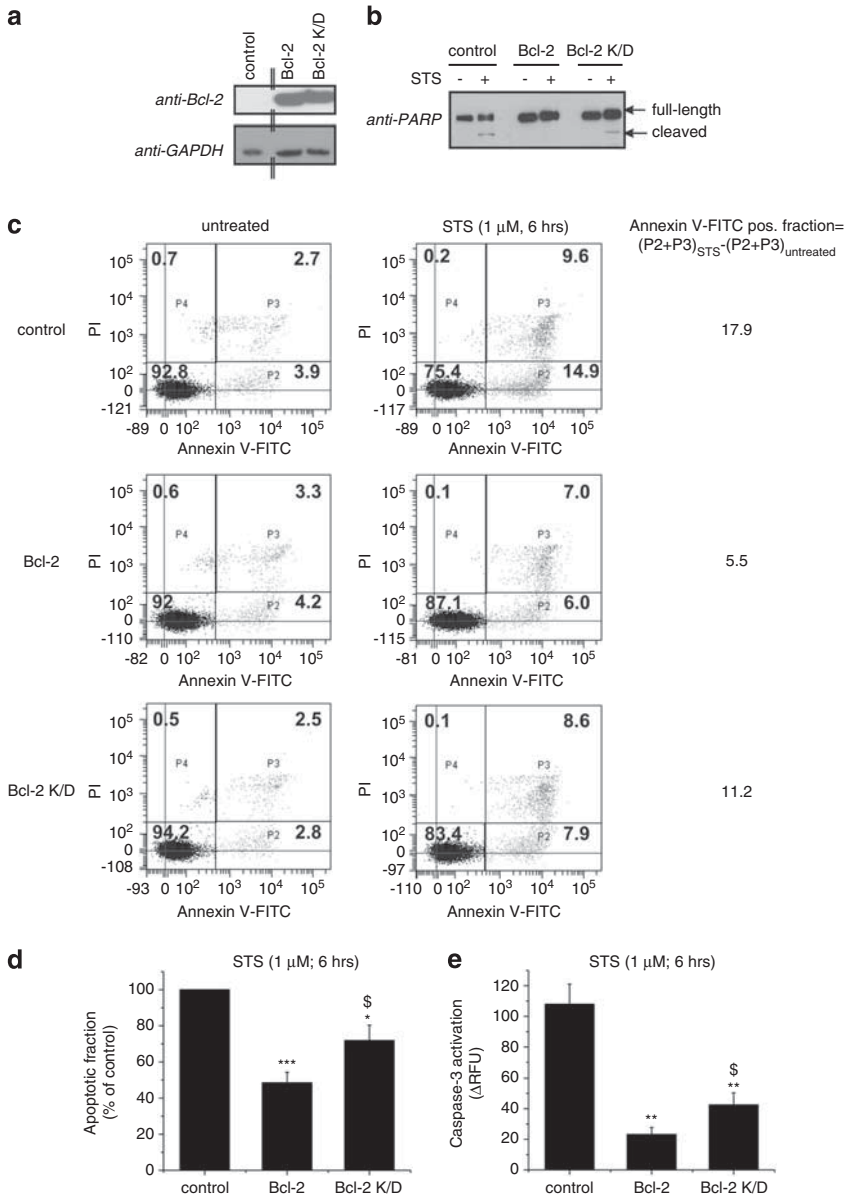

Figure 8 Bcl-2 K/D is less effective than Bcl-2 in protecting against STS-induced apoptosis in stable WEHI7.2 cell lines. (**a**) Stable WEHI7.2 cell lines expressing Bcl-2 or Bcl-2 K/D were created. The expression levels of Bcl-2 and Bcl-2 K/D were examined by western-blotting analysis using an anti-Bcl-2 antibody. Control WEHI7.2 cells display very low endogenous Bcl-2 levels. (**b**) The cleavage of poly(ADP-ribose)-polymerase (PARP) in control WEHI7.2 cells, WEHI7.2 cells expressing Bcl-2 and WEHI7.2 cells expressing Bcl-2 K/D was monitored by western-blotting analysis using an anti-PARP antibody. (**c**) FACS analysis of untreated and STS-treated PI/Annexin V-FITC-stained control, Bcl-2-overexpressing and Bcl-2 K/D-overexpressing WEHI7.2 cell lines (10 000 cells per analysis). The apoptotic population was identified as the AnnexinV-FITC-positive fraction (P2 + P3). The STS-induced apoptotic population was determined by the difference between the Annexin V-FITC-positive fraction of STS-treated cells and the untreated cells: $(P2 + P3)_{STS}$–$(P2 + P3)_{untreated}$. (**d**) Quantitative analysis from five independent experiments of the STS-induced apoptotic cell population, normalized to the values obtained for the control WEHI7.2 cells (% of control). (**e**) Fluorimetric analysis from three independent experiments of the caspase-3 activity in untreated and STS-treated control, Bcl-2-overexpressing and Bcl-2 K/D overexpressing WEHI7.2 cells using a plate-reader assay. The difference in relative fluorescence units between STS-treated and untreated cells was calculated and plotted. In all these experiments, both Bcl-2 and Bcl-2 K/D significantly (*) protected against STS-induced apoptosis, but Bcl-2 K/D was significantly ($) less potent than Bcl-2. Statistically significant differences are indicated as in Figure 5

Cell culture and transfections. MEF cells were cultured at 37°C in a 9% CO_2 incubator in DMEM/Ham's F12 medium (1 : 1; Invitrogen, Merelbeke, Belgium) supplemented with 10% fetal calf serum (Sigma-Aldrich), 3.8 mM L-glutamine (Glutamax, Invitrogen), 85 IU/ml penicillin and 85 μg/ml streptomycin (Invitrogen). C6 glioma cells were cultured in DMEM/Ham's F12 medium (1 : 1), containing 10% fetal calf serum, 100 IU/ml penicillin, 100 μg/ml streptomycin, 2.5 μg/ml fungizone and 2 mM L-glutamine at 37°C, 5% CO_2. COS-1 cells were seeded at a density of 15 000 cells/cm^2 and cultured in DMEM supplemented with 10% fetal bovine serum (Sigma-Aldrich) at 37°C, 10% CO_2. At 2 days after plating, COS-1 cells were transiently transfected with the empty p3xFLAG-Myc-CMV-24 vector (Sigma-Aldrich) or containing the cDNA of Bcl-2 or of the Bcl-2 K/D mutant. The transfection procedure was performed using JetPRIME transfection reagent (Polyplus Transfections, New York, NY, USA) and following the manufacturer's recommendations. For Ca^{2+}-imaging experiments, COS-1 cells were also co-transfected with a pcDNA 3.1-mCherry vector (Invitrogen) using a DNA ratio of 1 : 2 between pcDNA 3.1-mCherry and p3xFLAG-Myc-CMV-24 vectors.

Table 1 Overview of the sequence of different peptides used in this study

Peptide name	Peptide sequence
BH4-Bcl-2	RTGYDNREIVMKYIHYKLSQRGYEW
BH4-Bcl-Xl	MSQSNRELVVDFLSYKLSQKGYSW
BH4-Bcl-2SCR	WYEKQRSLHGIMYYVIEDRNTKGYR
BH4-Bcl-2BIND	RTGYANAEIVMKYIAEKLSAAGKEW
BH4-Bcl-2 K/D	RTGYDNREIVMKYIHYKLSQRGYEW
BH4-Bcl-Xl D/K	MSQSNRELVVDFLSYKLSQKGYSW
IDP	NVYTEIKCNSLLPLDDIVRV
Biotin-BH4-Bcl-2	Biotin-RTGYDNREIVMKYIHYKLSQRGYEW
Biotin-BH4-Bcl-Xl	Biotin-MSQSNRELVVDFLSYKLSQKGYSW
Biotin-BH4-Bcl-2SCR	Biotin-WYEKQRSLHGIMYYVIEDRNTKGYR
Biotin-BH4-Bcl-XlSCR	Biotin-WYSKQRSLSGLVMYVLEDKNSQFS
Biotin-BH4-Bcl-2BIND	Biotin-RTGYANAEIVMKYIAEKLSAAGKEW
Biotin-BH4-Bcl-2BINDSCR	Biotin-WKEKAASLAGIMEYVIEAANTKGYR
Biotin-BH4-Bcl-2 K/D	Biotin-RTGYDNREIVMDYIHYKLSQRGYEW
Biotin-BH4-Bcl-Xl D/K	Biotin-MSQSNRELVVKFLSYKLSQKGYSW

WEHI7.2 murine cells were grown as described previously[28] and nucleofected with either pSFFV-Neo, pSFFV-Neo-Bcl-2 or pSFFV-Neo-Bcl-2 K/D vectors, using the Amaxa nucleofector and the dedicated Mouse T cell Nucleofector Kit according to the manufacturer's instructions (Amaxa-Lonza AG, Basel, Switzerland). Subsequently, resistant cells were stably selected with 1 mg/ml G418 (Invitrogen) as described in Chen *et al*.,[21] but no clonal expansion was performed.

Western-blot analysis and antibodies. COS-1 and WEHI7.2 cells were lyzed in a buffer containing 25 mM Hepes, pH 7.5, 1% Triton X-100, 10% glycerol, 0.3 M NaCl, 1.5 mM $MgCl_2$, 1 mM DTT, 2 mM EDTA, 2 mM EGTA and protease inhibitor cocktail tablets (Roche, Basel, Switzerland). The protein concentration of samples was determined by Bradford assay (Sigma-Aldrich) using bovine serum albumin (BSA) as standard. Proteins (10–20 μg) were separated by NuPAGE 4–12% Bis/Tris SDS-polyacrylamide gels using MES/SDS-running buffer (Invitrogen) and transferred onto a polyvinylidene fluoride (PVDF) membrane. After blocking with TBS containing 0.1% Tween and 5% non-fat dry milk powder, the membrane was incubated with the primary antibody overnight. Next, membranes were incubated for 1 h with a secondary horseradish peroxidase (HRP)-conjugated antibody (dilution 1 : 2000 in 0.1% Tween/TBS). Protein detection was performed with Pierce ECL Western Blotting Substrate (Thermo Fisher Scientific; p/a Perbio Science BVBA, Erembodegem, Belgium). Bands quantification was done with ImageJ software (rsbweb.nih.gov/ij/).

Primary antibodies used in this study are: mouse monoclonal ANTI-FLAG M2-Peroxidase (HRP) (Sigma-Aldrich), rabbit polyclonal anti-PARP-1 (Alexis-Enzo Life Sciences, Farmingdale, NY, USA), mouse monoclonal Anti-GAPDH clone GAPDH-71.1 (Sigma-Aldrich) and mouse monoclonal anti-Bcl-2 (C2) (Santa Cruz Biotechnology, Santa Cruz, CA, USA).

Unidirectional $^{45}Ca^{2+}$-flux assay. The 12-well clusters containing MEF cells were fixed on a thermostated plate at 30°C on a mechanical shaker. The culture medium was aspirated, and the cells were permeabilized by incubating them for 10 min in a solution containing 120 mM KCl, 30 mM imidazole-HCl (pH 6.8), 2 mM $MgCl_2$, 1 mM ATP, 1 mM EGTA and 20 μg/ml saponin. The non-mitochondrial Ca^{2+} stores were then loaded for 45 min in 120 mM KCl, 30 mM imidazole-HCl (pH 6.8), 5 mM $MgCl_2$, 5 mM ATP, 0.44 mM EGTA, 10 mM NaN_3 to prevent mitochondrial Ca^{2+} uptake, and 150 nM free $^{45}Ca^{2+}$ (28 μCi/ml). After reaching steady-state loading, cells were washed twice with 500 μl of efflux medium (120 mM KCl, 30 mM imidazole-HCl (pH 6.8), 1 mM EGTA) supplemented with 4 μM thapsigargin (Enzo Life Sciences, Farmingdale, NY, USA) to block SERCA (sarcoplasmic-endoplasmic reticulum Ca^{2+} adenosine triphosphatase) Ca^{2+}-uptake activity. Then, efflux medium was added and replaced every 2 min. IP_3 (3 μM) was added for 2 min after 10 min of efflux. At the end of the experiment, all $^{45}Ca^{2+}$ remaining in the stores were released by incubation with 1 ml of a 2% (w/v) SDS solution for 30 min. Ca^{2+} release was plotted as fractional loss (%/2 min) as a function of time as previously described.[46] The fractional loss represents the amount of Ca^{2+} leaving the store in a 2-min time period divided by the total store Ca^{2+} content at that time point. The effect of these BH4-domain peptides on IICR was tested by preincubating the peptides 4 min before exposing the stores to IP_3.

Electroporation loading. *In situ* electroporation of monolayer cell cultures was performed as described before,[32] according to a procedure that was optimized for cell-death studies.[33] C6 cells were grown to near confluency on 13 mm diameter (apoptosis experiments) or 18 mm diameter (Fluo-3 Ca^{2+} imaging) glass coverslips. Cell-monolayer cultures were washed three times with Hanks' balanced salt solution buffered with Hepes (HBSS-Hepes) supplemented with D-glucose (0.81 mM $MgSO_4$, 0.95 mM $CaCl_2$, 137 mM NaCl, 0.18 mM Na_2HPO_4, 5.36 mM KCl, 0.44 mM KH_2PO_4, 5.55 mM D-glucose, 25 mM Hepes, pH 7.4) and subsequently three times with a low-conductivity electroporation buffer (4.02 mM KH_2PO_4, 10.8 mM K_2HPO_4, 1.0 mM $MgCl_2$, 300 mM sorbitol, 2.0 mM Hepes, pH 7.4). They were placed 400 μm underneath a two-wire Pt-Ir electrode on the microscopic stage and electroporated in the presence of a tiny amount of electroporation solution (10 μl). Electroporation was done with 50 kHz bipolar pulses applied as trains of 10 pulses of 2 ms duration each and repeated 15 times. The field strength was 100 V peak-to-peak applied over a 500 μm electrode separation distance. After electroporation, cells were thoroughly washed with HBSS-Hepes.

Fluo-3 Ca^{2+} imaging. C6 cells were seeded on 18 mm diameter glass coverslips and ester-loaded for 25 min with 5 μM Fluo-3-AM (Invitrogen) in HBSS-Hepes supplemented with 1 mM of probenecid (Sigma-Aldrich) and 0.01% pluronic F-127 (Invitrogen) at 37°C, followed by de-esterification over 15 min. Subsequently, cells were loaded with 100 μM Dextran Texas Red (DTR; Invitrogen) and 20 μM Bcl-2 peptides using the *in situ* electroporation technique as described above. For UV flash-photolysis experiments, 50 μM caged IP_3 (Invitrogen) was also included in the loading solution. Imaging was carried out using an inverted fluorescence microscope equipped with a $\times$ 40 oil-immersion objective and an intensified CCD camera (Extended Isis camera, Photonic Science, East Sussex, UK).

In the case of stimulation by ATP, cells were superfused for 1 min with HBSS-Hepes followed by 8 min with 1 μM of ATP (Sigma-Aldrich) in HBSS-Hepes, whereas for TG experiments, cells were superfused for 1 min with Ca^{2+}-free HBSS-Hepes containing 1 mM EGTA followed by 7 min with 2.5 μM TG (Invitrogen) in the same buffer. For IP_3-photoliberation experiments, cells were, after 10 s, spot illuminated with 1-kHz pulsed UV light (349 nm UV laser Explorer, Spectra-Physics, Oxfordshire, UK) during 20 ms (20 pulses of 90 μJ energy measured at the entrance of the microscope epifluorescence tube). The UV flash was applied at five different places along the electroporated area per dish. Images (1/s) were generated with software written in Microsoft Visual C^{++} 6.0 (http://msdn.microsoft.com/en-us/aa336402). Fluorescence-intensity changes in different cells (at least 20) were analyzed with custom-developed FluoFrames software (generated by L Leybaert Lab.). For UV flash photolysis experiments, fluorescence-intensity changes in all cells in a predefined 3950 μm^2 region were analyzed. Ca^{2+}-concentration, (Ca^{2+}), changes were quantified as the area under the curve (AUC) of the separate Ca^{2+} traces. *N* is equal to the number of dishes.

Preparation of GST-fusion proteins. BL21(DE3) *Escherichia coli* cells were transformed with pGEX-6p2 constructs containing cDNAs of IP_3R1 domain 3 (GST-Dom3 IP_3R1: a.a. 923–1581), IP_3R2 domain-3 analog (GST-Dom3 IP_3R2: a.a. 913–1562), IP_3R3 domain-3 analog (GST-Dom3 IP_3R3: a.a. 910–1427) or with

the empty vector. The expressed proteins were purified as previously described.[28] All fusion proteins were affinity purified and dialyzed against standard phosphate-buffered saline (PBS) without added Ca^{2+} or Mg^{2+} (2.67 mM KCl, 1.47 mM KH_2PO_4, 137.93 mM NaCl, 8.06 mM Na_2HPO_4; Invitrogen) using Slide-A-Lyzer with a cutoff of 3 kDa (Thermo Fisher Scientific, Pittsburg, PA, USA). After dialysis, the concentration of the purified GST-fusion proteins was determined using BCA Protein Assay Reagent (Thermo Fisher Scientific), and the quality and integrity were examined by SDS-PAGE and GelCode blue stain reagent (Thermo Fisher Scientific) before GST pull-downs or SPR analysis.

GST pull-downs. Equal amounts (30 μg) of the intact full-length GST-fusion proteins or parental GST (control) were incubated in Interaction Buffer (50 mM Tris-HCl, 300 mM NaCl, 1 mM EDTA, 1% NP-40, 0.5% sodium deoxycholate, 0.5% BSA and protease inhibitor cocktail, pH 7.0) with 30 μg of different BH4 domains (BH4-Bcl-2, BH4-Bcl-Xl or a non-binding mutant (BH4-Bcl-2BIND)) and immobilized on glutathione-Sepharose 4B beads (GE Healthcare Europe GmbH, Munich, Germany) via rotation in a head-over-head rotator for 2 h at 4°C. The beads were washed four times with modified Interaction Buffer (150 mM NaCl instead of 300 mM NaCl, without BSA) and complexed GST-fusion proteins were eluted by incubating the beads with 40 μl LDS (Invitrogen) for 3 min at 95°C and collected after centrifuging at 500 $\times$ *g* for 5 min. Eluates (10 μl) were subjected to western-blot analysis and the total protein content was visualized by GelCode blue staining of the gel.

For the pull-downs with full-length Bcl-2 proteins, 200 μg of cleared lysate from COS-1 cells transiently transfected with the 3xFLAG-Bcl-2 vector, 3xFLAG-Bcl-2-K/D or the empty vector were incubated with GST-tagged proteins using the same protocol as above. Eluates (10 μl) were subjected to western-blot and incubated with anti-FLAG HRP-conjugated antibody, diluted 1 : 4000 in 0.1% Tween/TBS.

SPR measurements. SPR experiments were performed as described before.[47] The binding of GST-Dom3 and parental GST (control) to the wild-type or mutated BH4 domain of Bcl-2 or Bcl-Xl was analyzed by SPR at 25°C using a Biacore 2000 instrument (Uppsala, Sweden). Equal amounts (200 ng or 58.2 pmol) of $>80\%$ pure biotinylated BH4 peptides were immobilized on four different flow cells of a streptavidin-coated sensor chip (BR-1000-32; Biacore, Uppsala, Sweden) using PBS supplemented with 0.005% P20 (Polysorbate-20) at pH 7.0. At least three independent sensor chips were used for the quantitative analysis.

Measurements with GST-fusion proteins as analyte were performed in PBS at a flow rate of 30 μl/min. Different concentrations of the analyte (injection volume 120 μl) were used in a random order to assess binding, expressed in terms of resonance units (RU). Bound peptide was removed by injection of 5 μl regeneration buffer (25 mM NaOH, 0.002% SDS) at 10 μl/min. Background signals were obtained from the reference flow cell, containing the BH4-scrambled peptide, and were subtracted to generate response curves using Biaevaluation 3.0 software (Biacore, http://www.biacore.com). In the analysis, only the association phase of the binding curve was taken into account. Data from two to three different sensorgrams for each condition were fitted by nonlinear regression analysis to a Hill–Langmuir binding isotherm using Origin 7.0 (OriginLab Corporation, Northampton, MA, USA) software.

Fura-2 Ca^{2+} imaging. At 2 days after co-transfection (mCherry + 3xFlag construct), COS-1 cells were loaded with Fura-2-AM (5 μM; Biotium, Inc., Hayward, CA, USA) in modified Krebs buffer (135 mM NaCl, 5.9 mM KCl, 1.2 mM $MgCl_2$, 11.6 mM Hepes, pH 7.3, 11.5 mM glucose and 1.5 mM Ca^{2+}) for 30 min, followed by de-esterification for 30 min. To buffer all free extracellular Ca^{2+}, 5 mM BAPTA (Invitrogen) was added before each measurement. ATP (1 μM) or TG (5 μM)-induced $[Ca^{2+}]$ rises were measured ratiometrically (excitation at 340 nm/380 nm, emission detection at 510 nm) using Zeiss Axio Observer Z1 Inverted Microscope equipped with a $\times$20 air objective and an high-speed digital camera (Axiocam Hsm, Zeiss, Jena, Germany). Intracellular cytoplasmic Ca^{2+} concentrations ($[Ca^{2+}]_{cyt}$) were calculated from the equation: $[Ca^{2+}]_{cyt}$ (nM) $= K_d \times Q \times (R–R_{min})/(R_{max}–R)$, where K_d is the dissociation constant of Fura-2 for Ca^{2+} at room temperature (220 nM), Q is the fluorescence ratio of the emission intensity excited by 380 nm in the absence of Ca^{2+} to that in the presence of saturating Ca^{2+}, R is the fluorescence ratio, R_{min} and R_{max} are the minimal and maximal fluorescence ratios, respectively. The R_{min} was measured by perfusion with 50 mM EGTA in Ca^{2+}-free Krebs solution and R_{max} was obtained by perfusion with 5 μM ionomycin and 250 mM $CaCl_2$. Only mCherry fluorescent (excitation 546 nm, emission 610 nm) and Fura-2 loaded cells were considered for data analysis. Per experiment, 10–15 cells were analyzed for a total of $\sim$80 cells per transfection condition on 3 different experimental days. Traces were normalized to baseline levels with Excel software (Microsoft Office) and for each experiment the average peak value ($\Delta[Ca^{2+}]_{cyt}$) was determined.

Apoptosis induction. For CytC-induced-apoptosis experiments, C6 cells were loaded by *in situ* electroporation in the presence of 100 μM DTR to identify the loaded zone, 20 μM of Bcl-2 peptides or 50 μM IP3RCYT peptide and 10 μM of CytC (Sigma). After electroporation, cells were kept in 200 μl culture medium for 25 min. For STS- and PAC-1-induced apoptosis experiments, cells were electroporated in the presence of 100 μM DTR and 20 μM Bcl-2 peptides. After electroporation, cells were kept in 200 μl culture medium containing 2 μM STS (Sigma-Aldrich) or 150 μM PAC-1 (Tocris Bioscience, Ellisville, MO, USA) for 6 h.

For STS-induced apoptosis, COS-1 cells transiently transfected with 3xFLAG-vectors and WEHI7.2 cells, and stably transfected with the various pSFFV-Neo vectors, were treated for 6 h with 1 μM STS (Sigma-Aldrich).

Detection of apoptosis by fluorescence microscopy. Glioma cells were stained first with 10 μM of the CaspACE FITC-VAD-FMK '*In situ* Marker' (Promega Benelux, Leiden, The Netherlands) in HBSS-Hepes for 40 min at 37°C. After fixing the cells with 4% paraformaldehyde (PFA) for 25 min at room temperature, nuclei were additionally stained for 5 min with 1 μg/ml DAPI (Sigma) in PBS supplemented with Ca^{2+} and Mg^{2+} (PBSD +). Cells were mounted with Vectashield fluorescent mounting medium (VWR International, Leuven, Belgium) on glass slides.

Five images (in each culture) were taken in the electroporated area using a Nikon TE300 epifluorescence microscope equipped with a $\times$10 objective (Plan APO, NA 0.45; Nikon) and a Nikon DS-5M camera (Nikon, Brussels, Belgium). The number of caspase-positive cells and DNA-fragmented nuclei were counted in each image and expressed relative to the number of nuclei present and stated as the AI. Small groups of apoptotic bodies were counted as remnants of a single apoptotic cell. Analyses were carried out blinded, making use of custom-developed counting software. For the STS- and PAC-1-treated cultures, five additional images were taken outside the electroporated area. The AI in the electroporated area was expressed relative to the AI outside the area.

FACS analysis and microplate-based apoptosis assay. WEHI7.2 cells were pelleted by centrifugation and incubated with Annexin-V-FITC (Becton Dickinson, USA) and PI (Invitrogen). Single-cell suspensions were analyzed by FACSCanto (Becton Dickinson, Franklin Lakes, NJ, USA). Cell death by apoptosis and secondary necrosis was scored by quantifying the population of Annexin-V-FITC-positive cells and Annexin-V-FITC/PI-positive cells. Flow-cytometric data were plotted and analyzed using BD FACSDiva Software (Becton Dickinson). Results were normalized as percentage decrease over control conditions.

Caspase-3 activity of STS-treated-WEHI7.2 cells was measured according to the protocol of the commercially available NucView 488 Caspase-3 Kit for live Cells (Biotium). Cells were transferred to a 96-well plate at a density of 400 000 cells/well and fluorescence was monitored using a FlexStation 3 microplate reader (Molecular Devices, Sunnyvale, CA, USA). The fluorescence intensity units collected from treated cells were normalized to untreated controls and plotted as changes in relative fluorescence units (ΔRFU).

Data and statistical analysis. Data are expressed as mean $\pm$ S.E.M., unless a typical experiment is shown (mean $\pm$ S.D.). Statistically significant differences were considered at $P<0.05$ (single symbols), $P<0.01$ (double symbols) and $P<0.001$ (triple symbols) after using a two-tailed paired Student's *t*-test (Excel Microsoft Office) or one-way ANOVA and a Bonferroni post-test using Origin 7.0.

Conflict of interest

The authors declare no conflict of interest.

Acknowledgements. We thank Marina Crabbe, Anja Florizoone and Kirsten Welkenhuyzen for excellent technical help. We thank Dr. Ylva Ivarsson for SPR training. We greatly appreciated the help of Dr. K Mikoshiba (Lab. for Developmental Neurobiology, Brain Science Institute, RIKEN, Japan), Dr. D Boehning (Department of Neuroscience and Cell Biology, University of Texas, Medical Branch, Texas, USA) and Dr. P Zimmermann (Dept. of Human Genetics,

KU Leuven), respectively, for providing the IP_3R2-expression plasmid, IP3RCYT peptide and the use of the BIAcore 2000. This work was supported by the Research Foundation-Flanders (FWO) Grant nos. G.0604.07N to HDS, G.0788.11N to GB and MDM and G.0134.09N to LL, by the Research Council of the KU Leuven via the Concerted Actions program (GOA/09/012) and via an OT START (STRT1/10/044), and by the Interuniversity Attraction Poles Program (Belgian Science Policy; P6/28 to HDS, JBP and LM and P6/31 to LL), and by National Institutes of Health RO1 CA085804 (to CWD). GM and ED were supported by a PhD fellowship from Research Foundation-Flanders (FWO). HA was supported by a postdoctoral fellowship from the Research Foundation-Flanders (FWO).

1. Chipuk JE, Moldoveanu T, Llambi F, Parsons MJ, Green DR. The BCL-2 family reunion. *Mol Cell* 2010; **37**: 299–310.
2. Brunelle JK, Letai A. Control of mitochondrial apoptosis by the Bcl-2 family. *J Cell Sci* 2009; **122**: 437–441.
3. Chipuk JE, Green DR. How do BCL-2 proteins induce mitochondrial outer membrane permeabilization? *Trends Cell Biol* 2008; **18**: 157–164.
4. Bertsch U, Deschermeier C, Fanick W, Girkontaite I, Hillemeier K, Johnen H *et al.* The second messenger binding site of inositol 1,4,5-trisphosphate 3-kinase is centered in the catalytic domain and related to the inositol trisphosphate receptor site. *J Biol Chem* 2000; **275**: 1557–1564.
5. Hunter JJ, Bond BL, Parslow TG. Functional dissection of the human Bc12 protein: sequence requirements for inhibition of apoptosis. *Mol Cell Biol* 1996; **16**: 877–883.
6. Huang DC, Adams JM, Cory S. The conserved N-terminal BH4 domain of Bcl-2 homologues is essential for inhibition of apoptosis and interaction with CED-4. *EMBO J* 1998; **17**: 1029–1039.
7. Oakes SA, Lin SS, Bassik MC. The control of endoplasmic reticulum-initiated apoptosis by the BCL-2 family of proteins. *Curr Mol Med* 2006; **6**: 99–109.
8. Oakes SA, Opferman JT, Pozzan T, Korsmeyer SJ, Scorrano L. Regulation of endoplasmic reticulum Ca^{2+} dynamics by proapoptotic BCL-2 family members. *Biochem Pharmacol* 2003; **66**: 1335–1340.
9. Scorrano L, Oakes SA, Opferman JT, Cheng EH, Sorcinelli MD, Pozzan T *et al.* BAX and BAK regulation of endoplasmic reticulum Ca^{2+}: a control point for apoptosis. *Science* 2003; **300**: 135–139.
10. Rong Y, Distelhorst CW. Bcl-2 protein family members: versatile regulators of calcium signaling in cell survival and apoptosis. *Annu Rev Physiol* 2008; **70**: 73–91.
11. Rizzuto R, Marchi S, Bonora M, Aguiari P, Bononi A, De Stefani D *et al.* Ca^{2+} transfer from the ER to mitochondria: when, how and why. *Biochim Biophys Acta* 2009; **1787**: 1342–1351.
12. Joseph SK, Hajnoczky G. IP_3 receptors in cell survival and apoptosis: Ca^{2+} release and beyond. *Apoptosis* 2007; **12**: 951–968.
13. Pinton P, Giorgi C, Siviero R, Zecchini E, Rizzuto R. Calcium and apoptosis: ER-mitochondria Ca^{2+} transfer in the control of apoptosis. *Oncogene* 2008; **27**: 6407–6418.
14. Hayashi T, Rizzuto R, Hajnoczky G, Su TP. MAM: more than just a housekeeper. *Trends Cell Biol* 2009; **19**: 81–88.
15. Spat A, Szanda G, Csordas G, Hajnoczky G. High- and low-calcium-dependent mechanisms of mitochondrial calcium signalling. *Cell Calcium* 2008; **44**: 51–63.
16. Decuypere JP, Monaco G, Missiaen L, De Smedt H, Parys JB, Bultynck G. IP_3 receptors, mitochondria, and Ca signaling: implications for aging. *J Aging Res* 2011; **2011**: 920178.
17. Bathori G, Csordas G, Garcia-Perez C, Davies E, Hajnoczky G. Ca^{2+}-dependent control of the permeability properties of the mitochondrial outer membrane and voltage-dependent anion-selective channel (VDAC). *J Biol Chem* 2006; **281**: 17347–17358.
18. Csordas G, Renken C, Varnai P, Walter L, Weaver D, Buttle KF *et al.* Structural and functional features and significance of the physical linkage between ER and mitochondria. *J Cell Biol* 2006; **174**: 915–921.
19. Jones RG, Bui T, White C, Madesh M, Krawczyk CM, Lindsten T *et al.* The proapoptotic factors Bax and Bak regulate T cell proliferation through control of endoplasmic reticulum Ca^{2+} homeostasis. *Immunity* 2007; **27**: 268–280.
20. Oakes SA, Scorrano L, Opferman JT, Bassik MC, Nishino M, Pozzan T *et al.* Proapoptotic BAX and BAK regulate the type 1 inositol trisphosphate receptor and calcium leak from the endoplasmic reticulum. *Proc Natl Acad Sci USA* 2005; **102**: 105–110.
21. Chen R, Valencia I, Zhong F, McColl KS, Roderick HL, Bootman MD *et al.* Bcl-2 functionally interacts with inositol 1,4,5-trisphosphate receptors to regulate calcium release from the ER in response to inositol 1,4,5-trisphosphate. *J Cell Biol* 2004; **166**: 193–203.
22. Zhong F, Davis MC, McColl KS, Distelhorst CW. Bcl-2 differentially regulates Ca^{2+} signals according to the strength of T cell receptor activation. *J Cell Biol* 2006; **172**: 127–137.
23. White C, Li C, Yang J, Petrenko NB, Madesh M, Thompson CB *et al.* The endoplasmic reticulum gateway to apoptosis by Bcl-xL modulation of the $InsP_3R$. *Nat Cell Biol* 2005; **7**: 1021–1028.
24. Foskett JK, Yang Y, Cheung KH, Vais H. Bcl-xL regulation of $InsP_3$ receptor gating mediated by dual Ca^{2+} release channel BH3 domains. *Biophys J* 2009; **96** (3 Suppl 1): 391a.
25. Eckenrode EF, Yang J, Velmurugan GV, Foskett JK, White C. Apoptosis protection by Mcl-1 and Bcl-2 modulation of inositol 1,4,5-trisphosphate receptor-dependent Ca^{2+} signaling. *J Biol Chem* 2010; **285**: 13678–13684.
26. Li C, Wang X, Vais H, Thompson CB, Foskett JK, White C. Apoptosis regulation by Bcl-xL modulation of mammalian inositol 1,4,5-trisphosphate receptor channel isoform gating. *Proc Natl Acad Sci USA* 2007; **104**: 12565–12570.
27. Hanson CJ, Bootman MD, Distelhorst CW, Wojcikiewicz RJ, Roderick HL. Bcl-2 suppresses Ca^{2+} release through inositol 1,4,5-trisphosphate receptors and inhibits Ca^{2+} uptake by mitochondria without affecting ER calcium store content. *Cell Calcium* 2008; **44**: 324–338.
28. Rong YP, Aromolaran AS, Bultynck G, Zhong F, Li X, McColl K *et al.* Targeting Bcl-2-IP_3 receptor interaction to reverse Bcl-2's inhibition of apoptotic calcium signals. *Mol Cell* 2008; **31**: 255–265.
29. Rong YP, Bultynck G, Aromolaran AS, Zhong F, Parys JB, De Smedt H *et al.* The BH4 domain of Bcl-2 inhibits ER calcium release and apoptosis by binding the regulatory and coupling domain of the IP_3 receptor. *Proc Natl Acad Sci USA* 2009; **106**: 14397–14402.
30. Rong YP, Barr P, Yee VC, Distelhorst CW. Targeting Bcl-2 based on the interaction of its BH4 domain with the inositol 1,4,5-trisphosphate receptor. *Biochim Biophys Acta* 2009; **1793**: 971–978.
31. Li C, Fox CJ, Master SR, Bindokas VP, Chodosh LA, Thompson CB. Bcl-X(L) affects Ca^{2+} homeostasis by altering expression of inositol 1,4,5-trisphosphate receptors. *Proc Natl Acad Sci USA* 2002; **99**: 9830–9835.
32. De Vuyst E, De Bock M, Decrock E, Van Moorhem M, Naus C, Mabilde C *et al.* In situ bipolar electroporation for localized cell loading with reporter dyes and investigating gap junctional coupling. *Biophys J* 2008; **94**: 469–479.
33. Decrock E, De Vuyst E, Vinken M, Van Moorhem M, Vranckx K, Wang N *et al.* Connexin 43 hemichannels contribute to the propagation of apoptotic cell death in a rat C6 glioma cell model. *Cell Death Differ* 2009; **16**: 151–163.
34. Muchmore SW, Sattler M, Liang H, Meadows RP, Harlan JE, Yoon HS *et al.* X-ray and NMR structure of human Bcl-xL, an inhibitor of programmed cell death. *Nature* 1996; **381**: 335–341.
35. Lee LC, Hunter JJ, Mujeeb A, Turck C, Parslow TG. Evidence for alpha-helical conformation of an essential N-terminal region in the human Bcl2 protein. *J Biol Chem* 1996; **271**: 23284–23288.
36. Boehning D, Patterson RL, Sedaghat L, Glebova NO, Kurosaki T, Snyder SH. Cytochrome c binds to inositol (1,4,5) trisphosphate receptors, amplifying calcium-dependent apoptosis. *Nat Cell Biol* 2003; **5**: 1051–1061.
37. Boehning D, van Rossum DB, Patterson RL, Snyder SH. A peptide inhibitor of cytochrome c/inositol 1,4,5-trisphosphate receptor binding blocks intrinsic and extrinsic cell death pathways. *Proc Natl Acad Sci USA* 2005; **102**: 1466–1471.
38. Kruman I, Guo Q, Mattson MP. Calcium and reactive oxygen species mediate staurosporine-induced mitochondrial dysfunction and apoptosis in PC12 cells. *J Neurosci Res* 1998; **51**: 293–308.
39. Nutt LK, Chandra J, Pataer A, Fang B, Roth JA, Swisher SG *et al.* Bax-mediated Ca^{2+} mobilization promotes cytochrome c release during apoptosis. *J Biol Chem* 2002; **277**: 20301–20308.
40. Putt KS, Chen GW, Pearson JM, Sandhorst JS, Hoagland MS, Kwon JT *et al.* Small-molecule activation of procaspase-3 to caspase-3 as a personalized anticancer strategy. *Nat Chem Biol* 2006; **2**: 543–550.
41. Palmer AE, Jin C, Reed JC, Tsien RY. Bcl-2-mediated alterations in endoplasmic reticulum Ca^{2+} analyzed with an improved genetically encoded fluorescent sensor. *Proc Natl Acad Sci USA* 2004; **101**: 17404–17409.
42. Kaufmann T, Schlipf S, Sanz J, Neubert K, Stein R, Borner C. Characterization of the signal that directs Bcl-xL, but not Bcl-2, to the mitochondrial outer membrane. *J Cell Biol* 2003; **160**: 53–64.
43. Shimizu S, Konishi A, Kodama T, Tsujimoto Y. BH4 domain of antiapoptotic Bcl-2 family members closes voltage-dependent anion channel and inhibits apoptotic mitochondrial changes and cell death. *Proc Natl Acad Sci USA* 2000; **97**: 3100–3105.
44. Cory S, Huang DC, Adams JM. The Bcl-2 family: roles in cell survival and oncogenesis. *Oncogene* 2003; **22**: 8590–8607.
45. Zhong F, Harr MW, Bultynck G, Monaco G, Parys JB, De Smedt H *et al.* Induction of Ca^{2+}-driven apoptosis in chronic lymphocytic leukemia cells by peptide-mediated disruption of Bcl-2-IP_3 receptor interaction. *Blood* 2011; **117**: 2924–2934.
46. Decuypere JP, Monaco G, Kiviluoto S, Oh-hora M, Luyten T, De Smedt H *et al.* STIM1, but not STIM2, is required for proper agonist-induced Ca^{2+} signaling. *Cell Calcium* 2010; **48**: 161–167.
47. Ponsaerts R, De Vuyst E, Retamal M, D'Hondt C, Vermeire D, Wang N *et al.* Intramolecular loop/tail interactions are essential for connexin 43-hemichannel activity. *FASEB J* 2010; **24**: 4378–4395.

Supplementary Information accompanies the paper on Cell Death and Differentiation website (http://www.nature.com/cdd)

PART I -*Supplementary information*

Selective regulation of IP_3-receptor-mediated Ca^{2+} signaling and apoptosis by the BH4 domain of Bcl-2 versus Bcl-Xl

Giovanni Monaco[1#], Elke Decrock[2#], Haidar Akl[1], Raf Ponsaerts[1], Tim Vervliet[1], Tomas Luyten[1], Marc De Maeyer[3], Ludwig Missiaen[1], Clark W. Distelhorst[4], Humbert De Smedt[1], Jan B. Parys[1], Luc Leybaert[2], Geert Bultynck[1]

Cell Death Differ. 2012,19:295-309.

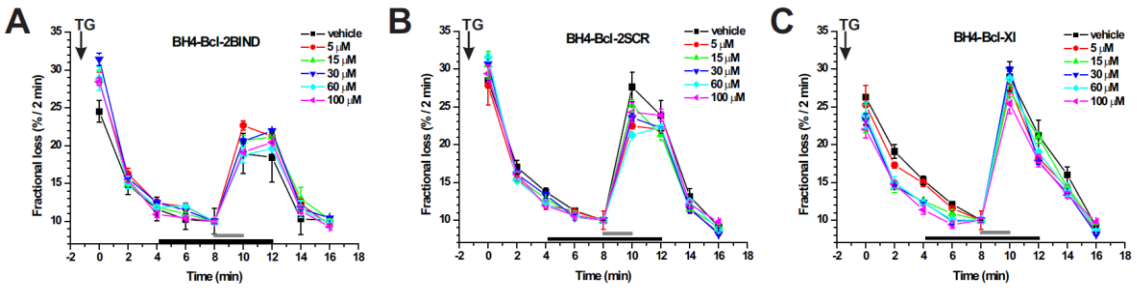

Supplemental Fig. 1. Unidirectional $^{45}Ca^{2+}$-flux assay shown as fractional loss (% / 2 min) as a function of time. The IP_3-induced Ca^{2+} release (gray bar) was measured in the presence of different concentrations of BH4-Bcl-2BIND (A), BH4-Bcl-2SCR (B) and BH4-Bcl-Xl (C) (black bars).

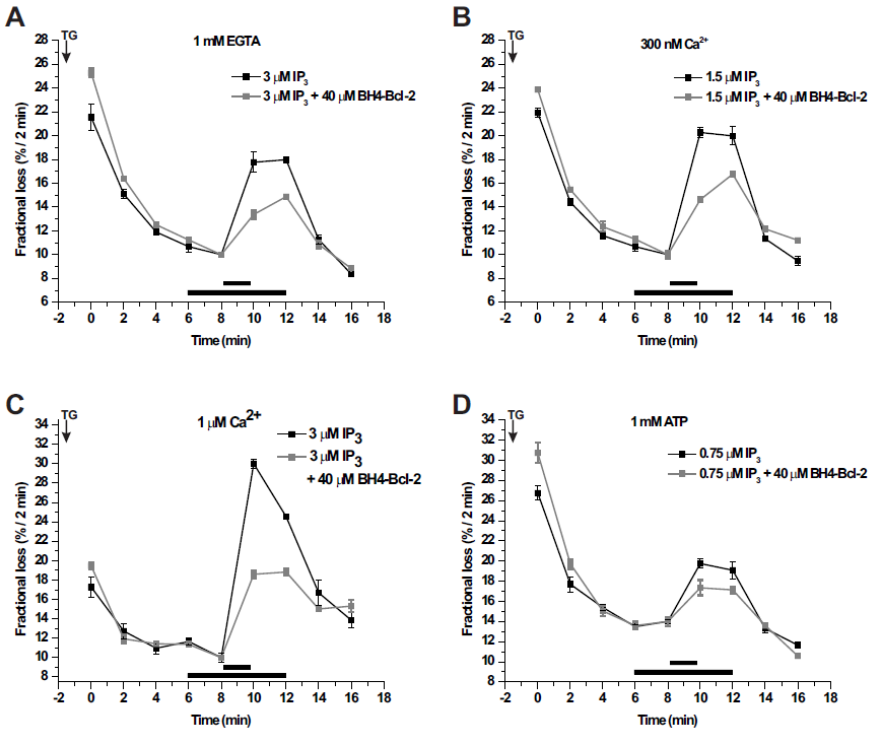

Supplemental Fig. 2. Unidirectional $^{45}Ca^{2+}$-flux assay shown as fractional loss (% / 2 min) as a function of time. The inhibitory effect of 40 μM BH4-Bcl-2 (long lower bars) on IP_3-induced Ca^{2+} release (short upper bar) was measured in the presence of 1 mM (A) EGTA, 300 nM free Ca^{2+}, 1 μM free Ca^{2+} and 1 mM ATP.

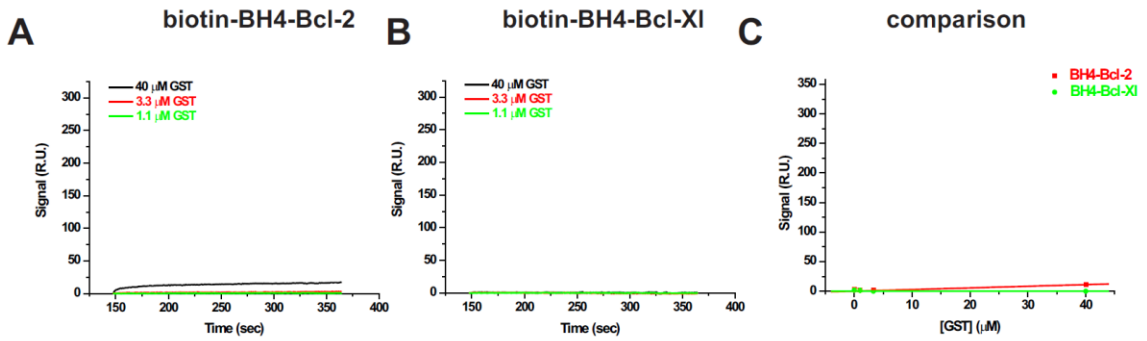

Supplemental Fig. 3. Results obtained with SPR for the binding of different concentrations of GST to biotin-BH4-Bcl-2 and biotin-BH4-Bcl-Xl. A, Typical sensorgrams for the association phase of the binding of GST to biotin-BH4-Bcl-2 corrected for the background binding to its scrambled version. B, Typical sensorgrams for the association phase of the binding of GST to biotin-BH4-Bcl-Xl corrected for the background binding to its scrambled version. C, Analysis of the maximal R.U. values obtained from at least three independent experiments.

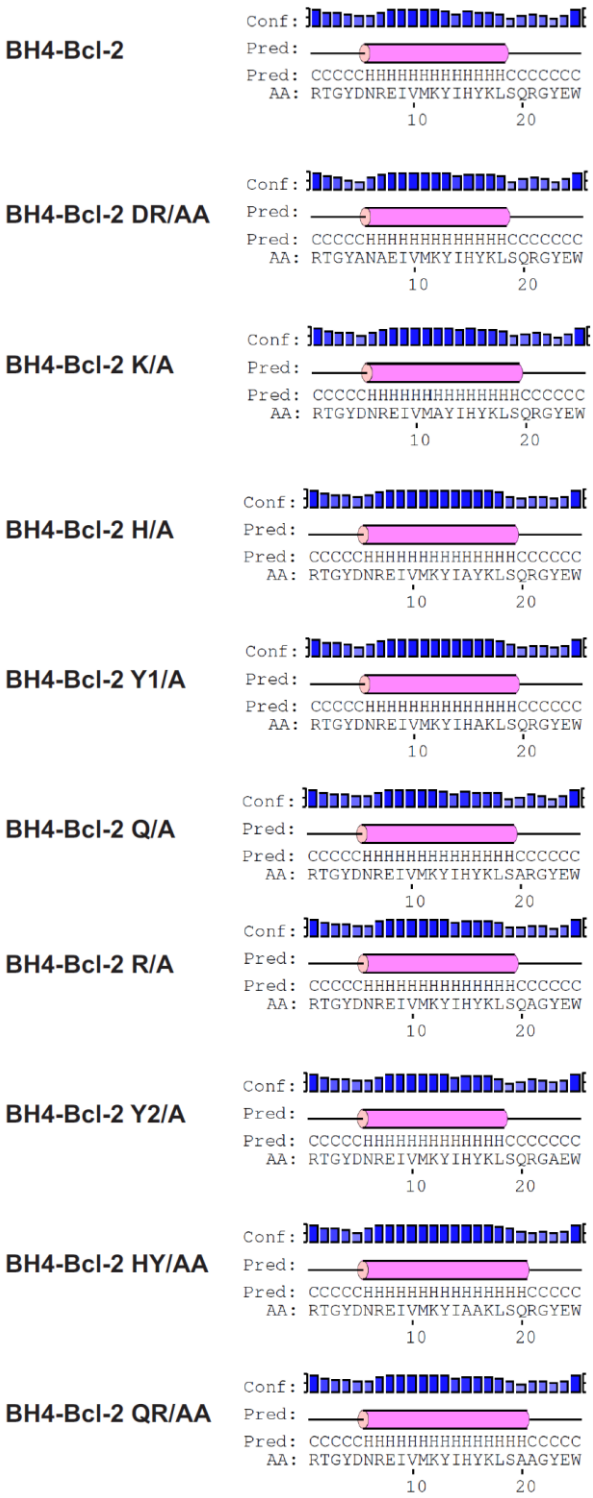

Supplemental Fig. 4. Secondary structure prediction of BH4-Bcl-2 its different Ala-mutant forms using PSIPREDv3.0 (H = α-helix, C = coiled).

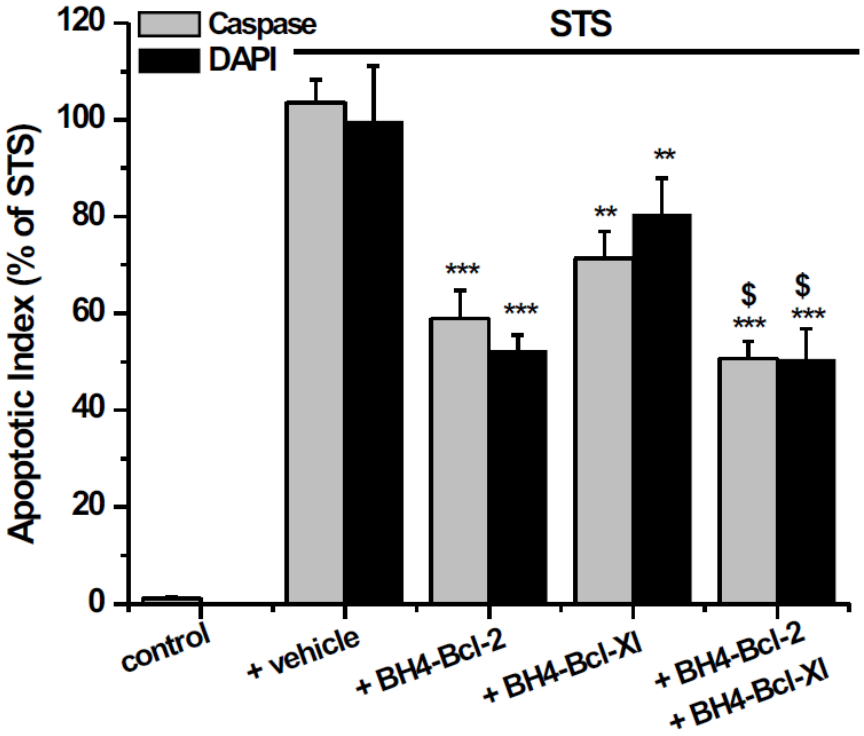

Supplemental Fig. 5. Staurosporin (STS)-induced apoptosis in C6-glioma cells and the effect of electroporating BH4-Bcl-2 (20 μM), BH4-Bcl-Xl (20 μM) or BH4-Bcl-2 (20 μM) + BH4-Bcl-Xl (20 μM). The combination of BH4-Bcl-2 of BH4-Bcl-Xl did not provoke an additive effect compared to the effects provoked by BH4-Bcl-2 and BH4-Bcl-Xl alone .

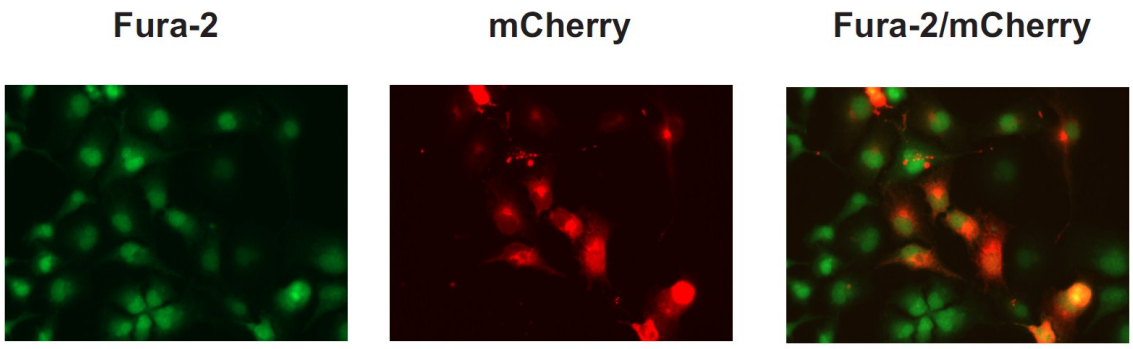

Supplemental Fig. 6. Typical images of COS-1 cells loaded with Fura-2 (green) and transfected with mCherry-expression plasmid (red). This analysis indicates that 30 to 40 % of the cells are transfected with the plasmid. Only mCherry-containing cells were analysed in the single cell Ca^{2+} experiments.

PART II

Addressing objective III.

Secondary structure determinants for the inhibition of the IP_3 receptor by a Bcl-2-BH4-domain peptide

Giovanni Monaco[1], Elke Decrock[2], Koen Nuyts[3], Larry E. Wagner II[4], Tomas Luyten[1], Sergei Strelkov[5], Ludwig Missiaen[1], Wim M. De Borggraeve[3], Luc Leybaert[2], David I. Yule[4], Humbert De Smedt[1], Jan B. Parys[1], Geert Bultynck[1]

[1] Laboratory of Molecular and Cellular Signaling, Department of Cellular and Molecular Medicine, KU Leuven, Leuven, Belgium

[2] Department of Basic Medical Sciences, Physiology Group, Faculty of Medicine and Health Sciences, Ghent University, Ghent, Belgium

[3] Section of Molecular Design and Synthesis, Department of Chemistry, KU Leuven, Heverlee, Belgium

[4] Department of Pharmacology & Physiology, School of Medicine and Dentistry, University of Rochester Medical Center, Rochester, NY, USA

[5] Laboratory for Biocrystallography, Department of Pharmaceutical and Pharmacological Sciences, KU Leuven, Leuven, Belgium.

under revision, PLoS One

Secondary structure determinants for the inhibition of the IP_3 receptor by a Bcl-2-BH4-domain peptide

Giovanni Monaco[1], Elke Decrock[2], Koen Nuyts[3], Larry E. Wagner II[4], Tomas Luyten[1], Sergei Strelkov[5], Ludwig Missiaen[1], Wim M. De Borggraeve[3], Luc Leybaert[2], David I. Yule[4], Humbert De Smedt[1], Jan B. Parys[1] and Geert Bultynck[1]

[1]Laboratory of Molecular and Cellular Signaling, Department of Cellular and Molecular Medicine, KU Leuven, Leuven, Belgium; [2]Department of Basic Medical Sciences, Physiology Group, Faculty of Medicine and Health Sciences, Ghent University, Ghent, Belgium; [3]Section of Molecular Design and Synthesis, Department of Chemistry, KU Leuven, Heverlee, Belgium; [4]Department of Pharmacology & Physiology, School of Medicine and Dentistry, University of Rochester Medical Center, Rochester, NY, USA; [5]Laboratory for Biocrystallography, Department of Pharmaceutical and Pharmacological Sciences, KU Leuven, Leuven, Belgium.

To whom correspondence should be addressed (E-mails: Geert.Bultynck@med.kuleuven.be; Giovanni.Monaco@med.kuleuven.be)

Page heading title: Bcl-2-BH4 peptide structure and IP_3R regulation

Abstract

The anti-apoptotic Bcl-2 protein is the founding member and namesake of the Bcl-2-protein family. It has recently been demonstrated that Bcl-2, apart from its anti-apoptotic role at mitochondrial membranes, can also directly interact with the inositol 1,4,5-trisphosphate receptor (IP_3R), the primary Ca^{2+}-release channel in the endoplasmic reticulum (ER). Bcl-2 can thereby reduce pro-apoptotic IP_3R-mediated Ca^{2+} release from the ER. Moreover, the Bcl-2 homology domain 4 (Bcl-2-BH4) has been identified as essential and sufficient for this IP_3R-mediated anti-apoptotic activity. In the present study, we investigated whether the reported inhibitory effect of a Bcl-2-BH4 peptide on the IP_3R was related to the distinctive alpha-helical conformation of the BH4 domain peptide. We therefore designed a peptide with two glycine "hinges" replacing residues I14 and V15, of the wild-type Bcl-2-BH4 domain (Bcl-2-BH4-IV/GG). By comparing the structural and functional properties of the Bcl-2-BH4-IV/GG peptide with its native counterpart, we found that the variant contained reduced alpha helicity, did neither bind nor inhibit the IP_3R channel, and in turn lost its anti-apoptotic effect. These results provide new insights for the further development of Bcl-2-BH4-derived peptides as specific inhibitors of the IP_3R with important pharmacological implications.

Key words: Intracellular Ca^{2+}-release channels / Anti-apoptotic Bcl-2-family members / Ca^{2+} signaling / Endoplasmic reticulum / BH4-domain peptide

Introduction

Intracellular Ca^{2+} homeostasis requires a tight cross-talk between the endoplasmic reticulum (ER) and the mitochondria. Although mitochondria need basal levels of Ca^{2+} to sustain cellular bioenergetics demands, mitochondrial Ca^{2+} overload leads to the onset of mitochondrial outer membrane permeabilization (MOMP) and downstream apoptosis activation [1,2,3,4]. Anti-apoptotic Bcl-2 family members have a dual role in MOMP prevention: 1) they antagonize the pore-forming activity of their pro-apoptotic relatives, BAX and BAK, on mitochondria and 2) they fine-tune the ER-mitochondria interplay towards pro-survival or anti-apoptotic Ca^{2+} signals [5,6,7,8,9]. In the latter scenario, numerous studies have shown that Bcl-2, localized at the ER membranes, is able to control the ER Ca^{2+} content and Ca^{2+} release. It was suggested that Bcl-2 could exert its protective function by decreasing the luminal Ca^{2+} content *via* an interaction with the sarco/endoplasmic-reticulum Ca^{2+}-ATPase (SERCA) [10,11] or more generally by increasing the passive leak of Ca^{2+} across the ER membrane [12,13,14,15,16]. In addition, Eckenrode et al. [17] proposed a direct interaction of anti-apoptotic proteins (Bcl-2, Bcl-Xl and Mcl-1) with the C-terminus of inositol 1,4,5-trisphosphate receptors (IP_3Rs), increasing the activity of these ER channels and therefore decreasing the steady-state $[Ca^{2+}]_{ER}$**.** On the other hand, Distelhorst and collaborators as well as our own group have demonstrated that Bcl-2, by interacting with the central, modulatory region of the IP_3R, inhibited pro-apoptotic Ca^{2+} signals from the ER without affecting steady-state Ca^{2+} concentration in the ER ($[Ca^{2+}]_{ER}$**)**. Our data identified the BH4 domain as an essential and sufficient component of Bcl-2 component responsible for the direct inhibition of IP_3-induced Ca^{2+} release (IICR) and apoptosis [18,19,20]. Furthermore, the BH4 domain is essential for many anti-apoptotic members of the Bcl-2 family (like Bcl-2 and Bcl-Xl) since its deletion abrogates their anti-apoptotic activity [21,22,23]. Remarkably, the isolated Bcl-2-BH4 domain was sufficient to protect against Ca^{2+}-mediated apoptosis by

selectively acting on the IP_3Rs [24,25], whereas the very similar Bcl-Xl-BH4 domain did not show any IP_3R-dependent-protective activity [24].

The functional BH4 domain in the native N-terminal domain of Bcl-2, comprises a stretch of 20 amino acids (a.a. 10 to 30) organized in an alpha-helical structure (α1) [26,27,28]. As we previously showed, some residues of the Bcl-2-BH4 domain (K17, H20, Y21 and R26, Fig. 1A) coordinate the inhibitory function of the Bcl-2-BH4 peptide on the IP_3Rs [24]. These residues are highly surface-accessible in the native Bcl-2 protein and proximal in the secondary structure-backbone [29]. Hence, we hypothesized that the Bcl-2-BH4 peptide may need a stable alpha-helical structure for inhibiting the IP_3R-channel activity. To test our hypothesis, we selected, by *in silico* analysis, a peptide modification that is predicted to affect BH4-alpha-helical stability. More specifically, we used a modified version of the Bcl-2-BH4 peptide that carries a change in two hydrophobic residues, which are part of the N-terminal alpha helix of the native Bcl-2 but display a poor surface accessibility in the full-length protein [28,29,30]. In this peptide, residues I14 and V15 have been replaced with two glycines to introduce high flexibility in the structure and destabilize helical conformation of the peptide. We applied this modified peptide in a series of functional experiments, addressing its ability to bind IP_3Rs, inhibit single-channel activity, curb IICR and protect against Ca^{2+}-dependent apoptosis.

Materials and methods

Peptides, plasmids and antibodies

The following peptides, obtained from Thermo Electron, Germany, were used: Bcl-2-BH4: *RTGYDNREIVMKYIHYKLSQRGYEW*; Bcl-2-BH4 IV/GG: *RTGYDNREGGMKYIHYKLSQRGYEW*. All peptides were more than 80% pure and their identity was confirmed via mass spectrometry (MS). The pGEX-6p2 construct (Amersham

Biosciences, GE healthcare) encoding amino acids 923-1581 of mouse IP_3R1 Domain 3 was obtained as previously described [24].

Cell culture and transfections

Mouse embryonic fibroblasts (MEF cells) [31] were cultured at 37°C in a 9% -CO_2 incubator in DMEM/Ham's F12 medium (1:1) (Invitrogen, Belgium) supplemented with 10% fetal calf serum (Sigma-Aldrich), 3.8 mM L-glutamine (Glutamax, Invitrogen), 85 IU/ml penicillin and 85 µg/ml streptomycin (Invitrogen). Rat C6 glioma cells [32,33] were cultured in DMEM/Ham's F12 medium (1:1), containing 10% fetal calf serum, 100 IU/ml penicillin, 100 µg/ml streptomycin, 2.5 µg/ml fungizone and 2 mM L-glutamine at 37°C and 5% CO_2. DT40-3KO cells, stably expressing rIP_3R1 [34], were cultured at 39°C in a 5% CO_2 incubator in RPMI (Invitrogen) supplemented with 2.05 mM L-glutamine, 10% fetal calf serum, 1% chicken serum, 100 IU/ml penicillin, and 100 µg/ml streptomycin (Invitrogen).

Peptide stability and secondary-structure predictions

To calculate the change in pseudo-thermodynamic stability induced by the GG substitutions, we used 4 different automated estimators of free-energy-change variations (ΔΔG), namely Concoord/Poisson-Bolzmann Surface Area [35], Eris [36], PoPMuSiC-2.1 [37] and SDM [38]. First, we extrapolated the structure of the Bcl-2-BH4 peptide from the PDB file corresponding to the NMR structure of Bcl-2 protein (PDB: 1G5M, [26]) and submitted it successively to the prediction servers. In some cases, we also needed to perform the computational mutation (single or double glycine substitutions) by ourselves using the PyMOL (http://pymol.sourceforge.net/) mutagenesis tool and energy minimizing the resulting structures with the short discrete molecular dynamics (DMD) simulations of the CHIRON server [39]. The ΔΔG values (in kcal/mol) reported in this study correspond to the average of

the 4 calculations ± SD. Additionally, the I-TASSER v2.1 webserver [40,41] was used to predict the secondary structure of Bcl-2-BH4 and Bcl-2-BH4 IV/GG peptides from their primary sequence. I-TASSER builds protein models using iterative assembling procedures and multiple threading alignments from template structures libraries. An estimate of accuracy of the predictions is provided based on the confidence score of the modeling. Only the predictive models with the highest confidence scores were considered from the server output page. These PDB files were downloaded and imported in PyMOL to generate high-quality images.

CD spectroscopy

CD spectra (Jasco J-810 circular dichroism spectropolarimeter, USA) were recorded at 1 nm intervals over the 190-260 nm wavelength range using 1 mm path length quartz cells (Hellma, Germany). Ten scans were performed. The experiments were run at 20 nm/min and the temperature was fixed at 298º K (25 °C). The secondary structure of the peptide (50 µM) was determined in 97.5% TFE and 2.5% methanol. To estimate the secondary structure of the peptide in terms of alpha-helical content, an analysis of the relevant CD spectra was carried out using the CDPro software (http://lamar.colostate.edu/~sreeram/CDPro/main.html) developed by Woody and coworkers [42]. The basis set 10 of the CDPro software was used [43]. The analysis was performed using the CONTIN/LL [44] a self-consistent method with an incorporated variable selection.

Preparation of GST-fusion proteins

BL21(DE3) **Escherichia coli** cells were transformed with pGEX-6p2 constructs containing cDNAs of IP_3R1 Domain 3 (GST-Dom3 IP_3R1: aa 923-1581). The expressed protein was purified as previously described [19]. GST-fused-IP_3R1 Domain 3 was affinity purified and

dialyzed against standard phosphate-buffered saline (PBS) without added Ca^{2+} or Mg^{2+} (2.67 mM KCl, 1.47 mM KH_2PO_4, 137.93 mM NaCl, 8.06 mM Na_2HPO_4; Invitrogen) using Slide-A-Lyzer with a cut-off of 3 kDa (Thermo Fisher Scientific, USA). After dialysis, the concentration of the purified GST-fusion protein was determined using BCA Protein-Assay Reagent (Thermo Fisher Scientific), and the quality and integrity were examined by SDS-PAGE and GelCode™ (Thermo Fisher Scientific) blue stain reagent prior to GST-pull downs.

GST-pull-down assays

Equal amounts (30 µg) of the intact full-length GST-Dom3 IP_3R1 or parental GST (control) were incubated in Interaction Buffer (50 mM Tris-HCl, 300 mM NaCl, 1 mM EDTA, 1% NP-40, 0.5% sodium deoxycholate, 0.5% bovine serum albumin (BSA) and protease inhibitor cocktail, pH 7.0) with 30 µg of different BH4 domains (Bcl-2-BH4, Bcl-2-BH4 IV/GG) and immobilized on glutathione-Sepharose 4B beads (GE Healthcare Europe GmbH, Belgium) *via* rotation in a head-over-head rotator for 2 h at 4°C. The beads were washed 4 times with modified Interaction Buffer (150 mM NaCl instead of 300 mM NaCl, without BSA) and complexed GST-fusion proteins were eluted by incubating the beads with 40 µl LDS® (Invitrogen) for 3 min at 95°C and collected after centrifuging at 500 g for 5 min. Eluates (10 µl) were subjected to SDS-PAGE.

SDS-PAGE

Sample protein concentrations were determined by Bradford assay (Sigma-Aldrich) using BSA as standard. Proteins (10-20 µg) were separated by NuPAGE 4–12% Bis/Tris SDS-polyacrylamide gels using MES/SDS-running buffer (Invitrogen). The gels were stained with

GelCode™ blue stain reagent following the manufacturer recommendations. The resulting bands were quantified by using ImageJ software (rsbweb.nih.gov/ij/).

Unidirectional $^{45}Ca^{2+}$-flux assay

$^{45}Ca^{2+}$-unidirectional flux experiments were performed as previously described [24]. Twelve-well clusters containing MEF cells were fixed on a thermostated plate at 30°C on a mechanical shaker. The culture medium was aspirated, and the cells were permeabilized by incubating them for 10 min in a solution containing 120 mM KCl, 30 mM imidazole-HCl (pH 6.8), 2 mM $MgCl_2$, 1 mM ATP, 1 mM EGTA and 20 µg/ml saponin. The non-mitochondrial Ca^{2+} stores were then loaded for 45 min in 120 mM KCl, 30 mM imidazole-HCl (pH 6.8), 5 mM $MgCl_2$, 5 mM ATP, 0.44 mM EGTA, 10 mM NaN_3 to prevent mitochondrial Ca^{2+} uptake, and 150 nM free $^{45}Ca^{2+}$ (28 µCi/ml). Then, 1 ml of efflux medium containing 120 mM KCl, 30 mM imidazole-HCl (pH 6.8) and 1 mM EGTA was added and replaced every 2 min. IP_3 (3 µM) was added for 2 min after 10 min of efflux. At the end of the experiment, all $^{45}Ca^{2+}$ remaining in the stores was released by incubation with 1 ml of a 2% (w/v) sodium dodecyl sulfate solution for 30 min. Ca^{2+} release was plotted as fractional loss (% / 2 min) as a function of time as previously described [24]. The effect of the BH4-domain peptides on IICR was tested by pre-incubating the peptides for 4 min before exposing the stores to IP_3.

Electroporation loading

In situ electroporation of adherent C6 cell monolayer cultures was performed as previously described [32], according to a procedure optimized for cell-death studies [45,46]. C6 cells were grown to near confluency on 13 mm- (apoptosis experiments) or 18 mm- (flash photolysis of caged IP_3 and $[Ca^{2+}]_{cyt}$ imaging) diameter glass coverslips. Cell monolayers were washed 3 times with Hanks' balanced salt solution buffered with Hepes (HBSS-Hepes) supplemented with D-glucose (0.81 mM $MgSO_4$, 0.95 mM $CaCl_2$, 137 mM NaCl, 0.18 mM

Na_2HPO_4, 5.36 mM KCl, 0.44 mM KH_2PO_4, 5.55 mM D-glucose, 25 mM Hepes, pH 7.4) and subsequently 3 times with a low-conductivity electroporation buffer (4.02 mM KH_2PO_4, 10.8 mM K_2HPO_4, 1.0 mM $MgCl_2$, 300 mM sorbitol, 2.0 mM Hepes, pH 7.4). They were placed 400 μm underneath a two-wire Pt-Ir electrode on the microscopic stage and electroporated in the presence of a tiny amount of electroporation solution (10 μl). Electroporation was done with 50 kHz bipolar pulses applied as trains of 10 pulses of 2 ms duration each and repeated 15 times. The field strength was 100 V peak-to-peak applied over a 500 μm electrode separation distance. After electroporation, cells were thoroughly washed with HBSS-Hepes.

Electrophysiology

Isolated DT40 nuclei were prepared by homogenization as previously described [34]. 3 μl of nuclear suspension were placed in 3 ml of bath solution which contained 140 mM KCl, 10 mM HEPES, 500 μM BAPTA, and 246 nM free Ca^{2+}, pH 7.1. Nuclei were allowed to adhere to a plastic culture dish for 10 minutes prior to patching. Single IP_3R channel potassium currents (i_k) were measured in the on-nucleus patch clamp configuration using PClamp 9 and an Axopatch 200B amplifier (Molecular Devices, Sunnydale, California) as previously described [47]. Pipette solution contained 140 mM KCl, 10 mM HEPES, 1 μM IP_3, 5 mM ATP, 100 μM BAPTA, and 200 nM free Ca^{2+}. Effects of the BH4 peptides on channel activity were examined by including 50 μM of the appropriate peptide in the pipette solution. Traces were recorded at -100 mV, sampled at 20 kHz and filtered at 5 kHz. A minimum of 15 seconds of recordings were considered for data analyses. Pipette resistances were typically 20 MΩ and seal resistances were >5 GΩ. Single channel open probabilities (P_o) were calculated by half-threshold crossing criteria using the event detection protocol in Clampfit 9. We assumed that the number of channels in any particular nuclear patch is represented by the maximum number of discrete stacked events observed during the experiment. Even at low P_o,

stacking events were evident [34]. Only patches with 1 apparent channel were considered for analyses.

Flash photolysis of caged IP_3 and $[Ca^{2+}]_{cyt}$ imaging

Changes in $[Ca^{2+}]_{cyt}$, triggered by photolytic release of IP_3 from a caged inactive precursor (caged IP_3; Invitrogen), were monitored according to a protocol described in detail in [46]. Briefly, C6 cells were seeded on 18 mm-diameter glass coverslips and ester-loaded for 25 min with 5 µM Fluo-3-AM (Invitrogen) in HBSS-Hepes supplemented with 1 mM probenecid (Sigma-Aldrich) and 0.01% pluronic F-127 (Invitrogen) at 37°C, followed by de-esterification over 15 min. Subsequently, cells were loaded with 100 µM Dextran Tetramethyl Rhodamine (DTR) (Invitrogen), 20 µM BH4 peptides and 50 µM caged IP_3 (Invitrogen) using the *in situ* electroporation technique as described above. Imaging was carried out using a Nikon Eclipse TE300 inverted epifluorescence microscope equipped with a 40x oil-immersion objective (Plan Fluor, NA 1.30; Nikon) and an EM-CCD camera (QuantEM™ 512SC CCD camera, Photometrics, Tucson, AZ). The UV flash (349 nm UV DPSS laser, Explorer; Spectra-Physics, Newport, Irvine, USA) was applied at 5 different places along the electroporated area per dish. Images (1 s) were generated with software written in Microsoft Visual C 6.0. Fluorescence-intensity changes in all cells in a predefined 3950µm^2 region were analyzed with custom-developed FluoFrames software (generated by L.L. and collaborators, Univ. Gent, Belgium.). $[Ca^{2+}]_{cyt}$ changes were quantified as the area under the curve of the separate Ca^{2+} traces. A minimum of 5 dishes have been used for each condition.

Apoptosis induction and detection

C6 glioma cells were electroporated in the presence of 100 µM DTR and 20 µM BH4 peptides. After electroporation, cells were kept in 200 µl culture medium containing 2 µM

STS (Sigma-Aldrich). Six hours later, cultures were stained first with 10 μM of the CaspACE FITC-VAD-FMK '*In situ* Marker' (Promega Benelux, Leiden, The Netherlands) in HBSS-Hepes for 40 min at 37°C. After fixing the cells with 4% paraformaldehyde for 25 min at room temperature, nuclei were additionally stained for 5 min with 1 μg/ml DAPI (Sigma) in PBS supplemented with Ca^{2+} and Mg^{2+} (PBSD+). Cells were mounted with Vectashield fluorescent mounting medium (VWR International, Leuven, Belgium) on glass slides. Five images (in each culture) were taken in the electroporated area and five outside the electroporated area using a Nikon TE300 epifluorescence microscope equipped with a 10x objective (Plan APO, NA 0.45; Nikon) and a Nikon DS-Ri1 camera (Nikon, Brussels, Belgium). The number of caspase-positive cells and DNA-fragmented nuclei were counted in each image and expressed relative to the number of nuclei present and expressed as the AI (apoptotic index). Small groups of apoptotic bodies were counted as remnants of a single apoptotic cell. Analyses were carried out blinded, making use of custom-developed counting software. The AI in the electroporated area was expressed relative to the AI outside the area.

Data and statistical analysis

Data are expressed as means ± SEM, unless a typical experiment is shown (mean ± SD). Statistically significant differences were considered at $P<0.05$ (single symbols), $P<0.01$ (double symbols) and $P<0.001$ (triple symbols) after using a two-tailed paired Student's *t* test (Excel Microsoft Office) or one-way ANOVA and a Bonferroni post-test using Origin7.0.

Results

Alpha-helix destabilization by I14G/V15G substitution in the Bcl-2-BH4-domain peptide (Bcl-2-BH4 IV/GG)

To maximize the chances of obtaining a peptide with decreased helical propensity, we opted for replacing two adjacent amino acids in the core of the Bcl-2-BH4 sequence with glycines. Glycines are well-known helix destabilizers by introducing an excessive degree of flexibility in the helix backbone [48,49,50]. The following rationale was adopted to select the target amino acids for the GG substitution: we avoided the residues previously proposed to be important in the IP_3R interaction (K17, H20, Y21 and R26), but we still aimed at the core of the alpha-helical structure. Therefore, we focused on four possible target residues (R12, E13, I14, V15, (Fig. 1A, 1B left panel) and predicted, by *in silico* analysis, the change in thermodynamic stability and secondary structure induced by glycine substitutions. The analysis suggested that by modifying I14 -V15 or E13-I14 into glycines one would obtain the highest degree of structure destabilization ($\Delta\Delta G$ of approximately 5 kcal/mol) (Fig. 1B, right panel). However, IV/GG would be the most suitable substitution since I14 and V15 are buried residues in the native structure of the full-length Bcl-2 protein and clearly not available for possible molecular interactions [29,30]. Accordingly, the I-TASSER webserver (http://zhanglab.ccmb.med.umich.edu/I-TASSER/) suggests that an alpha-helical structure covers at least 40% of the wild-type BH4-peptide sequence (Fig. 1C, upper panel) while the low confidence prediction for the IV/GG mutant (confidence scores ≤ 4) would indicate a much lower tendency to form an alpha helix (Fig. 1C, lower panel).

To validate the *in silico* findings, we performed circular dicroism (CD) spectroscopy and compared the propensity of Bcl-2-BH4 and Bcl-2-BH4 IV/GG peptides to form an alpha helix in 2,2,2-trifluoroethanol (TFE). This solvent has been shown to induce and stabilize alpha

helices in sequences with intrinsic helical propensity [51,52]. The far-UV CD spectrum of Bcl-2-BH4 demonstrated the presence of a stable alpha-helical structure, by showing the typical two spectral minima at 208 and 222 nm. A different pattern was observed for the Bcl-2-BH4-IV/GG mutant, which displayed a singular minimum of ellipticity detectable at about 215 nm. Therefore, the mutant appears to have less propensity to form an alpha helix, as compared to the wild-type BH4 domain, and rather displays a beta-sheet-like structure (Fig. 1D) [53]. Deconvolution of the CD traces provided us with an alpha-helical content of 20.4% and 8.4% for Bcl-2-BH4 and Bcl-2-BH4 IV/GG, respectively. This initial analysis indicated that amino acids I14 and V15 are important to properly stabilize the native alpha–helical conformation of the Bcl-2 BH4 peptide.

A

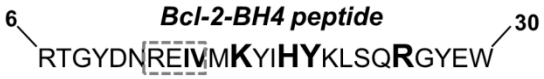

B

Peptide sequence	Pseudo Thermodynamic stability/free energy (ΔΔG)
RTGYDNREGGMKYIHYKLSQRGYEW	4.841 ± 2.979 kcal/mol
RTGYDNRGGVMKYIHYKLSQRGYEW	4.560 ± 2.937 kcal/mol
RTGYDNGGIVMKYIHYKLSQRGYEW	3.402 ± 2.888 kcal/mol

C

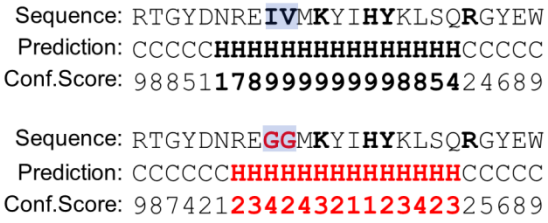

D

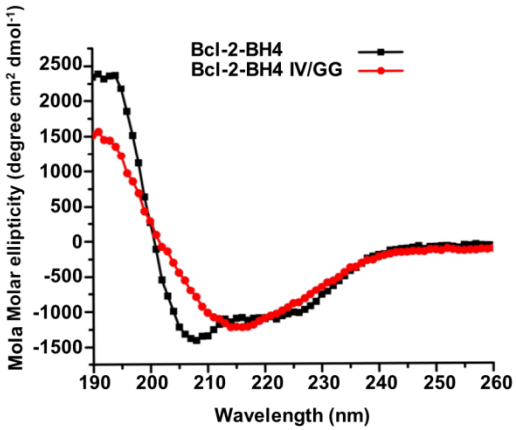

Figure 1. A Bcl-2-BH4 double-glycine variant (I14G/V15G) contains a decreased alpha-helical content. (A) Primary structure of the Bcl-2-BH4 peptide. The key residues involved in the regulation of IP_3Rs are depicted in black/bold and with greater font-size. The dotted square indicates the residues initially considered for the glycine substitution while I14 and V15 are in black/bold. (B) Table showing the values of ΔΔG, in kcal/mol, resulting from the *in silico* analysis of the following double GG substitutions: IV/GG, EI/GG and RE/GG. The position of the exchanged residues is indicated by the red double G in the sequence at the left. Positive ΔΔG values indicate destabilizing mutations. (C) Predicted-secondary structure assignments for the isolated BH4 domain of Bcl-2 (upper panel) and for its highly unstable IV/GG counterpart (lower panel). The panels show the primary sequence, the secondary-structure predictions (H= alpha helix; C= random coil, S= strand) and the level of confidence of the predictions (confidence scores from 0 to 9). Residues 14 and 15 of the BH4 domain are highlighted by a semi-transparent blue square. (D) CD spectra of synthetic Bcl-2-BH4 (black line) and Bcl-2-BH4 IV/GG peptides (red line). Bcl-2-BH4-IV/GG peptide lost the native alpha-helical conformation to adopt a more beta-sheet-like structure (210 nm-ellipticity minimum).

In contrast to Bcl-2-BH4, Bcl-2-BH4 IV/GG fails to bind IP_3R and inhibit its single-channel activity

To assess the IP3R-binding properties of BH4-Bcl-2-IV/GG, we performed GST-pull-down assays using the Bcl-2-BH4-IV/GG peptide and the domain 3 of IP_3R1 (GST-Domain 3, GST + aa 923-1581 of IP_3R1) fused to GST. Domain 3 corresponds to a tryptic subdomain of IP_3R1 containing the previously identified binding site for Bcl-2 [25,54]. Using SDS-PAGE, we showed that the Bcl-2-BH4–peptide strongly interacted with GST-Domain 3 while Bcl-2-BH4 IV/GG lost most of its IP_3R-binding properties (Fig. 2A). We quantified the binding from three independent experiments and observed no differences between GST-Domain 3 and GST for the binding of Bcl-2-BH4 IV/GG (Fig. 2B). Therefore, the residual Bcl-2-BH4-IV/GG peptide interaction with GST-Domain 3 was considered as non-specific. Next, we evaluated the effect of Bcl-2-BH4 and Bcl-2-BH4 IV/GG-peptides on IP_3R1-channel activity by utilizing the nuclear-membrane patch-clamp technique [34,55]. Nuclei were isolated from DT40 cells stably expressing IP_3R1 and channel openings were detected in the presence of submaximal doses of IP_3 (1 μM) and of 5 mM ATP and 200 nM Ca^{2+}. Fig. 2C shows representative traces of IP_3R1-channel openings at a pipette holding potential of -100 mV in the presence or absence of the different BH4 peptides. IP_3R1-channel activity is decreased by the Bcl-2-BH4 peptide (50 μM), in agreement with earlier reports [19,25]. The same concentration of Bcl-2-BH4-IV/GG peptide in contrast had no effect (Fig. 2C). Bcl-2-BH4 peptide reduced IP_3R1-open probability (**P**o) by approximately 80% from 0.2 ± 0.02 to 0.04 ± 0.01 whereas **P**o values in the presence of the Bcl-2-BH4-IV/GG peptide didn't significantly deviate from the control values (0.24 ± 0.03 Fig. 2D).

These data indicate that the IV/GG substitution not only destabilized the alpha helix of Bcl-2-BH4 peptide but also abrogated its binding to the IP_3R and its effect on IP_3R-channel activity.

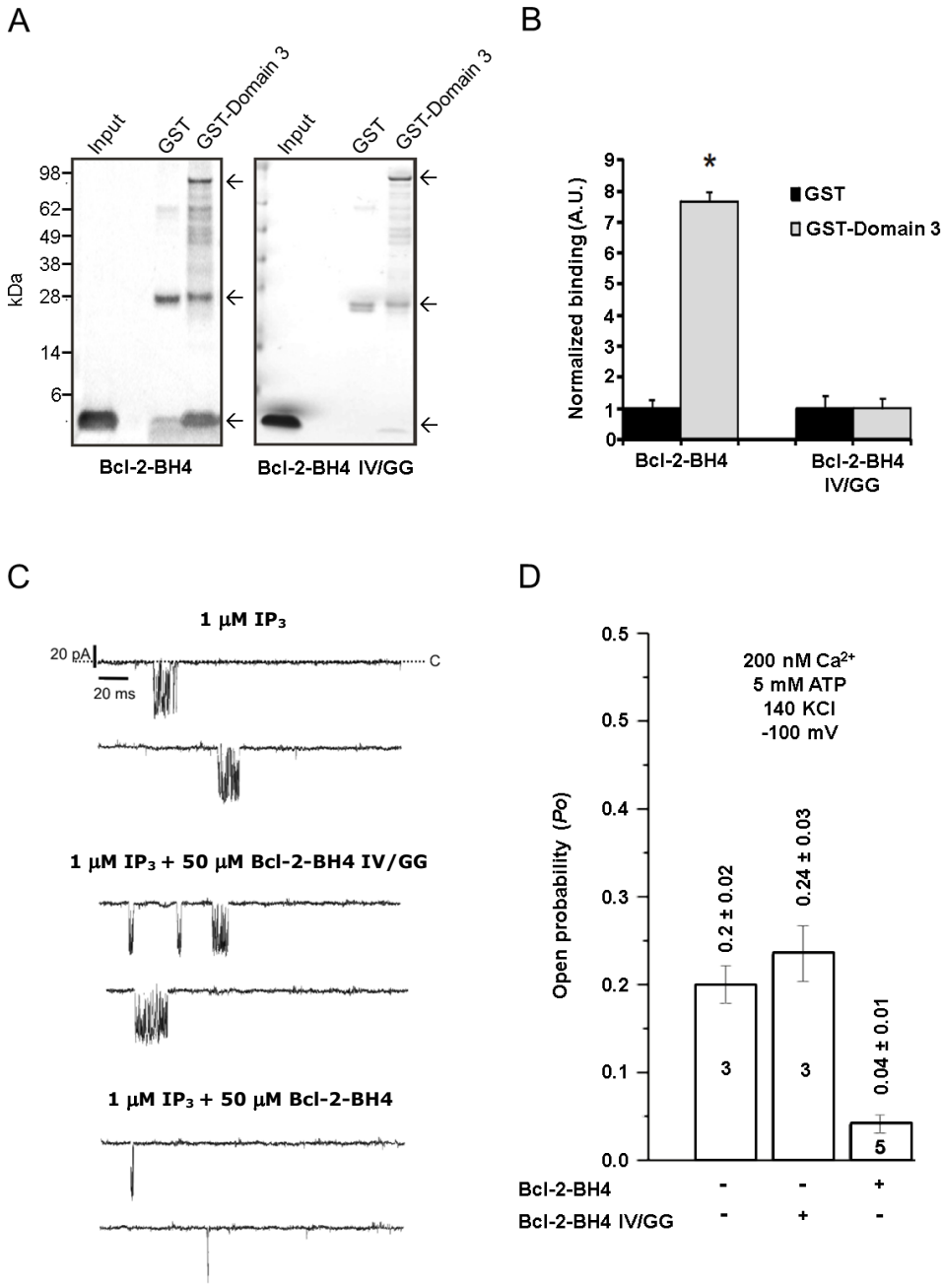

Figure 2. IV/GG substitution in BH4-Bcl-2 abolishes the direct interaction with IP_3R1-Domain 3 and the resulting inhibition of IP_3R-channel activity. (A-B) Pull-down assays of BH4 peptides with either purified GST-Domain 3 or GST alone. (A) Specific interactions between Bcl-2-BH4 or Bcl-2-BH4 IV/GG-peptides (30 µg) and the GST proteins (30 µg) detected by total protein staining (GelCode® Blue Stain Reagent) of SDS-PAGE runs. The arrows indicate the bands for, from top to bottom, GST-domain-3, GST and BH4-domain peptides (B) Bands corresponding to BH4-domain peptides were quantified using ImageJ software. Values were normalized relatively to the binding to GST and corrected for the amount of GST-fusion proteins. The results of at least 4 independent experiments are plotted as means ± SEM. * indicates a statistically significant difference from the GST control. (C) Representative single-channel recordings evoked by low [IP_3] (1 µM) at 200 nM Ca^{2+} and 5 mM ATP, in the presence or absence of the BH4 peptides. (D) Histogram depicting the open probability (*P*o) ± SD for the IP_3R1 under the previously described conditions. Within every bar is indicated the total number of recordings per each condition. The *P*o for IP_3R1 was ~5 fold lower when exposed to the Bcl-2-BH4 peptide whereas it was unaffected by the Bcl-2-BH4-IV/GG peptide.

In contrast to BH4-Bcl-2, BH4-Bcl-2 IV/GG does not inhibit IP_3-induced Ca^{2+} release (IICR) in permeabilized and intact cells

Next, to verify whether these effects could be reproduced in cellular systems, we compared the regulation of IICR by the Bcl-2-BH4 domain and its IV/GG mutant using unidirectional $^{45}Ca^{2+}$-flux assays in permeabilized mouse embryonic fibroblasts (MEF cells). This assay allows the quantitative assessment of Ca^{2+}-efflux properties under unidirectional conditions in the absence of ER and mitochondrial Ca^{2+}-uptake activity. The Ca^{2+} efflux of non-mitochondrial Ca^{2+}-stores, loaded to steady state with $^{45}Ca^{2+}$, is expressed as fractional loss (the amount of Ca^{2+} leaving the store in a 2-min time period divided by the total store Ca^{2+} content at that time). Adding IP_3 (3 μM) to the efflux medium provoked IICR from the ER Ca^{2+} stores, which is observed as a peak increase in the fractional loss. As hypothesized, the incubation with Bcl-2-BH4 (0.1, 3, 15, 30, 60, 100 μM) caused a potent concentration-dependent inhibition of IICR ($IC_{50} \approx 30$ μM) while Bcl-2-BH4 IV/GG didn't significantly affect IICR (Fig. 3A-B). In addition, we examined the effect of Bcl-2-BH4 or Bcl-2-BH4-IV/GG peptides on the IICR in intact C6 glioma cells. We loaded each peptide together with caged IP_3 in a small and defined zone of an adherent culture using an *in situ* electroporation technique [46], and successively released IP_3 by UV-flash photolysis in this area. While Bcl-2-BH4 inhibited the IICR, this was not the case for Bcl-2-BH4 IV/GG (Fig. 3C-D). Both, the $^{45}Ca^{2+}$-flux and the caged IP_3-release assays independently indicated that the inhibition of IICR by the Bcl-2-BH4 peptide was abrogated upon destabilization of its alpha-helical structure.

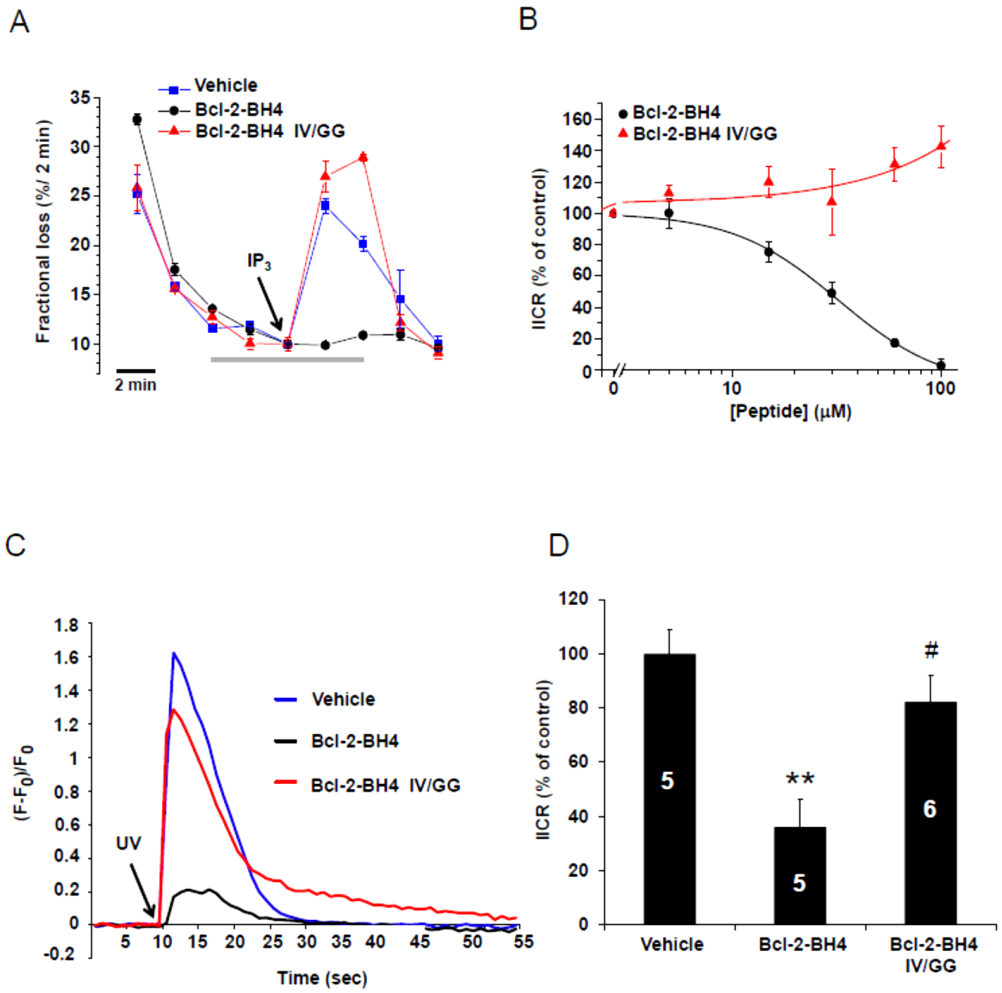

Figure 3. IV/GG substitution abrogates the inhibitory effect of Bcl-2-BH4 on IICR. (A) Representative unidirectional $^{45}Ca^{2+}$ fluxes in permeabilized MEF cells plotted as fractional loss (% / 2 min) as a function of time. Ca^{2+} release was activated 10 min after starting the experiment by applying 3 μM IP_3 (arrow) in the absence or presence of 100 μM of the different BH4-domain peptides (a gray bar indicates the peptide incubation period). (B) Concentration-response curves ([peptide]= 0,1; 3; 15; 30; 60; 100 μM) are shown for Bcl-2-BH4 and Bcl-2-BH4 IV/GG, obtained from 3 independent experiments. IICR was quantified as the difference of the fractional loss after 2 min of incubation with IP_3 and the fractional loss before the IP_3 addition. The 100% value corresponds to IICR in the presence of the vehicle and all the raw values were normalized to this control. Data points represent means ± SEM. (**C**) $[Ca^{2+}]_{cyt}$ increases in C6 glioma cells after photoliberation of caged IP_3 at 9980 ms of recording (arrow). Traces of individual cells are displayed that were loaded with different BH4-domain peptides (20 **μ**M) together with caged IP_3 (50 **μ**M). (**D**) Quantitative analysis of the area under the curve obtained from 5 or 6 independent experiments (as marked on each bar). Data were normalized to the vehicle condition, which was set as 100%, and are plotted as means ± SEM. These data indicate that Bcl-2-BH4 peptide significantly inhibited IICR (**), whereas Bcl-2-BH4 IV/GG peptides did not. # specifies the statistically significant difference between Bcl-2-BH4 and Bcl-2-BH4-IV/GG results.

In contrast to BH4-Bcl-2, Bcl-2-BH4 IV/GG does not protect against Staurosporine (STS)-induced apoptosis

Since STS is known to trigger Ca^{2+}-dependent apoptosis [56,57], our next step was to compare the protective activity of Bcl-2-BH4 and Bcl-2-BH4 IV/GG in STS-treated C6 glioma cells. Two typical biochemical hallmarks of apoptosis are caspase-3 activation and downstream DNA fragmentation, detectable by specific fluorescent probes (here by FITC-VAD-FMK and DAPI, respectively). Therefore, we related both events to the magnitude of the ongoing apoptosis in C6 glioma cultures subsequent to the loading of Bcl-2-BH4 or Bcl-2-BH4 IV/GG (20 μM) and treatment for 6 h with STS (2 μM). The apoptotic index (AI), defined as the ratio between dead cells and the total number of cells, was calculated and expressed relative to the cell profile outside the electroporated area. As shown in figure 4, Bcl-2-BH4 peptide significantly reduced apoptotic cell death in STS-treated cells while Bcl-2-BH4 IV/GG behaved similarly to the vehicle. The latter demonstrated that the BH4-IV/GG peptide lost its ability to inhibit the IP_3R and also its ability to counteract STS-induced apoptosis.

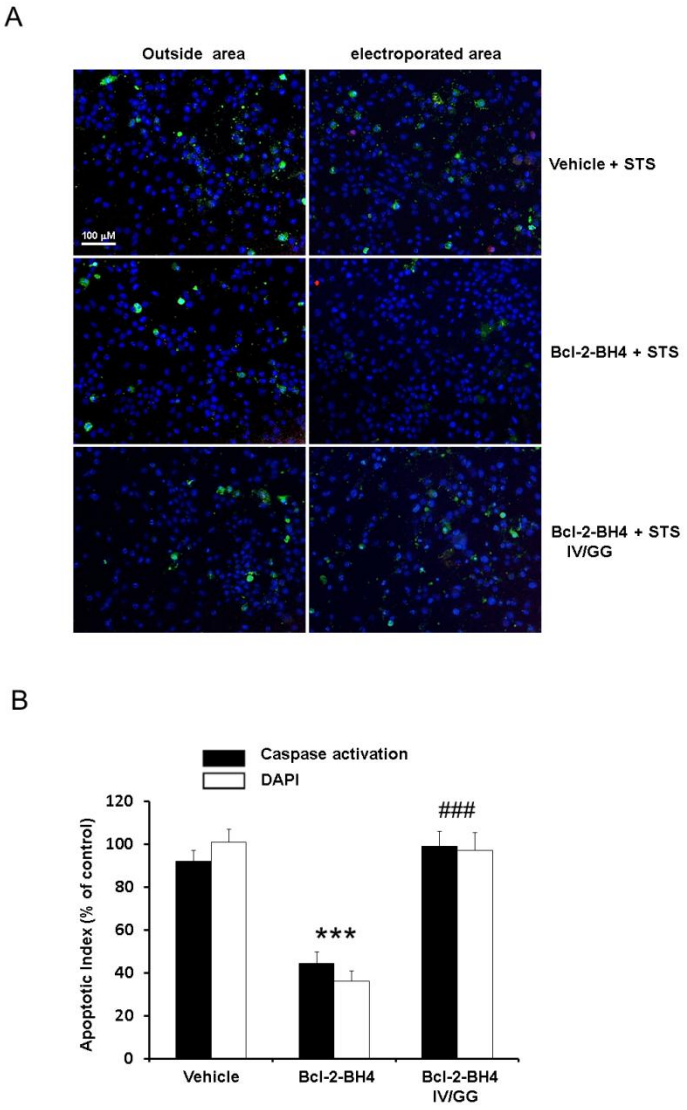

Figure 4. IV/GG substitution abolishes BH4-Bcl-2's protective function against STS-induced apoptosis. Simultaneous analysis of caspase activation (FITC-VAD-FMK, green) and nuclear fragmentation (DAPI staining, blue fragments) of STS-treated C6 glioma cells. (A) Representative images of cells electroporated with or without BH4 peptides (20 μM) and successively treated with STS (2 μM for 6 h). The left images are taken outside the electroporation area and are used as negative controls. (A, upper right) Electroporation in the absence of peptides (vehicle). (A, middle right) Electroporation of Bcl-2-BH4 peptide. (A, lower right) Electroporation of Bcl-2-BH4-IV/GG peptides. Red color is due to the spillover into the FITC channel of the intense DTR signal (the electroporation loading control). (B) Quantitative image based AI (number of apoptotic cells divided by the total cell number). The AI was normalized to the AI outside the electroporated area. All results were obtained from 5 independent experiments and are plotted as means ± SEM. Only Bcl-2-BH4 loading significantly reduced the AI when compared with the control vehicle (**). ### indicates that the results obtained with Bcl-2-BH4 IV/GG were significantly different from Bcl-2-BH4.

Discussion

Here, we examined the efficacy of Bcl-2-BH4 as an IP_3R-inhibitory peptide in relation to its intrinsic secondary structure. Our findings indicate that the alpha-helicity of Bcl-2-BH4 peptide is a key determinant for its ability to directly suppress IP_3R signaling and Ca^{2+}-mediated apoptosis.

Irrespective of any concerns on structural organization or selectivity, many studies already showed that a cell-penetrating peptide comprising the sequence for Bcl-2's BH4 domain is protective against various cellular stressors [58,59,60,61]. This can be attributed to a large extent to the direct inhibition of the IP_3Rs by Bcl-2's BH4 peptide as reported in our recent publications [19,24,25]. Notably, synthetic peptides derived from native protein sequences tend to shift conformations between helices, sheets and random coils, since they have been removed from the stabilizing effects of their protein context. The latter problem is not shared by the naturally occurring bioactive peptides, since they possess a secondary or tertiary structure "locked" by internal cysteine "knots" [62,63]. Remarkably, such a stable structure has been instrumental for the development of venom peptides as selective inhibitors of the voltage-dependent Ca^{2+} channels in the treatment of neuropathic pain [64,65,66,67]. Although ER Ca^{2+}-release channels are also implicated in a variety of muscular, cardiovascular and neurodegenerative diseases due to excessive intracellular Ca^{2+} signaling [68,69,70,71,72], no specific chemical compounds or peptide therapeutics are currently available for inhibiting the IP_3Rs [73,74,75]. The macrocyclic alkaloid xestospongin-B remains the only compound that seems to specifically target the IP_3Rs, though with a relatively low affinity [76,77]. Therefore, Bcl-2-BH4-peptide activity on IP_3Rs offers new opportunities for the development of a selective pharmacological modulator of IP_3Rs. Yet, it also raises new issues towards the stabilization of its "active" secondary structure. The Bcl-2-BH4 domain adopts a alpha-helical conformation in the native protein, a secondary

structure motif involved in many protein-protein interactions as well as in protein association with cellular membranes [78,79,80]. Isolated peptides corresponding to this region have been reported to adopt different secondary structures according to the surrounding environment: from an alpha helix or a beta sheet in an amphipathic/membrane-like environment to a random coil when present in an aqueous medium [28,81,82]. Here, we show that the Bcl-2's BH4 peptide has a substantial helical content (Fig. 1D), correlating with its ability to suppress the activity of the IP_3Rs and protect against STS-induced apoptosis. Consequently, introducing a double glycine amino acid in its alpha-helical core not only weakened the secondary structure organization of the peptide, but also abrogated its ability to bind to the IP_3R1 and reduced the related pro-apoptotic Ca^{2+} signaling. From our CD analysis, we estimated that approximately 20% of the Bcl-2's BH4 peptide is organized in an alpha helix when solubilized in TFE. This is in agreement with the 27% obtained by Lee at al. [28] in detergent micelles but in contrast with the higher value of 45% obtained by Khemtemourian et al. [81] in pure TFE. The apparent discrepancy is explicable by the slightly different experimental conditions (pH, temperature, solvent purity, membrane environment and peptide length) used by the two groups, which can drastically affect the peptide's secondary structure. However, it is clear from our data and from the previous work that this peptide displays improved stability in an alpha-helical conformation upon addition of the hydrogen-bond favoring solvent TFE [51] or of lipid membranes [28,81]. The relatively high doses of BH4 peptide necessary in the electrophysiological assays (Fig.2C-D) and in the $^{45}Ca^{2+}$ flux assays ($IC_{50} \approx 30$ μM, Fig.3D), might be therefore a consequence of the mixed unstructured/beta-sheet conformations present in an aqueous medium [28,81,83]. Bcl-2's BH4 peptide, which is amphiphilic and has a net positive charge at physiological pH, would still need to accumulate onto the acidic membrane environment and to assume a more alpha-helical conformation for gaining its ability to inhibit the IP_3Rs. On the other hand, the IV/GG-mutated BH4-peptide

shows a decrease of more than 50% in the extent of helix content (8% *vs* 20%) with a more beta-sheet-like CD spectrum, indicating a collapse of the alpha-helix in Bcl-2-BH4 IV/GG. The experimental evidence from the CD spectra suggests a shift in the secondary structure of the peptide, which causes a mis-positioning of the key BH4 amino acids necessary for its specific IP_3R inhibition and consequent protective role (Fig. 1B, left). Interestingly, Sani et al. showed that Bcl-2's BH4-peptide aggregates as a beta-sheet structure upon contact with mitochondrial-like membranes and would be able to protect against apoptosis by increasing the stiffness of the mitochondrial membrane [82]. Therefore, it is tempting to speculate that Bcl-2's BH4 peptide requires an alpha-helical conformation for modulating the IP_3R at the ER and a beta–sheet structure for increasing membrane cohesion on the mitochondria. In this scenario, our IV/GG mutant would be unable to act on both sites as it is more beta–sheet enriched but deprived of two hydrophobic residues (I14 and I15) putatively important for the proper aggregation on membranes. However, this point needs to be properly addressed by a simultaneous comparison of the accumulation of the peptides on ER and mitochondrial membranes.

Taken together, our results indicate that a precise secondary structure of the Bcl-2-BH4 peptide is required for its specific dampening of the IP_3R-dependent Ca^{2+} signaling and the resulting protection against Ca^{2+}-mediated apoptosis. Nonetheless, further structure-activity relationship studies are still necessary to interpret our findings in the context of the full-length Bcl-2 interaction with the IP_3Rs and in relation to the unknown mechanism of IP_3R channel inhibition [20]. Another challenge is to obtain from this anti-apoptotic peptide a stable, cell-permeable IP_3R-inhibitory tool that retains the specificity of the native BH4-domain alpha helix. Notably, the recent successes of two alpha-helix–stabilizing techniques, like the all-hydrocarbon and the triazole stapling [84,85,86,87] have already paved the way for accomplishing this task.

In conclusion, our study provides new opportunities for the rational design of selective IP_3R-inhibitors. Furthermore, it lays the basis for the development of a novel class of Bcl-2-BH4-derived molecules targeting disorders associated with aberrant intracellular Ca^{2+} signaling.

Acknowledgements

The authors thank Marina Crabbe, Anja Florizoone and Kirsten Welkenhuyzen for technical help. The authors also thank Dr. Raf Ponsaerts, Dr. Servaas Michielssens and Prof. Clark W. Distelhorst (Case Western Reserve University) for helpful discussions.

References

1. Grimm S (2012) The ER-mitochondria interface: the social network of cell death. Biochim Biophys Acta 1823: 327-334.
2. Rizzuto R, Marchi S, Bonora M, Aguiari P, Bononi A, et al. (2009) Ca2+ transfer from the ER to mitochondria: when, how and why. Biochim Biophys Acta 1787: 1342-1351.
3. Baumgartner HK, Gerasimenko JV, Thorne C, Ferdek P, Pozzan T, et al. (2009) Calcium elevation in mitochondria is the main Ca2+ requirement for mitochondrial permeability transition pore (mPTP) opening. J Biol Chem 284: 20796-20803.
4. Rasola A, Bernardi P (2011) Mitochondrial permeability transition in Ca2+-dependent apoptosis and necrosis. Cell Calcium 50: 222-233.
5. Westphal D, Dewson G, Czabotar PE, Kluck RM (2011) Molecular biology of Bax and Bak activation and action. Biochim Biophys Acta 1813: 521-531.
6. Walter L, Hajnoczky G (2005) Mitochondria and endoplasmic reticulum: the lethal interorganelle cross-talk. J Bioenerg Biomembr 37: 191-206.
7. Chipuk JE, Moldoveanu T, Llambi F, Parsons MJ, Green DR (2010) The BCL-2 family reunion. Mol Cell 37: 299-310.
8. Hardwick JM, Chen YB, Jonas EA (2012) Multipolar functions of BCL-2 proteins link energetics to apoptosis. Trends Cell Biol 22: 318-328.
9. Rong Y, Distelhorst CW (2008) Bcl-2 protein family members: versatile regulators of calcium signaling in cell survival and apoptosis. Annu Rev Physiol 70: 73-91.
10. Dremina ES, Sharov VS, Kumar K, Zaidi A, Michaelis EK, et al. (2004) Anti-apoptotic protein Bcl-2 interacts with and destabilizes the sarcoplasmic/endoplasmic reticulum Ca2+-ATPase (SERCA). Biochem J 383: 361-370.
11. Dremina ES, Sharov VS, Schoneich C (2012) Heat-shock proteins attenuate SERCA inactivation by the anti-apoptotic protein Bcl-2: possible implications for the ER Ca2+-mediated apoptosis. Biochem J 444: 127-139.
12. Pinton P, Ferrari D, Magalhaes P, Schulze-Osthoff K, Di Virgilio F, et al. (2000) Reduced loading of intracellular Ca2+ stores and downregulation of capacitative Ca2+ influx in Bcl-2-overexpressing cells. J Cell Biol 148: 857-862.

13. Foyouzi-Youssefi R, Arnaudeau S, Borner C, Kelley WL, Tschopp J, et al. (2000) Bcl-2 decreases the free Ca2+ concentration within the endoplasmic reticulum. Proc Natl Acad Sci U S A 97: 5723-5728.
14. Chami M, Prandini A, Campanella M, Pinton P, Szabadkai G, et al. (2004) Bcl-2 and Bax exert opposing effects on Ca2+ signaling, which do not depend on their putative pore-forming region. J Biol Chem 279: 54581-54589.
15. Palmer AE, Jin C, Reed JC, Tsien RY (2004) Bcl-2-mediated alterations in endoplasmic reticulum Ca2+ analyzed with an improved genetically encoded fluorescent sensor. Proc Natl Acad Sci U S A 101: 17404-17409.
16. Oakes SA, Lin SS, Bassik MC (2006) The control of endoplasmic reticulum-initiated apoptosis by the BCL-2 family of proteins. Curr Mol Med 6: 99-109.
17. Eckenrode EF, Yang J, Velmurugan GV, Foskett JK, White C (2010) Apoptosis protection by Mcl-1 and Bcl-2 modulation of inositol 1,4,5-trisphosphate receptor-dependent Ca2+ signaling. J Biol Chem 285: 13678-13684.
18. Distelhorst CW, Bootman MD (2011) Bcl-2 interaction with the inositol 1,4,5-trisphosphate receptor: role in Ca2+ signaling and disease. Cell Calcium 50: 234-241.
19. Rong YP, Aromolaran AS, Bultynck G, Zhong F, Li X, et al. (2008) Targeting Bcl-2-IP3 receptor interaction to reverse Bcl-2's inhibition of apoptotic calcium signals. Mol Cell 31: 255-265.
20. Monaco G, Vervliet T, Akl H, Bultynck G (2012) The selective BH4-domain biology of Bcl-2-family members: IP3Rs and beyond. Cellular and molecular life sciences Ahead of print.
21. Hunter JJ, Bond BL, Parslow TG (1996) Functional dissection of the human Bc12 protein: sequence requirements for inhibition of apoptosis. Mol Cell Biol 16: 877-883.
22. Huang DC, Adams JM, Cory S (1998) The conserved N-terminal BH4 domain of Bcl-2 homologues is essential for inhibition of apoptosis and interaction with CED-4. Embo J 17: 1029-1039.
23. Reed JC, Zha H, Aime-Sempe C, Takayama S, Wang HG (1996) Structure-function analysis of Bcl-2 family proteins. Regulators of programmed cell death. Adv Exp Med Biol 406: 99-112.
24. Monaco G, Decrock E, Akl H, Ponsaerts R, Vervliet T, et al. (2012) Selective regulation of IP3-receptor-mediated Ca2+ signaling and apoptosis by the BH4 domain of Bcl-2 versus Bcl-Xl. Cell Death Differ 19: 295-309.
25. Rong YP, Bultynck G, Aromolaran AS, Zhong F, Parys JB, et al. (2009) The BH4 domain of Bcl-2 inhibits ER calcium release and apoptosis by binding the regulatory and coupling domain of the IP3 receptor. Proc Natl Acad Sci U S A 106: 14397-14402.
26. Petros AM, Medek A, Nettesheim DG, Kim DH, Yoon HS, et al. (2001) Solution structure of the antiapoptotic protein bcl-2. Proc Natl Acad Sci U S A 98: 3012-3017.
27. Ku B, Liang C, Jung JU, Oh BH (2011) Evidence that inhibition of BAX activation by BCL-2 involves its tight and preferential interaction with the BH3 domain of BAX. Cell Res 21: 627-641.
28. Lee LC, Hunter JJ, Mujeeb A, Turck C, Parslow TG (1996) Evidence for alpha-helical conformation of an essential N-terminal region in the human Bcl2 protein. J Biol Chem 271: 23284-23288.
29. Rong YP, Barr P, Yee VC, Distelhorst CW (2009) Targeting Bcl-2 based on the interaction of its BH4 domain with the inositol 1,4,5-trisphosphate receptor. Biochim Biophys Acta 1793: 971-978.
30. Lama D, Sankararamakrishnan R (2010) Identification of core structural residues in the sequentially diverse and structurally homologous Bcl-2 family of proteins. Biochemistry 49: 2574-2584.

31. Kasri NN, Kocks SL, Verbert L, Hebert SS, Callewaert G, et al. (2006) Up-regulation of inositol 1,4,5-trisphosphate receptor type 1 is responsible for a decreased endoplasmic-reticulum Ca2+ content in presenilin double knock-out cells. Cell Calcium 40: 41-51.
32. De Vuyst E, De Bock M, Decrock E, Van Moorhem M, Naus C, et al. (2008) In situ bipolar electroporation for localized cell loading with reporter dyes and investigating gap junctional coupling. Biophys J 94: 469-479.
33. Bond SL, Bechberger JF, Khoo NK, Naus CC (1994) Transfection of C6 glioma cells with connexin32: the effects of expression of a nonendogenous gap junction protein. Cell Growth Differ 5: 179-186.
34. Wagner LE, 2nd, Yule DI (2012) Differential regulation of the InsP3 receptor type-1 and -2 single channel properties by InsP3, Ca2+ and ATP. J Physiol 590: 3245-3259.
35. Benedix A, Becker CM, de Groot BL, Caflisch A, Bockmann RA (2009) Predicting free energy changes using structural ensembles. Nat Methods 6: 3-4.
36. Yin S, Ding F, Dokholyan NV (2007) Eris: an automated estimator of protein stability. Nat Methods 4: 466-467.
37. Dehouck Y, Kwasigroch JM, Gilis D, Rooman M (2011) PoPMuSiC 2.1: a web server for the estimation of protein stability changes upon mutation and sequence optimality. BMC Bioinformatics 12: 151.
38. Worth CL, Preissner R, Blundell TL (2011) SDM--a server for predicting effects of mutations on protein stability and malfunction. Nucleic Acids Res 39: W215-222.
39. Ramachandran S, Kota P, Ding F, Dokholyan NV (2011) Automated minimization of steric clashes in protein structures. Proteins 79: 261-270.
40. Roy A, Kucukural A, Zhang Y (2010) I-TASSER: a unified platform for automated protein structure and function prediction. Nat Protoc 5: 725-738.
41. Zhang Y (2008) I-TASSER server for protein 3D structure prediction. BMC Bioinformatics 9: 40.
42. Sreerama N, Woody RW (1993) A self-consistent method for the analysis of protein secondary structure from circular dichroism. Anal Biochem 209: 32-44.
43. Sreerama N, Venyaminov SY, Woody RW (2000) Estimation of protein secondary structure from circular dichroism spectra: inclusion of denatured proteins with native proteins in the analysis. Anal Biochem 287: 243-251.
44. Sreerama N, Woody RW (2000) Estimation of protein secondary structure from circular dichroism spectra: comparison of CONTIN, SELCON, and CDSSTR methods with an expanded reference set. Anal Biochem 287: 252-260.
45. Decrock E, De Vuyst E, Vinken M, Van Moorhem M, Vranckx K, et al. (2009) Connexin 43 hemichannels contribute to the propagation of apoptotic cell death in a rat C6 glioma cell model. Cell Death Differ 16: 151-163.
46. Decrock E, De Bock M, Wang N, Bol M, Gadicherla A, et al. (2013) Electroporation loading and flash photolysis to investigate intra- and intercellular Ca2+ signaling. Cold spring Harbor protocols accepted for publication.
47. Betzenhauser MJ, Wagner LE, 2nd, Park HS, Yule DI (2009) ATP regulation of type-1 inositol 1,4,5-trisphosphate receptor activity does not require walker A-type ATP-binding motifs. The Journal of biological chemistry 284: 16156-16163.
48. Lyu PC, Wang PC, Liff MI, Kallenbach NR (1991) Local effect of glycine substitution in a model helical peptide. Journal of the American Chemical Society 113: 3568-3572.
49. Pace CN, Scholtz JM (1998) A helix propensity scale based on experimental studies of peptides and proteins. Biophysical journal 75: 422-427.
50. O'Neil KT, DeGrado WF (1990) A thermodynamic scale for the helix-forming tendencies of the commonly occurring amino acids. Science 250: 646-651.

51. Sönnichsen FD, Van Eyk JE, Hodges RS, Sykes BD (1992) Effect of trifluoroethanol on protein secondary structure: an NMR and CD study using a synthetic actin peptide. Biochemistry 31: 8790-8798.
52. Luo P, Baldwin RL (1997) Mechanism of helix induction by trifluoroethanol: a framework for extrapolating the helix-forming properties of peptides from trifluoroethanol/water mixtures back to water. Biochemistry 36: 8413-8421.
53. Greenfield NJ (2006) Using circular dichroism spectra to estimate protein secondary structure. Nat Protoc 1: 2876-2890.
54. Yoshikawa F, Iwasaki H, Michikawa T, Furuichi T, Mikoshiba K (1999) Trypsinized cerebellar inositol 1,4,5-trisphosphate receptor. Structural and functional coupling of cleaved ligand binding and channel domains. J Biol Chem 274: 316-327.
55. Stehno-Bittel L, Luckhoff A, Clapham DE (1995) Calcium release from the nucleus by InsP3 receptor channels. Neuron 14: 163-167.
56. Kruman I, Guo Q, Mattson MP (1998) Calcium and reactive oxygen species mediate staurosporine-induced mitochondrial dysfunction and apoptosis in PC12 cells. J Neurosci Res 51: 293-308.
57. Nutt LK, Chandra J, Pataer A, Fang B, Roth JA, et al. (2002) Bax-mediated Ca2+ mobilization promotes cytochrome c release during apoptosis. J Biol Chem 277: 20301-20308.
58. Cantara S, Donnini S, Giachetti A, Thorpe PE, Ziche M (2004) Exogenous BH4/Bcl-2 peptide reverts coronary endothelial cell apoptosis induced by oxidative stress. J Vasc Res 41: 202-207.
59. Trisciuoglio D, Gabellini C, Desideri M, Ragazzoni Y, De Luca T, et al. (2011) Involvement of BH4 domain of bcl-2 in the regulation of HIF-1-mediated VEGF expression in hypoxic tumor cells. Cell Death Differ 18: 1024-1035.
60. McDunn JE, Muenzer JT, Dunne B, Zhou A, Yuan K, et al. (2009) An anti-apoptotic peptide improves survival in lethal total body irradiation. Biochem Biophys Res Commun 382: 657-662.
61. Shimizu S, Konishi A, Kodama T, Tsujimoto Y (2000) BH4 domain of antiapoptotic Bcl-2 family members closes voltage-dependent anion channel and inhibits apoptotic mitochondrial changes and cell death. Proc Natl Acad Sci U S A 97: 3100-3105.
62. Mouhat S, Jouirou B, Mosbah A, De Waard M, Sabatier JM (2004) Diversity of folds in animal toxins acting on ion channels. Biochem J 378: 717-726.
63. Daly NL, Craik DJ (2011) Bioactive cystine knot proteins. Curr Opin Chem Biol 15: 362-368.
64. Lewis RJ, Garcia ML (2003) Therapeutic potential of venom peptides. Nat Rev Drug Discov 2: 790-802.
65. Pringos E, Vignes M, Martinez J, Rolland V (2011) Peptide neurotoxins that affect voltage-gated calcium channels: a close-up on omega-agatoxins. Toxins (Basel) 3: 17-42.
66. Park J, Luo ZD (2010) Calcium channel functions in pain processing. Channels (Austin) 4: 510-517.
67. Schroeder CI, Doering CJ, Zamponi GW, Lewis RJ (2006) N-type calcium channel blockers: novel therapeutics for the treatment of pain. Med Chem 2: 535-543.
68. Berridge MJ (2012) Calcium signalling remodelling and disease. Biochem Soc Trans 40: 297-309.
69. Varshney A, Ehrlich BE (2003) Intracellular Ca2+ signaling and human disease: the hunt begins with Huntington's. Neuron 39: 195-197.

70. Cheung KH, Shineman D, Muller M, Cardenas C, Mei L, et al. (2008) Mechanism of Ca2+ disruption in Alzheimer's disease by presenilin regulation of InsP3 receptor channel gating. Neuron 58: 871-883.
71. Xiao J, Liang D, Zhao H, Liu Y, Zhang H, et al. (2010) 2-Aminoethoxydiphenyl borate, a inositol 1,4,5-triphosphate receptor inhibitor, prevents atrial fibrillation. Exp Biol Med (Maywood) 235: 862-868.
72. Harzheim D, Talasila A, Movassagh M, Foo RS, Figg N, et al. (2010) Elevated InsP3R expression underlies enhanced calcium fluxes and spontaneous extra-systolic calcium release events in hypertrophic cardiac myocytes. Channels (Austin) 4: 67-71.
73. Bultynck G, Sienaert I, Parys JB, Callewaert G, De Smedt H, et al. (2003) Pharmacology of inositol trisphosphate receptors. Pflugers Arch 445: 629-642.
74. West DJ, Williams AJ (2007) Pharmacological regulators of intracellular calcium release channels. Curr Pharm Des 13: 2428-2442.
75. Boehning D, van Rossum DB, Patterson RL, Snyder SH (2005) A peptide inhibitor of cytochrome c/inositol 1,4,5-trisphosphate receptor binding blocks intrinsic and extrinsic cell death pathways. Proc Natl Acad Sci U S A 102: 1466-1471.
76. Jaimovich E, Mattei C, Liberona JL, Cardenas C, Estrada M, et al. (2005) Xestospongin B, a competitive inhibitor of IP3-mediated Ca2+ signalling in cultured rat myotubes, isolated myonuclei, and neuroblastoma (NG108-15) cells. FEBS Lett 579: 2051-2057.
77. Gafni J, Munsch JA, Lam TH, Catlin MC, Costa LG, et al. (1997) Xestospongins: potent membrane permeable blockers of the inositol 1,4,5-trisphosphate receptor. Neuron 19: 723-733.
78. Jochim AL, Arora PS (2009) Assessment of helical interfaces in protein-protein interactions. Mol Biosyst 5: 924-926.
79. Guharoy M, Chakrabarti P (2007) Secondary structure based analysis and classification of biological interfaces: identification of binding motifs in protein-protein interactions. Bioinformatics 23: 1909-1918.
80. Bechinger B (2010) Membrane association and pore formation by alpha-helical peptides. Adv Exp Med Biol 677: 24-30.
81. Khemtemourian L, Sani MA, Bathany K, Grobner G, Dufourc EJ (2006) Synthesis and secondary structure in membranes of the Bcl-2 anti-apoptotic domain BH4. J Pept Sci 12: 58-64.
82. Sani MA, Castano S, Dufourc EJ, Gröbner G (2008) Restriction of lipid motion in membranes triggered by β-sheet aggregation of the anti-apoptotic BH4 domain. FEBS Journal 275: 561-572.
83. Sani MA, Loudet C, Gröbner G, Dufourc EJ (2007) Pro-apoptotic bax-alpha1 synthesis and evidence for beta-sheet to alpha-helix conformational change as triggered by negatively charged lipid membranes. Journal of Peptide Science 13: 100-106.
84. Johanning GL (2012) Stapled Peptides as Anti-Apoptotic Drugs. Chemotherapy 1: 1-3.
85. Verdine GL, Walensky LD (2007) The challenge of drugging undruggable targets in cancer: lessons learned from targeting BCL-2 family members. Clin Cancer Res 13: 7264-7270.
86. Kawamoto SA, Coleska A, Ran X, Yi H, Yang CY, et al. (2012) Design of triazole-stapled BCL9 alpha-helical peptides to target the beta-catenin/B-cell CLL/lymphoma 9 (BCL9) protein-protein interaction. J Med Chem 55: 1137-1146.
87. Bird GH, Madani N, Perry AF, Princiotto AM, Supko JG, et al. (2010) Hydrocarbon double-stapling remedies the proteolytic instability of a lengthy peptide therapeutic. Proc Natl Acad Sci U S A 107: 14093-14098.

PART III

Addressing objective IV

Profiling of the Bcl-2/Bcl-Xl-binding sites on type 1 IP_3 receptor

Giovanni Monaco[#], Marjolein Beckers[#], Hristina Ivanova, Ludwig Missiaen, Jan B. Parys, Humbert De Smedt, Geert Bultynck

Laboratory of Molecular and Cellular Signaling, Department of Cellular and Molecular Medicine, KU Leuven Campus Gasthuisberg O/N-I bus 802, Herestraat 49, BE-3000 Leuven, Belgium

[#] These authors equally contributed to the work.

Biochem Biophys Res Commun. 2012,428:31-5.

Biochemical and Biophysical Research Communications 428 (2012) 31–35

Contents lists available at SciVerse ScienceDirect

Biochemical and Biophysical Research Communications

journal homepage: www.elsevier.com/locate/ybbrc

Profiling of the Bcl-2/Bcl-X_L-binding sites on type 1 IP_3 receptor

Giovanni Monaco [1], Marjolein Beckers [1], Hristina Ivanova, Ludwig Missiaen, Jan B. Parys, Humbert De Smedt, Geert Bultynck *

Laboratory of Molecular and Cellular Signaling, Department of Cellular and Molecular Medicine, KU Leuven Campus Gasthuisberg O/N-I bus 802, Herestraat 49, BE-3000 Leuven, Belgium

ARTICLE INFO

Article history:
Received 28 September 2012
Available online 8 October 2012

Keywords:
Ca^{2+} signaling
Inositol 1,4,5-trisphosphate receptor
Bcl-2
Bcl-X_L
Interaction
Protein-complex formation

ABSTRACT

Several members of the anti-apoptotic Bcl-2-protein family, including Bcl-2, Bcl-X_L and Mcl-1, directly bind and regulate the inositol 1,4,5-trisphosphate receptor (IP_3R), one of the two main intracellular Ca^{2+}-release channel types present in the endoplasmic reticulum. However, the molecular determinants underlying their binding to the IP_3R remained a matter of debate. One interaction site for Bcl-2 was proposed in the central part of the modulatory domain [Y.P. Rong, A.S. Aromolaran, G. Bultynck, F. Zhong, X. Li, K. McColl, S. Matsuyama, S. Herlitze, H.L. Roderick, M.D. Bootman, G.A. Mignery, J.B. Parys, H. De Smedt, C.W. Distelhorst, Targeting Bcl-2-IP3 receptor interaction to reverse Bcl-2's inhibition of apoptotic calcium signals, Mol. Cell 31 (2008) 255–265] and another site in the C-terminal domain of the IP_3R encompassing the sixth transmembrane domain, to which Bcl-2, Bcl-X_L and Mcl-1 can bind [E.F. Eckenrode, J. Yang, G.V. Velmurugan, J.K. Foskett, C. White, Apoptosis protection by Mcl-1 and Bcl-2 modulation of inositol 1,4,5-trisphosphate receptor-dependent Ca^{2+} signaling, J. Biol. Chem. 285 (2010) 13678–13684]. Here, we investigated and compared the binding of Bcl-2 and Bcl-X_L to both sites. Two different IP_3R domains were used for the C-terminal site: one lacking and one containing the sixth transmembrane domain. Our results show that elements preceding the C-terminal cytosolic tail located at the sixth transmembrane domain of IP_3R1 were critical for recruiting both Bcl-2 and Bcl-X_L to the C-terminal part of the IP_3R. Furthermore, consistent with our previous observations, Bcl-X_L bound with higher efficiency to the C-terminal part of the IP_3R and to a much lesser extent to the central, modulatory domain, while Bcl-2 targeted both sites with similar efficiencies. In conclusion, IP_3R harbors two different binding sites for anti-apoptotic Bcl-2 proteins, one in the central, modulatory domain and one in the C-terminal domain near the Ca^{2+}-channel pore.

1. Introduction

Intracellular Ca^{2+} signals originating from the endoplasmic reticulum (ER), the main intracellular Ca^{2+} store, control cell-survival and -death processes due to the close proximity between the ER and the mitochondria [1]. At the mitochondria-associated ER membranes (MAMs), there is physical contact between both organelles involving multi-protein complexes that participate in the privileged transfer of Ca^{2+} between them [2]. In the MAMs, the chaperone GRP75 links inositol 1,4,5-trisphosphate (IP_3) receptors (IP_3Rs), ER-located intracellular Ca^{2+}-release channels, to Ca^{2+}-permeable voltage-dependent anion channels, located in the mitochondrial outer membrane [3–5]. Several pro-survival and pro-death proteins regulate Ca^{2+} transfer between the ER and mitochondria [6,7]. Different members of the anti-apoptotic B-cell lymphoma 2 (Bcl-2) family, including Bcl-2, B-cell lymphoma extra large (Bcl-X_L) and myeloid cell leukemia sequence 1 (Mcl-1), control Ca^{2+} release from the ER. Different mechanisms were proposed, including a decrease in the steady-state ER Ca^{2+} levels [8–10] through a protein kinase A-dependent phosphorylation of the IP_3R [11] and a direct regulation of the Ca^{2+}-flux properties of the IP_3R through direct protein interactions [12–15]. Several groups provided evidence that anti-apoptotic Bcl-2 proteins directly bind and regulate IP_3R channels. However, the binding sites for Bcl-2 and Bcl-X_L on the IP_3R and the functional outcome of their interactions remained a matter of debate [16]. Foskett and co-workers reported that Bcl-X_L bound to the C-terminal part of the IP_3R containing the sixth transmembrane helix, thereby sensitizing IP_3R channels to low level of IP_3 and promoting pro-survival Ca^{2+}

Abbreviations: aa, amino acids; Bcl-2, B-cell lymphoma 2; Bcl-X_L, B-cell lymphoma extra large; ER, endoplasmic reticulum; GST, glutathione S-transferase; IP_3, inositol 1,4,5-trisphosphate; IP_3R, IP_3 receptor; Mcl-1, myeloid cell leukemia sequence 1; MAM, mitochondria-associated ER membrane; TMD, transmembrane domain.

* Corresponding author. Fax: +32 16 330732.
E-mail address: geert.bultynck@med.kuleuven.be (G. Bultynck).

[1] These authors have equally contributed to the work.

0006-291X/$ - see front matter © 2012 Elsevier Inc. All rights reserved.
http://dx.doi.org/10.1016/j.bbrc.2012.10.002

oscillations and mitochondrial bio-energetics [13,14]. The C-terminus of the IP_3R appeared to be a target not only for Bcl-X_L but also for Bcl-2 and Mcl-1 [17]. A different mechanism was proposed by C. Distelhorst in collaboration with our own group. We found that Bcl-2 bound to the central, modulatory domain of the IP_3R and suppressed IP_3R-channel activity, thereby preventing excessive pro-apoptotic Ca^{2+} transients [15]. Detailed molecular studies revealed the BH4 domain of Bcl-2 as sufficient and necessary for Bcl-2 binding to the IP_3R [16,18–20]. Furthermore, we showed that a critical difference between Bcl-2 and Bcl-X_L in the center of their respective BH4 domains may underpin the opposite outcome of Bcl-2 versus Bcl-X_L binding to IP_3R channels [16,21].

Here, we compared the Bcl-2/Bcl-X_L-binding properties of GST-fusion proteins of IP_3R1 covering (i) the central, modulatory domain (Domain3), (ii) the cytosolic C-terminal tail containing the distal 160 amino acids (Domain6) and (iii) the C-terminal domain encompassing the pore, including the putative pore helix, selectivity filter and the sixth transmembrane domain (TMD), and the C-terminal tail (TMD6 + Domain6). The first two proteins were developed before in our lab and used in previous studies [15,20,21]. For the third protein, we chose to develop exactly the same protein as the one used by Foskett and co-workers in their previous study [13]. Our experiments show that the C-terminal channel domain of the IP_3R is a target for Bcl-2/Bcl-X_L, demonstrating the presence of two differential binding sites for Bcl-2 proteins on IP_3R channels.

2. Materials and methods

2.1. Cloning, expression and purification of GST-constructs

Parental GST, GST-Domain3 (aa 923–1581) and GST-Domain6 (aa 2590–2749) were prepared as previously described [22]. The GST-fusion protein encompassing the sixth transmembrane domain and the C-terminal tail of IP_3R1, GST-TMD6 + Domain6 (aa 2512–2749 of mouse IP_3R1) was obtained by PCR amplification of the corresponding open reading frame (nucleotides 7536–8250 of mouse IP_3R1) using 5′-GCGGCGGGATCCGAGCTGCTCCCTGCC-GAAGAAACGG-3′ as forward primer and 5′-GCGGCGGAA TTCCTAGGCCGGCTGCTGTGGGTTGAC-3′ as reverse primer and cloning in the BamHI/EcoRI restriction site of the pGEX6p2 vector. The GST-TMD6 + Domain6 fusion protein was purified from BL21(DE3) *Escherichia coli* cells as described before [23], except that elution was done using a buffer containing 50 mM glutathione and 150 mM NaCl. Proteins were dialyzed using Slide-A-Lyzer cassettes with a cut-off of 10 kDa (Thermo Fisher Scientific, Pittsburg, PA). The protein concentration was determined using the Bradford assay (Sigma–Aldrich, Munich, Germany). After SDS–PAGE, the purity and quality of the purified GST-TMD6 + Domain6 was assessed via total protein gel staining using GelCode Blue Stain Reagent (Thermo Scientific, Rockford, IL) and Western-blotting analysis using anti-GST (dilution 1:2000, Invitrogen, Merelbeke, Belgium).

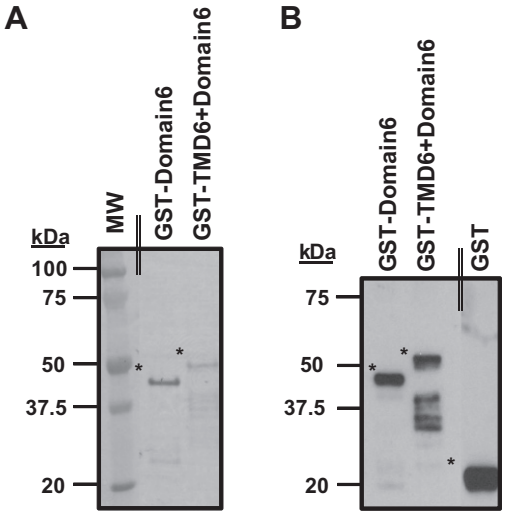

Fig. 1. Total protein staining and Western-blotting analysis of the purified GST-TMD6 + Domain6 fusion protein. (A) Total protein staining of the purified GST-Domain6 (~45 kDa protein) and GST-TMD6 + Domain6 (~50 kDa protein) obtained after purification using glutathione-Sepharose 4B beads and SDS–PAGE. Both full-length proteins are indicated with an asterisk. Similar amounts (2 μg) of both proteins were loaded. The first lane on the left shows the different molecular weight (MW) markers used as references and indicated on the left in kDa. (B) Western-blotting analysis of the purified GST-Domain6 and GST-TMD6 + Domain using an anti-GST antibody. Similar amounts of both proteins (500 ng) were loaded. Both full-length proteins are indicated with an asterisk. The double line on the Western blot indicates that lanes from another part of the same gel and exposure time were merged.

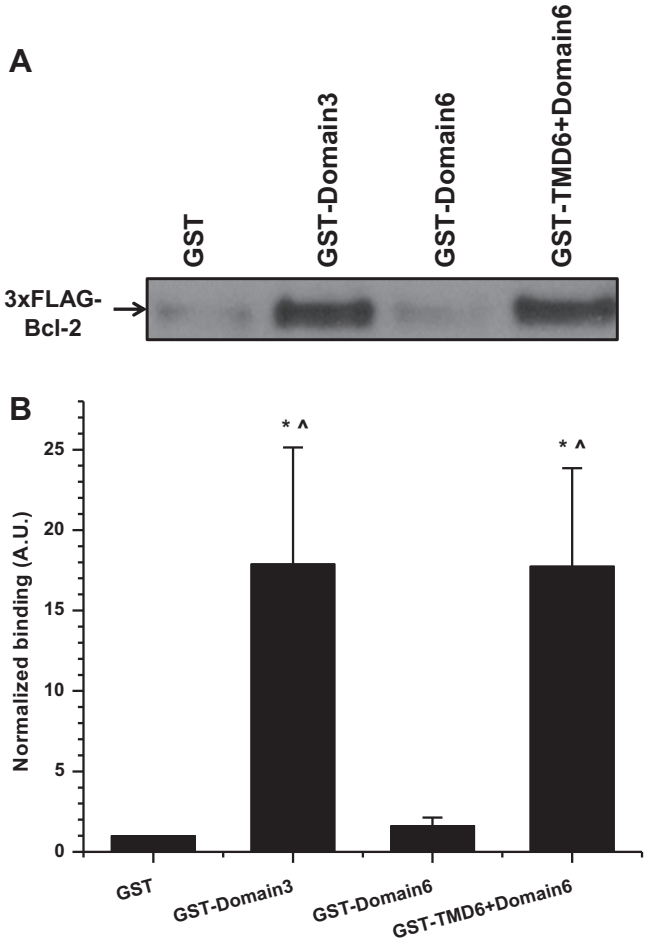

Fig. 2. GST-pull-down experiment showing the binding of 3×FLAG-Bcl-2 to the different purified GST-tagged IP_3R domains. (A) The amount of 3×FLAG-Bcl-2 retained by the different GST-fusion proteins was assessed via Western-blotting analysis using an anti-FLAG antibody. Parental GST was used as a negative control. The result of a representative GST-pull-down assay is shown out of three independent experiments. (B) The immunoreactive anti-FLAG signal was quantified using IMAGE-J and normalized to the signal obtained in the pull-down reactions using parental GST ($N = 3$). *indicates a significant difference ($p < 0.05$) compared to GST in a one-tailed t-test. ^A significant difference ($p < 0.05$) compared to GST-Domain6 in a one-tailed t-test.

2.2. GST-pull-down assays

Parental GST, GST-Domain3, GST-Domain6 and GST-TMD6 + Domain6 were used as bait in GST-pull-down assays to assess the binding of 3xFLAG-Bcl-2 or 3xFLAG-Bcl-X_L. The latter were expressed in COS-1 cells after transfection with 3xFLAG-MYC-pCMV-24 vectors (Sigma–Aldrich) encoding either Bcl-2 or Bcl-X_L. Three days after transfection, cell lysates were prepared using a buffer containing 25 mM Hepes, pH 7.5, 1% Triton X-100, 10% glycerol, 0.3 M NaCl, 1.5 mM $MgCl_2$, 1 mM DTT, 2 mM EDTA, 2 mM EGTA and protease inhibitor cocktail tablets (Roche, Basel, Switzerland). Protein concentrations were determined using Bradford analysis. Cell lysates (100 μg) were incubated for 1 h at 4 °C with equimolar amounts (~250 pmol/reaction) of the different purified GST-fusion proteins in a total reaction volume of 500 μl lysis buffer and captured using glutathione-Sepharose 4B beads (20 μl) for 1.5 h at 4 °C. The beads were washed 6 times with 500 μl reaction buffer and eluted in 40 μl of LDS sample buffer. These samples (15 μl) were analyzed on NuPAGE 4–12% Bis/Tris SDS–polyacrylamide gels using MES/SDS-running buffer (Invitrogen) and Western-blotting analysis was performed using anti-FLAG M2 antibody (dilution 1:6500, Sigma Aldrich).

3. Results and discussion

GST-TMD6 + Domain6 was purified and analyzed via SDS–PAGE along with GST-Domain6, developed and used in previous studies [15]. A total protein staining demonstrates the quality and purity of the purified GST-TMD6 + Domain6 (Fig. 1A). The presence of the full-length GST-TMD6 + Domain6 was confirmed using Western-blotting analysis using anti-GST antibody (Fig. 1B).

We then evaluated the Bcl-2-binding properties of GST-Domain6 and GST-TMD6 + Domain6 by performing semi-quantitative GST-pull-down assays with cell lysates obtained from COS-1 cells transiently transfected with 3xFLAG-tagged Bcl-2-encoding plasmids (Fig. 2A). Parental GST was used as a negative control, while GST-Domain3, which corresponds to the central, modulatory domain of IP_3R1 containing the previously identified Bcl-2-binding site [15], was used as positive control. Supplemental Fig. 1A shows a schematic representation of IP_3R1 with the different domains

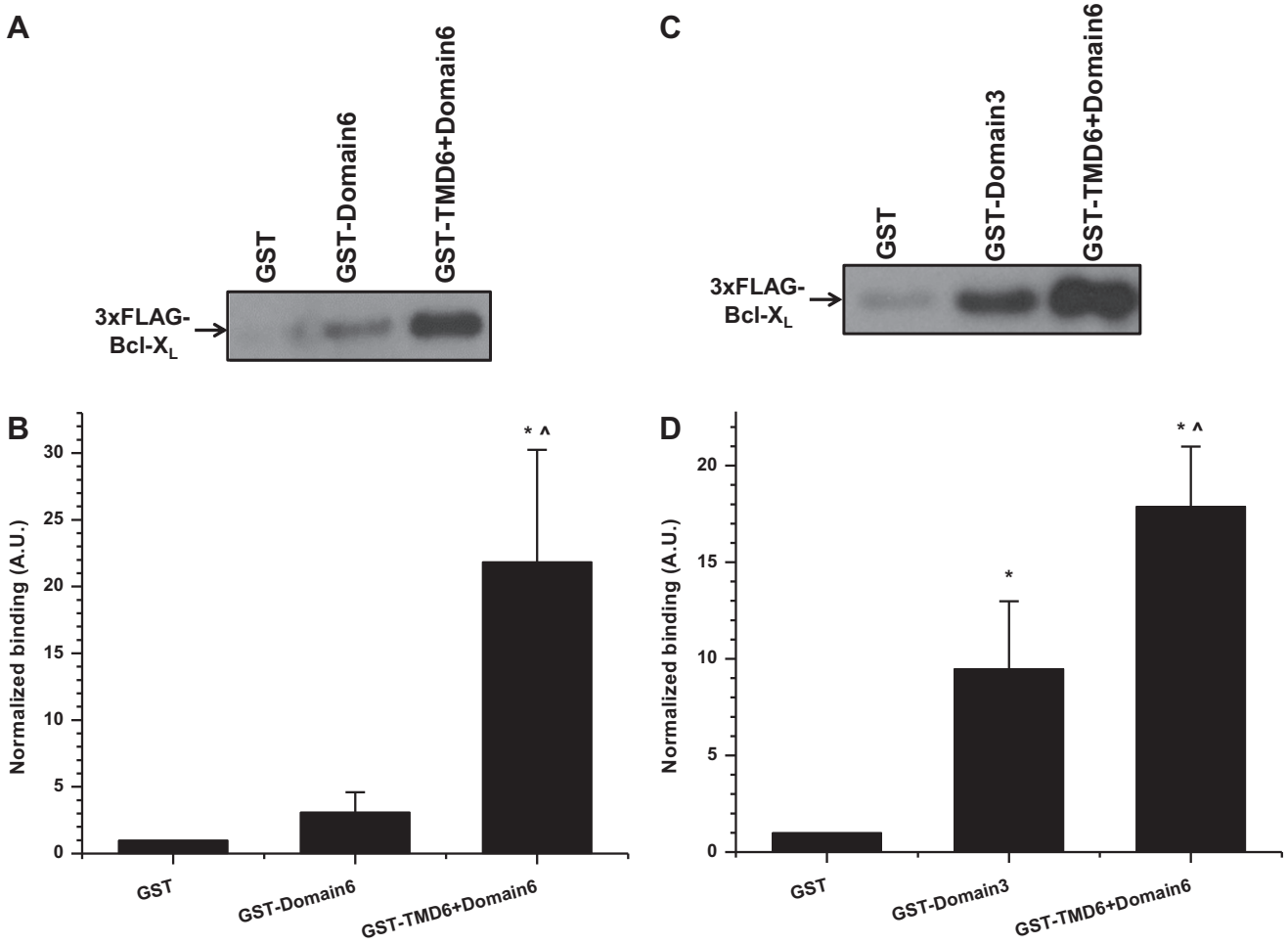

Fig. 3. GST-pull-down experiment showing the binding of 3×FLAG-Bcl-X_L to the different purified GST-tagged IP_3R domains. (A) The binding of 3×FLAG-Bcl-X_L to GST-Domain6 and GST-TMD6 + Domain6 was assessed via Western-blotting analysis using an anti-FLAG antibody. Parental GST was used a negative control. A typical experiment is shown out of three independent experiments. The double line on the Western blot indicates that lanes from another part of the same gel and exposure time were merged. (B) The immunoreactive anti-FLAG signal was quantified using IMAGE-J and normalized to the signal obtained in the pull-down reactions using parental GST ($N = 3$). *A significant difference ($p < 0.05$) compared to GST in a one-tailed t-test. ^A significant difference ($p < 0.05$) compared to GST-Domain6 in a one-tailed t-test. (C) The binding of 3×FLAG-Bcl-X_L to GST-TMD6 + Domain6 was compared to its binding to GST-Domain3. Parental GST was used as a negative control. A typical experiment is shown out of eight independent experiments. (D) The immunoreactive anti-FLAG signal was quantified using IMAGE-J and normalized to the signal obtained in the pull-down reactions using parental GST ($N = 8$). *indicates a significant difference ($p < 0.05$) compared to GST in a one-tailed t-test. ^A significant difference ($p < 0.05$) compared to GST-Domain3 in a one-tailed t-test.

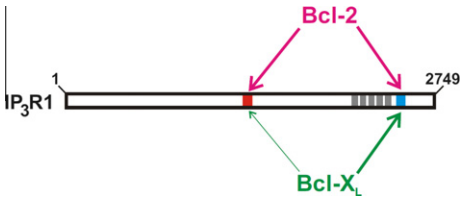

Fig. 4. Schematic representation of the IP_3R1 and its binding sites for Bcl-2 and Bcl-X_L. The IP_3R1 harbors two binding sites for Bcl-2 and Bcl-X_L. One binding site is located in the central, modulatory domain of the IP_3R1 (indicated in red) and one in the C-terminal channel domain including the sixth transmembrane domain (indicated in blue). Bcl-2 targets with similar efficiency both the central and C-terminal binding site in IP_3R1. In contrast, Bcl-X_L preferentially targets the C-terminal binding site in IP_3R1. These differences in IP_3R-binding profile between Bcl-2 and Bcl-X_L may underlie their different effects on Ca^{2+} fluxes through the IP_3R channel with Bcl-2 acting as an inhibitor and Bcl-X_L acting as an enhancer. (For interpretation of the references to color in this figure legend, the reader is referred to the web version of this article.)

used as GST-fusion proteins in this study. Supplemental Fig. 1B shows that similar amounts of GST-fusion proteins were present in the pull-downs. 3xFLAG-Bcl-2 binding to GST-Domain6 was not significantly higher than the binding of 3xFLAG-Bcl-2 to parental GST (Fig. 2B). In contrast, GST-TMD6 + Domain6 bound significantly higher amounts of 3xFLAG-Bcl-2. Furthermore, 3xFLAG-Bcl-2 bound to GST-Domain3 and GST-TMD6 + Domain6 with similar apparent affinities. These data indicate that elements preceding the cytosolic C-terminal tail of IP_3R1 are essential for Bcl-2 binding and that IP_3R1 contains two different Bcl-2-binding sites, which are targeted by Bcl-2 with comparable efficiencies.

A similar analysis was performed for 3xFLAG-tagged Bcl-X_L. Again, GST-pull-down assays revealed that binding of 3xFLAG-Bcl-X_L to GST-TMD6 + Domain6 was significantly higher than to GST-Domain6 and that binding of 3xFLAG-Bcl-X_L to GST-Domain6 was not significantly different from the binding to parental GST (Fig. 3A and B). This confirms that the sixth transmembrane domain of the IP_3R contains part of the interaction site for Bcl-X_L as well as for Bcl-2. In addition, we compared the binding of 3xFLAG-Bcl-X_L to the central, modulatory domain and the C-terminal domain of the IP_3R in a semi-quantitative manner (Fig. 3C and D). We found that 3xFLAG-Bcl-X_L binding to GST-Domain3 was significantly lower than the binding of 3xFLAG-Bcl-X_L to GST-TMD6 + Domain6. The latter data indicate that, different from Bcl-2, Bcl-X_L preferentially binds to the C-terminal binding domain of the IP_3R. This result is fully consistent with our previous study showing that the BH4 domain of Bcl-X_L is critically different from the BH4 domain of Bcl-2. BH4-Bcl-X_L binds with a much lower affinity to the central, modulatory domain of the IP_3R than BH4-Bcl-2, due to a critical single amino-acid modification in this domain (Asp11 versus Lys17) [21].

Thus, these experiments clearly indicate that the IP_3R harbors at least two different Bcl-2/Bcl-X_L-binding sites. The binding site in the C-terminal part of the IP_3R critically depends on elements preceding the C-terminal cytosolic tail, like the presence of the sixth transmembrane domain (Fig. 4). This is underpinned by a recent study by Eckenrode et al. showing that a GST-fusion protein containing the sixth transmembrane domain and the C-terminal tail of IP_3R1 binds various anti-apoptotic Bcl-2-family members with similar affinities [17]. Remarkably, Bcl-2 binds with equal efficiencies to both domains, while Bcl-X_L binds with significantly higher efficiency to the C-terminal domain than to the central, modulatory domain of IP_3R1. These differences in binding modes between Bcl-2 and Bcl-X_L may underlie their different properties with respect to the regulation of IP_3R channels. Bcl-2 may predominantly act as an effective inhibitor of excessive IP_3R-channel activity [24], whereas Bcl-X_L may predominantly operate as an enhancer of basal IP_3R-channel activity [13]. Thus, Bcl-XL by mainly targeting the a region close to the Ca^{2+}-channel pore which is also physically linked to the N-terminal IP_3-binding domain may facilitate the opening of the Ca^{2+}-channel pore upon binding of IP_3 [23,25]. Remarkably, a similar mechanism has recently been described for Bax Inhibitor-1 and IP_3Rs [26]. Furthermore, these data may also explain why Bcl-2 is a very effective regulator of the Ca^{2+}-flux properties of the IP_3R despite the relatively low affinity of the isolated BH4 domain to bind and regulate IP_3Rs. The presence of an additional binding site for Bcl-2 in the C-terminal part of the IP_3R may tether the BH4 domain of Bcl-2 in the close proximity of the central, modulatory domain. These findings are also in line with detailed molecular and modeling studies obtained for Bcl-2/ASPP2-protein complexes in which different Bcl-2 domains establish different contact sites for binding ASPP2, resulting in an overall high-affinity binding of Bcl-2 to ASPP2 [27]. Similarly as for the IP_3R, the BH4 domain of Bcl-2, which contains an additional positive charge (Lys17), has a higher affinity for ASPP2 than the BH4 domain of Bcl-X_L, which contains an additional negative charge (Asp11).

Collectively, these data in combination with previous observations [17] identify the sixth transmembrane domain of IP_3R1 as a critical component of the binding site for anti-apoptotic Bcl-2 proteins in the C-terminal part of the IP_3R channel. In addition, this binding site for anti-apoptotic Bcl-2 proteins may be more promiscuous for binding Bcl-2 and Bcl-X_L than the one in the central, modulatory domain that is more selective for binding Bcl-2 than Bcl-X_L through critical differences in the BH4-domain biology. Finally, differences in binding modes between various Bcl-2-family members targeting both binding sites with different affinities may underlie their distinct properties towards IP_3R-channel regulation, either inhibition (e.g. like for Bcl-2) or sensitization (like for Bcl-X_L).

Competing interests

The authors declare that there no competing interests.

Author contributions

GM and MB performed the experimental work. GB and GM designed the study, GB supervised the study. All authors were involved in analyzing and interpreting the data, GB prepared the manuscript in collaboration with the other authors.

Acknowledgments

We thank Kirsten Welkenhuyzen, Marina Crabbé and Anja Florizoone for excellent technical help. This work has been supported by research grants provided by the Research Council of the KU Leuven (OT/STRT1/10/044), the Research Foundation – Flanders (FWO; grants numbers G.0788.11 and G.0571.12) and by the Royal Flemish Academy of Belgium for Science and the Arts (Research Award from the Octaaf Dupont Foundation 2010). GM is holder of a PhD fellowship of the Research Foundation – Flanders (FWO). The authors thank Dr. Kevin Foskett (University of Pennsylvania) and Dr. Clark W. Distelhorst (Case Western Reserve University) for helpful discussions.

Appendix A. Supplementary data

Supplementary data associated with this article can be found, in the online version, at http://dx.doi.org/10.1016/j.bbrc.2012.10.002.

References

[1] P. Pinton, C. Giorgi, R. Siviero, E. Zecchini, R. Rizzuto, Calcium and apoptosis: ER-mitochondria Ca^{2+} transfer in the control of apoptosis, Oncogene 27 (2008) 6407–6418.
[2] C. Giorgi, F. Baldassari, A. Bononi, M. Bonora, E. De Marchi, S. Marchi, S. Missiroli, S. Patergnani, A. Rimessi, J.M. Suski, M.R. Wieckowski, P. Pinton, Mitochondrial Ca^{2+} and apoptosis, Cell Calcium 52 (2012) 36–43.
[3] C. Giorgi, D. De Stefani, A. Bononi, R. Rizzuto, P. Pinton, Structural and functional link between the mitochondrial network and the endoplasmic reticulum, Int. J. Biochem. Cell Biol. 41 (2009) 1817–1827.
[4] R. Rizzuto, S. Marchi, M. Bonora, P. Aguiari, A. Bononi, D. De Stefani, C. Giorgi, S. Leo, A. Rimessi, R. Siviero, E. Zecchini, P. Pinton, Ca^{2+} transfer from the ER to mitochondria: when, how and why, Biochim. Biophys. Acta 1787 (2009) 1342–1351.
[5] J.P. Decuypere, G. Monaco, G. Bultynck, L. Missiaen, H. De Smedt, J.B. Parys, The IP_3 receptor-mitochondria connection in apoptosis and autophagy, Biochim. Biophys. Acta 2011 (1813) 1003–1013.
[6] Y. Rong, C.W. Distelhorst, Bcl-2 protein family members: versatile regulators of calcium signaling in cell survival and apoptosis, Annu. Rev. Physiol. 70 (2008) 73–91.
[7] P. Pinton, C. Giorgi, P.P. Pandolfi, The role of PML in the control of apoptotic cell fate: a new key player at ER-mitochondria sites, Cell Death Differ. 18 (2011) 1450–1456.
[8] P. Pinton, D. Ferrari, E. Rapizzi, F. Di Virgilio, T. Pozzan, R. Rizzuto, The Ca2+ concentration of the endoplasmic reticulum is a key determinant of ceramide-induced apoptosis: significance for the molecular mechanism of Bcl-2 action, EMBO J. 20 (2001) 2690–2701.
[9] P. Pinton, D. Ferrari, P. Magalhaes, K. Schulze-Osthoff, F. Di Virgilio, T. Pozzan, R. Rizzuto, Reduced loading of intracellular Ca^{2+} stores and downregulation of capacitative Ca^{2+} influx in Bcl-2-overexpressing cells, J. Cell Biol. 148 (2000) 857–862.
[10] L. Scorrano, S.A. Oakes, J.T. Opferman, E.H. Cheng, M.D. Sorcinelli, T. Pozzan, S.J. Korsmeyer, BAX and BAK regulation of endoplasmic reticulum Ca^{2+}: a control point for apoptosis, Science 300 (2003) 135–139.
[11] S.A. Oakes, L. Scorrano, J.T. Opferman, M.C. Bassik, M. Nishino, T. Pozzan, S.J. Korsmeyer, Proapoptotic BAX and BAK regulate the type 1 inositol trisphosphate receptor and calcium leak from the endoplasmic reticulum, Proc. Natl. Acad. Sci. USA 102 (2005) 105–110.
[12] R. Chen, I. Valencia, F. Zhong, K.S. McColl, H.L. Roderick, M.D. Bootman, M.J. Berridge, S.J. Conway, A.B. Holmes, G.A. Mignery, P. Velez, C.W. Distelhorst, Bcl-2 functionally interacts with inositol 1,4,5-trisphosphate receptors to regulate calcium release from the ER in response to inositol 1,4,5-trisphosphate, J. Cell Biol. 166 (2004) 193–203.
[13] C. White, C. Li, J. Yang, N.B. Petrenko, M. Madesh, C.B. Thompson, J.K. Foskett, The endoplasmic reticulum gateway to apoptosis by Bcl-X_L modulation of the $InsP_3R$, Nat. Cell Biol. 7 (2005) 1021–1028.
[14] C. Li, X. Wang, H. Vais, C.B. Thompson, J.K. Foskett, C. White, Apoptosis regulation by Bcl-x(L) modulation of mammalian inositol 1,4,5-trisphosphate receptor channel isoform gating, Proc. Natl. Acad. Sci. USA 104 (2007) 12565–12570.
[15] Y.P. Rong, A.S. Aromolaran, G. Bultynck, F. Zhong, X. Li, K. McColl, S. Matsuyama, S. Herlitze, H.L. Roderick, M.D. Bootman, G.A. Mignery, J.B. Parys, H. De Smedt, C.W. Distelhorst, Targeting Bcl-2-IP3 receptor interaction to reverse Bcl-2's inhibition of apoptotic calcium signals, Mol. Cell 31 (2008) 255–265.
[16] G. Monaco, T. Vervliet, H. Akl, G. Bultynck, The selective BH4-domain biology of Bcl-2-family members: IP_3Rs and beyond, Cell. Mol. Life Sci. In press. http://dx.doi.org/10.1007/s00018-012-1118-y.
[17] E.F. Eckenrode, J. Yang, G.V. Velmurugan, J.K. Foskett, C. White, Apoptosis protection by Mcl-1 and Bcl-2 modulation of inositol 1,4,5-trisphosphate receptor-dependent Ca^{2+} signaling, J. Biol. Chem. 285 (2010) 13678–13684.
[18] Y.P. Rong, G. Bultynck, A.S. Aromolaran, F. Zhong, J.B. Parys, H. De Smedt, G.A. Mignery, H.L. Roderick, M.D. Bootman, C.W. Distelhorst, The BH4 domain of Bcl-2 inhibits ER calcium release and apoptosis by binding the regulatory and coupling domain of the IP3 receptor, Proc. Natl. Acad. Sci. USA 106 (2009) 14397–14402.
[19] C.W. Distelhorst, M.D. Bootman, Bcl-2 interaction with the inositol 1,4,5-trisphosphate receptor: role in Ca(2+) signaling and disease, Cell Calcium 50 (2011) 234–241.
[20] F. Zhong, M.W. Harr, G. Bultynck, G. Monaco, J.B. Parys, H. De Smedt, Y.P. Rong, J.K. Molitoris, M. Lam, C. Ryder, S. Matsuyama, C.W. Distelhorst, Induction of Ca(2)+-driven apoptosis in chronic lymphocytic leukemia cells by peptide-mediated disruption of Bcl-2-IP3 receptor interaction, Blood 117 (2011) 2924–2934.
[21] G. Monaco, E. Decrock, H. Akl, R. Ponsaerts, T. Vervliet, T. Luyten, M. De Maeyer, L. Missiaen, C.W. Distelhorst, H. De Smedt, J.B. Parys, L. Leybaert, G. Bultynck, Selective regulation of IP3-receptor-mediated Ca^{2+} signaling and apoptosis by the BH4 domain of Bcl-2 versus Bcl-Xl, Cell Death Differ. 19 (2012) 295–309.
[22] G. Bultynck, P. De Smet, D. Rossi, G. Callewaert, L. Missiaen, V. Sorrentino, H. De Smedt, J.B. Parys, Characterization and mapping of the 12 kDa FK506-binding protein (FKBP12)-binding site on different isoforms of the ryanodine receptor and of the inositol 1,4,5-trisphosphate receptor, Biochem. J. 354 (2001) 413–422.
[23] G. Bultynck, K. Szlufcik, N.N. Kasri, Z. Assefa, G. Callewaert, L. Missiaen, J.B. Parys, H. De Smedt, Thimerosal stimulates Ca^{2+} flux through inositol 1,4,5-trisphosphate receptor type 1, but not type 3, via modulation of an isoform-specific Ca^{2+}-dependent intramolecular interaction, Biochem. J. 381 (2004) 87–96.
[24] F. Zhong, M.C. Davis, K.S. McColl, C.W. Distelhorst, Bcl-2 differentially regulates Ca^{2+} signals according to the strength of T cell receptor activation, J. Cell Biol. 172 (2006) 127–137.
[25] D. Boehning, S.K. Joseph, Direct association of ligand-binding and pore domains in homo- and heterotetrameric inositol 1,4,5-trisphosphate receptors, EMBO J. 19 (2000) 5450–5459.
[26] S. Kiviluoto, L. Schneider, T. Luyten, T. Vervliet, L. Missiaen, H. De Smedt, J.B. Parys, A. Methner, G. Bultynck, Bax Inhibitor-1 is a novel IP_3 receptor-interacting and -sensitizing protein, Cell Death Dis. 3 (2012) e367.
[27] C. Katz, H. Benyamini, S. Rotem, M. Lebendiker, T. Danieli, A. Iosub, H. Refaely, M. Dines, V. Bronner, T. Bravman, D.E. Shalev, S. Rudiger, A. Friedler, Molecular basis of the interaction between the antiapoptotic Bcl-2 family proteins and the proapoptotic protein ASPP2, Proc. Natl. Acad. Sci. USA 105 (2008) 12277–12282.

PART III-*Supplementary information*

Profiling of the Bcl-2/Bcl-Xl-binding sites on type 1 IP_3 receptor

Giovanni Monaco[#], Marjolein Beckers[#], Hristina Ivanova, Ludwig Missiaen, Jan B. Parys, Humbert De Smedt, Geert Bultynck

Biochem Biophys Res Commun. 2012,428:31-5.

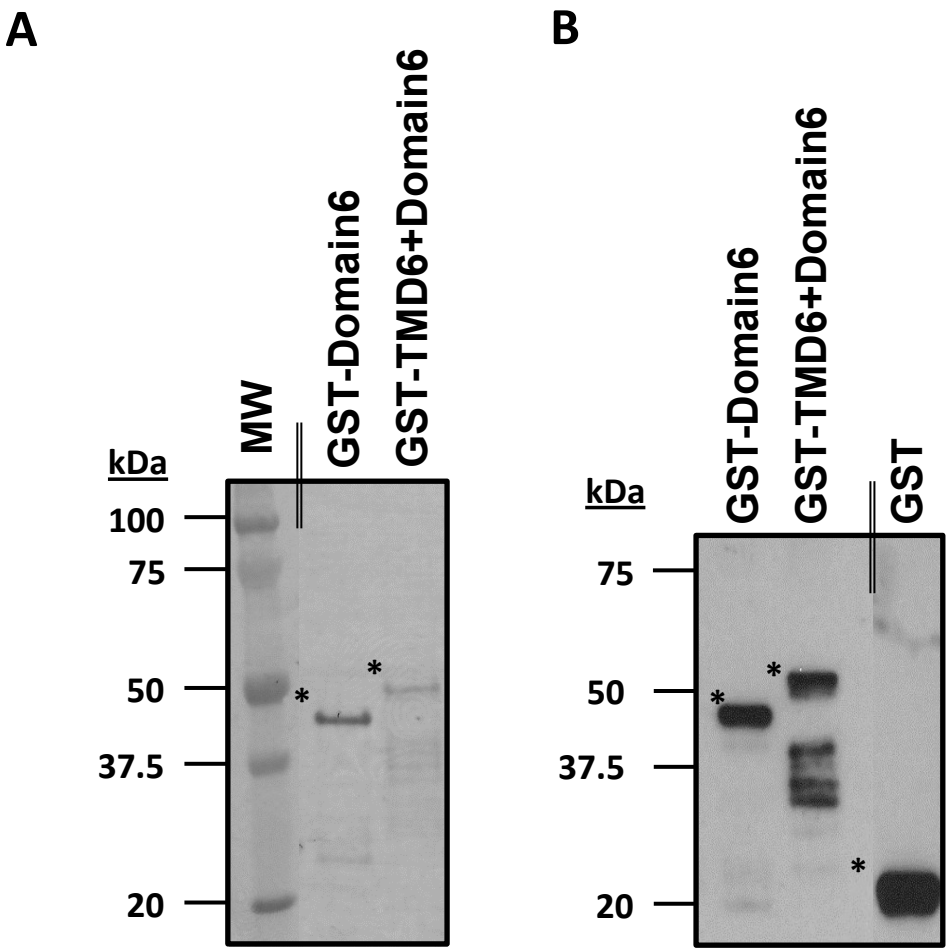

Supplementary figure 1. IP_3R domains used in this study. (A) Schematic representation of Domain3, Domain6 and TMD6 + Domain6 on the linear structure of the IP_3R1, which contains six transmembrane domains (gray boxes). (B) GST-fusion proteins of the different domains of the IP_3R1 depicted in panel A. The samples were obtained from LDS-treated beads at the end of the pull-down experiment. The asterisks indicate the presence of the respective full-length GST-fusion proteins. Their respective molecular mass is indicated at the left. Total protein staining, confirming the presence of similar amounts of GST-fusion proteins (indicated with asterisks) in the pull-down reaction, was obtained using GelCode Blue Stain Reagent.

GENERAL CONCLUSIONS AND FUTURE PERSPECTIVES

1 GENERAL CONCLUSIONS

The discussion presented in this section is partly based on the following review:

Giovanni Monaco, Tim Vervliet, Haidar Akl, Geert Bultynck (2013). The selective BH4-domain biology of Bcl-2-family members: IP_3Rs and beyond. *Cellular and Molecular Life Sciences, 2013 Apr; 70(7):1171-83*.

1 GENERAL CONCLUSIONS

Taken together, the results illustrated in the above research papers converge into the general conclusion that Bcl-2 and Bcl-Xl bear distinctive properties concerning their interaction with the IP_3Rs and subsequent protection against Ca^{2+}-mediated apoptosis. This statement is justified by the contrasting BH4-domain biology of Bcl-2 versus Bcl-Xl as well as by the specific pattern of interactions of these anti-apoptotic proteins with IP_3Rs. More specifically, the novel findings of this study can be summarized as follows:

i) *The BH4 domain of Bcl-2, but not of Bcl-Xl, inhibits IP_3R-mediated Ca^{2+} release.*

ii) *Isolated BH4 domains of Bcl-2 and Bcl-Xl are both protective against Ca^{2+}-mediated apoptosis but only the effect of BH4-Bcl-2 requires the interaction with the IP_3R.*

iii) *The conserved Lys17 in the BH4 domain of Bcl-2 determines (at the domain and full-protein level) its selective protective action via IP_3Rs.*

iv) *The alpha-helicity of the isolated BH4 domain of Bcl-2 is a key determinant for its ability to suppress IP_3R signaling and Ca^{2+}- mediated apoptosis.*

v) *Full-length Bcl-2 binds with similar affinity to the two reported interaction sites on IP_3R1, while Bcl-Xl binds more effectively to the IP_3R1 C-terminal site.*

Bcl-2 and Bcl-Xl are highly similar in sequence and structure and they share approximately 60% of homology and 43% of identity [45, 183, 184]. They were therefore so far considered as virtually exchangeable for regulating both, Ca^{2+} signaling and apoptosis. Early mutagenesis studies of Bcl-2 and Bcl-Xl revealed that the hydrophobic cleft is critical for heterodimerization with the pro-apoptotic relatives Bax and Bak and for protection against apoptosis [185, 186]. Nevertheless, in some cases, mutants no longer able to bind to Bax or Bak were yet retaining part of their anti-apoptotic activity [187-189] . This hydrophobic cleft-independent effect substantiates the protective role observed for the isolated BH4 domain of both Bcl-2 and Bcl-Xl in many experimental conditions [133, 171-173, 190, 191]. However,

most of these studies focused on the BH4 domain of either Bcl-2 or Bcl-Xl without any side-by-side comparison or in-depth molecular analysis.

As presented in the first research paper (Results, Part I), both BH4 domains protected against apoptosis induced by staurosporine, an apoptotic inducer discharging ER Ca^{2+}, but only Bcl-2's BH4 domain bound to and inhibited IP_3Rs. We identified a selective Bcl-2 anti-apoptotic activity at the level of the IP_3R due to specific molecular and functional characteristics of its BH4 domain. Indeed, IDP, a competitive peptide representing the BH4-Bcl-2-binding site on the IP_3R1 (a.a. 1389–1408), seems to inhibit only the protective effects of Bcl-2 without affecting Bcl-Xl's anti-apoptotic function. Importantly, no reduction in the ER Ca^{2+} content was observed following the incubation with the different BH4 domains or the overexpression of Bcl-2, in line with our previous results [170]. The anti-apoptotic effect of Bcl-2's BH4 domain was instead strictly due to the inhibition of the IP_3R1. It should be noticed that the latter mechanism may be valid also for the other IP_3R isoforms since all of them showed in our hands a similar affinity for binding to the BH4 domain of Bcl-2.

Furthermore, we elucidated one critical amino acid in this selective action of Bcl-2 *versus* Bcl-Xl on the IP_3Rs: while most residues are conserved between the BH4 domains of Bcl-2 and Bcl-Xl, a critical difference in one single surface-accessible residue is present in the center of this domain (Fig. 1, general conclusions). We found that Lys17 in BH4-Bcl-2 is not conserved in BH4-Bcl-Xl, in which it corresponds to an Asp residue. After performing a vast set of molecular and functional studies, we could pinpoint this residue as the underlying factor responsible for the difference in the BH4 domains of Bcl-2 and Bcl-Xl. Indeed, replacing Asp11 by Lys in BH4-Bcl-Xl led to a variant that was able to bind and inhibit IP_3Rs, while replacing Lys17 by Asp in BH4-Bcl-2 led to a variant that completely lost its IP_3R-binding and inhibitory properties. The importance of this difference for the biological properties of

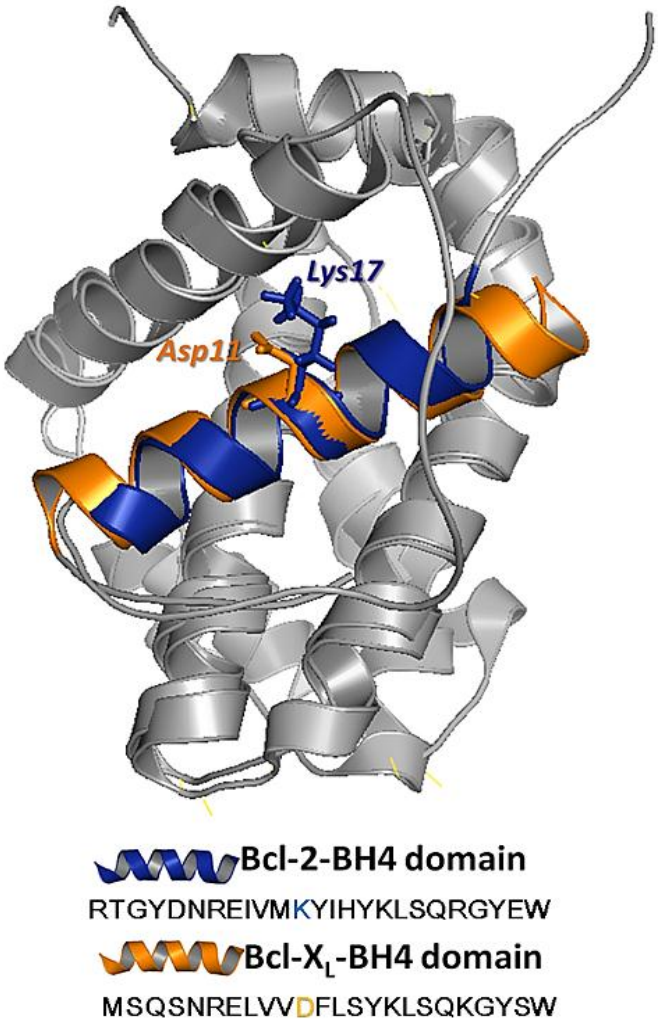

Fig. 1: A representation of the overlapping Bcl-2 and Bcl-Xl structures. The respective BH4 domains (blue for Bcl-2, orange for Bcl-Xl) are indicated together with the critical difference between Bcl-2 (Lys17) and Bcl-Xl (Asp11), which determines the ability of Bcl-2, but not of Bcl-Xl, to interact with the central, modulatory domain of the IP_3R. The lower part shows the sequence alignment of the BH4 domains of Bcl-2 and Bcl-Xl with highlighted Lys17 and Asp11. Adapted from [164].

these proteins is highlighted by the fact that altering this residue in full-length Bcl-2 impaired its ability to regulate IP_3Rs and to protect against Ca^{2+}-mediated apoptosis. This is further highlighted by the relative conservation of this critical residue switch across the vertebrate orthologs of Bcl-2 and Bcl-Xl [164]. Eventually, this may suggest that the property of Bcl-2-dependent regulation of IP_3Rs is conserved during evolution.

Apart from Lys17 a detailed alanine-scan analysis disclosed the further participation of other BH4-surface accessible residues (His20, Tyr21 and Arg26) in the interaction with the IP_3R. Ultimately, this raised the intriguing possibility that the three-dimensional organization of the BH4 domain might also contribute to its IP_3R-binding ability. Therefore, our study was extended towards examining the role played by the secondary structure of Bcl-2's BH4 domain. As presented in the second research paper (Results, Part II), the alpha helical organization seemed necessary, among the different conformations that the Bcl-2's BH4 peptide can assume in aqueous solution, to bind and inhibit IP_3Rs. This is in agreement with the secondary structure observed for the BH4 domain in the full-length Bcl-2 protein by NMR analysis and X-ray crystallography [183, 192]. However, the question still remained whether the BH4 alpha helix is equally essential to inhibit the IP_3R in the full-length protein considering the different protein context and the proximity of the hydrophobic cleft region. Interestingly, the dicodon mutation (I14G-V15G) that we used to destabilize the alpha-helical-BH4 peptide was previously reported to abolish Bcl-2's anti-apoptotic function, supposedly by effecting Bcl-2 heterodimerization with Bax [50, 55, 172, 174].

As previously discussed, only the BH4 domain of Bcl-2 binds to the IP_3R1 central/regulatory domain whereas the hydrophobic cleft of both proteins, formed by the BH3, BH1 and BH2 domains, has been proposed to bind IP_3R1 at a more distal C-terminal region [163, 166, 168, 169]. This interaction site was originally only identified for Bcl-Xl, and comprises the IP_3R1 C-terminal tail (the gating domain) together with part of the last TMD (TMD6) (a.a. 2512–2749). However, for Bcl-2 a controversy was still present in the field since a later study found that Bcl-2 did not interact with the C-terminal tail of the IP_3R1 (a.a. 2590–2749) [170]. Therefore, we decided to also measure the binding properties of Bcl-2 and Bcl-Xl to the C-terminal binding site on the IP_3R. As described in the third research paper (Results, Part III), the reasons behind the apparent discrepancy between published data was due to the use of

different IP_3R1 regions as representative for the C-terminal binding site. We indeed found that the presence of part of the TMD6 region was critical for the binding of both Bcl-2 and Bcl-Xl to the C-terminal binding domain of IP_3R1. Moreover, we also included in our comparative analysis of Bcl-2 and Bcl-Xl the previously characterized IP_3R1 central/regulatory domain. Consistent with our earlier observations, Bcl-Xl bound with higher efficiency to the C-terminal part of the IP_3R1 and to a lesser extent to the central, regulatory domain, while Bcl-2 targeted both sites with similar efficiencies (Fig. 2, General Conclusions). Collectively, we propose that the predominant effect of Bcl-2 on Ca^{2+} signaling is executed *via* its BH4 domain targeting the central, regulatory domain of the IP_3R, thereby imposing IP_3R inhibition and preventing large pro-apoptotic Ca^{2+} transients. For Bcl-Xl, we postulate a role for its hydrophobic cleft targeting a supposedly BH3-like structure near the C-terminal Ca^{2+}-channel pore of the IP_3R. This C-terminal interaction could then lead to increased IP_3R-channel gating and/or increased sensitivity towards activation by IP_3. Additionally, we confirmed that Bcl-2 too targets this C-terminal site, but functionally the inhibitory effect exerted by its BH4 domain may overrule the sensitizing effect of the interaction at the C-terminus. It is also conceivable that Bcl-2 may switch from an inhibitory position in the central modulatory domain to a stimulatory position at the C-terminus, depending on as yet unknown cellular conditions (*e.g.* regulation by phosphorylation). Finally, it should be mentioned that the molecular features that could explain a residual interaction of Bcl-Xl with the IP_3R1 central/regulatory domain need still to be further assessed.

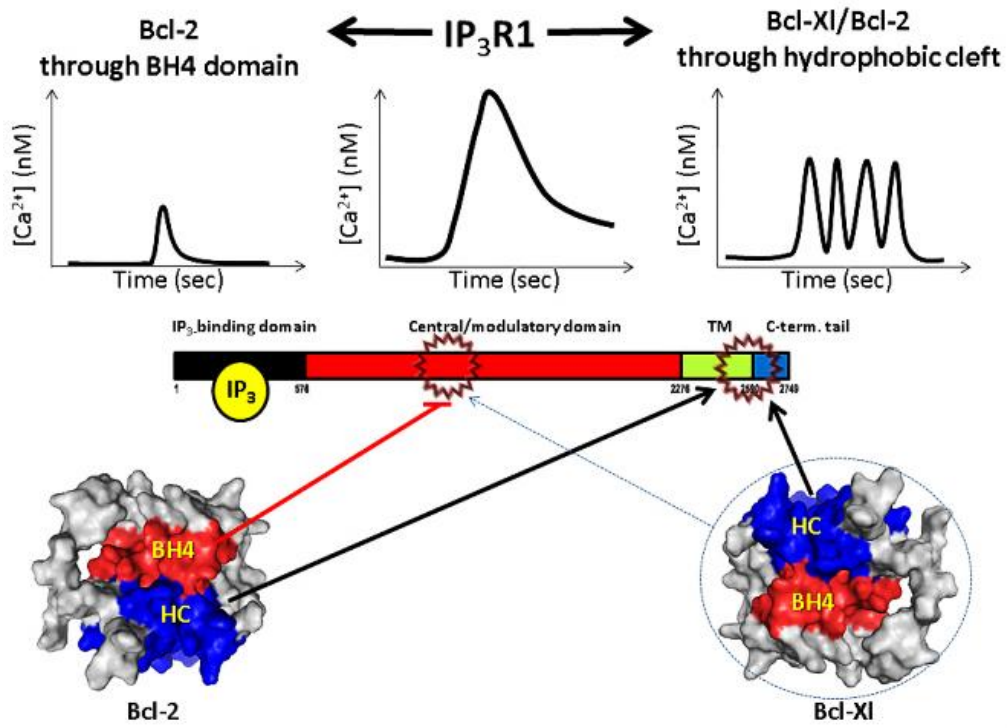

Fig. 2: An updated model for the regulation of IP_3R channels by Bcl-2 *versus* Bcl-Xl. The Ca^{2+}-flux properties of the IP_3R are thought to be critically controlled by Bcl-2-family members to promote cell survival or to protect against cell death. We propose that distinct anti-apoptotic Bcl-2-family members have a distinct interaction pattern with at least two binding sites on the IP_3R. In this paradigm, Bcl-2 through its BH4 domain may primarily target the central, modulatory domain of the IP_3R (a.a. 923–1581 for the mouse IP_3R1), thereby reducing large global pro-apoptotic Ca^{2+} transients (left); while Bcl-Xl through its hydrophobic cleft (HC) may primarily target the C-terminal region of the IP_3R (a.a. 2512–2749 for the mouse IP_3R1) close to the channel pore, thereby increasing IP_3R sensitivity to basal IP_3 levels and promoting pro-survival Ca^{2+} oscillations (right). In addition, we established that Bcl-2 was also able to target the C-terminal region of the IP_3R possibly *via* its hydrophobic cleft and it may in this way also contribute to the pro-survival Ca^{2+} signaling. On the other hand, we also showed some Bcl-Xl residual interactivity (see blue dotted frame and arrow) on the IP_3R's central, modulatory domain. The molecular parameters of the latter interaction are not yet clear, but we tend to exclude that it was mediated by its BH4 domain due to a critical single amino-acid difference in this domain (Asp11 in Bcl-Xl versus Lys17 in Bcl-2).

2 FUTURE PERSPECTIVES

The discovery of a specific Bcl-2/IP_3R liaison opens novel avenues to selectively suppress malignant Bcl-2 function in cancer cells by targeting its BH4 domain, while maintaining essential Bcl-Xl functions in normal cells. In this respect, ABT-737 and ABT-263, potent Bcl-2 inhibitors which are already in clinical development against hematological and solid tumors [63, 65, 193-196], act as Bad BH3-mimetic molecules that do not discriminate between Bcl-2 and Bcl-Xl. Hence, the targeting of Bcl-2's and Bcl-Xl's hydrophobic cleft results in the inhibition of the pro-survival activity of both proteins. This may not be desirable in cancer patients and cause adverse effects, since Bcl-2 and Bcl-Xl have distinct biological functions. While some types of cancer cells may need the elevated Bcl-2 levels to compensate for the on-going upstream pro-apoptotic signaling and the elevated levels of BH3-only proteins, normal cells may still need Bcl-Xl for their survival. As a proof of concept, drugs like ABT-737 that kill Bcl-2-dependent cancer cells (like CLL), lead to *in vivo* dose-dependent transient thrombocytopenia and thrombocytopathy [197, 198]. The latter is due to the simultaneous inhibition of Bcl-Xl, which is essential to sustain platelet survival by limiting Bax activity [199]. Henceforth, specifically targeting the BH4 domain of Bcl-2 with IDP may be a very promising approach to promote cell death in a more specific way *via* the induction of pro-apoptotic Ca^{2+} signaling in Bcl-2-dependent malignancies. This is further sustained by our observation that IDP (exclusively targeting Bcl-2) did not kill blood platelets (Akl, Monaco unpublished observations), as these cells mainly depend on Bcl-Xl for survival. Moreover, the co-administration of the IDP peptide with a newly developed Bcl-2-specific BH3-mimetic named ABT-199 [66, 200] could potentiate the killing of malignant blood cells but still spare the platelets. Finally, also the peptide encompassing the Bcl-2's BH4 domain has a promising future. As pointed out by part II of the results, this domain possesses indeed an independent anti-apoptotic activity exploitable for its development as a therapeutic tool. Particularly,

molecules derived from the BH4 domain would be useful in the treatment of some neurodegenerative or psychiatric diseases associated with aberrant intracellular Ca^{2+} signaling and consequently accelerated cell death. For instance, excessive IP_3R-mediated Ca^{2+} release has been implicated as contributing to the pathogenesis of Alzheimer's disease and a cell-permeable BH4 peptide can reduce Aβ peptide-induced apoptosis [201]. Since we just characterized the secondary structure of the BH4 domain required for its IP_3Rs inhibition, BH4 helical foldamers may have a future as lead compounds for therapeutics or at least as pharmacological tools.

Apart from this therapeutic and pharmacological potential, the results of this PhD research not only provided some important answers but also raised new questions, as we have addressed below.

What is the molecular mechanism behind the modulation of the IP_3Rs by Bcl-2's BH4 domain?

Although the function of Bcl-2's BH4 domain on the IP_3Rs is now clarified, the molecular mechanism that leads to the inhibition of the channel activity needs to be characterized. Bcl-2's BH4 domain may be an allosteric inhibitor of the IP_3Rs, in other words regulating channel gating through its binding to the central, regulatory region of the IP_3Rs which does not correspond to the channel activation site. Supporting this concept, IP_3R's central region has indeed been proven, in previous studies, to function in relaying the IP_3- and Ca^{2+}-stimulatory signals down to the channel region following a conformational rearrangement [90, 167]. However, mutagenesis, structural and computational studies of this BH4's binding site on the IP_3Rs are necessary and underway in order to gain experimental evidences. Additionally, some of our very recent data show a competitive behavior between IP_3 and the BH4 domain suggesting an even more complex regulatory mechanism. The IP_3R-LBD region might

therefore be recruited for an accessory role of the BH4 domain or the latter could electrostatically interfere with IP_3 to hamper its activity. IP_3-binding experiments in the presence and absence of the BH4 domain or of more electroneutral variants of this domain will elucidate the matter.

Which molecular determinants are responsible for Bcl-2 and Bcl-Xl interaction with the IP_3R's C-terminal region?

Our data pinpoint that the primary mechanism by which Bcl-2 impinges on Ca^{2+}-mediated apoptosis involves the activity of its BH4 domain on the IP_3Rs. We also know, from the present study as well as from earlier analysis [170], that BH4 prevents apoptosis by inhibiting the IP_3R in the same manner as reported for full-length Bcl-2. On the contrary, we do not know the exact molecular determinants involved in Bcl-2/Bcl-Xl interaction with the IP_3R's C-terminal site. Is the hydrophobic cleft truly the region that interacts with this portion of the channel or is the hydrophobic cleft only functional at the mitochondria? Certainly, the additive pro-apoptotic effect of IDP when administered together with the BH3-mimetic ABT-737[174] in cancer cells envisions that the anti-apoptotic mechanism of the BH4 domain on the IP_3R is independent of and complementary to the hydrophobic-cleft mechanism at the mitochondria. Further supporting this concept, the Bcl-2-IP_3R interaction appears increased in cells lacking the pro-apoptotic BH3-only family member Bim [202]. Accordingly, we also recently found that the smaller protective effect by the Bcl-2 K/D mutant seems solely imputable to BH4-domain loss of binding with the IP_3Rs, since the *in vitro* Bax-binding properties of the full-length protein were intact (preliminary results not yet published). However, all the above experimental results do not offer clear information about the putative hydrophobic-cleft interaction with the IP_3R's C-terminal site. At first glance, by exploiting a mutagenesis approach for the hydrophobic cleft or using the BH3-mimetic tool ABT-737, we

observed that, at least in unstressed conditions, the binding of Bcl-2 and Bcl-Xl to the IP_3R1 did not occur *via* the hydrophobic cleft (preliminary observations). These initial results leave open many possibilities: 1) Bcl-2's hydrophobic cleft may be only required during apoptosis for structurally allowing BH4 domain interaction with the IP_3R1 central, regulatory domain; 2) Bcl-2's hydrophobic cleft may not exploit the same BH3-domain-binding determinants to interact with the C-terminal part of the IP_3R; 3) Bcl-2's hydrophobic cleft may simply not be involved at all in the interaction because perhaps the C-terminal part of the IP_3R1 doesn't really contain BH3-like domains. In the first two cases, strong literature or experimental hints are lacking to guide our investigation, whereas in the last case we can already envisage some plausible additional paradigms. Even though Bcl-2's and Bcl-Xl's TMD seemed dispensable for their anti-apoptotic activity [203, 204], we observed, in further preliminary experiments, that cells overexpressing the TMD-truncated variant of Bcl-2 showed no inhibition of IICR if compared with wild-type Bcl-2-overexpressing cells. Hypothetically, Bcl-2 may hold tight the IP_3R through a membranous interaction involving its TMD and perhaps the IP_3R's C-terminal region in order to permit the BH4-domain activity at the central, regulatory domain. This would also be in agreement with the many biophysical data suggesting that the natural habitat for Bcl-2 family's interactions is the membrane environment [205, 206]. Alternatively, the TMD-truncated variant of Bcl-2 may have assumed a conformation unable to expose the BH4 domain for interactions or may have simply lost is ER-membrane localization signal [207]. Furthermore, we *cannot* exclude among the potential IP_3R C-terminal targets the large, highly flexible and intrinsically disordered loop located between the BH4 and BH3 domain of Bcl-2 [45, 183]. Such region is typically a target of many phosphorylation and dephosphorylation events which tune Bcl-2's anti-apoptotic activity [208, 209]. However, Bcl-2's phosphorylation status has also been proven to mediate protein-protein interactions involving the flexible loop itself [210, 211]. Finally, few of the above proposed mechanisms might be

valid for Bcl-Xl as well (*e.g.* the loop hypothesis) although the scenario might be here even more complicated, since Bcl-Xl's BH4 domain residual interaction with the IP_3R1 has still no reported molecular or functional role. Interestingly, by computational comparison of Bcl-2's and Bcl-Xl's tertiary structure, we recently observed that Bcl-Xl might bear a similar IP_3R-interaction surface outside its BH4-domain region as the one formed by Bcl-2 within its BH4 domain. Apparently, the key molecular determinants behind Bcl-2's BH4-domain interaction with the IP_3Rs (*e.g.* the positive residue Lys17) even though not present on Bcl-Xl's BH4 domain, might still be embodied more downstream on the Bcl-Xl structure (e.g Lys87, collaboration with L. Martens, VIB, Ghent).

Hereafter, Bcl-2/Bcl-Xl's molecular and structural role on the IP_3R1 C-terminal site will need appropriate characterization and validation in all above hypotheses. In any case, competitive peptides, derived from the IP_3R1 or Bcl-2/Bcl-Xl, will be useful to delineate the precise interaction profile in biochemical and biophysical experiments.

Is the protective effect of Bcl-Xl's BH4 domain due to its regulation of a mitochondrial target involved in the ER-mitochondria Ca^{2+} transfer?

It has recently become clear that specific sites of physical association between ER and mitochondria, named "mitochondrial associated membranes" (MAMs), are directly involved in the efficient channeling of Ca^{2+} from the ER into the mitochondria. Indeed, MAMs create a physical link between the mitochondria and the ER involving a vast set of inter-organelle proteins. In this regard, our experimental work pointed out that BH4-Bcl-Xl protects against apoptotic stimuli in an IP_3R–independent fashion suggesting that the target of its anti-apoptotic activity would be elsewhere, perhaps in the MAMs (see Fig. 1, future perspectives). In agreement with this hypothesis, our experimental results (see supplemental material of the first research paper [Results, Part I]) showed that by co-administering BH4 peptides derived

from both Bcl-Xl and Bcl-2, no additive protection was observed. Moreover, both BH4 peptides were unable to protect downstream of Cyt c release. Therefore, BH4-Bcl-Xl likely acts on a target downstream of the IP_3Rs probably in the same signaling cascade upstream of Cyt c. Considering the preferential distribution of Bcl-Xl to the mitochondrial outer membrane [207], we considered a mitochondrial target. In the MAMs at least one of the three subtypes of the IP_3R seems connected to VDAC-1 *via* a physical link provided by the chaperone glucose-regulated protein 75 (Grp75) [84, 212]. This would certainly make VDAC-1 a good candidate as a Bcl-Xl target because of its prominent role in the ER-mitochondria Ca^{2+}-cross-talk and of its demonstrated involvement in mitochondrial Ca^{2+} overload, MOMP and apoptosis [112]. Several studies have already suggested that the anti-apoptotic Bcl-2-family members could interact with the N-terminal region of VDAC-1 to regulate mitochondria-mediated apoptosis [133, 134, 213]. In addition, we already obtained preliminary evidence that VDAC-1 is a target of BH4-Bcl-Xl but not of BH4-Bcl-2. Importantly, the relevance of the IP_3R/Grp75/VDAC-1 complex and consequently of appropriate ER–mitochondrial coupling in healthy *versus* malignant cells is not fully understood. A very interesting parameter thereby would be the localization in the MAMs of particular IP_3R isoforms that have a different basal sensitivity to IP_3. The sensitivity of the IP_3R in the IP_3R/Grp75/VDAC-1 complex could be a crucial and as yet unappreciated parameter in determining the ER-to-mitochondrial Ca^{2+} flux and Ca^{2+}-dependent cell death.

In summary, we are now moving our research focus from an ER-centric view to a more comprehensive overall view of the ER-mitochondria Ca^{2+} crosstalk. Therefore, we are zooming out of Bcl-2's and Bcl-Xl's anti-apoptotic role at the IP_3Rs and investigating the wider scenario of the IP_3R/Grp75/VDAC-1 complex in Ca^{2+} mediated cell death. Moreover, the composition of such multi-protein complexes in the MAMs may be different in cancer cells as compared to normal healthy cells. In a future perspective, the composition of the

MAMs in cancer cells should be analyzed in order to appreciate and target potential defense systems of cancer cells against Ca^{2+}-mediated cell death.

Last but not least, although our laboratory has focused mainly on the interactions of Bcl-2 and Bcl-Xl with the IP_3R, BH4 interacts with a growing list of targets beyond IP_3Rs and even VDACs, including calcineurin/PP2B, murine leukemia viral oncogene homolog 1 (Raf-1), rat sarcoma small-GTPase (Ras), *Caenorhabditis elegans* death gene 4 (CED-4), paxillin, nuclear factor kappa-light-chain-enhancer of activated B cells (NF-kB), Bax inhibitor 1 (BI-1) and apoptosis-stimulating of p53 protein 2 (ASPP2) [164]. They all may contribute, together with the Bcl-2/IP_3R interaction, to enable Bcl-2/Bcl-Xl regulation of a wide range of signaling pathways, not only related to Bcl-2 and Bcl-Xl anti-apoptotic function [161, 214, 215].

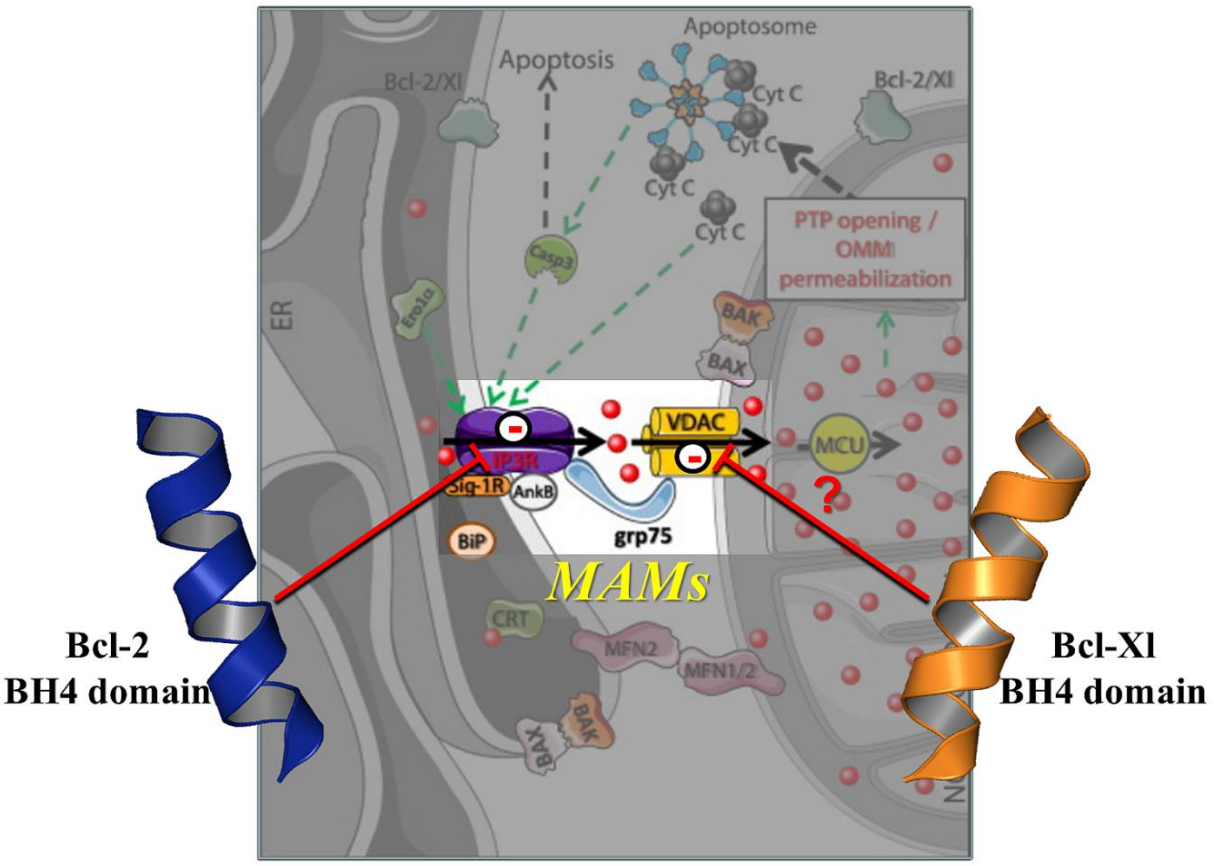

Fig. 1: The proposed roles of Bcl-2's and Bcl-Xl's BH4 domains at the ER-mitochondria contact sites. An excessive Ca^{2+} transfer from the ER to the mitochondria *via* the MAMs stimulates the progression of apoptosis. According to our results, Bcl-2 protects against Ca^{2+}-mediated apoptosis mainly by using its BH4 domain to interact and inhibit IP_3Rs on the ER. On the other hand, since Bcl-Xl is preferentially distributed to the mitochondrial outer membrane, we propose a specific role for the BH4 domain of Bcl-Xl in the reduction of mitochondrial Ca^{2+} uptake. Our preliminary data suggest that BH4-Bcl-Xl acts as an inhibitor of the Ca^{2+}-channel properties of VDAC-1, likely by controlling its N-terminal tail. Additionally, a more complex role at the level of IP_3R/Grp75/VDAC-1 Ca^{2+}-channeling function cannot be excluded and needs to be investigated. Adapted from [106].

SUMMARY
SAMENVATTING

SUMMARY

The anti-apoptotic proteins Bcl-2 and Bcl-Xl are highly similar in sequence and structure, and so far considered as virtually exchangeable for regulating apoptosis. Both proteins conventionally promote cell survival by employing their hydrophobic cleft in the heterodimerizion process with pro-apoptotic Bcl-2 members, like Bax and Bak, and consequently preserving mitochondrial integrity. In addition to this, Bcl-2 safeguards against MOMP by preventing mitochondrial Ca^{2+} overload. The latter role seems primarily due to Bcl-2's interaction with ER–resident IP_3Rs on their central, regulatory domain, thereby preventing IP_3R-dependent Ca^{2+} release and transfer to the mitochondria. The only Bcl-2 portion sufficient for IP_3R inhibition is the N-terminal BH4 domain, which is exclusive for the anti-apoptotic Bcl-2-family members and also reported to be essential for their pro-survival function. Bcl-Xl too has been reported to bind and modulate IP_3Rs but the molecular determinants involved in both binding partners are still unknown. In particular, Bcl-Xl may bind to the receptor on a different site, located close to the C-terminal, and stimulate basal/physiological IP_3R-mediated Ca^{2+} oscillations in favor of a proper mitochondrial respiration. In this respect, Bcl-Xl seems to predominantly enhance the pro-survival IP_3Rs signaling instead of hampering the anti-apoptotic one.

During this Ph.D. research, we first examined side-by-side the molecular features of Bcl-2 and Bcl-Xl in this seemingly conflicting regulation of IP_3R-dependent Ca^{2+} signaling and apoptosis. In more detail, we mainly compared the anti-apoptotic inhibition of IP_3R-mediated Ca^{2+} release by the BH4 domains of Bcl-2 *versus* Bcl-Xl. In molecular (pull downs; surface plasmon resonance [SPR] analysis) and functional (Ca^{2+} measurements and apoptotic assays) experiments, the BH4-domain biology of Bcl-2 and Bcl-Xl at the level of IP_3Rs appeared very different. BH4-Bcl-2 protected against Ca^{2+}-mediated apoptosis by binding the IP_3Rs and inhibiting IP_3-induced Ca^{2+} release, whereas BH4-Bcl-Xl protection proceeded without any

binding and regulation of the IP_3R channel although acting on the same signaling cascade. Interestingly, the selective molecular liaison between Bcl-2 and the IP_3Rs relates to a Lys17 in BH4-Bcl-2 that is not conserved in BH4-Bcl-Xl, in which it corresponds to an Asp residue, having an opposite charge.

Next, we examined the structural features of the Bcl-2-BH4 domain in even more detail. Hence, we investigated the role played by the three-dimensional structure of a Bcl-2-BH4 peptide in the aforedescribed IP_3R interaction. We thereby found that the isolated Bcl-2-BH4 domain requires an alpha-helical organization for binding the IP_3Rs and to inhibit the pro-apoptotic channel activity.

Finally, we extended our study towards an initial characterization of the full-length Bcl-2 and Bcl-Xl interactions with their proposed binding sites on IP_3R1. In this way, we partially solved a molecular controversy in the Ca^{2+} field by demonstrating that the full-length Bcl-2 bound with similar efficiency to the two reported interaction sites on IP_3R1, while Bcl-Xl bound more effectively to the IP_3R1 C-terminal site.

Collectively, these data support a selective and unique inhibition of the IP_3Rs by Bcl-2. Bcl-2-BH4 domain is therefore in charge of targeting the channel's central, regulatory domain and of curbing the pro-apoptotic ER Ca^{2+} release. Accordingly, even though both Bcl-2 and Bcl-Xl interact with the site next to the IP_3R1-channel pore, Bcl-Xl is more likely acting as an endogenous IP_3R sensitizer and promoter of pro-survival ER Ca^{2+} release. Indeed, its BH4 domain does not bear any function towards the IP_3Rs and seems instead protecting against Ca^{2+}-mediated apoptosis by acting downstream of the IP_3Rs probably just prior to the MOMP.

SAMENVATTING

De anti-apoptotische Bcl-2- en Bcl-Xl -proteïnen zijn zeer gelijkend in sequentie en structuur. Tot nu toe werden deze anti-apoptotische proteïnen als functioneel inwisselbaar beschouwd. Beide proteïnen zorgen voor celoverleving en het behouden van de mitochondriële integriteit door *via* hun hydrofobe groeve pro-apoptotische proteïnen van de Bcl-2-familie (zoals Bax en Bak) te neutraliseren. Bovendien verhindert Bcl-2 het overladen van de mitochondriën met Ca^{2+} en beschermt hierdoor tegen de permeabilisatie van het buitenste mitochondriële membraan (MBMP). Het onderliggende moleculaire mechanisme hiervoor is de interactie van Bcl-2 met de inositol 1,4,5-trisfosfaatreceptor (IP_3R), een intracellulair Ca^{2+}-vrijzettingskanaal in het ER membraan. Bcl-2 interageert daarbij *via* het centraal, regulatorische domein van de IP_3R. De interactie tussen Bcl-2 en de IP_3R onderdruk IP_3R-afhankelijke Ca^{2+}-vrijzetting en Ca^{2+}-overdracht naar de mitochondriën. Het BH4-domein van Bcl-2 is noodzakelijk en voldoende voor de inhibitie van IP_3R-activiteit. Dit BH4-domein is een exclusief kenmerk van anti-apoptotische Bcl-2-familieleden en is ook essentieel voor hun anti-apoptotische functie. Anderzijds zijn er ook meldingen dat het verwante anti-apoptotische Bcl-Xl aan de IP_3R bindt en daarbij de Ca^{2+}-flux eigenschappen moduleert en versterkt. De moleculaire determinanten van deze interactie tussen Bcl-Xl en de IP_3R werden nog niet verder gekarakteriseerd. Er werd voorgesteld dat Bcl-Xl zou binden aan een bindingsplaats in het C-terminale gedeelte van de IP_3R dichtbij het Ca^{2+}-porievormende gedeelte. Bcl-Xl zorgt hierbij voor een stimulatie van IP_3R-afhankelijke Ca^{2+}-oscillaties die betrokken zijn bij het aandrijven van de mitochondriële ademhalingsketen. In dat opzicht kan men Bcl-Xl beschouwen als een proteïne die celoverleving bevordert door het in stand houden van een basale, fysiologische IP_3R-gemedieerde Ca^{2+}-signaaltransductie.

Wij hebben gedurende dit PhD-onderzoekswerk eerst de moleculaire eigenschappen van Bcl-2 en Bcl-Xl met elkaar vergeleken, gezien hun schijnbaar tegengestelde effecten op IP_3R-

afhankelijke Ca^{2+}-signaaltransductie en celdood. Hierbij hebben wij de anti-apoptotische inhibitie van IP_3R-afhankelijke Ca^{2+}-vrijzetting onderzocht en werd het effect van de overeenkomstige BH4-domeinen van Bcl-2 en Bcl-Xl vergeleken. Uit verschillende moleculaire en functionele analyses bleken de biologische eigenschappen van de BH4-domeinen van Bcl-2 en Bcl-Xl zeer verschillend te zijn wat betreft de regeling van de IP_3R. BH4-Bcl-2 beschermde tegen Ca^{2+}-gemedieerde apoptose door te binden aan de IP_3R en de Ca^{2+}-vrijzetting doorheen deze kanalen zeer effectief te onderdrukken. In tegenstelling hiermee bleek BH4-Bcl-Xl veel minder sterk te binden aan de IP_3R. BH4-Bcl-Xl vertoonde wel bescherming tegen apoptose maar deze was onafhankelijk van de binding aan de IP_3R en van de regeling van zijn Ca^{2+}-vrijzettingsactiviteit. BH4-Bcl-2 en BH4-Bcl-Xl bleken echter wel in dezelfde signaalcascade te werken maar duidelijk op een verschillende plaats. De selectiviteit van de inhibitie van IP_3Rs door BH4-Bcl-2 bleek veroorzaakt te worden door de aanwezigheid van het positief geladen Lys17 in BH4-Bcl-2. Dit residu is uniek voor BH4-Bcl-2 en het overeenkomstige aminozuur in BH4-Bcl-Xl is het negatief geladen Asp11.

In een tweede deel werden de structurele eigenschappen van het BH4-Bcl-2-domein bepaald die noodzakelijk zijn voor zijn interactie met de IP_3R. Uit analyse van het geïsoleerde BH4-Bcl-2-domein en door gebruik te maken van specifieke mutaties in het BH4-Bcl-2-domein hebben wij aangetoond dat een alfa helixstructuur noodzakelijk was voor de binding aan en de inhibitie van de IP_3R.

Tenslotte hebben wij een eerste karakterisatie gedaan van de verschillende potentiële interactieplaatsen op de type-1 IP_3R-isovorm (IP_3R1) voor de volledige Bcl-2 en Bcl-Xl proteïnen. Deze analyse heeft althans ten dele een controverse betreffende deze bindingsplaatsen opgeklaard. Wij konden aantonen dat Bcl-2 zowel bond aan het centrale als aan het C-terminale domein van de IP_3R1 met gelijkaardige efficiëntie, terwijl Bcl-Xl veel efficiënter bond aan het C-terminale domein dan aan het centrale domein. Dit bevestigt

daarbij het verschillende functioneel effect van deze verwante proteïnen op cellulaire Ca^{2+}-signalen.

Wij kunnen besluiten dat deze data een selectieve en unieke rol voor Bcl-2 aantonen *via* zijn uniek BH4-domein, waarbij de pro-apoptotische activiteit van de IP_3R geïnhibeerd wordt. BH4-Bcl-2 heeft daarbij het centrale, regulatorische domein van de IP_3R als doelwit. BH4-Bcl-Xl heeft deze functie niet maar interageert vermoedelijk met een andere target in dezelfde signaalcascade. Anderzijds kunnen zowel het volledige Bcl-2 als het volledige Bcl-Xl binden aan de C-terminale kanaalregio. Daarom postuleren wij dat vooral Bcl-Xl kan beschouwd worden als een endogeen IP_3R-sensitizerend proteïne en een stimulator van IP_3R-gemedieerde Ca^{2+}-oscillaties die een pro-celoverlevingseffect hebben. Het geïsoleerde BH4-domein van Bcl-Xl bleek echter ook betrokken bij het onderdrukken van de pro-apoptotische Ca^{2+}-transfer naar de mitochondriën "downstream" van de IP_3R. Daarom stellen wij voor dat BH4-Bcl-Xl een "downstream" doelwit heeft in de IP_3R-Ca^{2+}-signaaltransductiecascade ter hoogte van de mitochondriën.

REFERENCES

REFERENCES FOR GENERAL INTRODUCTION, GENERAL CONCLUSIONS AND FUTURE PERSPECTIVES

1. Mizushima, N. and M. Komatsu, *Autophagy: Renovation of cells and tissues.* Cell, 2011. **147**(4): p. 728-41.
2. Clarke, P.G. and J. Puyal, *Autophagic cell death exists.* Autophagy, 2012. **8**(6): p. 867-9.
3. Hotchkiss, R.S., A. Strasser, J.E. McDunn, and P.E. Swanson, *Cell death.* N Engl J Med, 2009. **361**(16): p. 1570-83.
4. Kerr, J.F., A.H. Wyllie, and A.R. Currie, *Apoptosis: A basic biological phenomenon with wide-ranging implications in tissue kinetics.* Br J Cancer, 1972. **26**(4): p. 239-57.
5. Edinger, A.L. and C.B. Thompson, *Death by design: Apoptosis, necrosis and autophagy.* Curr Opin Cell Biol, 2004. **16**(6): p. 663-9.
6. Kreuzaler, P. and C.J. Watson, *Killing a cancer: What are the alternatives?* Nat Rev Cancer, 2012. **12**(6): p. 411-24.
7. Galluzzi, L., I. Vitale, J.M. Abrams, E.S. Alnemri, E.H. Baehrecke, M.V. Blagosklonny, . . . G. Kroemer, *Molecular definitions of cell death subroutines: Recommendations of the nomenclature committee on cell death 2012.* Cell Death Differ, 2012. **19**(1): p. 107-20.
8. Schlegel, R.A. and P. Williamson, *Phosphatidylserine, a death knell.* Cell Death Differ, 2001. **8**(6): p. 551-63.
9. Wickman, G., L. Julian, and M.F. Olson, *How apoptotic cells aid in the removal of their own cold dead bodies.* Cell Death Differ, 2012. **19**(5): p. 735-42.
10. Elmore, S., *Apoptosis: A review of programmed cell death.* Toxicol Pathol, 2007. **35**(4): p. 495-516.
11. Cejna, M., G. Fritsch, D. Printz, R. Schulte-Hermann, and W. Bursch, *Kinetics of apoptosis and secondary necrosis in cultured rat thymocytes and S49 mouse lymphoma and CEM human leukemia cells.* Biochem Cell Biol, 1994. **72**(11-12): p. 677-85.
12. Zhou, S., L. Zhao, M. Kuang, B. Zhang, Z. Liang, T. Yi, . . . X. Zhao, *Autophagy in tumorigenesis and cancer therapy: Dr. Jekyll or mr. Hyde?* Cancer Lett, 2012. **323**(2): p. 115-27.
13. Hannun, Y.A., *Apoptosis and the dilemma of cancer chemotherapy.* Blood, 1997. **89**(6): p. 1845-53.
14. Roehner, B.M., *Apoptosis* in *Driving forces in physical, biological and socio-economic phenomena-a network science investigation of social bonds and interactions.* 2007, Cambridge University Press. p. 1-14.
15. Favaloro, B., N. Allocati, V. Graziano, C. Di Ilio, and V. De Laurenzi, *Role of apoptosis in disease.* Aging (Albany NY), 2012. **4**(5): p. 330-49.
16. Cavallucci, V. and M. D'Amelio, *Matter of life and death: The pharmacological approaches targeting apoptosis in brain diseases.* Curr Pharm Des, 2011. **17**(3): p. 215-29.
17. Moffitt, K.L., S.L. Martin, and B. Walker, *From sentencing to execution--the processes of apoptosis.* J Pharm Pharmacol, 2010. **62**(5): p. 547-62.
18. Falschlehner, C., U. Schaefer, and H. Walczak, *Following trail's path in the immune system.* Immunology, 2009. **127**(2): p. 145-54.
19. Ola, M.S., M. Nawaz, and H. Ahsan, *Role of Bcl-2 family proteins and caspases in the regulation of apoptosis.* Mol Cell Biochem, 2011. **351**(1-2): p. 41-58.

20. Riedl, S.J. and Y. Shi, *Molecular mechanisms of caspase regulation during apoptosis.* Nat Rev Mol Cell Biol, 2004. **5**(11): p. 897-907.
21. Crawford, E.D. and J.A. Wells, *Caspase substrates and cellular remodeling.* Annu Rev Biochem, 2011. **80**: p. 1055-87.
22. Szegezdi, E., S.E. Logue, A.M. Gorman, and A. Samali, *Mediators of endoplasmic reticulum stress-induced apoptosis.* EMBO Rep, 2006. **7**(9): p. 880-5.
23. Ashkenazi, A., *Targeting death and decoy receptors of the tumour-necrosis factor superfamily.* Nat Rev Cancer, 2002. **2**(6): p. 420-30.
24. Robbins, S.L., V. Kumar, A.K. Abbas, R.S. Cotran, and N. Fausto, *Cell injury, cell death, and adaptations*, in *Robbins and cotran pathologic basis of disease* 2010, Elsevier Limited. p. 1-30.
25. Kantari, C. and H. Walczak, *Caspase-8 and bid: Caught in the act between death receptors and mitochondria.* Biochim Biophys Acta, 2011. **1813**(4): p. 558-63.
26. Bagnoli, M., S. Canevari, and D. Mezzanzanica, *Cellular FLICE-inhibitory protein (c-FLIP) signalling: A key regulator of receptor-mediated apoptosis in physiologic context and in cancer.* Int J Biochem Cell Biol, 2010. **42**(2): p. 210-3.
27. Tait, S.W. and D.R. Green, *Mitochondria and cell death: Outer membrane permeabilization and beyond.* Nat Rev Mol Cell Biol, 2010. **11**(9): p. 621-32.
28. Boyer, P.D., *The ATP synthase--a splendid molecular machine.* Annu Rev Biochem, 1997. **66**: p. 717-49.
29. Zamaraeva, M.V., R.Z. Sabirov, E. Maeno, Y. Ando-Akatsuka, S.V. Bessonova, and Y. Okada, *Cells die with increased cytosolic ATP during apoptosis: A bioluminescence study with intracellular luciferase.* Cell Death Differ, 2005. **12**(11): p. 1390-7.
30. Bender, T. and J.C. Martinou, *Where killers meet--permeabilization of the outer mitochondrial membrane during apoptosis.* Cold Spring Harb Perspect Biol, 2013. **5**(1): p. a011106.
31. Saelens, X., N. Festjens, L. Vande Walle, M. van Gurp, G. van Loo, and P. Vandenabeele, *Toxic proteins released from mitochondria in cell death.* Oncogene, 2004. **23**(16): p. 2861-74.
32. Robertson, J.D., S. Orrenius, and B. Zhivotovsky, *Review: Nuclear events in apoptosis.* J Struct Biol, 2000. **129**(2-3): p. 346-58.
33. Kinnally, K.W., P.M. Peixoto, S.Y. Ryu, and L.M. Dejean, *Is mPTP the gatekeeper for necrosis, apoptosis, or both?* Biochim Biophys Acta, 2011. **1813**(4): p. 616-22.
34. Rasola, A. and P. Bernardi, *Mitochondrial permeability transition in Ca^{2+}-dependent apoptosis and necrosis.* Cell Calcium, 2011. **50**(3): p. 222-33.
35. Westphal, D., G. Dewson, P.E. Czabotar, and R.M. Kluck, *Molecular biology of Bax and Bak activation and action.* Biochim Biophys Acta, 2011. **1813**(4): p. 521-31.
36. Wei, M.C., W.X. Zong, E.H. Cheng, T. Lindsten, V. Panoutsakopoulou, A.J. Ross, . . . S.J. Korsmeyer, *Proapoptotic Bax and bak: A requisite gateway to mitochondrial dysfunction and death.* Science, 2001. **292**(5517): p. 727-30.
37. Llambi, F., T. Moldoveanu, S.W. Tait, L. Bouchier-Hayes, J. Temirov, L.L. McCormick, . . . D.R. Green, *A unified model of mammalian Bcl-2 protein family interactions at the mitochondria.* Mol Cell, 2011. **44**(4): p. 517-31.
38. Reed, J.C., *Bcl-2-family proteins and hematologic malignancies: History and future prospects.* Blood, 2008. **111**(7): p. 3322-30.
39. Vaux, D.L., S. Cory, and J.M. Adams, *Bcl-2 gene promotes haemopoietic cell survival and cooperates with c-myc to immortalize pre-B cells.* Nature, 1988. **335**(6189): p. 440-2.

40. Chipuk, J.E., T. Moldoveanu, F. Llambi, M.J. Parsons, and D.R. Green, *The Bcl-2 family reunion.* Mol Cell, 2010. **37**(3): p. 299-310.
41. Shamas-Din, A., H. Brahmbhatt, B. Leber, and D.W. Andrews, *BH3-only proteins: Orchestrators of apoptosis.* Biochim Biophys Acta, 2011. **1813**(4): p. 508-20.
42. Aouacheria, A., V. Rech de Laval, C. Combet, and J.M. Hardwick, *Evolution of Bcl-2 homology motifs: Homology versus homoplasy.* Trends Cell Biol, 2013. **23**(3): p.103-11.
43. Kvansakul, M., H. Yang, W.D. Fairlie, P.E. Czabotar, S.F. Fischer, M.A. Perugini, . . . P.M. Colman, *Vaccinia virus anti-apoptotic F1l is a novel Bcl-2-like domain-swapped dimer that binds a highly selective subset of BH3-containing death ligands.* Cell Death Differ, 2008. **15**(10): p. 1564-71.
44. Kelekar, A. and C.B. Thompson, *Bcl-2-family proteins: The role of the BH3 domain in apoptosis.* Trends Cell Biol, 1998. **8**(8): p. 324-30.
45. Muchmore, S.W., M. Sattler, H. Liang, R.P. Meadows, J.E. Harlan, H.S. Yoon, . . . S.W. Fesik, *X-ray and nmr structure of human Bcl-Xl, an inhibitor of programmed cell death.* Nature, 1996. **381**(6580): p. 335-41.
46. Suzuki, M., R.J. Youle, and N. Tjandra, *Structure of Bax: Coregulation of dimer formation and intracellular localization.* Cell, 2000. **103**(4): p. 645-54.
47. Moldoveanu, T., Q. Liu, A. Tocilj, M. Watson, G. Shore, and K. Gehring, *The x-ray structure of a Bak homodimer reveals an inhibitory zinc binding site.* Mol Cell, 2006. **24**(5): p. 677-88.
48. Lama, D. and R. Sankararamakrishnan, *Identification of core structural residues in the sequentially diverse and structurally homologous Bcl-2 family of proteins.* Biochemistry, 2010. **49**(11): p. 2574-84.
49. Basanez, G. and J.M. Hardwick, *Unravelling the Bcl-2 apoptosis code with a simple model system.* PLoS Biol, 2008. **6**(6): p. e154.
50. Hunter, J.J., B.L. Bond, and T.G. Parslow, *Functional dissection of the human Bc1-2 protein: Sequence requirements for inhibition of apoptosis.* Mol Cell Biol, 1996. **16**(3): p. 877-83.
51. Lee, L.C., J.J. Hunter, A. Mujeeb, C. Turck, and T.G. Parslow, *Evidence for alpha-helical conformation of an essential N-terminal region in the human Bcl-2 protein.* J Biol Chem, 1996. **271**(38): p. 23284-8.
52. Hanada, M., C. Aime-Sempe, T. Sato, and J.C. Reed, *Structure-function analysis of Bcl-2 protein. Identification of conserved domains important for homodimerization with Bcl-2 and heterodimerization with Bax.* J Biol Chem, 1995. **270**(20): p. 11962-9.
53. Zha, H., C. Aime-Sempe, T. Sato, and J.C. Reed, *Proapoptotic protein Bax heterodimerizes with Bcl-2 and homodimerizes with Bax via a novel domain (BH3) distinct from BH1 and BH2.* J Biol Chem, 1996. **271**(13): p. 7440-4.
54. Cheng, E.H., D.G. Kirsch, R.J. Clem, R. Ravi, M.B. Kastan, A. Bedi, . . . J.M. Hardwick, *Conversion of Bcl-2 to a Bax-like death effector by caspases.* Science, 1997. **278**(5345): p. 1966-8.
55. Hirotani, M., Y. Zhang, N. Fujita, M. Naito, and T. Tsuruo, *NH2-terminal bh4 domain of Bcl-2 is functional for heterodimerization with Bax and inhibition of apoptosis.* J Biol Chem, 1999. **274**(29): p. 20415-20.
56. Puthalakath, H. and A. Strasser, *Keeping killers on a tight leash: Transcriptional and post-translational control of the pro-apoptotic activity of BH3-only proteins.* Cell Death Differ, 2002. **9**(5): p. 505-12.
57. Kim, H., H.C. Tu, D. Ren, O. Takeuchi, J.R. Jeffers, G.P. Zambetti, . . . E.H. Cheng, *Stepwise activation of Bax and Bak by tBid, Bim, and PUMA initiates mitochondrial apoptosis.* Mol Cell, 2009. **36**(3): p. 487-99.

58. Kuwana, T., L. Bouchier-Hayes, J.E. Chipuk, C. Bonzon, B.A. Sullivan, D.R. Green, and D.D. Newmeyer, *BH3 domains of BH3-only proteins differentially regulate Bax-mediated mitochondrial membrane permeabilization both directly and indirectly.* Mol Cell, 2005. **17**(4): p. 525-35.
59. Certo, M., V. Del Gaizo Moore, M. Nishino, G. Wei, S. Korsmeyer, S.A. Armstrong, and A. Letai, *Mitochondria primed by death signals determine cellular addiction to antiapoptotic Bcl-2 family members.* Cancer Cell, 2006. **9**(5): p. 351-65.
60. Chen, L., S.N. Willis, A. Wei, B.J. Smith, J.I. Fletcher, M.G. Hinds, . . . D.C. Huang, *Differential targeting of prosurvival Bcl-2 proteins by their BH3-only ligands allows complementary apoptotic function.* Mol Cell, 2005. **17**(3): p. 393-403.
61. Kim, H., M. Rafiuddin-Shah, H.C. Tu, J.R. Jeffers, G.P. Zambetti, J.J. Hsieh, and E.H. Cheng, *Hierarchical regulation of mitochondrion-dependent apoptosis by Bcl-2 subfamilies.* Nat Cell Biol, 2006. **8**(12): p. 1348-58.
62. Green, D.R. and G. Kroemer, *The pathophysiology of mitochondrial cell death.* Science, 2004. **305**(5684): p. 626-9.
63. Zhang, L., L. Ming, and J. Yu, *BH3 mimetics to improve cancer therapy; mechanisms and examples.* Drug Resist Updat, 2007. **10**(6): p. 207-17.
64. Park, C.M., M. Bruncko, J. Adickes, J. Bauch, H. Ding, A. Kunzer, . . . S.W. Elmore, *Discovery of an orally bioavailable small molecule inhibitor of prosurvival B-cell lymphoma 2 proteins.* J Med Chem, 2008. **51**(21): p. 6902-15.
65. Tse, C., A.R. Shoemaker, J. Adickes, M.G. Anderson, J. Chen, S. Jin, . . . S.W. Elmore, *ABT-263: A potent and orally bioavailable Bcl-2 family inhibitor.* Cancer Res, 2008. **68**(9): p. 3421-8.
66. Davids, M.S. and A. Letai, *ABT-199: Taking dead aim at Bcl-2.* Cancer Cell, 2013. **23**(2): p. 139-41.
67. Akao, Y., Y. Otsuki, S. Kataoka, Y. Ito, and Y. Tsujimoto, *Multiple subcellular localization of Bcl-2: Detection in nuclear outer membrane, endoplasmic reticulum membrane, and mitochondrial membranes.* Cancer Res, 1994. **54**(9): p. 2468-71.
68. Krajewski, S., S. Tanaka, S. Takayama, M.J. Schibler, W. Fenton, and J.C. Reed, *Investigation of the subcellular distribution of the Bcl-2 oncoprotein: Residence in the nuclear envelope, endoplasmic reticulum, and outer mitochondrial membranes.* Cancer Res, 1993. **53**(19): p. 4701-14.
69. Szegezdi, E., D.C. Macdonald, T. Ni Chonghaile, S. Gupta, and A. Samali, *Bcl-2 family on guard at the ER.* Am J Physiol Cell Physiol, 2009. **296**(5): p. C941-53.
70. Berridge, M.J., M.D. Bootman, and H.L. Roderick, *Calcium signalling: Dynamics, homeostasis and remodelling.* Nat Rev Mol Cell Biol, 2003. **4**(7): p. 517-29.
71. Case, R.M., D. Eisner, A. Gurney, O. Jones, S. Muallem, and A. Verkhratsky, *Evolution of calcium homeostasis: From birth of the first cell to an omnipresent signalling system.* Cell Calcium, 2007. **42**(4-5): p. 345-50.
72. Berridge, M.J., *Calcium signalling remodelling and disease.* Biochem Soc Trans, 2012. **40**(2): p. 297-309.
73. Berridge, M.J., P. Lipp, and M.D. Bootman, *The versatility and universality of calcium signalling.* Nat Rev Mol Cell Biol, 2000. **1**(1): p. 11-21.
74. Verkhratsky, A., *Calcium and cell death.* Subcell Biochem, 2007. **45**: p. 465-80.
75. Harr, M.W. and C.W. Distelhorst, *Apoptosis and autophagy: Decoding calcium signals that mediate life or death.* Cold Spring Harb Perspect Biol, 2010. **2**(10): a005579.
76. Rong, Y. and C.W. Distelhorst, *Bcl-2 protein family members: Versatile regulators of calcium signaling in cell survival and apoptosis.* Annu Rev Physiol, 2008. **70**: p. 73-91.

77. Brini, M. and E. Carafoli, *The plasma membrane Ca^{2+} ATPase and the plasma membrane sodium calcium exchanger cooperate in the regulation of cell calcium.* Cold Spring Harb Perspect Biol, 2011. **3**(2):a004168.
78. Schwaller, B., *The regulation of a cell's Ca^{2+} signaling toolkit: The Ca^{2+}homeostasome.* Adv Exp Med Biol, 2012. **740**: p. 1-25.
79. Schwaller, B., *Cytosolic Ca^{2+} buffers.* Cold Spring Harb Perspect Biol, 2010. **2**(11): a004051.
80. Antkiewicz-Michaluk, L., *Voltage-operated calcium channels: Characteristics and their role in the mechanism of action of psychotropic drugs.* Pol J Pharmacol, 1999. **51**(2): p. 179-86.
81. Karlstad, J., Y. Sun, and B.B. Singh, *Ca^{2+} signaling: An outlook on the characterization of Ca^{2+} channels and their importance in cellular functions.* Adv Exp Med Biol, 2012. **740**: p. 143-57.
82. Muik, M., R. Schindl, M. Fahrner, and C. Romanin, *Ca^{2+} release-activated Ca^{2+} (CRAC) current, structure, and function.* Cell Mol Life Sci, 2012. **69**(24): p. 4163-76.
83. Ginzburg, L., Y. Kacher, and A.H. Futerman, *The pathogenesis of glycosphingolipid storage disorders.* Semin Cell Dev Biol, 2004. **15**(4): p. 417-31.
84. Rizzuto, R., D. De Stefani, A. Raffaello, and C. Mammucari, *Mitochondria as sensors and regulators of calcium signalling.* Nat Rev Mol Cell Biol, 2012. **13**(9): p. 566-78.
85. De Stefani, D., A. Bononi, A. Romagnoli, A. Messina, V. De Pinto, P. Pinton, and R. Rizzuto, *VDAC-1 selectively transfers apoptotic Ca^{2+} signals to mitochondria.* Cell Death Differ, 2012. **19**(2): p. 267-73.
86. Raffaello, A., D. De Stefani, and R. Rizzuto, *The mitochondrial Ca^{2+} uniporter.* Cell Calcium, 2012. **52**(1): p. 16-21.
87. Bernardi, P. and S. von Stockum, *The permeability transition pore as a Ca^{2+} release channel: New answers to an old question.* Cell Calcium, 2012. **52**(1): p. 22-7.
88. Berridge, M.J., *The endoplasmic reticulum: A multifunctional signaling organelle.* Cell Calcium, 2002. **32**(5-6): p. 235-49.
89. Lanner, J.T., D.K. Georgiou, A.D. Joshi, and S.L. Hamilton, *Ryanodine receptors: Structure, expression, molecular details, and function in calcium release.* Cold Spring Harb Perspect Biol, 2010. **2**(11): p. a003996.
90. Parys, J.B. and H. De Smedt, *Inositol 1,4,5-trisphosphate and its receptors.* Adv Exp Med Biol, 2012. **740**: p. 255-79.
91. Bootman, M., E. Niggli, M. Berridge, and P. Lipp, *Imaging the hierarchical Ca^{2+} signalling system in HeLa cells.* J Physiol, 1997. **499** (Pt 2): p. 307-14.
92. Lipp, P. and E. Niggli, *Fundamental calcium release events revealed by two-photon excitation photolysis of caged calcium in guinea-pig cardiac myocytes.* J Physiol, 1998. **508** (Pt 3): p. 801-9.
93. Burdakov, D., O.H. Petersen, and A. Verkhratsky, *Intraluminal calcium as a primary regulator of endoplasmic reticulum function.* Cell Calcium, 2005. **38**(3-4): p. 303-10.
94. Zhivotovsky, B. and S. Orrenius, *Calcium and cell death mechanisms: A perspective from the cell death community.* Cell Calcium, 2011. **50**(3): p. 211-21.
95. Guo, J., Y. Lao, and D.C. Chang, *Calcium and apoptosis*, in *Handbook of neurochemistry and molecular neurobiology* 2009, Spinger. p. 597-622.
96. Ozaki, T., T. Yamashita, and S. Ishiguro, *Mitochondrial m-calpain plays a role in the release of truncated apoptosis-inducing factor from the mitochondria.* Biochim Biophys Acta, 2009. **1793**(12): p. 1848-59.
97. Giansanti, V., A. Torriglia, and A.I. Scovassi, *Conversation between apoptosis and autophagy: "Is it your turn or mine?".* Apoptosis, 2011. **16**(4): p. 321-33.

98. Brnjic, S., M.H. Olofsson, A.M. Havelka, and S. Linder, *Chemical biology suggests a role for calcium signaling in mediating sustained jnk activation during apoptosis.* Mol Biosyst, 2010. **6**(5): p. 767-74.
99. Dhanasekaran, D.N. and E.P. Reddy, *JNK signaling in apoptosis.* Oncogene, 2008. **27**(48): p. 6245-51.
100. Yano, S., H. Tokumitsu, and T.R. Soderling, *Calcium promotes cell survival through CaM-k kinase activation of the protein-kinase-b pathway.* Nature, 1998. **396**(6711): p. 584-7.
101. Hogan, P.G., L. Chen, J. Nardone, and A. Rao, *Transcriptional regulation by calcium, calcineurin, and nfat.* Genes Dev, 2003. **17**(18): p. 2205-32.
102. Vance, J.E., *Phospholipid synthesis in a membrane fraction associated with mitochondria.* J Biol Chem, 1990. **265**(13): p. 7248-56.
103. Rowland, A.A. and G.K. Voeltz, *Endoplasmic reticulum-mitochondria contacts: Function of the junction.* Nat Rev Mol Cell Biol, 2012. **13**(10): p. 607-25.
104. Rizzuto, R., P. Pinton, W. Carrington, F.S. Fay, K.E. Fogarty, L.M. Lifshitz, . . . T. Pozzan, *Close contacts with the endoplasmic reticulum as determinants of mitochondrial Ca^{2+} responses.* Science, 1998. **280**(5370): p. 1763-6.
105. Csordas, G., A.P. Thomas, and G. Hajnoczky, *Quasi-synaptic calcium signal transmission between endoplasmic reticulum and mitochondria.* Embo J, 1999. **18**(1): p. 96-108.
106. Decuypere, J.P., G. Monaco, G. Bultynck, L. Missiaen, H. De Smedt, and J.B. Parys, *The IP_3 receptor-mitochondria connection in apoptosis and autophagy.* Biochim Biophys Acta, 2011. **1813**(5): p. 1003-13.
107. Giorgi, C., K. Ito, H.K. Lin, C. Santangelo, M.R. Wieckowski, M. Lebiedzinska, . . . P.P. Pandolfi, *PML regulates apoptosis at endoplasmic reticulum by modulating calcium release.* Science, 2010. **330**(6008): p. 1247-51.
108. Miyakawa, T., A. Maeda, T. Yamazawa, K. Hirose, T. Kurosaki, and M. Iino, *Encoding of Ca^{2+} signals by differential expression of IP_3 receptor subtypes.* Embo J, 1999. **18**(5): p. 1303-8.
109. Cardenas, C., R.A. Miller, I. Smith, T. Bui, J. Molgo, M. Muller, . . . J.K. Foskett, *Essential regulation of cell bioenergetics by constitutive $InsP_3$ receptor Ca^{2+} transfer to mitochondria.* Cell, 2010. **142**(2): p. 270-83.
110. McCormack, J.G., A.P. Halestrap, and R.M. Denton, *Role of calcium ions in regulation of mammalian intramitochondrial metabolism.* Physiol Rev, 1990. **70**(2): p. 391-425.
111. Hayashi, T., R. Rizzuto, G. Hajnoczky, and T.P. Su, *MAM: More than just a housekeeper.* Trends Cell Biol, 2009. **19**(2): p. 81-8.
112. Shoshan-Barmatz, V., V. De Pinto, M. Zweckstetter, Z. Raviv, N. Keinan, and N. Arbel, *VDAC, a multi-functional mitochondrial protein regulating cell life and death.* Mol Aspects Med, 2010. **31**(3): p. 227-85.
113. Nakatsu, Y. and T. Asano, *[regulation of energy metabolism via AMPK].* Nihon Yakurigaku Zasshi, 2012. **140**(3): p. 138-9.
114. Cardenas, C. and J.K. Foskett, *Mitochondrial Ca^{2+} signals in autophagy.* Cell Calcium, 2012. **52**(1): p. 44-51.
115. Gomes, L.C., G. Di Benedetto, and L. Scorrano, *During autophagy mitochondria elongate, are spared from degradation and sustain cell viability.* Nat Cell Biol, 2011. **13**(5): p. 589-98.
116. Giorgi, C., A. Romagnoli, P. Pinton, and R. Rizzuto, *Ca^{2+} signaling, mitochondria and cell death.* Curr Mol Med, 2008. **8**(2): p. 119-30.

117. Sato, C., K. Hamada, T. Ogura, A. Miyazawa, K. Iwasaki, Y. Hiroaki, . . . K. Mikoshiba, *Inositol 1,4,5-trisphosphate receptor contains multiple cavities and l-shaped ligand-binding domains.* J Mol Biol, 2004. **336**(1): p. 155-64.
118. Patel, S., S.K. Joseph, and A.P. Thomas, *Molecular properties of inositol 1,4,5-trisphosphate receptors.* Cell Calcium, 1999. **25**(3): p. 247-64.
119. Taylor, C.W., A.A. Genazzani, and S.A. Morris, *Expression of inositol trisphosphate receptors.* Cell Calcium, 1999. **26**(6): p. 237-51.
120. Iino, M., *Biphasic Ca^{2+} dependence of inositol 1,4,5-trisphosphate-induced Ca^{2+}release in smooth muscle cells of the guinea pig taenia caeci.* J Gen Physiol, 1990. **95**(6): p. 1103-22.
121. Finch, E.A., T.J. Turner, and S.M. Goldin, *Calcium as a coagonist of inositol 1,4,5-trisphosphate-induced calcium release.* Science, 1991. **252**(5004): p. 443-6.
122. Bezprozvanny, I., J. Watras, and B.E. Ehrlich, *Bell-shaped calcium-response curves of ins(1,4,5)p3- and calcium-gated channels from endoplasmic reticulum of cerebellum.* Nature, 1991. **351**(6329): p. 751-4.
123. Berridge, M., *Ion channels*. Cell Signalling Biology, 2012. module 3:p. 1-72, doi: 10.1042/csb0001003.
124. Schug, Z.T. and S.K. Joseph, *The role of the s4-s5 linker and c-terminal tail in inositol 1,4,5-trisphosphate receptor function.* J Biol Chem, 2006. **281**(34): p. 24431-40.
125. Choe, C.U. and B.E. Ehrlich, *The inositol 1,4,5-trisphosphate receptor (IP_3R) and its regulators: Sometimes good and sometimes bad teamwork.* Sci STKE, 2006. **363**: re15.
126. Mikoshiba, K., *IP_3 receptor/Ca^{2+} channel: From discovery to new signaling concepts.* J Neurochem, 2007. **102**(5): p. 1426-46.
127. Foskett, J.K., C. White, K.H. Cheung, and D.O. Mak, *Inositol trisphosphate receptor Ca^{2+} release channels.* Physiol Rev, 2007. **87**(2): p. 593-658.
128. Vanderheyden, V., B. Devogelaere, L. Missiaen, H. De Smedt, G. Bultynck, and J.B. Parys, *Regulation of inositol 1,4,5-trisphosphate-induced Ca^{2+} release by reversible phosphorylation and dephosphorylation.* Biochim Biophys Acta, 2009. **1793**(6): p. 959-70.
129. Vanden Abeele, F., R. Skryma, Y. Shuba, F. Van Coppenolle, C. Slomianny, M. Roudbaraki, . . . N. Prevarskaya, *Bcl-2-dependent modulation of Ca^{2+} homeostasis and store-operated channels in prostate cancer cells.* Cancer Cell, 2002. **1**(2): p. 169-79.
130. Rong, Y.P., A.S. Aromolaran, G. Bultynck, F. Zhong, X. Li, K. McColl, . . . C.W. Distelhorst, *Targeting Bcl-2-IP_3 receptor interaction to reverse Bcl-2's inhibition of apoptotic calcium signals.* Mol Cell, 2008. **31**(2): p. 255-65.
131. Joseph, S.K. and G. Hajnoczky, *IP_3 receptors in cell survival and apoptosis: Ca^{2+} release and beyond.* Apoptosis, 2007. **12**(5): p. 951-68.
132. Pinton, P., C. Giorgi, R. Siviero, E. Zecchini, and R. Rizzuto, *Calcium and apoptosis: ER-mitochondria Ca^{2+} transfer in the control of apoptosis.* Oncogene, 2008. **27**(50): p. 6407-18.
133. Shimizu, S., A. Konishi, T. Kodama, and Y. Tsujimoto, *BH4 domain of antiapoptotic Bcl-2 family members closes voltage-dependent anion channel and inhibits apoptotic mitochondrial changes and cell death.* Proc Natl Acad Sci U S A, 2000. **97**(7): p. 3100-5.
134. Arbel, N. and V. Shoshan-Barmatz, *Voltage-dependent anion channel 1-based peptides interact with Bcl-2 to prevent antiapoptotic activity.* J Biol Chem, 2010. **285**(9): p. 6053-62.

135. Baffy, G., T. Miyashita, J.R. Williamson, and J.C. Reed, *Apoptosis induced by withdrawal of interleukin-3 (IL-3) from an IL-3-dependent hematopoietic cell line is associated with repartitioning of intracellular calcium and is blocked by enforced Bcl-2 oncoprotein production.* J Biol Chem, 1993. **268**(9): p. 6511-9.
136. Lam, M., G. Dubyak, L. Chen, G. Nunez, R.L. Miesfeld, and C.W. Distelhorst, *Evidence that Bcl-2 represses apoptosis by regulating endoplasmic reticulum-associated Ca^{2+} fluxes.* Proc Natl Acad Sci U S A, 1994. **91**(14): p. 6569-73.
137. Pinton, P., D. Ferrari, P. Magalhaes, K. Schulze-Osthoff, F. Di Virgilio, T. Pozzan, and R. Rizzuto, *Reduced loading of intracellular Ca^{2+} stores and downregulation of capacitative Ca^{2+} influx in Bcl-2-overexpressing cells.* J Cell Biol, 2000. **148**(5): p. 857-62.
138. Pinton, P., D. Ferrari, E. Rapizzi, F. Di Virgilio, T. Pozzan, and R. Rizzuto, *The Ca^{2+} concentration of the endoplasmic reticulum is a key determinant of ceramide-induced apoptosis: Significance for the molecular mechanism of Bcl-2 action.* Embo J, 2001. **20**(11): p. 2690-701.
139. Palmer, A.E., C. Jin, J.C. Reed, and R.Y. Tsien, *Bcl-2-mediated alterations in endoplasmic reticulum Ca^{2+} analyzed with an improved genetically encoded fluorescent sensor.* Proc Natl Acad Sci U S A, 2004. **101**(50): p. 17404-9.
140. Schendel, S.L., Z. Xie, M.O. Montal, S. Matsuyama, M. Montal, and J.C. Reed, *Channel formation by antiapoptotic protein Bcl-2.* Proc Natl Acad Sci U S A, 1997. **94**(10): p. 5113-8.
141. Saito, M., S.J. Korsmeyer, and P.H. Schlesinger, *Bax-dependent transport of Cytochrome c reconstituted in pure liposomes.* Nat Cell Biol, 2000. **2**(8): p. 553-5.
142. Chami, M., A. Prandini, M. Campanella, P. Pinton, G. Szabadkai, J.C. Reed, and R. Rizzuto, *Bcl-2 and Bax exert opposing effects on Ca^{2+} signaling, which do not depend on their putative pore-forming region.* J Biol Chem, 2004. **279**(52): p. 54581-9.
143. Kuo, T.H., H.R. Kim, L. Zhu, Y. Yu, H.M. Lin, and W. Tsang, *Modulation of endoplasmic reticulum calcium pump by Bcl-2.* Oncogene, 1998. **17**(15): p. 1903-10.
144. Vento, M.T., V. Zazzu, A. Loffreda, J.R. Cross, J. Downward, M.P. Stoppelli, and I. Iaccarino, *Praf2 is a novel bcl-xl/Bcl-2 interacting protein with the ability to modulate survival of cancer cells.* PLoS One, 2010. **5**(12): p. e15636.
145. Kobrinsky, E.M. and M.A. Kirchberger, *Evidence for a role of the sarcoplasmic/endoplasmic reticulum Ca^{2+}-ATPase in thapsigargin and Bcl-2 induced changes in xenopus laevis oocyte maturation.* Oncogene, 2001. **20**(8): p. 933-41.
146. Dremina, E.S., V.S. Sharov, K. Kumar, A. Zaidi, E.K. Michaelis, and C. Schoneich, *Anti-apoptotic protein Bcl-2 interacts with and destabilizes the sarcoplasmic/endoplasmic reticulum Ca^{2+}-ATPase (SERCA).* Biochem J, 2004. **383**(2): p. 361-70.
147. Dremina, E.S., V.S. Sharov, and C. Schoneich, *Displacement of serca from sr lipid caveolae-related domains by Bcl-2: A possible mechanism for serca inactivation.* Biochemistry, 2006. **45**(1): p. 175-84.
148. Chen, R., I. Valencia, F. Zhong, K.S. McColl, H.L. Roderick, M.D. Bootman, . . . C.W. Distelhorst, *Bcl-2 functionally interacts with inositol 1,4,5-trisphosphate receptors to regulate calcium release from the er in response to inositol 1,4,5-trisphosphate.* J Cell Biol, 2004. **166**(2): p. 193-203.
149. Bassik, M.C., L. Scorrano, S.A. Oakes, T. Pozzan, and S.J. Korsmeyer, *Phosphorylation of Bcl-2 regulates er Ca^{2+} homeostasis and apoptosis.* Embo J, 2004. **23**(5): p. 1207-16.

150. Li, C., C.J. Fox, S.R. Master, V.P. Bindokas, L.A. Chodosh, and C.B. Thompson, *Bcl-Xl affects Ca^{2+} homeostasis by altering expression of inositol 1,4,5-trisphosphate receptors.* Proc Natl Acad Sci U S A, 2002. **99**(15): p. 9830-5.
151. Oakes, S.A., S.S. Lin, and M.C. Bassik, *The control of endoplasmic reticulum-initiated apoptosis by the Bcl-2 family of proteins.* Curr Mol Med, 2006. **6**(1): p. 99-109.
152. Scorrano, L., S.A. Oakes, J.T. Opferman, E.H. Cheng, M.D. Sorcinelli, T. Pozzan, and S.J. Korsmeyer, *Bax and bak regulation of endoplasmic reticulum Ca^{2+}: A control point for apoptosis.* Science, 2003. **300**(5616): p. 135-9.
153. Distelhorst, C.W. and G.C. Shore, *Bcl-2 and calcium: Controversy beneath the surface.* Oncogene, 2004. **23**(16): p. 2875-80.
154. Erin, N., S.K. Bronson, and M.L. Billingsley, *Calcium-dependent interaction of calcineurin with Bcl-2 in neuronal tissue.* Neuroscience, 2003. **117**(3): p. 541-55.
155. Erin, N. and M.L. Billingsley, *Domoic acid enhances Bcl-2-calcineurin-inositol-1,4,5-trisphosphate receptor interactions and delayed neuronal death in rat brain slices.* Brain Res, 2004. **1014**(1-2): p. 45-52.
156. Xu, L., D. Kong, L. Zhu, W. Zhu, D.W. Andrews, and T.H. Kuo, *Suppression of IP_3-mediated calcium release and apoptosis by Bcl-2 involves the participation of protein phosphatase 1.* Mol Cell Biochem, 2007. **295**(1-2): p. 153-65.
157. Nutt, L.K., A. Pataer, J. Pahler, B. Fang, J. Roth, D.J. McConkey, and S.G. Swisher, *Bax and Bak promote apoptosis by modulating endoplasmic reticular and mitochondrial Ca^{2+} stores.* J Biol Chem, 2002. **277**(11): p. 9219-25.
158. Zong, W.X., C. Li, G. Hatzivassiliou, T. Lindsten, Q.C. Yu, J. Yuan, and C.B. Thompson, *Bax and Bak can localize to the endoplasmic reticulum to initiate apoptosis.* J Cell Biol, 2003. **162**(1): p. 59-69.
159. Mathai, J.P., M. Germain, and G.C. Shore, *BH3-only bik regulates Bax,Bak-dependent release of Ca^{2+} from endoplasmic reticulum stores and mitochondrial apoptosis during stress-induced cell death.* J Biol Chem, 2005. **280**(25): p. 23829-36.
160. Luo, X., Q. He, Y. Huang, and M.S. Sheikh, *Transcriptional upregulation of puma modulates endoplasmic reticulum calcium pool depletion-induced apoptosis via Bax activation.* Cell Death Differ, 2005. **12**(10): p. 1310-8.
161. Hardwick, J.M., Y.B. Chen, and E.A. Jonas, *Multipolar functions of Bcl-2 proteins link energetics to apoptosis.* Trends Cell Biol, 2012. **22**(6): p. 318-28.
162. Distelhorst, C.W. and M.D. Bootman, *Bcl-2 interaction with the inositol 1,4,5-trisphosphate receptor: Role in Ca^{2+} signaling and disease.* Cell Calcium, 2011. **50**(3): p. 234-41.
163. White, C., C. Li, J. Yang, N.B. Petrenko, M. Madesh, C.B. Thompson, and J.K. Foskett, *The endoplasmic reticulum gateway to apoptosis by bcl-Xl modulation of the $InsP_3R$.* Nat Cell Biol, 2005. **7**(10): p. 1021-8.
164. Monaco, G., T. Vervliet, H. Akl, and G. Bultynck, *The selective bh4-domain biology of Bcl-2-family members: Ip3rs and beyond.* Cell Mol Life Sci, 2013. **70**(7): p.1171-83.
165. Davis, M.C. and C.W. Distelhorst, *Live free or die: An immature t cell decision encoded in distinct Bcl-2 sensitive and insensitive Ca^{2+} signals.* Cell Cycle, 2006. **5**(11): p. 1171-4.
166. Li, C., X. Wang, H. Vais, C.B. Thompson, J.K. Foskett, and C. White, *Apoptosis regulation by bcl-Xl modulation of mammalian inositol 1,4,5-trisphosphate receptor channel isoform gating.* Proc Natl Acad Sci U S A, 2007. **104**(30): p. 12565-70.

167. Chan, J., H. Yamazaki, N. Ishiyama, M.D. Seo, T.K. Mal, T. Michikawa, . . . M. Ikura, *Structural studies of inositol 1,4,5-trisphosphate receptor: Coupling ligand binding to channel gating.* J Biol Chem, 2010. **285**(46): p. 36092-9.
168. Foskett, J.K., J. Yang, K.H. Cheung, and H. Vais, *Bcl-Xl regulation of $InsP_3$ receptor gating mediated by dual Ca^{2+} release channel BH3 domains.* Biophys J, 2009. **96**(3): p. 391a.
169. Eckenrode, E.F., J. Yang, G.V. Velmurugan, J.K. Foskett, and C. White, *Apoptosis protection by Mcl-1 and Bcl-2 modulation of inositol 1,4,5-trisphosphate receptor-dependent Ca^{2+} signaling.* J Biol Chem, 2010. **285**(18): p. 13678-84.
170. Rong, Y.P., G. Bultynck, A.S. Aromolaran, F. Zhong, J.B. Parys, H. De Smedt, . . . C.W. Distelhorst, *The BH4 domain of Bcl-2 inhibits er calcium release and apoptosis by binding the regulatory and coupling domain of the IP_3 receptor.* Proc Natl Acad Sci U S A, 2009. **106**(34): p. 14397-402.
171. Cantara, S., S. Donnini, A. Giachetti, P.E. Thorpe, and M. Ziche, *Exogenous BH4/Bcl-2 peptide reverts coronary endothelial cell apoptosis induced by oxidative stress.* J Vasc Res, 2004. **41**(2): p. 202-7.
172. Trisciuoglio, D., C. Gabellini, M. Desideri, Y. Ragazzoni, T. De Luca, E. Ziparo, and D. Del Bufalo, *Involvement of BH4 domain of Bcl-2 in the regulation of HIF-1-mediated vegf expression in hypoxic tumor cells.* Cell Death Differ, 2011. **18**(6): p. 1024-35.
173. McDunn, J.E., J.T. Muenzer, B. Dunne, A. Zhou, K. Yuan, A. Hoekzema, . . . R.S. Hotchkiss, *An anti-apoptotic peptide improves survival in lethal total body irradiation.* Biochem Biophys Res Commun, 2009. **382**(4): p. 657-62.
174. Rong, Y.P., P. Barr, V.C. Yee, and C.W. Distelhorst, *Targeting Bcl-2 based on the interaction of its bh4 domain with the inositol 1,4,5-trisphosphate receptor.* Biochim Biophys Acta, 2009. **1793**(6): p. 971-8.
175. Zhong, F., M.W. Harr, G. Bultynck, G. Monaco, J.B. Parys, H. De Smedt, . . . C.W. Distelhorst, *Induction of Ca^{2+}-driven apoptosis in chronic lymphocytic leukemia cells by peptide-mediated disruption of Bcl-2-IP_3 receptor interaction.* Blood, 2011. **117**(10): p. 2924-34.
176. Boehning, D., R.L. Patterson, L. Sedaghat, N.O. Glebova, T. Kurosaki, and S.H. Snyder, *Cytochrome c binds to inositol (1,4,5) trisphosphate receptors, amplifying calcium-dependent apoptosis.* Nat Cell Biol, 2003. **5**(12): p. 1051-61.
177. Boehning, D., D.B. van Rossum, R.L. Patterson, and S.H. Snyder, *A peptide inhibitor of Cytochrome c/inositol 1,4,5-trisphosphate receptor binding blocks intrinsic and extrinsic cell death pathways.* Proc Natl Acad Sci U S A, 2005. **102**(5): p. 1466-71.
178. Assefa, Z., G. Bultynck, K. Szlufcik, N. Nadif Kasri, E. Vermassen, J. Goris, . . . H. De Smedt, *Caspase-3-induced truncation of type 1 inositol trisphosphate receptor accelerates apoptotic cell death and induces inositol trisphosphate-independent calcium release during apoptosis.* J Biol Chem, 2004. **279**(41): p. 43227-36.
179. Hirota, J., T. Furuichi, and K. Mikoshiba, *Inositol 1,4,5-trisphosphate receptor type 1 is a substrate for caspase-3 and is cleaved during apoptosis in a caspase-3-dependent manner.* J Biol Chem, 1999. **274**(48): p. 34433-7.
180. Verbert, L., B. Lee, S.L. Kocks, Z. Assefa, J.B. Parys, L. Missiaen, . . . G. Bultynck, *Caspase-3-truncated type 1 inositol 1,4,5-trisphosphate receptor enhances intracellular Ca^{2+} leak and disturbs Ca^{2+} signalling.* Biol Cell, 2008. **100**(1): p. 39-49.
181. Hanson, C.J., M.D. Bootman, and H.L. Roderick, *Cell signalling: IP_3 receptors channel calcium into cell death.* Curr Biol, 2004. **14**(21): p. R933-5.
182. Kopil, C.M., A.P. Siebert, J.K. Foskett, and R.W. Neumar, *Calpain-cleaved type 1 inositol 1,4,5-trisphosphate receptor impairs ER Ca^{2+} buffering and causes*

neurodegeneration in primary cortical neurons. J Neurochem, 2012. **123**(1): p. 147-58.

183. Petros, A.M., A. Medek, D.G. Nettesheim, D.H. Kim, H.S. Yoon, K. Swift, . . . S.W. Fesik, *Solution structure of the antiapoptotic protein Bcl-2.* Proc Natl Acad Sci U S A, 2001. **98**(6): p. 3012-7.
184. Fiebig, A.A., W. Zhu, C. Hollerbach, B. Leber, and D.W. Andrews, *Bcl-Xl is qualitatively different from and ten times more effective than Bcl-2 when expressed in a breast cancer cell line.* BMC Cancer, 2006. **6**: p. 213.
185. Yin, X.M., Z.N. Oltvai, and S.J. Korsmeyer, *BH1 and bH2 domains of Bcl-2 are required for inhibition of apoptosis and heterodimerization with Bax.* Nature, 1994. **369**(6478): p. 321-3.
186. Sedlak, T.W., Z.N. Oltvai, E. Yang, K. Wang, L.H. Boise, C.B. Thompson, and S.J. Korsmeyer, *Multiple Bcl-2 family members demonstrate selective dimerizations with Bax.* Proc Natl Acad Sci U S A, 1995. **92**(17): p. 7834-8.
187. Cheng, E.H., B. Levine, L.H. Boise, C.B. Thompson, and J.M. Hardwick, *Bax-independent inhibition of apoptosis by bcl-Xl.* Nature, 1996. **379**(6565): p. 554-6.
188. Minn, A.J., C.S. Kettlun, H. Liang, A. Kelekar, M.G. Vander Heiden, B.S. Chang, . . . C.B. Thompson, *Bcl-Xl regulates apoptosis by heterodimerization-dependent and -independent mechanisms.* Embo J, 1999. **18**(3): p. 632-43.
189. Zha, H. and J.C. Reed, *Heterodimerization-independent functions of cell death regulatory proteins Bax and Bcl-2 in yeast and mammalian cells.* J Biol Chem, 1997. **272**(50): p. 31482-8.
190. Boisguerin, P., C. Redt-Clouet, A. Franck-Miclo, S. Licheheb, J. Nargeot, S. Barrere-Lemaire, and B. Lebleu, *Systemic delivery of BH4 anti-apoptotic peptide using cpps prevents cardiac ischemia-reperfusion injuries in vivo.* J Control Release, 2011. **156**(2): p. 146-53.
191. Cantara, S., P.E. Thorpe, M. Ziche, and S. Donnini, *Tat-BH4 counteracts abeta toxicity on capillary endothelium.* FEBS Lett, 2007. **581**(4): p. 702-6.
192. Ku, B., C. Liang, J.U. Jung, and B.H. Oh, *Evidence that inhibition of Bax activation by Bcl-2 involves its tight and preferential interaction with the BH3 domain of Bax.* Cell Res, 2011. **21**(4): p. 627-41.
193. High, L.M., B. Szymanska, U. Wilczynska-Kalak, N. Barber, R. O'Brien, S.L. Khaw, . . . R.B. Lock, *The Bcl-2 homology domain 3 mimetic ABT-737 targets the apoptotic machinery in acute lymphoblastic leukemia resulting in synergistic in vitro and in vivo interactions with established drugs.* Mol Pharmacol, 2010. **77**(3): p. 483-94.
194. Ackler, S., M.J. Mitten, K. Foster, A. Oleksijew, M. Refici, S.K. Tahir, . . . A.R. Shoemaker, *The Bcl-2 inhibitor ABT-263 enhances the response of multiple chemotherapeutic regimens in hematologic tumors in vivo.* Cancer Chemother Pharmacol, 2010. **66**(5): p. 869-80.
195. Shoemaker, A.R., M.J. Mitten, J. Adickes, S. Ackler, M. Refici, D. Ferguson, . . . S.W. Elmore, *Activity of the Bcl-2 family inhibitor ABT-263 in a panel of small cell lung cancer xenograft models.* Clin Cancer Res, 2008. **14**(11): p. 3268-77.
196. Vogler, M., D. Dinsdale, M.J. Dyer, and G.M. Cohen, *Bcl-2 inhibitors: Small molecules with a big impact on cancer therapy.* Cell Death Differ, 2009. **16**(3): p. 360-7.
197. Schoenwaelder, S.M., K.E. Jarman, E.E. Gardiner, M. Hua, J. Qiao, M.J. White, . . . S.P. Jackson, *Bcl-Xl-inhibitory BH3 mimetics can induce a transient thrombocytopathy that undermines the hemostatic function of platelets.* Blood, 2011. **118**(6): p. 1663-74.

198. Mason, K.D., M.R. Carpinelli, J.I. Fletcher, J.E. Collinge, A.A. Hilton, S. Ellis, . . . B.T. Kile, *Programmed anuclear cell death delimits platelet life span.* Cell, 2007. **128**(6): p. 1173-86.
199. Qi, B. and J.M. Hardwick, *A Bcl-Xl timer sets platelet life span.* Cell, 2007. **128**(6): p. 1035-6.
200. Souers, A.J., J.D. Leverson, E.R. Boghaert, S.L. Ackler, N.D. Catron, J. Chen, . . . S.W. Elmore, *ABT-199, a potent and selective Bcl-2 inhibitor, achieves antitumor activity while sparing platelets.* Nat Med, 2013. **19**(2): p. 202-8.
201. Berridge, M.J., *Dysregulation of neural calcium signaling in alzheimer disease, bipolar disorder and schizophrenia.* Prion, 2013. **7**(1): p. 2-13.
202. Ludwinski, M.W., J. Sun, B. Hilliard, S. Gong, F. Xue, R.J. Carmody, . . . Y.H. Chen, *Critical roles of Bim in T cell activation and t cell-mediated autoimmune inflammation in mice.* J Clin Invest, 2009. **119**(6): p. 1706-13.
203. Borner, C., R. Olivier, I. Martinou, C. Mattmann, J. Tschopp, and J.C. Martinou, *Dissection of functional domains in Bcl-2 alpha by site-directed mutagenesis.* Biochem Cell Biol, 1994. **72**(11-12): p. 463-9.
204. Borner, C., I. Martinou, C. Mattmann, M. Irmler, E. Schaerer, J.C. Martinou, and J. Tschopp, *The protein Bcl-2 alpha does not require membrane attachment, but two conserved domains to suppress apoptosis.* J Cell Biol, 1994. **126**(4): p. 1059-68.
205. Garcia-Saez, A.J., *The secrets of the Bcl-2 family.* Cell Death Differ, 2012. **19**(11): p. 1733-40.
206. Leber, B., J. Lin, and D.W. Andrews, *Embedded together: The life and death consequences of interaction of the Bcl-2 family with membranes.* Apoptosis, 2007. **12**(5): p. 897-911.
207. Kaufmann, T., S. Schlipf, J. Sanz, K. Neubert, R. Stein, and C. Borner, *Characterization of the signal that directs bcl-Xl, but not Bcl-2, to the mitochondrial outer membrane.* J Cell Biol, 2003. **160**(1): p. 53-64.
208. Blagosklonny, M.V., *Unwinding the loop of Bcl-2 phosphorylation.* Leukemia, 2001. **15**(6): p. 869-74.
209. Ruvolo, P.P., X. Deng, and W.S. May, *Phosphorylation of bcl2 and regulation of apoptosis.* Leukemia, 2001. **15**(4): p. 515-22.
210. Kang, C.B., J. Tai, J. Chia, and H.S. Yoon, *The flexible loop of Bcl-2 is required for molecular interaction with immunosuppressant FK-506 binding protein 38 (FKBP38).* FEBS Lett, 2005. **579**(6): p. 1469-76.
211. Kang, C., N. Bharatham, J. Chia, Y. Mu, K. Baek, and H.S. Yoon, *The natively disordered loop of Bcl-2 undergoes phosphorylation-dependent conformational change and interacts with pin1.* PLoS One, 2012. **7**(12): p. e52047.
212. Bononi, A., S. Missiroli, F. Poletti, J.M. Suski, C. Agnoletto, M. Bonora, . . . P. Pinton, *Mitochondria-associated membranes (MAMs) as hotspot Ca^{2+} signaling units.* Adv Exp Med Biol, 2012. **740**: p. 411-37.
213. Arbel, N., D. Ben-Hail, and V. Shoshan-Barmatz, *Mediation of the antiapoptotic activity of bcl-Xl protein upon interaction with VDAC-1 protein.* J Biol Chem, 2012. **287**(27): p. 23152-61.
214. Bonneau, B., J. Prudent, N. Popgeorgiev, and G. Gillet, *Non-apoptotic roles of Bcl-2 family: The calcium connection.* Biochim Biophys Acta, 2013. Ahead of print.
215. Hardwick, J.M. and L. Soane, *Multiple functions of Bcl-2 family proteins.* Cold Spring Harb Perspect Biol, 2013. **5**(2): a008722.

PROFESSIONAL CAREER:

Giovanni MONACO

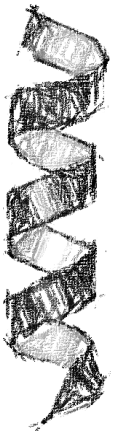

PROFESSIONAL CAREER: *Giovanni MONACO*

Education

16/10/2006
Msc Degree in Pharmaceutical Biotechnology, University of Padua, Italy
Experimental research thesis: "Characterization of flavopiridol-cytotoxic effect on ALCL lymphoma cells". Degree grade: 104/110

Research experience

10/2008-04/2013 || *Ph.D. student*
Laboratory of Molecular and Cellular Signalling,
KU Leuven/F.W.O., Leuven, Belgium
Research project: "Regulation of intracellular Ca^{2+} signalling by anti-apoptotic Bcl-2-family members".
Supervisor: Dr. Geert Bultynck

03/2007-07/2008 || *Research Assistant*
Laboratory of Circuit Formation and Function in the Olfactory System,
Venetian Institute of Molecular Medicine, VIMM, Padua, Italy
Research project: "Roles of second messengers in circuit formation and function in the olfactory system".
Supervisor: Dr. Claudia Lodovichi

10/2005-10/2006 || *Laboratory traineeship as under-graduate*
Laboratory of Pediatric Oncohematology,
Clinica di Oncoematologia Pediatrica, Padua, Italy
Experimental research thesis (see above).
Supervisor: Dr. Paolo Bonvini

List of publications

Research papers

Monaco G, Decrock E, Nuyts K, Wagner II LE, Luyten T, Strelkov S, Missiaen L, De Borggraeve WM, Leybaert L, Yule DI, De Smedt H, Parys JB and Bultynck G:
Secondary structure determinants for the inhibition of the IP_3 receptor by a Bcl-2-BH4-domain peptide. *PLoS One*, 2013, under final revision.

Akl H, **Monaco G**, La Rovere R, Welkenhuyzen K, Kiviluoto S, Vervliet T, Molgó J, Distelhorst CW, Missiaen L, Mikoshiba K, Parys JB, De Smedt H and Bultynck G:
IP_3R2 levels dictate the apoptotic sensitivity of diffuse large B cell lymphoma cells to an IP_3R-derived peptide targeting the BH4 domain of Bcl-2. *Cell Death and Disease*. 2013, Ahead of Print.

Akl A, Vandecaetsbeek I, **Monaco G**, Kauskot A, Luyten T, Welkenhuyzen K, Hoylaerts M, De Smedt H, Parys JB and Bultynck G:
HA14-1, but not the BH3 mimetic ABT-737, causes Ca^{2+} dysregulation in platelets and human cell lines. *Hematologica*. 2013, Apr; 98(4):e49-51.

Monaco G[*], Beckers M[*], Ivanova H, Missiaen L, Parys JB, De Smedt H and Bultynck G:
Profiling of the Bcl-2/Bcl-Xl-binding sites on type 1 IP_3 receptor. *Biochemical and Biophysical Research Communications*. 2012 Nov 9; 428(1):31-5. *(*shared first authorship).*

Monaco G[*], Decrock E[*], Ponsaerts R, Akl H, Luyten T, Vervliet T, De Maeyer M, Missiaen L, Distelhorst CW, De Smedt H, Parys JB, Leybaert L and Bultynck G:
Selective regulation of IP_3-receptor-mediated Ca^{2+} signaling and apoptosis by the BH4 domain of Bcl-2 versus Bcl-Xl. *Cell Death and Differentiation.* 2012 Feb; 19(2):295-309. *(*shared first authorship).*

Zhong F, Harr MW, Bultynck G, **Monaco G**, Parys JB, De Smedt H, Rong YP, Molitoris JK, Lam M, Ryder C, Matsuyama S and Distelhorst CW:
Induction of Ca^{2+}-driven apoptosis in chronic lymphocytic leukemia cells by peptide-mediated disruption of Bcl-2-IP_3 receptor interaction. *Blood*. 2011 Mar; 117(10):2924-34.

Decuypere JP[*], **Monaco G**[*], Kiviluoto S, Oh-hora M, Luyten T, De Smedt H, Parys JB, Missiaen L and Bultynck G:
STIM1, but not STIM2, is required for proper agonist-induced Ca^{2+} signaling. *Cell Calcium*. 2010 Aug-Sep; 48(2-3):161-7. *(*shared first authorship).*

Bonvini P, Zorzi E, Mussolin L, **Monaco G,** Pigazzi M, Basso G and Rosolen A:
The effect of the cyclin-dependent kinase inhibitor flavopiridol on anaplastic large cell lymphoma cells and relationship with NPM-ALK kinase expression and activity. *Haematologica*. 2009 Jul; 94(7):944-55.

Maritan M, **Monaco G**, Zamparo I, Zaccolo M, Pozzan T, Lodovichi C:
Odorant receptors at the growth cone are coupled to localized cAMP and Ca^{2+} increases. *Proceedings of the National Academy of Sciences of the United States of America*. 2009 Mar 3; 106(9):3537-42.

Reviews

Monaco G[*], Vervliet T[*], Akl H[*] and Bultynck G:
The selective BH4-domain biology of Bcl-2-family members: IP_3Rs and beyond. *Cellular and Molecular Life Sciences*. 2013 Apr; 70(7):1171-83. *(*shared first authorship).*

Decuypere JP, **Monaco G,** Bultynck G, Missiaen L, De Smedt H and Parys JB:
The IP_3 receptor-mitochondria connection in apoptosis and autophagy. *Biochimica et Biophysica Acta-Molecular Cell Research.* 2011 May; 1813(5):1003-13.

Decuypere JP, **Monaco G**, Missiaen L, De Smedt H, Parys JB and Bultynck G:
IP_3 receptors, mitochondria and Ca^{2+} signaling: implications for aging. *Journal of Aging Research.* 2011 March; 2011:920178.

List of abstracts 2008-2013

Oral presentations

Monaco G, Decrock E, Ponsaerts R, Missiaen L, Distelhorst CW, De Smedt H, Parys JB, Leybaert L, Bultynck G: IP_3-receptor-mediated Ca^{2+} signaling and apoptosis are selectively regulated by the BH4 domain of Bcl-2, but not of Bcl-Xl. Cell Death in Cancer, European Association for Cancer Research, January 26-28, 2012, Amsterdam, The Netherlands, *(oral presentation by Geert Bultynck)*.

Monaco G, Decrock E, Ponsaerts R, Akl H, Luyten T, Vervliet T, De Maeyer M, Missiaen L, Distelhorst CW, De Smedt H, Parys JB, Leybaert L, Bultynck G: The BH4 domains of Bcl-2 and Bcl-Xl differentially regulate inositol 1,4,5-trisphosphate receptors and apoptosis. European Calcium Society (ECS) Meeting, September 6-9, 2010, Warsaw, Poland.

Poster presentations

Akl H, Vandecaetsbeek I, **Monaco G**, Kauskot T, Luyten T, Welkenhuyzen K, Missiaen L, Hoylaerts MF, Parys JB, De Smedt H, Bultynck G: BH3-mimetic ABT-737 has a safe Ca^{2+}-signaling profile and does not disrupt intracellular Ca^{2+} homeostasis and dynamics in platelets and human cells. Annual Meeting Belgian Association for Cancer Research (BACR), Death and Cancer, February 2, 2013, Antwerp, Belgium

Akl H, Vandecaetsbeek I, **Monaco G**, Kauskot T, Luyten T, Welkenhuyzen K, Missiaen L, Hoylaerts MF, Parys JB, De Smedt H, Bultynck G: BH3-mimetic ABT-737 has a safe Ca^{2+}-signaling profile and does not disrupt intracellular Ca^{2+} homeostasis and dynamics in platelets and human cells. Genes & Cancer, 29th Annual Meeting, December 10-12, 2012, Warwick, UK.

Dubron K, Akl H, **Monaco G**, Baes M, Erneux C, Missiaen L, De Smedt H, Parys JB, Bultynck G: Chronic IP_3 signaling contributes to cell death in response to peptides disrupting IP_3R/Bcl-2 complexes in diffuse large-B-cell lymphoma cell models. Genes & Cancer, 29th Annual Meeting, December 10-12, 2012, University of Warwick, UK.

Monaco G, Ponsaerts R, La Rovere R, Decrock E, Nuyts K, Luyten T, Welkenhuysen K, Strelkov S, Leybaert L, De Borggraeve W, De Smedt H, Parys JB, Bultynck G: A dicodon mutation in the BH4 domain of Bcl-2 reveals new structural determinants involved in the inhibition of inositol 1,4,5-trisphosphate receptors (IP_3Rs). 2012's Meeting of the Belgian Society of Physiology and Pharmacology, October 26th, 2012, Brussels, Belgium.

Monaco G, Ponsaerts R, La Rovere R, Decrock E, Nuyts K, Luyten T, Welkenhuysen K, Strelkov S, Leybaert L, De Borggraeve W, De Smedt H, Parys JB, Bultynck G: A dicodon mutation in the BH4 domain reveals new structural determinants involved in the inhibition of inositol 1,4,5-trisphosphate receptors (IP_3Rs) by Bcl-2. 12th meeting of the European Calcium Society, September 9-12, 2012, Toulouse, France.

Akl H, La Rovere R, **Monaco G**, Kauskot A, Molgo J, Distelhorst CW, Missaen L, Parys JB, De Smedt H, Bultynck G: IP_3R2/IP_3R ratio dictates apoptotic sensitivity towards peptide-mediated disruption of IP_3R/Bcl-2 interaction in Diffuse Large-B-cell Lymphomas."Cell Death" Gordon Research Conference, July 15-20, 2012, Lucca, Italy.

Monaco G, Ponsaerts R, La Rovere R, Decrock E, Nuyts K, Luyten T, Welkenhuysen K, Strelkov S, Leybaert L, De Borggraeve W, De Smedt H, Parys JB, Bultynck G: New structural insights into the pro-survival inhibition of inositol 1,4,5-trisphosphate receptors (IP_3Rs) by the BH4 domain of Bcl-2. "Cell Death" Gordon Research Conference, July 15-20, 2012, Lucca, Italy.

Akl H, La Rovere R, **Monaco G**, Kauskot A, Molgo J, Distelhorst CW, Missiaen L, Parys JB, De Smedt H, Bultynck G: Up-regulation of the type-2 IP_3R isoform dictates the apoptotic response to disrupting IP_3R/Bcl-2 complexes in diffuse-large B-cell lymphoma. Calcium & Cell Function. June 17-22, 2012, Snowmass Village, Colorado, USA.

Akl H, La Rovere R, **Monaco G**, Kauskot A, Molgo J, Distelhorst CW, Missaen L, Parys JB, De Smedt H, Bultynck G: Up-regulation of the type-2 IP_3R isoform dictates the apoptotic response to disrupting IP_3R/Bcl-2 complexes in diffuse-large B-cell lymphoma. Apoptosis and Cancer meeting. June 14-15, 2012, Cambridge, UK.

Monaco G, Decrock E, Akl H, Ponsaerts R, Vervliet T, Luyten T, De Maeyer M, Missiaen L, Distelhorst CW, De Smedt H, Parys JB, Leybaert L, Bultynck G: Selective regulation of IP_3-receptor-mediated Ca^{2+} signaling and apoptosis by the BH4 domain of Bcl-2 versus Bcl-Xl. Mitochondrial Dynamics: from Mechanism to Disease, September 11-15, 2011, Sardinia, Italy.

Monaco G, Decrock E, Ulens T, Akl H, , Missiaen L, De Maeyer M, Leybaert L, Distelhorst CW, Parys JB, De Smedt H, Bultynck G: BH4 domains of Bcl-2 and Bcl-Xl differentially regulate apoptosis by modulating inositol 1,4,5-trisphosphate receptors activity. 18th European Cell Death Organization (ECDO) Euroconference, September 1-4, 2010, Ghent, Belgium.

Akl H, Van Melckebeke H, **Monaco G**, Vanhoecke B, Missiaen L, Parys JB, Offner F, De Smedt H, Bultynck G: Abnormal IP_3R-induced Ca^{2+} release correlates with anti-apoptotic signaling in Diffuse large B-cell lymphoma and B-cell chronic lymphocytic leukemia. 18th European Cell Death Organization (ECDO) Euroconference, September 1-4, 2010 Ghent, Belgium.

Monaco G, Akl H, Ulens T, Rong YP, Parys JB, Missiaen L, De Smedt H, De Maeyer M, Distelhorst CW, Bultynck G: Exploting the BH4 domain of Bcl-2 as a novel strategy to provoke pro-apoptotic Ca^{2+} signaling in cancer cells. Annual Meeting Belgian Association for Cancer Research (BACR), January, 2010, Leuven, Belgium.

Maritan M, **Monaco G**, Zaccolo M, Lodovichi C: Real time cAMP and Ca^{2+} dynamics in the olfactory system. 10th ECS (European Calcium Society) Symposium, September 17-20, 2008, Leuven, Belgium.

Participation in international meetings

9-12/09/2012
European Calcium Society (ECS) Meeting, Toulouse, France.

15-20/07/2012
"Cell Death" Gordon research conference, Lucca, Italy.

11-15/09/2011
Mitochondrial Dynamics: from Mechanism to Disease, Sardinia, Italy.

6-9/09/2010
European Calcium Society (ECS) Meeting, Warsaw, Poland.

1-4/09/2010
18th European Cell Death Organization (ECDO) Euroconference, Ghent, Belgium.

17-20/09/2008
European Cacium Society (ECS) Meeting, Leuven, Belgium.

Supervising experiences

Supervisor of Marjolein Beckers for her master's thesis work entitled: "Molecular interactions of anti-apoptotic Bcl-2 and Bcl-Xl proteins with IP_3R1-domains", Faculty of Pharmaceutical Science, academic year 2012-2013

Fellowships/honors/awards

Research Foundation Flanders/Fonds Wetenschappelijk Onderzoek-Vlaanderen (FWO)
Ph.D. fellowship holder 2009-2013

Travel scholarship sponsored by the School of Molecular Medicine (SMM), September 6th-9th 2010, Warsaw, Poland

Article by Monaco et al., "Selective regulation of IP_3-receptor-mediated Ca^{2+} signaling and apoptosis by the BH4 domain of Bcl-2 versus Bcl-Xl", Cell Death Differ;19(2):295-309, 2012 recommended and ranked by F1000's Faculty of 5,000 renowned researchers and clinicians, assisted by 5,000 associates. - F1000